Synthesis and Applications of Amide-Based Pd(II) NNN-pincer Complexes

By

Thomas S. Johnson

Submitted to the graduate degree program in Chemistry
and the Graduate Faculty of the University of Kansas in partial fulfillment of the requirements for the degree of Master of Science.

_____

Kristin Bowman-James, *co-chairperson*

_____

Helena C. Malinakova, *co-chairperson*

_____

Jon A. Tunge

_____

Thomas E. Prisinzano

Date Defended: February 1, 2016

The Thesis Committee for Thomas S. Johnson

certifies that this is the approved version of the following thesis:

Synthesis and Applications of Amide-Based Pd(II) NNN-pincer Complexes

_____

Kristin Bowman-James, *co-chairperson*

_____

Helena C. Malinakova, *co-chairperson*

_____

Jon A. Tunge

_____

Thomas E. Prisinzano

Date approved: February 8, 2016

Abstract

The first project is described in Chapter 2, and details the synthesis of a series of mono- and multimetallic Pd(II) NNN-pincer complexes which—to the best of our knowledge—represent the first examples of these types of complexes being employed as catalysts in a Heck reaction. Chapter 3 discusses the design and synthesis of a hybrid pincer/imidazolium salt ligand and its transition metal chemistry, with the ultimate goal of synthesizing heterobimetallic complexes for bifunctional catalysis. The work in Chapter 4 strays away from the catalysis theme, and includes preliminary investigations into the synthesis of metal-organic frameworks (MOF) derived from the combination of a bis[palladium(II)] complex with a pyridine-appended ditopic macrocycle.

Acknowledgements

First, I would like to thank my two Ph.D. advisors – Professors Helena Malinakova and Kristin Bowman-James – for their ongoing support of me throughout my Ph.D. career. Also, I would like to thank all the past and present group members that I have had the privilege to work with: Qi-Qiang Wang, Rowshan Begum, Pedro Metola, Hanumaiah Telikepalli, Chuandong Jia, Jorge Gonzales, Thomas Robben, James Mills, Jess Lohrman, Lucas McCormick, Sandeep Raikar, Rachel Scheetz, Pavel Ryabchuk, John Hershberger, Atsushi Shiota, Kevin Godber, Benoy Pal, Sarvesh, Kumar, and Jayanth Thatai. An additional thanks goes to the members of my defense committee: Professors Jon Tunge, Tom Prisinzano, and Misha Barybin.

Second, I would like to thank everyone that has been involved with the Chemical Biology Training Grant. This includes Professors Paul Hanson, Tom Prisinzano, and Audrey Lamb, as well as the rotating cast of student fellows. The training grant was a profound opportunity for me to experience as a graduate student. I sincerely hope that the diverse courses, lab rotations, conferences, and opportunities for personal interactions with guest speakers will be available to more graduate students in the future because it has provided me and my peers with invaluable information that will guide us through the rest of our careers. I also would like to thank Dr. Leo Qiang of Combi-Block Inc. (San Diego, CA) and Dr. Tomislav Rovis of Colorado State University (Fort Collins, CO) for allowing me to conduct lab rotations in their groups. Lastly, I would like to again thank Dr. Bowman-James, for encouraging me to apply for this program.

Third, I would like to thank my family. My mom: Thank you for always encouraging and believing in me. Your kindness, hard work, and creativity will always be an inspiration to me. My dad: You have never left my side. My wife: There is no question I would not be in this position without you. For many reasons, graduate school has consisted of the toughest trials of my life. Having to cope with the loss of my father, grandmother, and one of my closest college friends; without the never-ending support of my wife, my mom, and countless other family and friends, I could not have come this far. Lastly, I would also like to thank everyone in the Lawrence community that has helped me keep my head up along the way and continued to encourage me. The future is bright.

This thesis is dedicated to my great great grandfather,

George Washington, who escaped from slavery

at the Miller plantation in Missouri

and settled near Clinton, Kansas.

TABLE OF CONTENTS

List of Abbreviations

AAS	atomic absorption spectroscopy
acac	acetylacetonate
CEES	2-chloroethyl sulphide
Cp	cyclopentadiene
dba	dibenzylideneacetone
DCM	dichloromethane
DEPT	distortionless enhancement by polarization transfer
DFT	density functional theory
ditz	1,2,4-trimethyltriazolylidene
DMA	*N*,*N*-dimethylacetamide
DMF	*N*,*N*-dimethylformamide
DMSO	dimethyl sulfoxide
ee	enantiomeric excess
EPR	electron paramagnetic resonance
ESI	electrospray ionization
Et_3N	triethylamine
FT-IR	fourier-transform infrared spectroscopy
HOMO	highest occupied molecular orbital
HRMS	high-resolution mass spectrometry
KHMDS	potassium bis(trimethylsilyl)amide
LUMO	lowest unoccupied molecular orbital
m/z	mass-to-charge ratio
MOF	metal-organic framework
NaOAc	sodium acetate
NHC	*N*-heterocyclic carbene

NMP	*N*-methyl-2-pyrrolidone
NMR	nuclear magnetic resonance
OAc	acetate
OTf	triflate
P(*o*-Tol)$_3$	tri(*o*-tolyl)phosphine
PEG	polyethylene glycol
PS-Pd	polystyrene-bound palladium
PPh_3	triphenylphosphine
RCM	ring-closing metathesis
SWNT	single wall nanotube
TBA	tetrabutylammonium
TEM	tunneling-electron microscopy
TFA	trifluoroacetic acid
THF	tetrahydrofuran
tht	tetrahydrothiophene
TMED	*N*,*N*,*N*′,*N*′-tetramethylethane-1,2-diamine
TMS	tetramethylsilane
TPMA	tris(2-pyridylmethyl)amine
tren	tris(2-aminoethyl)amine
TOF	time of flight
TON	turnover number
XRD	X-ray diffraction

Chapter 1

Introduction

The ability to efficiently form carbon–carbon bonds is an important facet of modern synthetic organic chemistry.[1] The discoveries of palladium-catalyzed cross coupling reactions, such as the Heck, Suzuki, Sonogashira, and Stille reactions, have enabled the efficient syntheses of many types of complex organic compounds. However, the typical catalysts employed in these reactions (e.g. $Pd(OAc)_2$, $Pd(PPh_3)_4$, $PdCl_2(PPh_3)_2$) sometimes suffer due to a lack of thermal stability and necessitate the use of excess phosphine stabilizing ligands.[2] Transition metal complexes derived from tridentate six-electron donor "pincer ligands" (Figure 1.1) can provide stable and highly selective alternatives to traditional catalysts.[3] Pincer ligands bind to the metal center via a central donor atom (traditionally an anionic carbon donor atom) along with two *ortho* pendant donor atoms (traditionally neutral phosphorus donor atoms). Owing in part to this tridentate coordination, the resulting "pincer complexes" enjoy a high thermal stability, which has led to their widespread exploration in a number of cross coupling reactions.

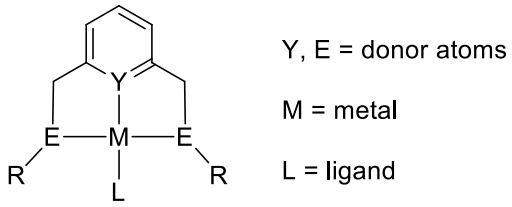

Figure 1.1. Schematic representation of a pincer complex.

As illustrated in Figure 1.2, the last two decades have seen a dramatic surge in the number of reports of "palladium pincer complexes." In addition to their use in C–C coupling reactions, they have been studied in supramolecular chemistry, chemical sensing, and investigations of luminescence for light emitting devices.[4] In addition to palladium, other transition metal complexes with pincer ligands have been extensively investigated in

catalysis and in other applications, but are beyond the scope of this review. This chapter will highlight the synthesis and applications of some of the representative examples of Pd(II) pincer complexes. Whereas research in the Dr. Bowman-James research group has concentrated on the supramolecular[5-17] and transition metal[18-24] chemistry of amide- and thioamide-based pincer ligands, the second part of this chapter will focus on the transition metal chemistry of NNN-pincer ligands.

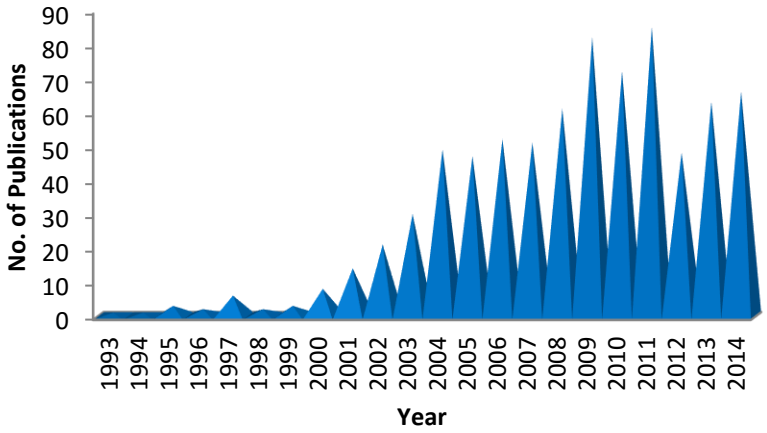

Figure 1.2. Number of publications containing the concept "palladium pincer" arranged by publication year (source: SciFinder).[25]

1.1 *Properties and Synthesis of Pd(II) Pincer Complexes*

Pincer ligands and their corresponding metal complexes were first described in 1976 by Moultan and Shaw (Figure 1.3).[26] The study of these ligands was an extension of the earlier discovery that bulky monophosphine ligands (PBu^t_2R, R = alkyl or aryl) could be used to stabilize metals in unusual oxidation states, as well as promote *ortho*-metalation.[27,28] Pincer ligands are classified based on the identity of their donor atoms. For example, a phosphorus-carbon-phosphorus pincer ligand can be described as a 'PCP'-

pincer ligand. Although the term "pincer complex," as coined by van Koten in 1989,[29] was first intended to describe these tridentate PCP-type ligands, the term can also be used to describe ligands derived from a variety of donor atoms, including phosphorus, carbon, nitrogen, sulfur, and selenium. The most common oxidation state of palladium in pincer complexes is +2, although a number of studies have investigated the stability of Pd(IV) complexes with pincer ligands.[30] The tridentate coordination of the pincer ligand imparts a strong chelate effect on the metal center which helps to prevent ligand exchange and results in the high thermal stability enjoyed by these complexes.[31] Also, as a result of the tridentate pincer chelation, at least one site is available for coordinating additional ligands.

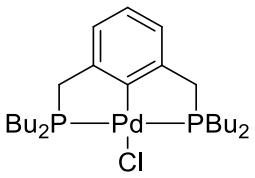

1.1

Figure 1.3. Pd(II) PCP-pincer complex reported by Moulton and Shaw.[26]

Two of the most direct methods to synthesize Pd(II) ECE-type (E = heteroatom) pincer complexes are 1) C–H activation by an electron deficient Pd(II) source (usually a tetrachloropalladate salt) and 2) oxidative addition of a C–X bond (X = Cl, Br, or I) to a Pd(0) source. In 2006, our group reported the synthesis of a Pd(II) SCS-pincer complex from pincer ligand **1.2a** (Y = CH) via the C–H insertion method (Scheme 1.1).[19] Treatment of **1.2a** with K_2PdCl_4 affords Pd(II) SCS-pincer complex **1.3** in 70% yield. To satisfy the +2 oxidation state of palladium, the fourth coordination site is occupied by a chloride ligand. Similarly, other monoanionic pincer ligands (e.g. phosphine-based PCP-, amine-based NCN-, and thioether-based SCS-pincer ligands) often contain a negative donor

ligand in the fourth coordination site. Alternatively, if the "Y" atom in the thioamide pincer ligand is nitrogen—as in ligand **1.2b**—metalation occurs with deprotonation of one of the thioamide hydrogens to give Pd(II) SNS-pincer complex **1.4**.

Scheme 1.1. Synthesis of pincer complexes by C–H insertion or single deprotonation.[19]

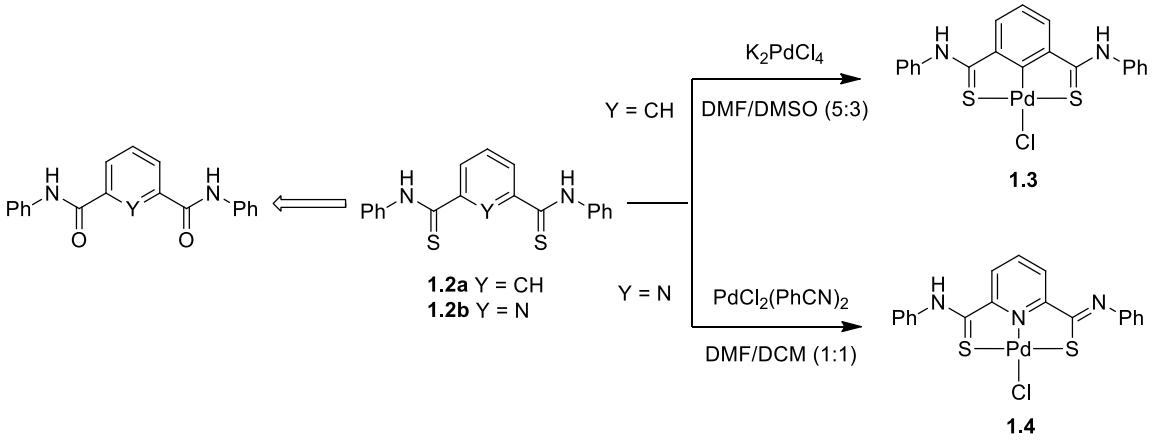

Alternatively, Pd(II) pincer complexes can be readily formed from ligands containing a central C–X (X = halogen) bond using Pd(0) sources such as $Pd(dba)_2$ (dba = dibenzylideneacetone), $Pd_2(dba)_3$ or $Pd(PPh_3)_4$ (PPh_3 = triphenylphosphine). This method has been successfully employed by the van Koten group to selectively introduce metals into the bifunctional ligand **1.5** (Scheme 1.2).[32] Treatment of **1.5** with $Pd_2(dba)_3{\cdot}CHCl_3$ at -80 ^oC affords Pd(II) SCS-pincer complex **1.6** via oxidative addition of the C–Br bond to Pd(0). The resulting Pd(II) complex is stabilized by the N-donor pendant group atoms to afford the air-stable NCN-pincer complex. Alternatively, treatment of **1.5** with $Pd(PPh_3)_4$ at 50 ^oC affords Pd(II) complex **1.7** via oxidative addition of the C–I bond to Pd(0).

Scheme 1.2. Synthesis of pincer complexes via oxidative addition of Pd(0) to a C–X bond.[32]

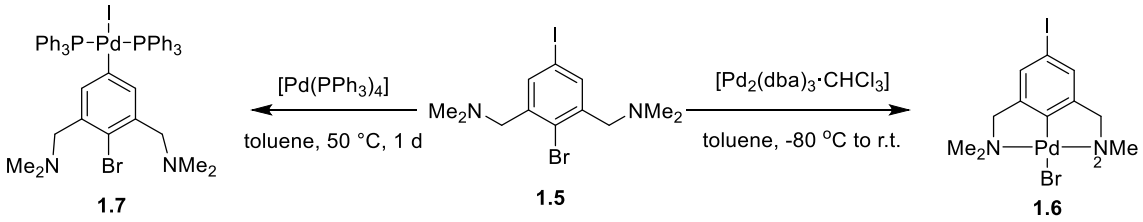

If a C–H or C–X direct metalation route is not possible—particularly if the ligand contains sterically demanding side arms—a transmetalation route can be employed. In their synthesis of Pd(II) NCN-pincer complexes, Jung and coworkers describe a transmetalation route which proceeds via an *in situ* generated Li–C intermediate (Scheme 1.3).[33] When R = H, as in ligand **1.8a**, direct palladation failed to give the corresponding pincer complex when treated with $PdCl_2$. However, if a bromide atom is introduced into the pincer ligand (R = Br), as in ligand **1.8b**, halogen-lithium exchange occurs with *n*-BuLi. Transmetalation of this intermediate occurs in the presence of $PdBr_2$ or $PdCl_2$ to afford the desired NCN-pincer complex **1.9**.

Scheme 1.3. Synthesis of a Pd(II) NCN-pincer complex by transmetallation.[33]

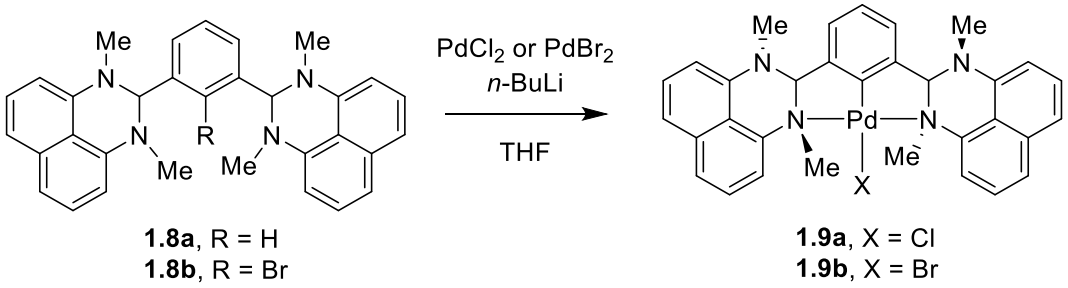

1.2 *Pd(II) Pincer Complexes in Catalysis*

Interest in pincer complexes grew in the mid-1990s, when numerous reports documented their applications as catalysts for a variety of reactions. In 1994, Venanzi and coworkers demonstrated the use of Pt(II) PCP-pincer complex **1.10** for the preparation of *trans*- and *cis*-oxazolines **1.11** and **1.12** via an asymmetric aldol condensation (Scheme 1.4).[34] The first Heck coupling reaction in which a Pd(II) pincer complex was employed as the catalyst was reported by Milstein and coworkers in 1997.[35] Since these two seminal reports, Pd(II) pincer complexes have been exploited as catalysts in a variety of reactions, including the Suzuki,[36-41] Negishi,[42-44] aldol,[45-47] Michael,[45,48-50] Sonogashira,[51,52] Hiyama,[51,52] Stille,[53] and asymmetric allylation reactions.[54-58] Many excellent reviews and books have focused on the transition metal chemistry of pincer ligands as well as their catalytic applications.[3] This section will highlight some of the representative examples of Pd(II) pincer complexes as catalysts for coupling reactions.

Scheme 1.4. Synthesis of oxazolines using chiral pincer complex **1.10**.[34]

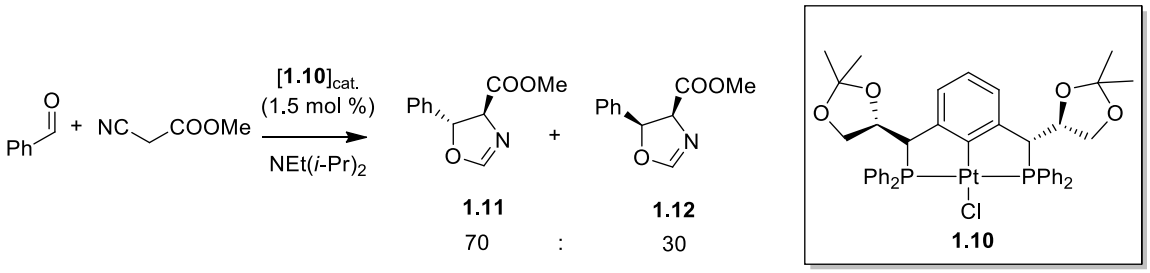

1.2.1 *Mizoroki-Heck Reaction*

The Mizoroki-Heck reaction, discovered independently by Tsutomu Mizoroki (1971)[59] and Richard F. Heck (1972),[60] represents an important C–C coupling reaction used in industry for the synthesis of a variety of fine chemicals (e.g. Prosulfuron™ by Novartis, Naproxen™ by Albemarle, and Singulair™ by Merck).[61] The prelude to the two seminal papers by Mizoroki and Heck came in the form of a series of seven letters published in *J. Am. Chem. Soc*. in 1968 by Heck.[62] In these letters, Heck reports the arylation of olefins using an *in situ*-generated palladium species derived from stoichiometric amounts of $Pd(OAc)_2$ or $PdCl_2$. However, the fact that the arylating agents were based on organo-mercury, -tin, and -lead compounds, limited the practical applications of these reactions. Thus, the later reports by Mizoroki and Heck represented major improvements over these reactions in that they used catalytic amounts of palladium (1 mol %) and were able to employ aryl halides as the arylating agents. Both groups used the model coupling reaction of 4-iodotoluene and styrene to access stilbene **1.13** (Scheme 1.5). In the last 40 years, a number of variants of the Mizoroki-Heck reaction have been developed that employ different aryl halides, solvents, bases, and catalysts.[63] Today, typical protocols for Heck-type couplings utilize $PdCl_2$ or $Pd(OAc)_2$, in combination with an excess of phosphine ligand (Ph_3P or *o*-Tol_3P), and in the presence of a base (Et_3N or NaOAc).

Scheme 1.5. Examples of the first reported Heck reactions.[59,60,64]

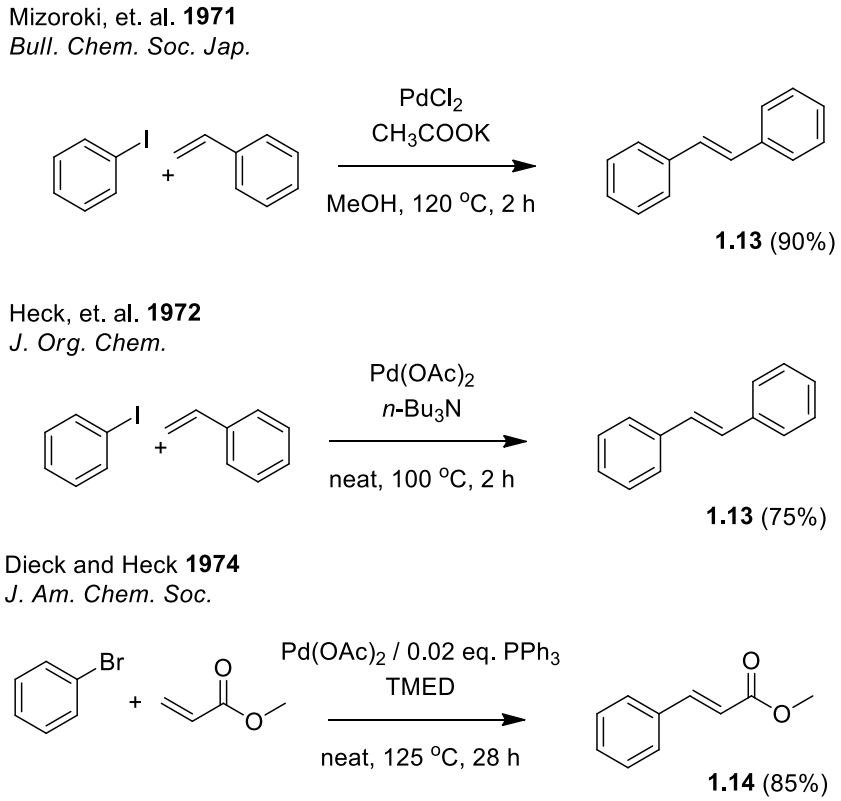

The first full mechanism for the Heck reaction was proposed in Heck's 1972 paper.[60] In this mechanism, it was suggested that aryl halides oxidatively add to an *in situ* generated Pd(0) species formed from reduction of the Pd(II) source by the olefin. In 1974, Dieck and Heck reported a variant of the Heck reaction that employed phosphine ligands in the synthesis of compound **1.14** (Scheme 1.5), and subsequently proposed a slightly different mechanism.[64] In the first step of the catalytic cycle, the aryl halide oxidatively adds to Pd(0) to give Pd(II) complex **1.15** (Scheme 1.6). This complex coordinates the olefin substrate to give complex **1.16**, which is followed by *syn* insertion to give Pd(II) complex **1.17**. Complex **1.17** undergoes β-hydride elimination to generate the stilbene complex **1.18**, which dissociates to give Pd(II) complex **1.19**. Base-assisted reductive

elimination/deprotonation furnishes the original Pd(0) catalyst. The order of reactivity for aryl halides (ArI > ArBr > ArCl) suggests that oxidative addition is the rate limiting step, which reflects the relative abilities for different aryl halides to oxidatively add to palladium.[65] Additionally, aryl halides that contain *para*-electron withdrawing groups have been found to be more active Heck substrates compared to aryl halides with *para*-electron donating groups.

Scheme 1.6. Pd(0)-Pd(II) catalytic cycle for the Heck reaction.

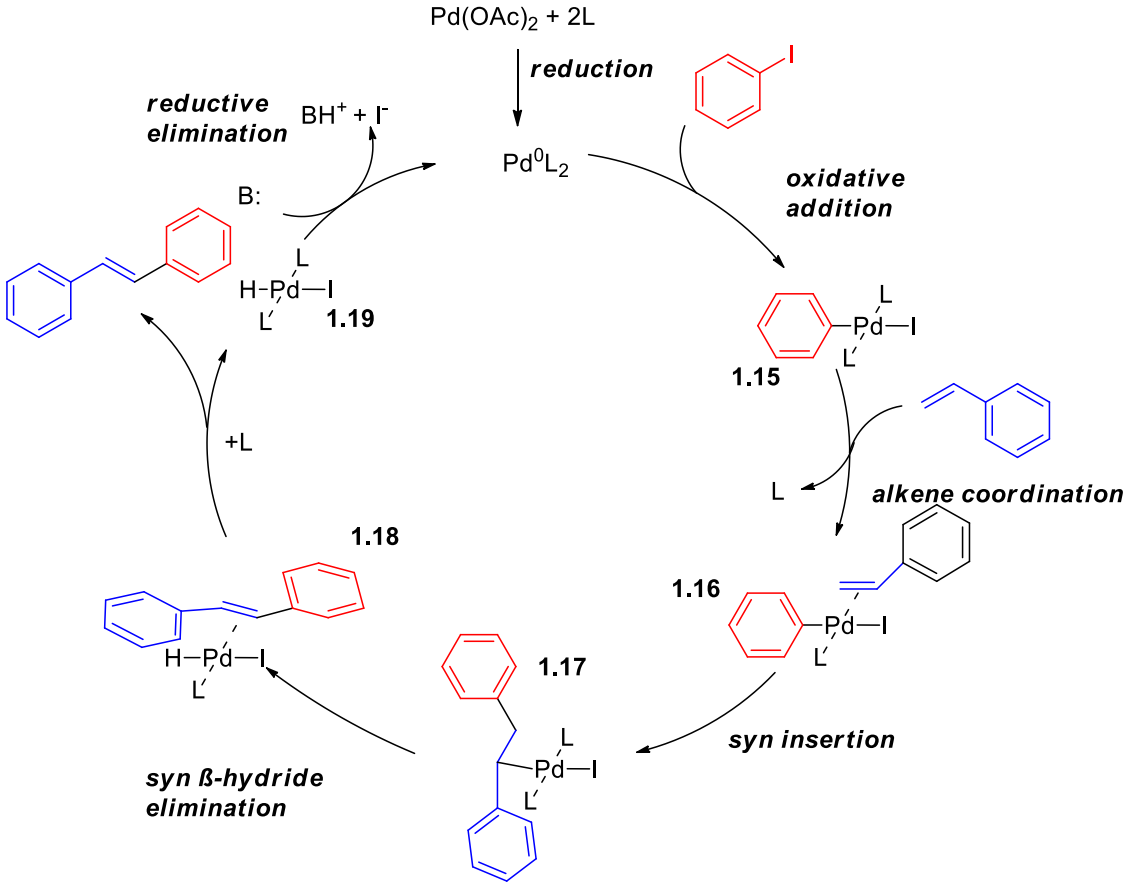

Although the first palladium pincer complexes were reported by Shaw in 1976 (Figure 1.3, *vide supra*),[26] it was over 20 years until the catalytic activity of a pincer complex in the Heck reaction was reported. In 1997, Milstein and coworkers investigated

Pd(II) PCP-pincer complexes **1.20**, **1.21**, and **1.22** (Scheme 1.7) in the Heck coupling of a variety of iodo- and bromo-arenes with styrene or methyl acrylate.[35] Quantitative yields and turnover numbers (TON) of up to 500,000 were observed in the coupling of iodobenzene and methyl acrylate using complexes **1.20** and **1.21**. The Heck coupling of methyl acrylate with either bromobenzene or 4-bromoanisole also produced the Heck products in good yields (79-93%) using **1.21** as the catalyst, although longer reaction times were required.

Scheme 1.7. Heck coupling in the presence of Pd(II) PCP-pincer complexes.[35]

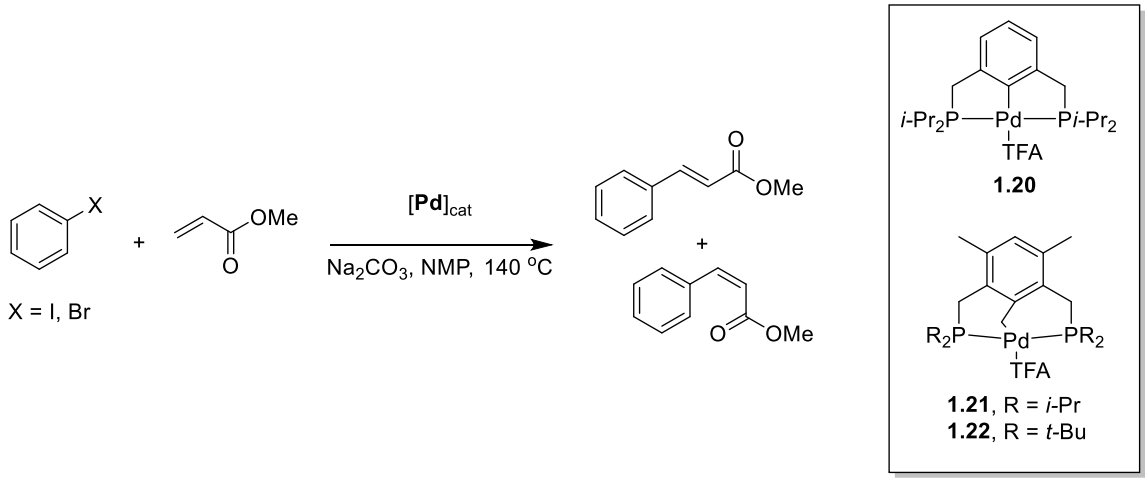

As an alternative to phosphine-derived catalysts, Crabtree and coworkers have investigated the coordination chemistry of Pd(II) with *N*-heterocyclic carbene (NHC)-based pincer ligands (Figure 1.4).[31,66] The authors reasoned that the strong electron donating character of carbenes relative to phosphines could help facilitate oxidative addition to the palladium center. To this extent, they synthesized the bidentate and tridentate CN- and CNC-pincer complexes illustrated in Figure 1.4. In contrast to conventional protocols for the Heck reaction which commonly employ phosphine ligands,

these reactions were not air sensitive. Complex **1.23a** (R = Me) showed good activity in the Heck coupling of iodobenzene and styrene using a catalyst loading of 0.2 mol %. The coupling of bromobenzene with styrene was also accomplished with this complex, using 5 mol % catalyst loading. The catalyst **1.23b** (R = *n*-Bu) was determined to be more efficient than **1.23a** (R = Me), which the authors attributed to enhanced solubility. Six successive reactions using complex **1.23b** (R = *n*-Bu) (with additional substrates added after each conversion) were carried out with yields ranging from 98 to 87% (first and last runs respectively). Complex **1.23b** proved to be a robust catalyst for the coupling of aryl chlorides with styrene, although the additive tetrabutylammonium bromide (TBAB) was necessary for the conversion to take place (95% yield, 22 h, TON = 47,500). The authors proposed that the Br^- ion may help facilitate catalyst activation and prevent the active species from forming catalytically inactive palladium black.

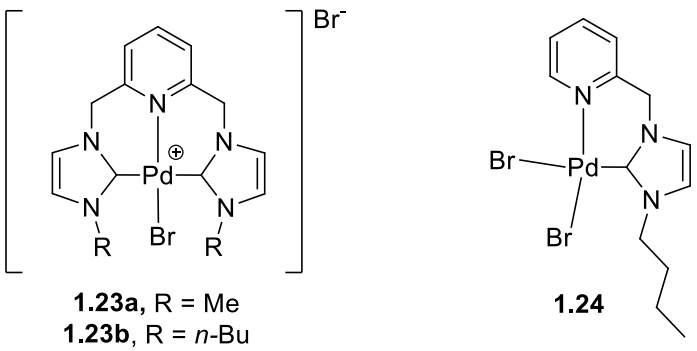

1.23a, R = Me
1.23b, R = *n*-Bu

1.24

Figure 1.4. Pd(II) CNC-pincer and CN palladacycles reported by Crabtree *et al*.[31,66]

The immobilization of pincer complexes onto polymer supports has been explored by Bergbreiter and coworkers,[67] who prepared a series of Pd(II) complexes with an SCS-pincer ligand (Figure 1.5). As a control, SCS-pincer complex **1.25** was examined in the Heck reaction of aryl iodides and bromides with a variety of alkenes. Using 0.1 mol % of

the catalyst, yields of 91-96% were obtained in the coupling of aryl iodides with a variety of alkenes. Complex **1.25** was less successful as a catalyst for the Heck reaction using aryl bromides. In the best result, a 30% conversion was observed after 20 hours using 2 mol % of complex **1.25** as the catalyst in the Heck coupling of *p*-bromoanisole and *tert*-butyl acrylate. Polyethylene glycol (PEG) appended Pd(II) SCS-pincer complex **1.26** was successfully recycled three times in the coupling of iodobenzene with different olefins, with yields ranging from 85-95%.

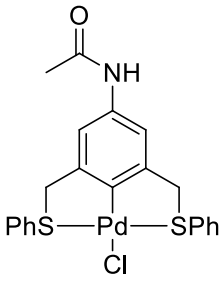

1.25

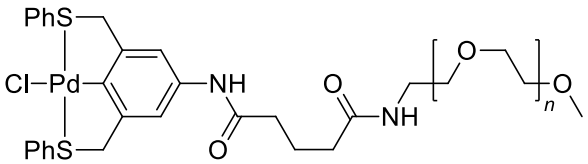

1.26

Figure 1.5. Pd(II) SCS-pincer complexes prepared by Bergbreiter *et al*.[67]

In 2004, the Bowman-James group investigated the catalytic activity of bis[palladium(II)] complex **1.27** (Figure 1.6) in the Heck reaction of 4-iodotoluene and styrene.[18] The solid state structure of **1.27** reveals that the two Pd(II) SCS-pincer scaffolds are configured in an *anti* orientation, with a Pd···Pd separation of 6.74(2) Å. Remarkably, a catalyst TON of 94,300 was obtained after 48 hours using 1 x 10^{-3} mol % catalyst loading. As opposed to traditional PCP-pincer complexes, which are known to have decreased activity in the presence of Pd(0) scavengers such as Hg(0),[68-70] no reduction in yield was observed when **1.27** was employed as the catalyst in the Heck reaction of 4-iodotoluene and styrene in the presence of Hg(0). In order to further evaluate the role of thioamides in

pincer chemistry, the Bowman-James group later investigated the Heck reaction using Pd(II) SCS- and SNS-pincer complexes derived from acyclic ligands.[19] Pd(II) complexes **1.28** and **1.29** and Pt(II) complex **1.30** (Figure 1.6) were synthesized and investigated in the cross coupling reaction of 4-iodotoluene with styrene. Similar to bis[palladium(II)] complex **1.27**, the use of complex **1.28** as the catalyst resulted in 98% conversion to the stilbene products. However, when Pd(II) SNS-pincer complex **1.29** was employed as the catalyst, only 59% conversion to the stilbene products was observed after 16 hours. As anticipated, when Pt(II) complex **1.30** was used, no Heck product was observed.

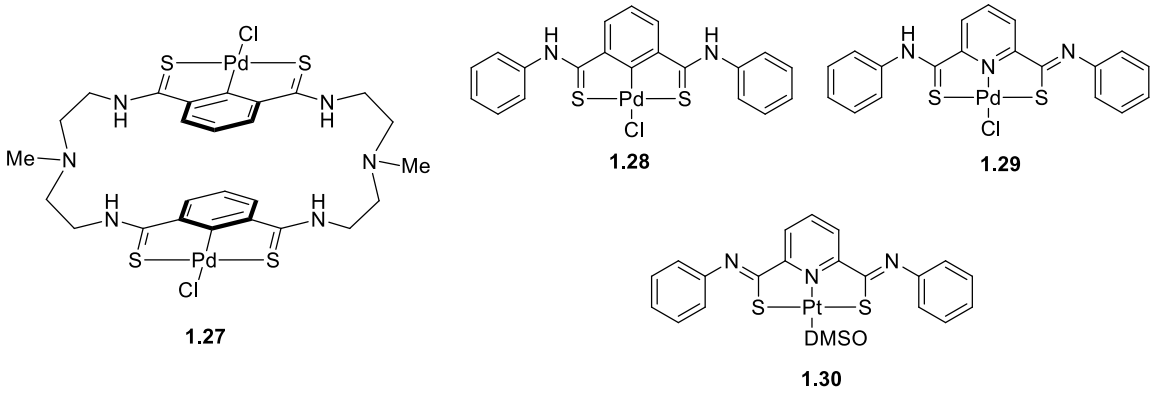

Figure 1.6. Thioamide-derived Pd(II) SCS- and SNS-pincer complexes prepared by the Bowman-James group.[18,19]

Reports in the late 1990s that indicated Pd(II) pincer complexes were thermally stable and did not show visible signs of decomposition at the elevated temperatures required for the Heck reaction[33,71-73] led some authors to propose a mechanism for Pd(II) pincer-mediated Heck reactions that involved a Pd(II)–Pd(IV) catalytic cycle.[74-76] Additional support for a Pd(II)–Pd(IV) cycle came from the isolation of unchanged Pd(II) pincer complexes following catalysis by Dupont and coworkers[77] and the observation that different palladacycles gave different reaction rates by Shibasaki and coworkers.[78] A shift

in sentiment began when several studies in the early 2000s showed that—under the harsh reaction conditions typically employed for the Heck reaction—Pd(II) SCS- and PCP-pincer complexes might not be the active catalysts. In their study of polymer supported Pd(II) SCS-pincer complexes, Bergbreiter and coworkers found evidence that a catalytically active Pd(0) species was leached from the complex during catalysis.[67] Interestingly, the authors determined that only <1% of the original complex decomposed during catalysis, thus providing a possible explanation for the aforementioned cases in which no Pd black was observed. Similar results were obtained by Weck and Jones in their investigation of both soluble and insoluble supported Pd(II) SCS-pincer complexes.[79] A follow-up study by the same group found that Pd(II) PCP-pincer complexes follow a similar fate, though the extent of Pd(II) decomposition was less.[80] Eberhard and coworkers have investigated four electronically different Pd(II) PCP-pincer complexes and concluded that complexes which decompose more readily tend to have improved catalytic activity.[70] The authors point out that the observation of induction periods or S-shaped kinetic curves means that more than one process is taking place during catalysis. Additionally, positive poisoning tests employing Pd(0) scavengers such as Hg(0), CS_2, thiophene, and PPh_3 suggest that Pd(0) plays an active role in the catalytic cycle.[80] Together, these results provide strong evidence that Pd(II) pincer complexes are precatalysts for a catalytically active Pd(0) species that follows the classical Pd(0)-Pd(II) cycle.[81]

While an exact decomposition pathway is not known, Weck and coworkers have proposed the initial steps of a decomposition pathway using Pd(II) PCP- and SCS-pincer complexes in Heck coupling reactions (Scheme 1.8; Pd(II) PCP-pincer complex shown).[82] In the first step, a molecule of triethylamine coordinates the Pd(II) center of complex **1.31**,

forcing one of the phosphine donor atoms to dissociate to give complex **1.32**. This complex undergoes a β-hydride elimination to generate the Pd(II)-hydride complex **1.33**. Based on preliminary computations using a related SCS-pincer analogue of this complex, the authors speculate that the next step of the decomposition pathway could involve an intramolecular hydride transfer—and simultaneous Pd–C bond cleavage—to provide Pd(0).

Scheme 1.8. Initial steps in proposed mechanism for ligand dissociation, redrawn from Weck and coworkers.[82]

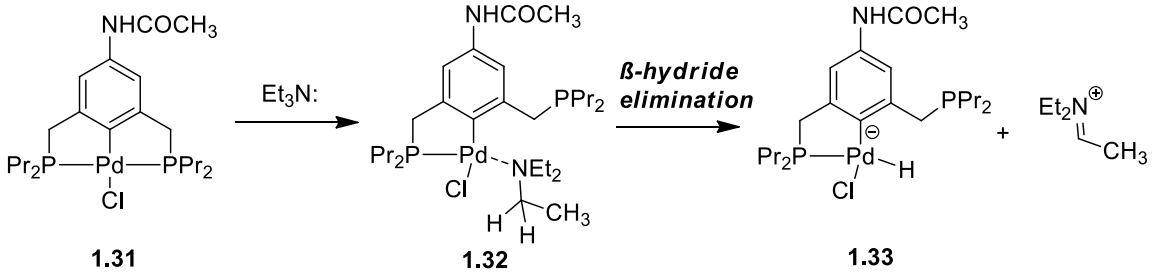

1.2.2 *Suzuki-Miyaura Coupling*

First reported in 1979,[83] the Suzuki reaction features the coupling of an aryl halide with a boronic acid. Its wide-spread use in industry has been spurred by the availability of boronic acids.[84] Further, the use of halide-substitutes—or "pseudohalides"—has made the large-scale production of biaryl compounds using the Suzuki reaction very efficient (e.g. CI-1034, an Endothelin Antagonist, can be made on an 80 kg scale in 95% yield).[85]

Many Pd(II) pincer complexes employed as catalysts in the Heck reaction are also efficient catalysts in the Suzuki reaction. In one of the first examples, Bedford and coworkers studied the coupling of activated bromo- and chlorobenzene derivatives using Pd(II) PCP-pincer complexes **1.34a** and **1.34b** (Scheme 1.9).[36] In this work, the authors

found similar activities for both catalysts although, on average, catalyst **1.34b** performed better at a catalyst loading of 0.0001 mol %. Conversions as high as 92% were achieved using 0.001 mol % of catalyst **1.34a** in the coupling of 4-bromoacetophenone (R = COMe, X = Br) with phenylboronic acid. When **1.34a** was used in the coupling of 4-chloronitrobenzene with phenylboronic acid, the biaryl product was observed in yields of up to 67%. A study by Olsson and Wendt investigated the kinetics of the Suzuki reaction using Pd(II) PCP-pincer complexes.[37] The authors reasoned that the absence of an induction period suggests that the Pd(II) complexes are active catalysts in the Suzuki reaction and remain intact throughout the catalytic cycle. Further, mercury drop poisoning experiments did not significantly hinder the catalytic activities of these complexes. Similar studies employing different pincer scaffolds have corroborated these results.[38]

Scheme 1.9. Suzuki coupling in the presence of Pd(II) PCP-pincer complexes.[36]

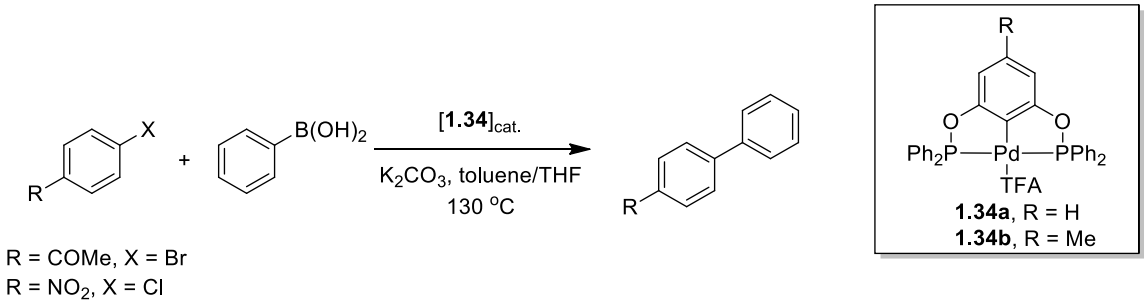

R = COMe, X = Br
R = NO_2, X = Cl

Phosphine-free pincer catalysts have also been successfully employed in the Suzuki reaction.[39-41] For example, Nishiyama and coworkers have studied the reactivity of chiral Pd(II) NCN-pincer complex **1.35** in the coupling of 1-napthylboronic acid and 2-alkyl or methoxy-1-iodonaphthalene at 50 °C (Scheme 1.10).[40] Chirality was transferred to the product, though the selectivity was not high (39-49% ee). However, based on the observation of any enantioselectivity, the authors proposed that the pathway includes a

Pd(II)-Pd(IV) redox cycle in which the Pd(II) pincer complex remains intact during the reaction.

Scheme 1.10. Enantioselective Suzuki coupling using chiral catalyst **1.35**.[40]

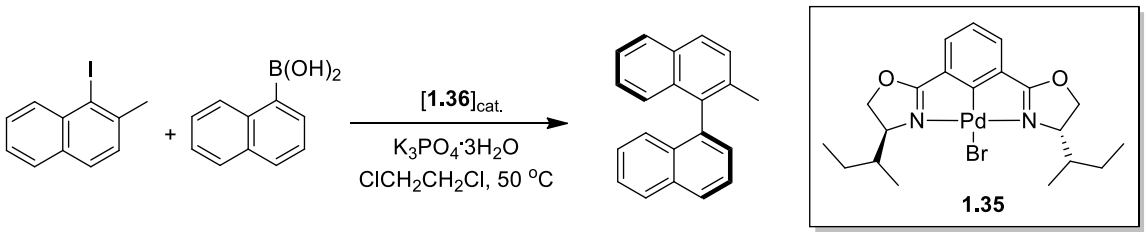

Recently, Nishioka and coworkers reported the use of NHC-based Pd(II) CCN-pincer complex **1.36** for a Suzuki coupling reaction in water (Scheme 1.11).[41] When 4'-bromoacetophenone was coupled phenyl boronic acid, a 94% conversion to the coupling product was observed after 16 hours. When the less reactive 4'-chloroacetopheneone was used as the substrate, a 56% conversion to the coupling product was observed after 41 hours. Interestingly, the catalytic activity of **1.36** was not influenced by the presence of Hg(0). Thus, the authors theorize that the pincer complex is an active catalyst, although they did not investigate the kinetics of the reaction (i.e. induction periods) and a mechanism for such a process was not proposed.

Scheme 1.11. Suzuki coupling in water using sugar appended complex **1.36**.[41]

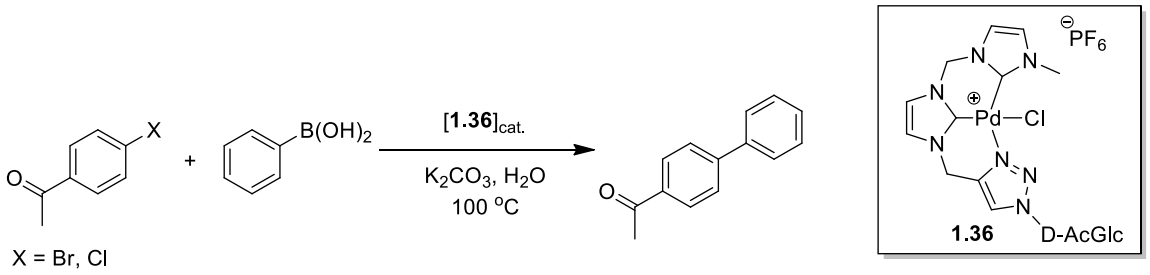

1.2.3 *Negishi Reaction*

In a series of studies,[42-44] Lei and coworkers have investigated the use of Pd(II) SNS-pincer complex **1.37** in the Negishi reaction of various primary and secondary alkyl zinc substrates with aryl halids (Scheme 1.12). Notably, these reactions took place at temperatures as low as 0 ^{o}C. An extremely high TON of 6.1 x 10^6 was observed when the reaction was carried out on a large scale (0.1 moles with respect to the alkyl zinc substrate).

Scheme 1.12. Negishi coupling employing Pd(II) SNS-pincer complex **1.37** as a direct catalyst.[42]

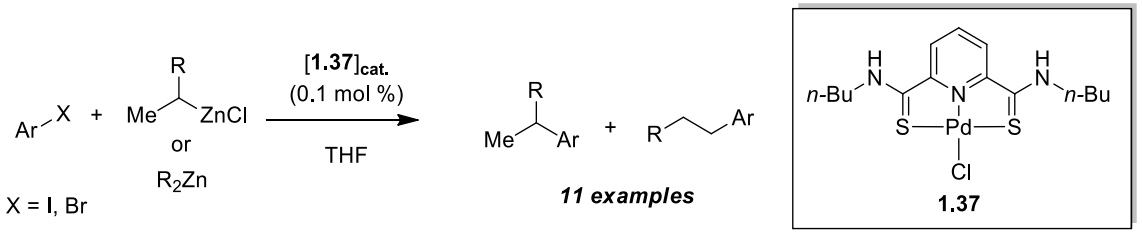

In subsequent studies, Lei and coworkers studied the mechanism of the Negishi coupling of ethyl 2-iodobenzoate with cyclohexylzinc chloride.[43] Interestingly, a small induction period was observed when **1.37** was employed as the catalyst. Treatment of **1.37** with excess cyclohexylzinc chloride (a reducing agent) led to the formation of the tetrameric complex **1.41**, suggesting that the source of this induction period was not due to catalyst decomposition. When **1.37** was treated with a more powerful alkylating agent, such as methylmagnesium bromide, formation of the electron rich intermediate anionic Pd(II) complex **1.40a** was observed by both ^{1}H and ^{13}C NMR spectroscopies. Interestingly, addition of ethyl 2-iodobenzoate to a solution of **1.37**, pretreated with cyclohexylmagnesium bromide led to formation of the coupling product with no induction period, even at temperatures as low as -20 ^{o}C. Thus, the authors proposed a mechanism

for the Pd(II) SCS-pincer mediated Negishi coupling, which is illustrated in Scheme 1.13. In the first step, deprotonation of the thioamide protons in **1.37** leads to bis-iminothiolate complex **1.38**. This complex can undergo alkylation to give complex **1.40**, which subsequently undergoes oxidative addition to the Ar–I bond to afford hexacoordinate Pd(IV) complex **1.41**. Reductive elimination releases the product and regenerates bis-iminothiolate complex **1.38**, which can undergo subsequent alkylation or aggregate to form tetrameric complex **1.39**. The authors believe that the aforementioned induction period may be due to the tendency for **1.37** to form **1.39** in the presence of cyclohexylzinc chloride.

Scheme 1.13. Proposed mechanism for r.t. Pd(II) pincer-mediated Negishi coupling reaction, redrawn from Lei *et al.*[43]

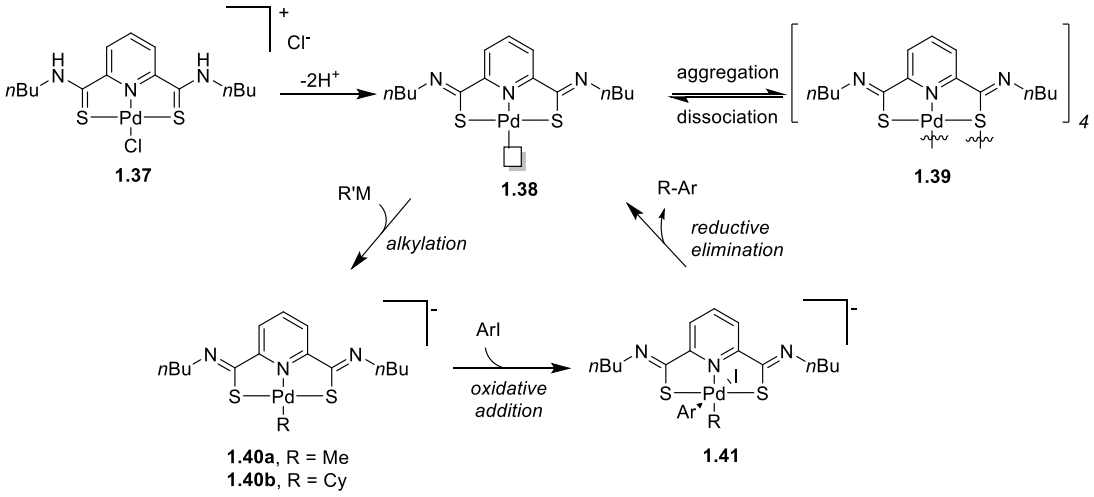

1.2.4 *Enantioselective Aldol and Michael Type Reactions*

The asymmetric aldol and Michael reactions (Scheme 1.14) have been studied using chiral pincer complexes. As previously mentioned, the first asymmetric aldol reaction using a pincer complex was performed using a Pt(II) complex (Scheme 1.4, *vide supra*).[15] Since then, Pd(II) complexes been able to achieve similar results. Richards and Stark were

among the first to investigate aldol and Michael reactions using a chiral Pd(II) pincer complex using chiral Pd(II) SCS-pincer complex **1.42** (Figure 1.7).[45,48] The model aldol coupling of benzaldehyde with methyl isocyanoacetate was carried out to in the presence of **1.42** and Hunig's base to give oxazolines in a 4:1 *trans* to *cis* ratio. Additionally, the Michael reaction between an α-cyanocarboxylate and methyl vinyl ketone was carried out to afford methyl vinyl ketone with enantioselecivities up to 34% ee. Five years later, Nishiyama and coworkers investigated a chiral NCN-pincer complex in the the aldol reaction of α-cyanocarboxylate and benzaldehyde.[46] Using complex **1.43**, a promising selectivity of 57% ee was achieved. In 2008, the Szabo group realized enantioselectivies as high as 86% ee using catalyst **1.44** for a sequential aldol condensation/hydrolysis of imines with methyl isocyanoacetate to afford α,β-diamino acids.[47] More recently, the van Koten group has reported the synthesis and catalytic properties of immobilized pincer complexes, such as **1.45**, in the Michael reaction of double ethyl cyanoacetate and methyl vinyl ketone.[49] In this case, the catalytic activity of the immobilized catalyst was not diminished compared to the homogenous (monomeric) forms of the catalyst. Earlier this year, Zhang and coworkers described the use of PNP-pincer complex **1.46** in the Michael addition of diphenylphosphine to β,γ-unsaturated α-keto esters with up to 93% ee.[50]

Scheme 1.14. (**A**) Generic aldol reaction between methyl isocyanoacetate and an aldehyde and (**B**) generic Michael reaction between methyl cyanopropanoate and methyl vinyl ketone.

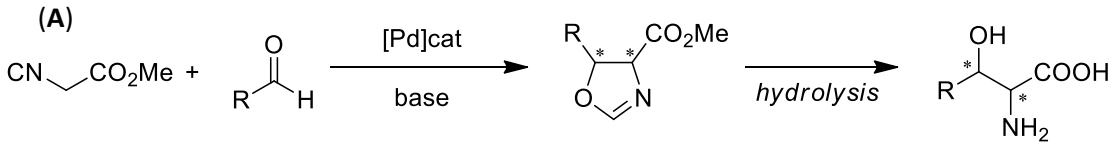

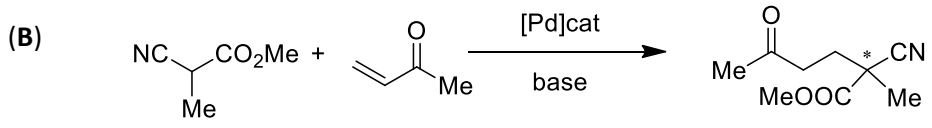

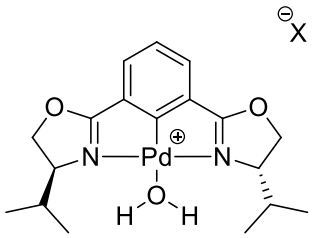

1.42, X = SBF_6
1.43, X = BF_4

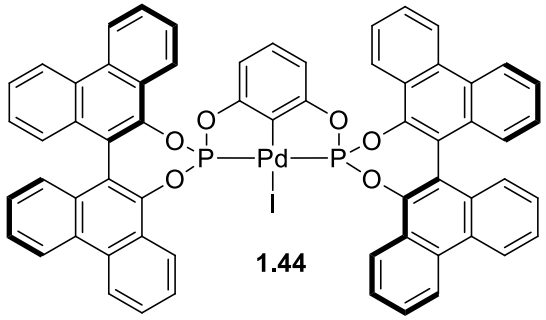

1.44

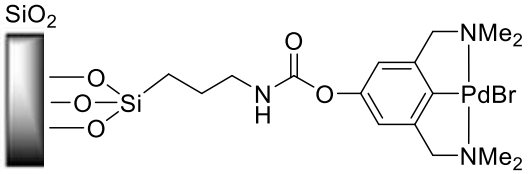

1.45

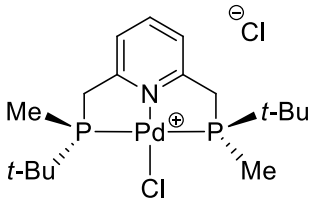

1.46

Figure 1.7. Pd(II) pincer complexes investigated in aldol or Michael type reactions.[45-50]

1.3 *Amide-Based NNN-Pincer Complexes*

Recent efforts in the Bowman-James group have exploited amide-based NNN-pincer ligands for anion recognition[5-10,12-15,17] and for metal coordination.[18-24] These ligands are an attractive scaffold in pincer chemistry due to their ease of synthesis and derivatization. Although the first amide-based NNN-pincer ligand was synthesized in the 1970s,[86] their transition metal complexes were not extensively explored until the 1990s. Metalation of the pincer ligand is usually preceded by deprotonation of bis-amide ligand **1.47** to afford the dianionic NNN-pincer ligand **1.48** (Scheme 1.15). Due to their similarity to peptides, amide-based NNN-pincer ligands were initially investigated using a variety of first row transition metals, notably with Fe, Co, Ni, and Cu in different oxidation states.[20,24,87-99] More recently, these ligands have been used to access stable Pd(II) complexes.[21-23,102-106]

Scheme 1.15. Formation of dianionic NNN-pincer ligand **1.48**.

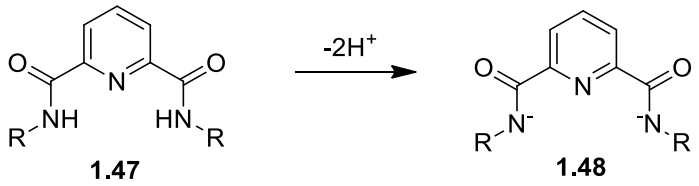

1.47 **1.48**

1.3.1 *NNN^{2-} Pincer Complexes with First Row Transition Metals*

Hirao was among the early pioneers of amide-based NNN-pincer chemistry.[87,88] In an early study, Hirao and coworkers investigated catalytic oxygenation systems employing a wide variety of NNN-pincer ligands—including ligands **1.49** through **1.53** illustrated in Figure 1.8—in combination with different metal salts. Notably, imidazolyl-substituted ligand **1.52** in combination with $FeCl_2$ or $Co(OAc)_2$ led to the epoxidation of 2-norbornene

to form *exo*-2,3-epoxynorbornane in 22% and 24% GLC yields, respectively. Although the Fe(II) complex with ligand **1.52** was not isolated, evidence that the complex is formed *in situ* was provided by the observation that, in the absence of ligand **1.52**, only a 4% yield of *exo*-2,3-epoxynorborane was observed. Whereas the use of ligands **1.51** or **1.53** resulted in lower yields, the authors proposed that the imidazolyl moiety in **1.52** plays an important role in the catalysis. When the oxygenation reaction was carried out with a combination of ligand **1.52** and Fe(III), Rh(III), Ru(III), Ni(II), Mn(II), or Cu(II), little or no product was observed.

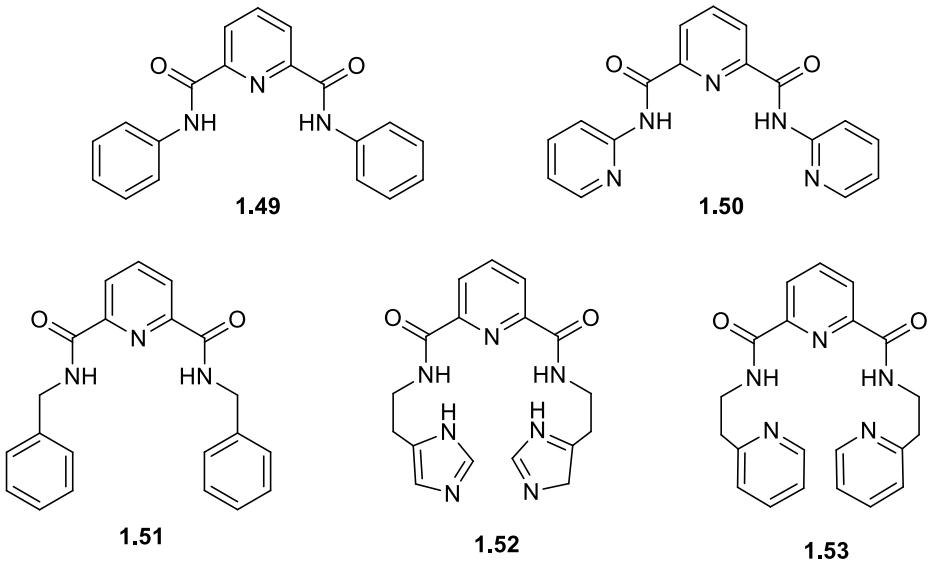

Figure 1.8. Sample of NNN-pincer ligands investigated by Hirao and coworkers.[87,88]

The isolation of high-valent metal complexes has been achieved in a number of cases by employing pincer ligands. Specifically, ligands containing bis-amide functionalities have received interest in this area of study because deprotonation of the amide hydrogens results in two anionic nitrogen donor atoms, which can be used to facilitate the stabilization of metals in higher oxidation states. Mukherjee and coworkers have investigated the coordination chemistry of ligand **1.49** with Co(III) and Fe(III)

(Scheme 1.16).[89-91] Treatment of the sodium salt of deprotonated **1.49** with either $Fe(MeCN)_4(ClO_4)_2$ and $TBACl{\cdot}H_20$ or $Co(OAc)_2{\cdot}4H_20$ and $TBA[MeCO_2]{\cdot}4H_20$ yields complexes **1.54** and **1.55**, respectively, after oxidation by O_2. In a later report by the same group, Ni(II), Ni(III), and Ni(IV) complexes were synthesized from the same bis-amide ligand. Treatment of ligand **1.49** with $NiCl_2{\cdot}6H_20$, followed by addition of $TBACl{\cdot}H_20$, affords air-stable complex **1.56**. A one-electron chemical oxidation was achieved when **1.56** was treated with 1.2 equivalents of $[Fe(\eta^5\text{-}C_5H_5)_2][PF_6]$ to afford a Ni(III) complex. Alternatively, the treatment of Ni(II) complex **1.56** with three equivalents of ceric ammonium nitrate leads to a two-electron chemical oxidation to afford a Ni(IV) complex. In a separate study, the Mukherjee group explored the Ru(II) and Ru(III) chemistry with ligand **1.49**.[92]

Scheme 1.16. Synthesis of iron, nickel, and cobalt NNN-pincer complexes.[89-92]

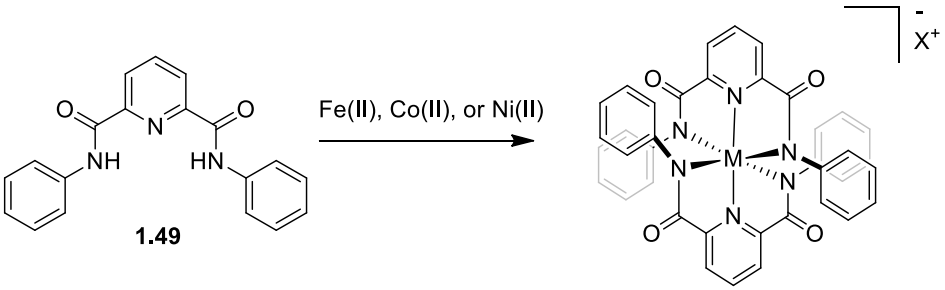

Borovik and coworkers have explored the coordination chemistry of Cu(II) with a variety of amide-based NNN-pincer ligands.[93-96] In one study, deprotonation of ligand **1.57** followed by addition of $Cu(OAc)_2$ yields Cu(II) complex **1.58** (Scheme 1.17). In the solid state, **1.58** exists as a metallohelix, with the amide appendages oriented *anti* to each other on opposite sides of the Cu(II) coordination plane. The addition of pyridine to **1.58** results

in a significant structural rearrangement, driven by the breaking both Cu–O(amide) bonds in **1.58**. Interestingly, the chirality of the resulting metallohelix extends to the crystal lattice of the complex, as extended helices stabilized by several edge-to-face π–π stacking interactions were observed.

Scheme 1.17. Synthesis of a helical Cu(II) NNN-pincer complex.[94]

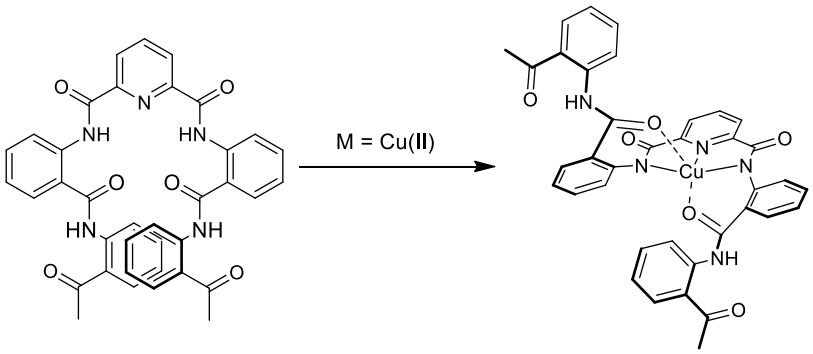

1.57 **1.58**

In 2000, Mukherjee and coworkers investigated the coordination complexes of NNN-pincer ligand **1.49** with Cu(II).[91] Treatment of **1.49** with three equivalents of sodium hydride, followed by the addition of $Cu(OAc)_2 \cdot H_20$, affords dimer **1.59** (Scheme 1.18). Rather than forming a bis-chelate structure similar to the aforementioned Co, Fe and Ni complexes (Scheme 1.16, *vide supra*), the structure of **1.59** with Cu(II) is a hydroxo-bridged dimer. Copper hydroxide complexes are proposed intermediates in a number of reactions, including the hydrolysis of nitriles and fixation of CO_2. At the time, this structure represented one of the only examples of a hyrdroxo-bridged Cu(II) dimer, the first with NNN-pincer coordination. The presence of a hydroxo bridge results in antiferromagnetic exchange between the two Cu(II) centers.

Scheme 1.18. Synthesis of hydroxo-bridged dimeric Cu(II) complex **1.59**.[91]

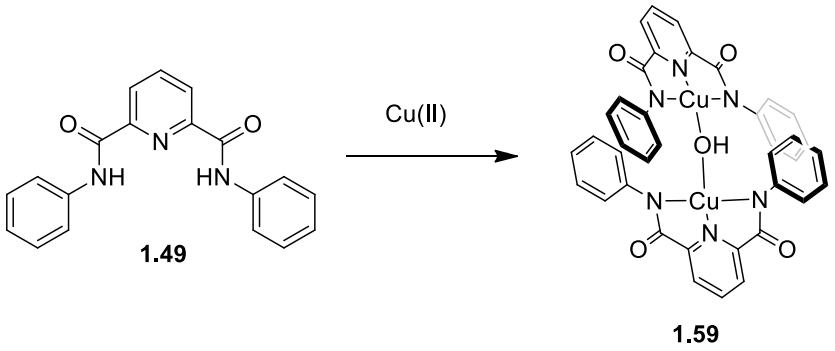

Holm *et al.*[97] and Tolman *et al.*[98,99] have independently investigated the synthesis of Ni(II) and Cu(II) hydroxo complexes with NNN-pincer ligand **1.60**. In Holm's work, treatment of **1.60** with Et_4NOH and $Ni(OTf)_2$ yields Ni(II)-hydroxo complex **1.61** (Scheme 1.19). The authors suggest that a monomer is formed rather than a dimer (see complex **1.59**, Scheme 1.18, *vide supra*) due to the increased sterics enforced on the Ni(II) binding site by the *ortho*-substitued phenyl amide appendages. The hydroxide ligand can be exchanged with other anionic ligands, including Cl^-, OMe^-, SH^-, CN^-, OAc^-, and CN^-, in the presence of their tetraethylammonium salts. Treatment of Ni(II)-cyano complex **1.62** with [Fe(Me_6tren)-(OTf)](OTf) yields heterobimetallic Ni(II)/Fe(III) complex **1.63**. Conversely, **1.61** reacts with CO_2 to form the η^1-bicarbonate ligated complex **1.64**. In order to construct a synthetic mimic of carbon monoxide dehydrogenase (which features a bridged Ni/Fe active site) the group also synthesized a binucleating macrocyclic ligand containing NNN-pincer and tren nucleating sites. Tolman and coworkers have studied the Cu(II) NNN-pincer chemistry with the same macrocyclic binucleating ligand in their synthesis of bimetallic Cu(II)/Cu(II), Cu(II)/Pd(II), and Cu(II)/Pt(II) complexes. See Section 3.2 (*vide infra*) of this dissertation for further details of these studies by Holm and Tolman.

Scheme 1.19. Stepwise synthesis of bridged Ni(II)/Fe(III) complex **1.63**.[97] Complexes **1.61**, **1.62**, and **1.64** were isolated as Et_4N^+ salts. Complex **1.63** was obtained as the triflate salt.

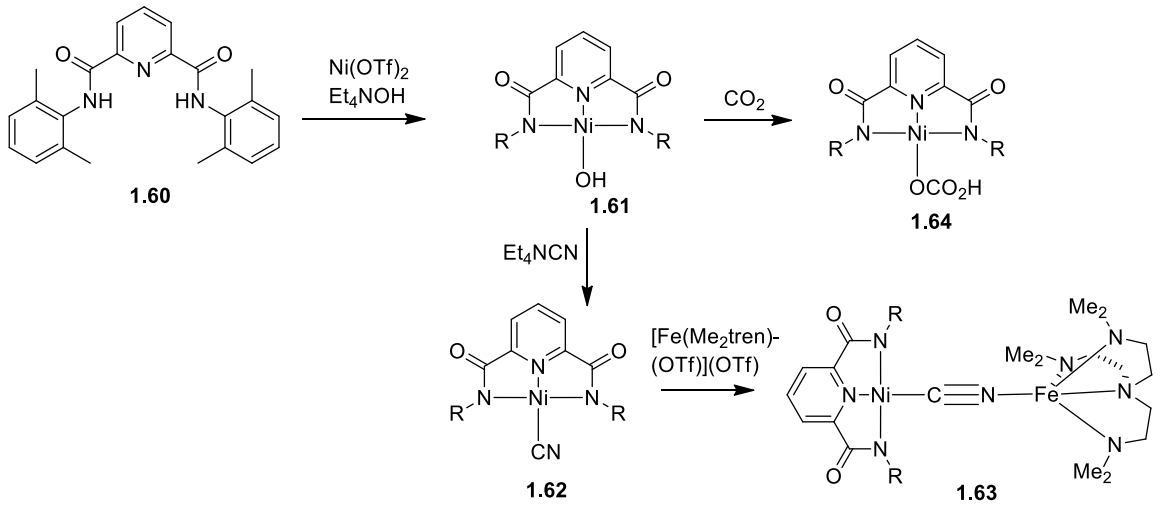

Copper superoxo complexes have also received increased attention in the last two decades, as they serve an important role as intermediates in aerobic oxidations. Tolman and coworkers have reported an anionic Cu(II) superoxide complex with the sterically hindered pyridinecarboxamide ligand **1.65**.[99] Treatment of Cu(II)-MeCN complex **1.65** with KO_2 and 18-crown-6 yields superoxide complex **1.66** (Scheme 1.20), which is stable at -80 ^oC. The reaction of superoxide complex **1.66** with [(TPMA)Cu(CH_3CN)]OTf [TPMA = tris(2-pyridylmethyl)amine] affords bis[copper(II)] complex **1.67**, which was characterized *in situ* by UV-Vis spectrosocpy. This structure is exciting given the role that M-O_2-M dimeric complexes play in a variety of biological catalytic cycles.[100,101] Preliminary investigations of superoxide complex **1.66** with phenol suggest that the anionic superoxide ligand assists in the conversion of 4-nitrophenol to 4-nitrophenoxide by acting as a base in the first deprotonation step.[99]

Scheme 1.20. [a]Conditions: [(tpma)Cu(CH$_3$CN)]OTf, -80 °C. Redrawn from Tolman *et al.*[99]

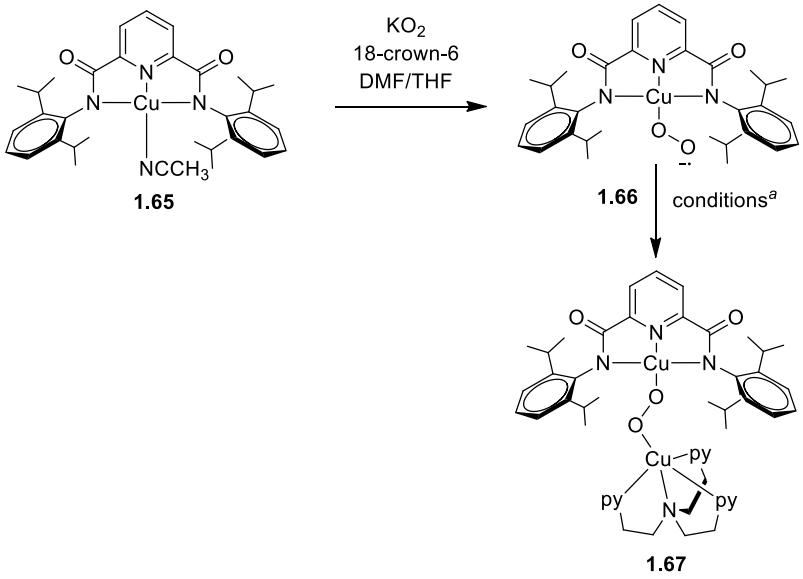

In 2007, Bowman-James and coworkers reported the crystal structures of the ditopic tetraamide macrocycle **1.68** with Cu(II), Ni(II), Co(III), Fe(III), $Cr_2O_7^{2-}$, and ReO_4^- (Scheme 1.21).[20] The formation of the $Cr_2O_7^{2-}$, and ReO_4^- structures **1.69** and **1.70** coincides with protonation of the macrocycle tertiary amines in order to maintain a net neutral charge. Alternatively, formation of homobimetallic Cu(II) and Ni(II) complexes **1.71** and **1.72** is driven by the deprotonation of all four amide protons. Each of the two Cu(II) atoms coordinates one of the pincer binding sites and an amide nitrogen of the opposing pincer binding site, resulting in an overall square-pyramidal coordination. This coordination mode, along with π–π stacking between the two pyridyl moieties of the ligand, results in each complex folding in a "face-to-face" conformation in the solid state, similar to that of the Ni(II), $Cr_2O_7^{2-}$ and ReO_4^- structures. The monometallic Co(III) and Fe(III) solid state structures of **1.73** and **1.74** are isomorphous. Each metal ion in these complexes has a hexadentate coordination with the ligand.

Scheme 1.21. Synthesis of mono- and bimetallic complexes from macrocyclic ligand **1.68**.[20]

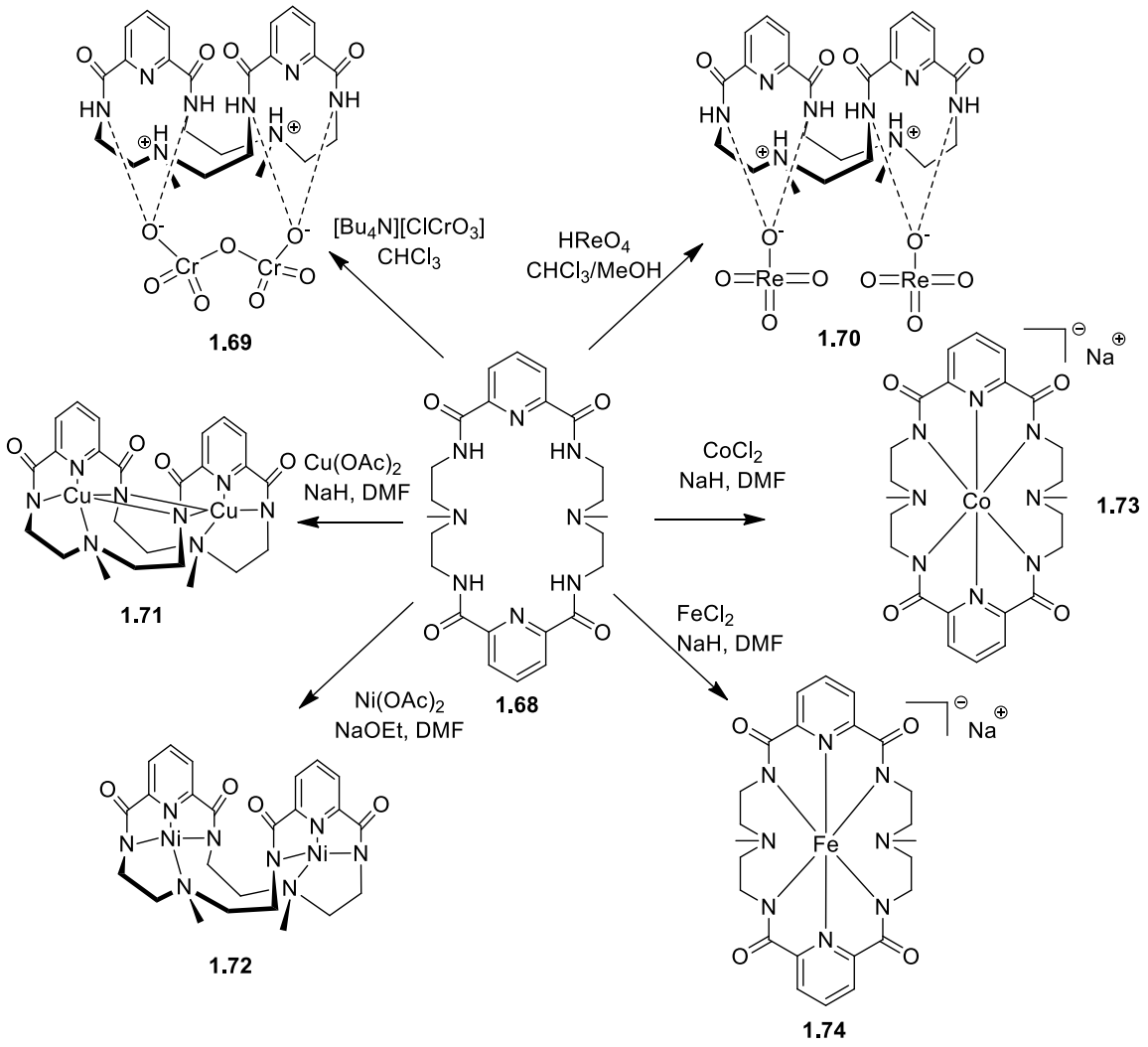

Recently, the Bowman-James group studied Ni(II) and Cu(II) dimeric complexes of ligands **1.75** and **1.76** (Scheme 1.22).[24] Treatment of pyridyl ligand **1.75** with $Ni(OAc)_2 \cdot 2H_2O$ affords Ni(II) dimer **1.77**. The solid state structure of **1.77** reveals that the Ni(II) metal center is coordinated to the pyridine nitrogen of the pincer complex by a covalent bond to give it an octahedral geometry. Likewise, treatment of ligand **1.75** with

$Cu(OAc)_2 \cdot H_2O$ affords **1.78** as a dimer. Interestingly, treatment of phenyl ligand **1.76** with $Cu(OAc)_2 \cdot 4H_2O$ yields dimeric complex **1.79**, which features a very short Cu–C(phenyl) distance, indicative of a possible agostic interaction. Further analysis of this complex by density functional theory (DFT) studies revealed that, rather than a Cu–C(phenyl) agostic interaction, the complex is folded due to π–π stacking interactions between the phenyl groups and the connectivity of the two Cu(II) metal atoms.

Scheme 1.22. Synthesis of bimetallic complexes from NNN-pincer ligands **1.75** and **1.76**. Redrawn from Begum *et al.*[24]

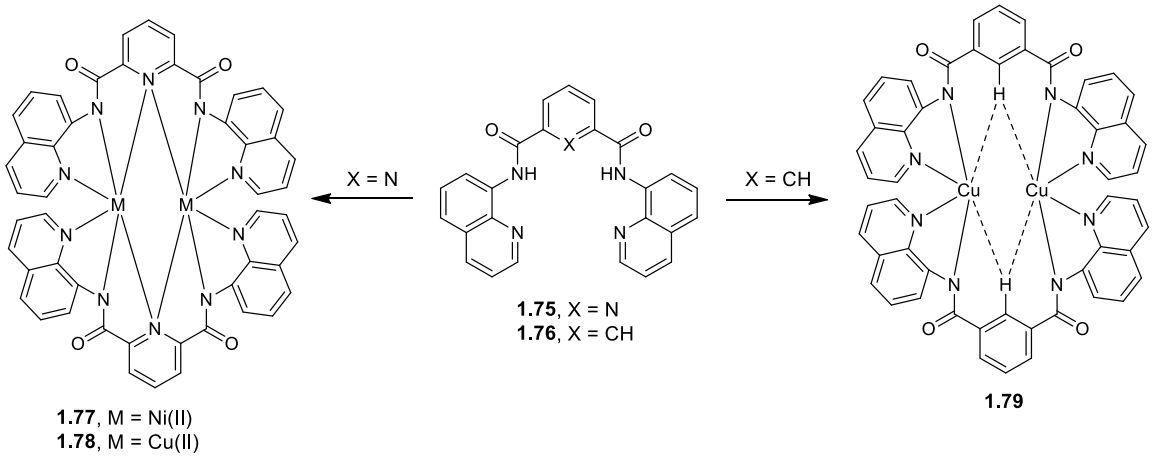

1.3.2 *NNN^{2-} Palladium Complexes*

In contrast to the other metals already discussed, the complexation of the NNN-pincer ligand with Pd(II) is usually accompanied by the coordination of a neutral ancillary ligand. Hirao and coworkers have employed a Pd(II) NNN-pincer complex to synthesize a Pd(II)/Fe(II) heterobimetallic system (Scheme 1.23).[102] Treatment of the NNN-pincer ligand with $Pd(OAc)_2$ in acetonitrile affords Pd(II) complex **1.81**. As is common in the synthesis of Pd(II) NNN-pincer complexes in coordinating solvents such as acetonitrile, a

molecule of solvent resides in the fourth coordination site. The utility of complex **1.81** as a metalloreceptor was demonstrated by the reaction of **1.81** with [3]ferrocenophene **1.80**, which contains an appended pyridyl ligand. The pyridyl nitrogen replaces the labile acetonitrile molecule in complex **1.81** to afford heterobimetallic complex **1.82**. Free rotation about the Pd–N(py) bond in **1.82** is hindered by the steric replusion between ferrocenophene and the amide appendages of the pincer complex.

Scheme 1.23. Synthesis of heterobimetallic Pd(II)/Fe(II) complex **1.82**.[102]

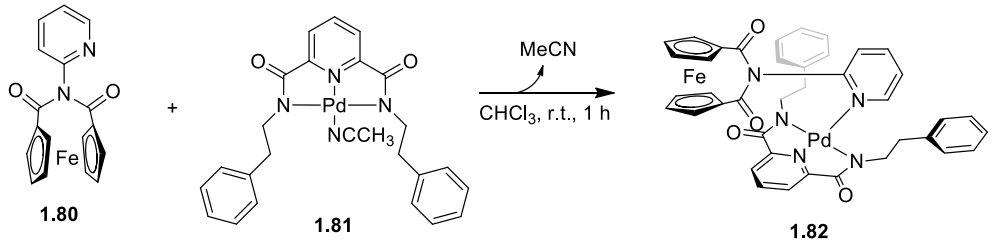

The lability of the acetonitrile molecule in **1.81** was further exploited by the Hirao group in 2001 in their synthesis of homobimetallic dimers **1.84a** and **1.84b** (Scheme 1.24).[103] Treatment of complex **1.81** with π-conjugated diimine ligand **1.83** results in the redox-active dimeric complex **1.84a**. The 2:1 pincer to diamine ligand ratio was confirmed by X-ray crystallography. Although the *anti* isomer formed in the solid state, the *syn* isomer **1.84b** was determined by a van't Hoff plot of $\ln K_{eq}$ vs. T^{-1} to be favored enthropically by 1 kcal/mol (K_{eq} was determined by ^{1}H NMR spectroscopy). The same group has used similar chemistry to construct chiral polymers based on the chelation of a Pd(II) NNN-pincer complex with an emeraldine base of poly(o-toluidine).[104] Complexes of this type could have several unique applications in materials and asymmetric catalysis.

Scheme 1.24. Synthesis of *anti* and *syn* dimeric complexes from Pd(II) complex **1.81**.[103]

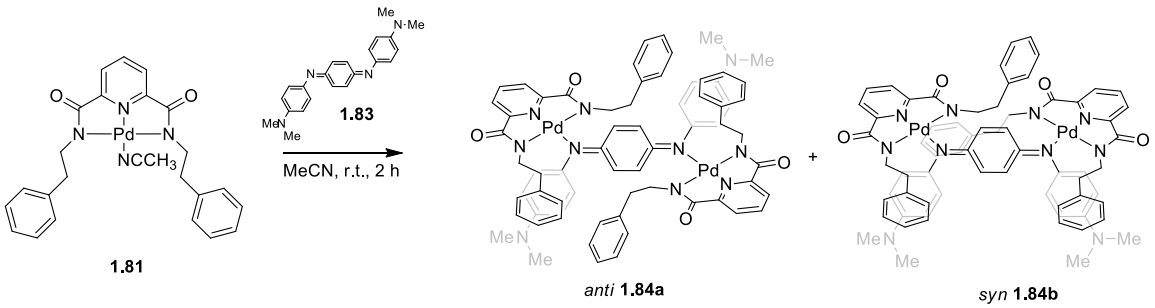

In 2006, Dell'Amico and coworkers reported the synthesis of complexes **1.85** and **1.86** (Scheme 1.25) from the treatment of NNN-pincer ligand **1.49** (Figure 1.8, *vide supra*) with $Pd(OAc)_2$ in acetonitrile.[105] When **1.85** is dissolved in chloroform, the ancillary acetonitrile ligand dissociates and is replaced by the amide oxygen of an adjacent pincer complex, resulting in the formation of tetrameric complex **1.87**. Complex **1.87** is soluble in $CDCl_3$, and was characterized by IR, ^1H and ^{13}C NMR spectroscopies, mass spectrometry, and XRD. A similar structure was obtained in our group by Dr. Wang, who crystallized hexamer **1.88** from complex **1.86** in $CHCl_3$ (Scheme 1.25).[22] Interestingly, in contrast to **1.87**, complex **1.88** is insoluble in noncoordinating solvents (i.e. $CHCl_3$, CH_2Cl_2, benzene, toluene), making further spectroscopic analysis difficult.

Scheme 1.25. Formation of tetrameric and hexamer structures from the dissociation of acetonitrile in complexes **1.85** and **1.86** in the presence of chloroform.[22,105]

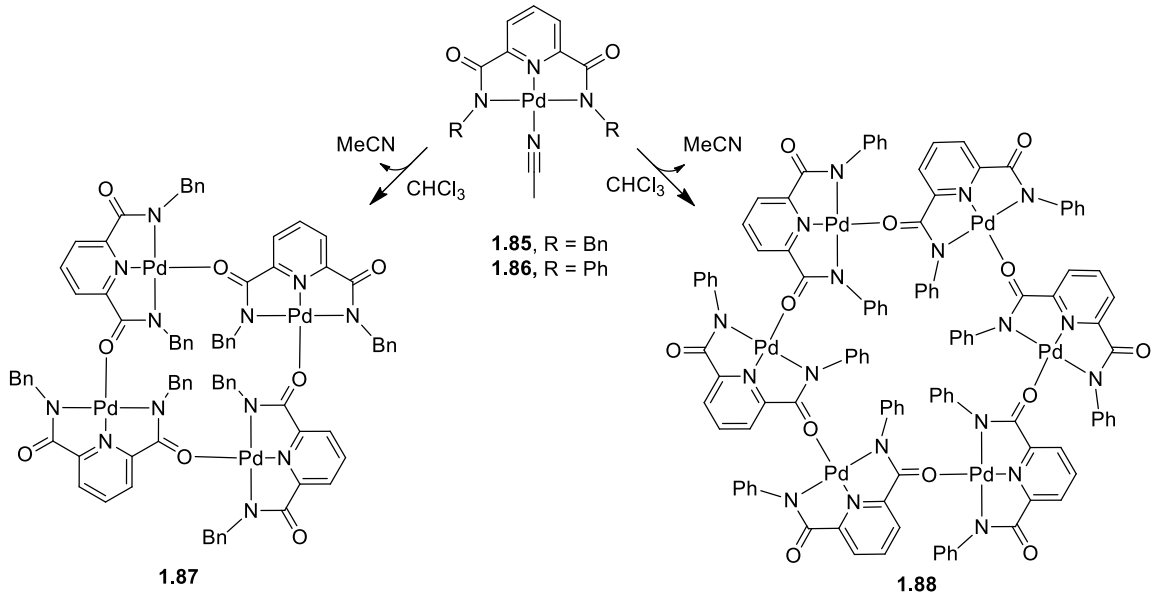

The small molecule recognition properties of complexes **1.85** and **1.86** have been studied by both the Dell'Amico[105] and Bowman-James groups.[21,23] Dell'Amico and coworkers found that the reaction of **1.85** with SEt_2 or $SeEt_2$ results in the formation of Pd-pincer-YEt_2 (Y = S or Se) complexes. An equilibrium constant K = 15 was observed for the complexation of **1.85** with SEt_2. Likewise, the reaction of **1.85** with $SeEt_2$ results in quantitative conversion to a Se-coordinated complex. The SEt_2-bound complex can also be formed from tetramer **1.86**, suggesting that the binding preference for ancillary ligands follows the order $SeEt_2$ > SEt_2 > O(amide) > MeCN for derivatives of complex **1.85**.

Recently, the Bowman-James group investigated the targeting of a sulfur mustard surrogate, 2-chloroethyl sulfide (CEES).[23] Treatment of Pd(II) NNN-pincer complex **1.86** with CEES in $CDCl_3$ results in the exchange of acetonitrile with CEES (Scheme 1.26). This exchange was observed spectroscopically via ^{1}H NMR in $CDCl_3$, with an equilibrium

constant K = 15. The equilibrium constant was not dramatically influenced by the introduction of electron-donating groups (i.e. -Me, -OMe) to the *para* position of the phenyl amide appendage. The use of a naphthalene derivative of **1.86** led to a modest increase in the equilibrium constant (K = 76). The most significant increase in K was obtained when the anthracene derivative of **1.86** was employed. The solid state structures of CEES-Pd(II)-NNN-pincer complexes **1.89a**, **1.90**, and **1.91** show an alignment between the mustard surrogate and the walls of the amide-appended aromatic groups. This alignment is particularly noticeable in Pd(II)-CEES complex **1.91**, in which the walls run roughly the length of the CEES ligand, suggesting that van der Waals forces contribute to the increased K observed for the formation of this complex.

Scheme 1.26. Binding properties of Pd(II) pincer complexes with 2-chloroethyl sulfide (a mustard gas surrogate).[23]

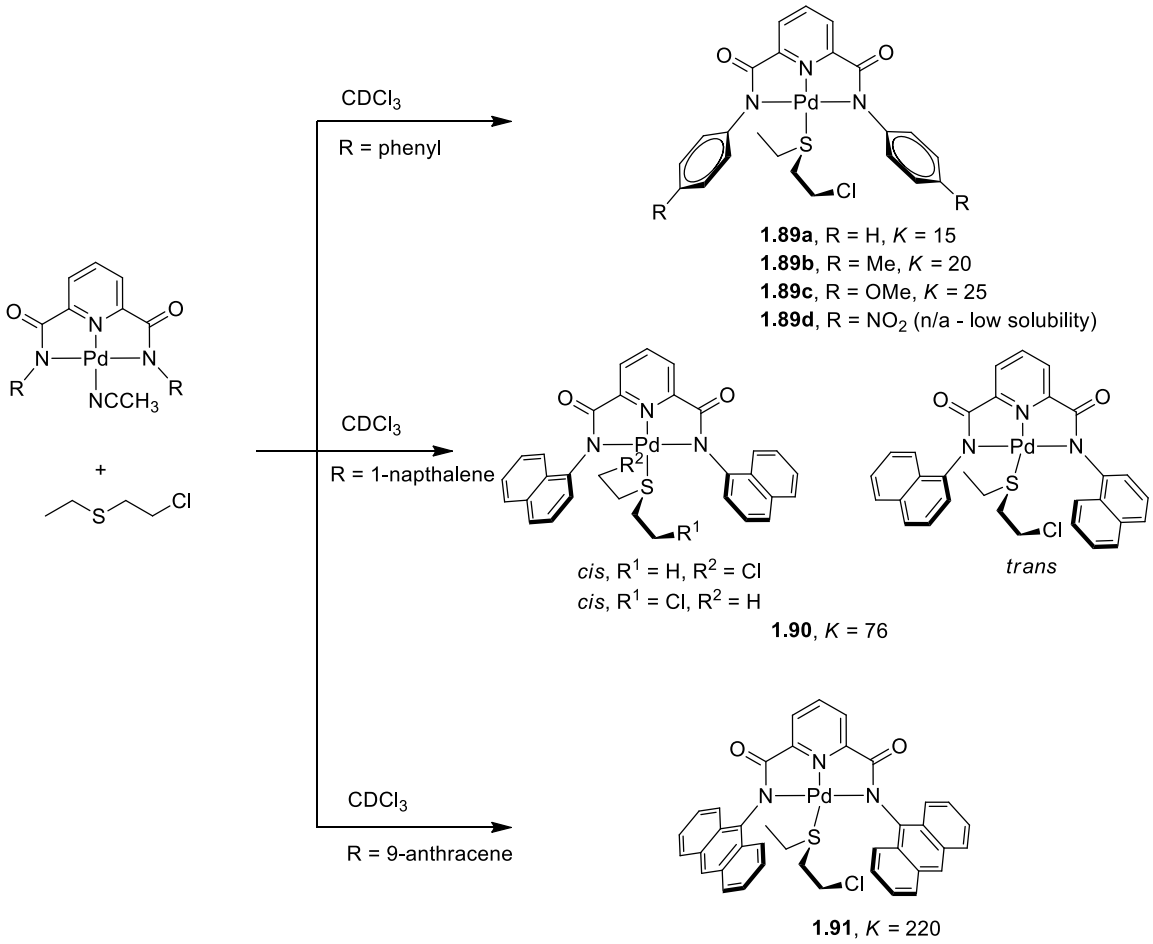

In an elegant extension of this Pd(II)-CEES chemistry, Mishra and coworkers studied the immobilization of Pd(II)-CEES complex **1.89a** with superparamagnetic carbon nanotubes (Scheme 1.27).[106] Treatment of CEES-bound complex **1.89a** with 3-aminopropyl trimethoxysilane functionalized single wall nanotubes (SWNTs) affords the immobilized complex **1.92**. Immobilization was confirmed using both FT-IR and EPR analysis, and the morphology of these supramolecular structures was analyzed using both tunneling-electron microscopy (TEM) and atomic absorption spectroscopy (AAS). A TON

of 1946 was obtained when complex **1.92** was employed as a catalyst in the oxidation of cyclohexane. The recycling of **1.92** was carried out with an 8.1% decrease in conversion after five runs, suggesting that the catalyst slowly decomposes in the presence of the reaction conditions that were investigated (150 ^{o}C, 10 bar pressure of O_2, 6 h).

Scheme 1.27. Synthesis of immobilized Pd(II) NNN-pincer complex **1.92**.[106]

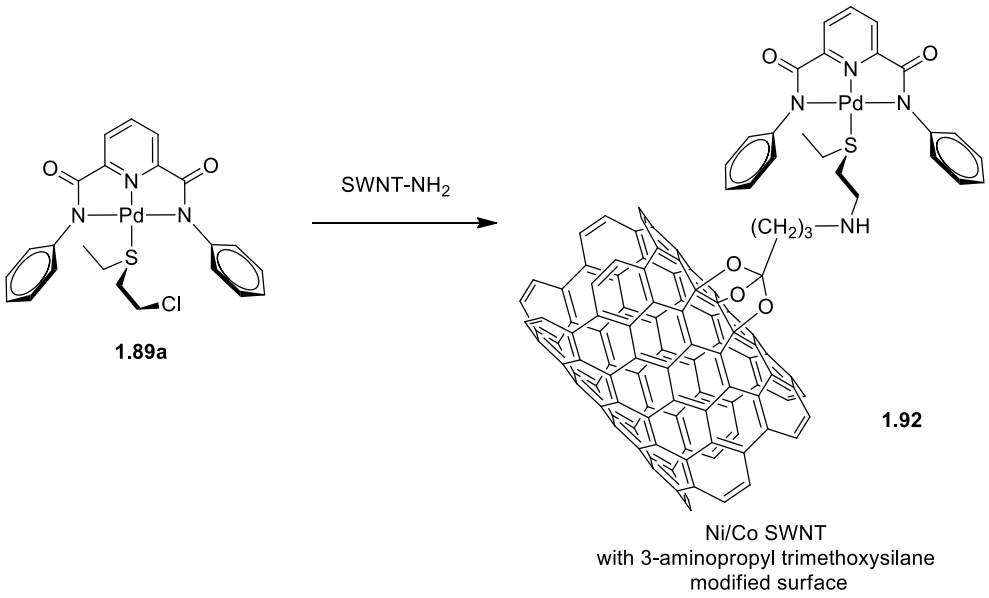

1.4 *Concluding Remarks*

It is surprising that, although pincer complexes were first synthesized in the 1970s as analogues to diphosphine Pd(II) complexes—which were at the time being researched as stable cross coupling catalysts—that the first reports of the use of pincer complexes in catalysis did not come for another two decades. Nonetheless, the last 20 years (1995 to the present) have seen a remarkable amount of interest into the development of pincer complexes. Most of the research in cross coupling reactions has been performed employing Pd(II) PCP-pincer complexes. Less common relative to their PCP-pincer counterparts, amide-based NNN-pincer ligands and their metal complexes are an attractive tool for research due to the ease of synthesis of amide pincer ligands and the versatility of these ligands toward metal chelation. Currently, there are no examples of the use of Pd(II) NNN-pincer complexes in the Heck reaction. Thus, the bulk of the work contained in this doctoral thesis aims to build upon the current body of knowledge in the field of amide-based NNN-pincer complexes by examining the use of novel Pd(II) NNN-pincer complexes as catalysts for the Mizoroki-Heck reaction.

1.5 *References*

1. Seechum, C. C. C. J.; Kitching, M. O.; Colacot, T. J.; Snieckus, V. "Palladium-Catalyzed Cross-Coupling: A Historical Contextual Perspective to the 2010 Nobel Prize" *Angew. Chem. Int. Ed.* **2012**, *51*, 5062–5085.
2. Herrmann, W. A.; Brossmer, C.; Reisinger, C-. P.; Riermeier, T. H.; Őfele, K.; Beller, M. "Palladacycles: Efficient New Catalysts for the Heck Vinylation of Aryl Halides" *Chem. Eur. J.* **1997**, *8*, 1357–1364.
3. (a) Peris, E.; Crabtree, R. H. "Recent Homogeneous Catalytic Applications of Chelate and Pincer *N*-Heterocyclic Carbenes" *Coord. Chem. Rev.* **2004**, *248*, 2239–2246; (b) Morales-Morales, D. "Pincer Complexes Applications in Catalysis" *Rev. Soc. Quim. Méx.* **2004**, *48*, 338–346; (c) *The Chemistry of Pincer Compounds*, ed. D. Morales-Morales and C. G. M. Jensen, Elsevier, Amsterdam, **2007**; (d) Serrano-Becerra, J. M.; Morales-Morales, D. "Organic Transformations Mediated by Platinum Group PCP and PNP Aromatic-Based Pincer Complexes" *Curr. Org. Syn.* **2009**, *6*, 169–192; (e) Selander, N.; Szabó, K. J. "Catalysis by Palladium Pincer Complexes" *Chem. Rev.* **2011**, *111*, 2048–2076; (f) Gelman, D.; Musa, S. "Coordination Versatility of sp3‑Hybridized Pincer Ligands toward Ligand−Metal Cooperative Catalysis" *ACS Catal.* **2012**, *2*, 2456–2466; (g) *Organometallic Pincer Chemistry*, ed. G. van Koten and D. Milstein, Springer-Verlag, Berlin, **2013**.
4. Dupont, J.; Consorti, C. S.; Spencer, J. "The Potential of Palladacycles: More Than Just Precatalysts" *Chem. Rev.* **2005**, *105*, 2527–2571.
5. Hossain, M. A.; Llinares, J. M.; Powell, D.; Bowman-James, K. "Multiple Hydrogen Bond Stabilization of a Sandwich Complex of Sulfate between Two Macrocyclic Tetraamides" *Inorg. Chem.* **2001**, *40*, 2936−2937.
6. Hossain, M. A.; Kang, S. O.; Powell, D.; Bowman-James, K. "Anion Receptors: A New Class of Amide/Quaternized Amine Macrocycles and the Chelate Effect" *Inorg. Chem.* **2003**, *42*, 1397−1399.
7. Kang, S. O.; Llinares, J. M.; VanderVelde, D.; Powell, D.; Bowman-James, K. "New Polyamide Cryptand for Anion Binding" *J. Am. Chem. Soc.* **2003**, *125*, 10152−10153.

8. Kang, S. O.; Powell, D.; Bowman-James, K. “Anion Binding Motifs: Topicity and Charge in Amidocryptands” *J. Am. Chem. Soc.* **2005**, *127*, 13478−13479.
9. Kang, S. O.; Powell, D.; Day, V. W.; Bowman-James, K. “Trapped Bifluoride” *Angew. Chem., Int. Ed.* **2006**, *45*, 1921−1925.
10. Kang, S. O.; Day, V. W.; Bowman-James, K. “The Influence of Amine Functionalities on Anion Binding in Polyamide-Containing Macrocycles” *Org. Lett.* **2009**, *11*, 3654−3657.
11. Kang, S.O.; Llinares, J. M.; Day, V. W.; Bowman-James, K. “Cryptand-Like Anion Receptors” *Chem. Soc. Rev.* **2010**, *39*, 3980–4003.
12. Kang, S. O.; Day, V. W.; Bowman-James, K. “Tricyclic Host for Linear Anions” *Inorg. Chem*. **2010**, *49*, 8629−8636.
13. Wang, Q.-Q.; Day, V. W.; Bowman-James, K. “Tunable, Shape-Shifting Capsule for Dicarboxylates” *Chem. Sci*. **2011**, *2*, 1735−1738.
14. Hossain, M. A.; Kang, S. O.; Kut, J. A.; Day, V. W.; Bowman-James, K. “Influence of Charge on Anion Receptivity in Amide-Based Macrocycles” *Inorg. Chem*. **2012**, *51*, 4833−4840.
15. Wang, Q.-Q.; Day, V. W.; Bowman-James, K. “Supramolecular Encapsulation of Tetrahedrally Hydrated Guests in a Tetrahedron Host” *Angew. Chem., Int. Ed*. **2012**, *51*, 2119−2123.
16. Wang, Q.-Q.; Begum, R. A.; Day, V. W.; Bowman-James, K. “Alfred Werner’s Expanded Legacy: Anion and Metal Ion Coordination in an Unsymmetrical, Octaamido Cryptand” *Polyhedron*, **2013**, *52*, 515−523.
17. Wang, Q.-Q.; Day, V. W.; Bowman-James, K. “Chemistry and Structure of a Host–Guest Relationship: The Power of NMR and X-ray Diffraction in Tandem” *J. Am. Chem. Soc.* **2013**, *135*, 392−399.
18. Hossain, Md. A.; Lucarini, S.; Powell, D.; Bowman-James, K. “Ditopic Double Pincer Palladacycle Catalyst for C–C Coupling” *Inorg. Chem*. **2004**, *43*, 7275–7277.
19. Begum, R. A.; Powell, D.; Bowman-James, K. “Thioamide Pincer Ligands with Charge Versatility” *Inorg. Chem.* **2006**, *45*, 964–966.

20. Ghosh, S.; Roehm, B.; Begum, R. A.; Kut, J.; Hossain, M. A.; Day, V. W.; Bowman-James, K. “Versatile Host for Metallo Anions and Cations” *Inorg. Chem.* **2007**, *46*, 9519−9521.
21. Wang, Q.-Q.; Begum, R. A.; Day, V. W.; Bowman-James, K. “Molecular Thioamide⇔Iminothiolate Switches for Sulfur Mustards” *Inorg. Chem*. **2012**, *51*, 760−762.
22. Wang, Q.-Q.; Day, V. W.; Bowman-James, K. “Hexagonal Molecular ‘Palladawheel’” *Chem. Commun*. **2013**, *49*, 8042−8044.
23. Wang, Q.-Q.; Begum, R.A.; Day, V.W.; Bowman-James, K. “Chemical Mustard Containment Using Simple Palladium Pincer Complexes: The Influence of Molecular Walls” *J. Am. Chem. Soc*. **2013**, *135*, 17193−17199.
24. Begum, R. A.; Day, V. W.; Kumar, M.; Gonzalez, J. Jackson, T. A.; Bowman-James, K. “M···H-C Interaction – Agostic or Not: A Comparison of Phenyl- Versus Pyridyl-Bridged Transition Metal Dimers” *Inorg. Chem. Acta.* **2014**, *417*, 287−293.
25. *Scifinder,* web version; Chemical Abstracts Service: Columbus, OH, 2007; RN 58-08-2 (Accessed Feb 17, 2015).
26. Moulton, C. J.; Shaw, B. L. Transition Metal-Carbon Bonds. “Part XLII. Complexes of Nickel, Palladium, Platinum, Rhodium and Iridium with the Tridentate Ligand 2,6-Bis[(di-t-butylphosphino)methyl]phenyl” *J. Chem. Soc., Dalton Trans*. **1976**, 1020–1024.
27. Kane-Maguire, L. A. P.; Thomas, K. “Kinetics and mechanism of substitution on square-planar palladium(II) complexes in mixed aqueous solvents” *J.C.S. Dalton* **1975**, 1890–1894.
28. Shaw, B. L.; Uttley, M. F. “Dihydro-Platinum(II) and Related Complexes” *J.C.S. Chem. Comtn*. **1974**, 918–919.
29. Coining of the name “pincer”: Van Koten, G. “Tuning the Reactivity of Metals Held in a Rigid Ligand Environment” *Pure Appl. Chem.* **1989**, *61*, 1681–1694.
30. Canty, A. J. “Development of Organopalladium(IV) Chemistry: Fundamental Aspects and Systems for Studies of Mechanism in Organometallic Chemistry and Catalysis” *Acc. Chem. Res.* **1992**, *25*, 83–90.

31. Peris, E.; Loch, J. A.; Mata, J.; Crabtree, R. H. “A Pd Complex of a Tridentate Pincer CNC Bis-Carbene Ligand as a Robust Homogeneous Heck Catalyst” *Chem. Commun.* **2001**, 201–202.
32. Rodriguez, G.; Albrecht, M.; Schoenmaker, J.; Ford, A.; Lutz, M.; Spek, A. L.; van Koten, G. “Bifunctional Pincer-type Organometallics as Substrates for Organic Transformations and as Novel Building Blocks for Polymetallic Materials” *J. Am. Chem. Soc.* **2002**, *124*, 5127–5138.
33. Jung, I. G.; Son, S. U.; Park, K. H.; Chung, K-. C.; Lee, J. W.; Chung, Y. K. “Synthesis of Novel Pd−NCN Pincer Complexes Having Additional Nitrogen Coordination Sites and Their Application as Catalysts for the Heck Reaction” *Organometallics,* **2003**, *22,* 4715–4720.
34. Gorla, F.; Togni, A.; Venanzi, L. M. “Synthesis of an Optically Active Platinum(I1) Complex Containing a New Terdentate P-C-P Ligand and Its Catalytic Activity in the Asymmetric Aldol Reaction of Methyl Isocyanoacetate. X-ray Crystal Structure of [2,6-Bis[(1’5,2’5)-1’-(diphenylphosphino)-2',3'-dihydroxypropyl]phenyl](η^1-nitrato) platinum(II)” *Organometallics*, **1994**, *13*, 1607–1616.
35. Ohff, M.; Ohff, A.; van der Boom, M. E.; Milstein, D. “Highly Active Pd(II) PCP–Type Catalysts for the Heck Reaction” *J. Am. Chem. Soc.* **1997**, *119*, 11687–11688.
36. Bedford, R. B.; Draper, S. M.; Scully, P. N.; Welch, S. L. “Palladium bis(phosphinite) ‘PCP ’-pincer complexes and their application as catalysts in the Suzuki reaction” *New J. Chem.* **2000**, *24*, 745–747.
37. Olsson, D.; Wendt, O. F. J. “Suzuki Reaction Catalysed by a PC(sp^3)P Pincer Pd(II) Complex: Evidence for a Mechanism Involving Molecular Species” *J. Organomet. Chem.* **2009**, *694*, 3112–3115.
38. Bolliger, J. L.; Blacque, O.; Frech, C. M. “Short, Facile, and High-Yielding Synthesis of Extremely Efficient Pincer-Type Suzuki Catalysts Bearing Aminophosphine Substituents” *Angew. Chem., Int. Ed.,* **2007**, *46,* 6514–6517.
39. Zim, D.; Gruber, A. S.; Ebeling, G.; Dupont, J.; Monteiro, A. L. “Sulfur-Containing Palladacycles: Efficient Phosphine-Free Catalyst Precursors for the Suzuki Cross-Coupling Reaction at Room Temperature” *Org. Lett.* **2000**, *2*, 2881–2884.

40. Takemoto, T.; Iwasa, S.;Hamada, H.; Shibatomi, K.; Kameyama, M.; Motoyama, Y.; Nishiyama, H. "Highly efficient Suzuki-Miyaura coupling reactions catalyzed by bis(oxazolinyl)phenyl-Pd(II) complex" *Tetrahedron Lett*. **2007**, *48*, 3397–3401.
41. Imanaka, Y.; Hashimoto, H.; Kinoshita, I.; Nishioka, T. "Incorporation of a Sugar Unit into a C-C-N Pincer Pd Complex Using Click Chemistry and Its Dynamic Behavior in Solution and Catalytic Ability toward the Suzuki-Miyaura Coupling in Water" *Chem. Lett.* **2014**,*43*, 687–689.
42. Liu, J.; Wang, H.; Zhang, H.; Wu, X.; Zhang, H.; Deng, Y.; Yang, Z.; Lei, A. "Identification of a Highly Efficient Alkylated Pincer Thioimido–Palladium(II) Complex as the Active Catalyst in Negishi Coupling" *Chem. Eur. J.* **2009**, *15*, 4437–4445.
43. Wang, H.; Liu, J.; Deng, Y.; Min, T.; Yu, G.; Wu, X.; Yang, Z.; Lei, A. "Pincer Thioamide and Pincer Thioimide Palladium Complexes Catalyze Highly Efficient Negishi Coupling of Primary and Secondary Alkyl Zinc Reagents at Room Temperature" *Chem. Eur. J.* **2009**, *15*, 1499–1507.
44. Liu, J.; Deng, Y.; Lin, C.; Lei, A. "Push Effect'' of Sulfur Coordination: Promoting the Breaking of C(sp^2)–I Bond by Pincer Thioimido-Pd(II) Complexes" *Chem. Sci*. **2012**, *3*, 1211–1214.
45. Stark, M. A.; Richards, C. J. "Synthesis and application of cationic 2,6-bis(2-oxazolinyl)phenylpalladium(II) complexes" *Tetrahedron Lett*. **1997**, *38*, 5881–5884.
46. Motoyama, Y.; Kawakami, H.; Shimozono, K.; Aoki, K.;Nishiyama, H. "Synthesis and X-ray Crystal Structures of Bis(oxazolinyl)phenyl-Derived Chiral Palladium(II) and Platinum(II) and -(IV) Complexes and Their Use in the Catalytic Asymmetric Aldol-Type Condensation of Isocyanides and Aldehydes" *Organometallics* **2002**, *21*, 3408–3416.
47. Aydin, J.; Ryden, A.; Szabo, K. J. "Chiral Palladium-Pincer Complex Catalyzed Asymmetric Condensation of Sulfonimines and Isocyanoacetate" *Tetrahedron: Asymmetry* **2008**, *19*, 1867–1870.

48. Stark, M. A.; Jones, G.; Richards, C. J. "Cationic [2,6-Bis(2'-oxazolinyl)phenyl]palladium(II) Complexes: Catalysts for the Asymmetric Michael Reaction" *Organometallics* **2000**, *19*, 1282–1291.
49. McDonald, A. R.; Dijkstra, H. P.; Suijkerbuijk, B. M. J. M.; van Klink, G. P. M.; van Koten, G. "'Click' Immobilization of Organometallic Pincer Catalysts for C–C Coupling Reactions" *Organometallics* **2009**, *28*, 4689–4699.
50. Xu, Y.; Yang, Z.; Ding, B.; Liu, D.; Liu, Y.; Sugiya, M.; Imamoto, T.; Zhang, W. "Asymmetric Michael Addition of Diphenylphosphine to β,γ-Unsaturated α-Keto Esters Catalyzed by a P-Stereogenic Pincer-Pd Complex" *Tetrahedron* **2015**, *71*, 6832–6839.
51. Gu, S.; Chen, W. "Pincer Complexes of Palladium- and Nickel-Containing 3-Butyl-1-(1,10-phenanthrolin-2-yl)imidazolylidene as Efficient Aqueous Sonogashira and Kumada Coupling Reactions" *Organometallics* **2009**, *28*, 909–914.
52. Ines, B.; SanMartin, R.; Churruca, F.; Domínguez, E.; Urtiaga, M. K.; Arriortua, M. I. "A Nonsymmetric Pincer-Type Palladium Catalyst In Suzuki, Sonogashira, and Hiyama Couplings in Neat Water" *Organometallics* **2008**, *27*, 2833–2839.
53. Olsson, D.; Nilsson, P.; El Masnaouy, M.; Wendt, O. F. "A catalytic and mechanistic investigation of a PCP pincer palladium complex in the Stille reaction" *Dalton Trans*. **2005**, 1924–1929.
54. Wallner, O. A.; Szabo, K. J. "Palladium Pincer Complex-Catalyzed Allylic Stannylation with Hexaalkylditin Reagents" *Org. Lett.* **2004**, *6*, 1829–1831.
55. Aydin, J.; Szabo, K. J. "Palladium−Pincer Complex Catalyzed C−C Coupling of Allyl Nitriles with Tosyl Imines via Regioselective Allylic C−H Bond Functionalization" *Org. Lett.* **2008**, *10*, 2881–2884.
56. Piechaczyk, O.; Cantat, T.; Mezailles, N.; Le Floch, P. "A Joint Experimental and Theoretical Study of the Palladium-Catalyzed Electrophilic Allylation of Aldehydes" *J. Org. Chem*. **2007**, 72, 4228–4237.
57. Solin, N.; Kjellgren, J.; Szabo, K. J. "Pincer Complex-Catalyzed Allylation of Aldehyde and Imine Substrates via Nucleophilic η^1-Allyl Palladium Intermediates" *J. Am. Chem. Soc.* **2004**, *126*, 7026–7033.

58. Mazzeo, M.; Lamberti, M.; Massa, A.; Scettri, A.; Pellechia, C.; Peters, J. C. "Phosphido Pincer Complexes of Palladium as New Efficient Catalysts for Allylation of Aldehydes" *Organometallics* **2008**, *27*, 5741–5743.

59. Mizoroki, T.; Mori, K.; Ozaki, A. "Arylation of Olefin with Aryl Iodide Catalyzed by Palladium" *Bull. Chem. Soc. Jap*. **1971**, *44*, 581.
60. Heck, R. F.; Nolley, J. P., Jr. "Palladium-catalyzed Vinylic Hydrogen Substitution Reactions with Aryl, Benzyl, and Styryl Halides" *J. Org. Chem.* **1972**, *37*, 2320–2322.
61. De Vries, J. G. "The Heck Reaction in the Production of Fine Chemicals" *Can. J. Chem.* **2001**, *79*, 1086–1092.
62. (a) Heck, R.F. "Acylation, Methylation, and Carboxyalkylation of Olefins by Group VIII Metal Derivatives" *J. Am. Chem. Soc.* **1968**, *90*, 5518–5526; (b) Heck, R.F. "The Arylation of Allylic Alcohols with Organopalladium Compounds. A New Synthesis of 3-Aryl Aldehydes and Ketones" *J. Am. Chem. Soc.* **1968**, *90*, 5526–5531; (c) Heck, R.F. "Allylation of Aromatic Compounds with Organopalladium Salts" *J. Am. Chem. Soc.* **1968**, *90*, 5531–5534; (d) Heck, R.F. "The Palladium-catalyzed Arylation of Enol Esters, Ethers, and Halides. A New Synthesis of 2-Aryl Aldehydes and Ketones" *J. Am. Chem. Soc.* **1968**, *90*, 5535–5538; (e) Heck, R.F. "Aromatic haloethylation with palladium and copper halides" *J. Am. Chem. Soc.* **1968**, *90*, 5538–5542; (f) Heck, R.F. "The Addition of Alkyl- and Arylpalladium Chlorides to Conjugated Dienes" *J. Am. Chem. Soc.* **1968**, *90*, 5542–5546; (g) Heck, R.F. "A Synthesis of Diaryl Ketones from Arylmercuric salts" *J. Am. Chem. Soc.* **1968**, *90*, 5546–5548.
63. Beletskaya, I. P.; Cheprakov, A. V. "The Heck Reaction as a Sharpening Stone of Palladium Catalysis" *Chem. Rev*. **2000**, *100*, 3009–3066.
64. Dieck, H. A.; Heck, R. F. "Organophosphinepalladium Complexes as Catalysts for Vinylic Hydrogen Substitution Reactions" *J. Am. Chem. Soc.* **1974**, *96*, 1133–1136.
65. Whitcombe, N. J.; Hii, K. K.; Gibson, S. E. "Advances in the Heck Chemistry of Aryl Bromides and Chlorides" *Tetrahedron* **2001**, *57*, 7449–7476.

66. Loch, J. A.; Albrecht, M.; Peris, E.; Mata, J.; Faller, J. W.; Crabtree, R. H. "Palladium Complexes with Tridentate pincer Bis-Carbene Ligands as Efficient Catalysts for C–C Coupling" *Organometallics* **2002**, *21*, 700–706.
67. Bergbreiter, D. E.; Osburn, P. L.; Frels, J. D. "Mecahnistic Studies of SCS-Pd Complexes Used in Heck Catalysis" *Adv. Synth. Catal.* **2005**, *347*, 172–184.
68. Anton, D. R.; Crabtree, R. H. "Dibenzo[a,e]cyclooctatetraene in a Proposed Test for Heterogeneity in Catalysts Formed from Soluble Platinum-group Metal Complexes" *Organometallics* **1983**, *2*, 855–859.
69. Foley, P.; DiCosimo, R.; Whitesides, G. M. "Mechanism of Thermal Decomposition of Dineopentylbis(triethylphosphine)platinum(II): Formation of Bis(triethylphosphine)-3,3-Dimethylplatinacyclobutane" *J. Am. Chem. Soc.* **1980**,*102*, 6713–6725.
70. Eberhard, M. R. "Insights into the Heck Reaction with PCP Pincer Palladium(II) Complexes" *Org. Lett.* **2004**, *6*, 2125–2128.
71. Ohff, M.; Ohff, A.; van der Boom, M. E.; Milstein, D. "Highly Active Pd(II) PCP-Type Catalysts for the Heck Reaction" *J. Am. Chem. Soc.* **1998**, *120*, 3273–3273.
72. Beletskaya, I. P.; Chuchuryukin, A. V.; van Koten, G.; Dijkstra, H. P.; van Klink, G. P. M.; Kashin, A. N.; Nefedov, S. E.; Eremenko, I. L. "Synthesis and Catalytic Properties of Di- and Trinuclear Palladium Complexes with PCP-Pincer Ligands" *Russ. J. Org. Chem.* **2003**, *39*, 1268–1281.
73. Sjövall, S.; Wendt, O. F.; Andersson, C. "Synthesis, Characterisation and Catalytic Investigation of a New Type of PC(sp^3)P pincer Pd(II) Complex" *J. Chem. Soc.Dalton Trans*. **2002**, 1396–1400.
74. Morales-Morales, D.; Redon, R.; Yung, C.; Jensen, C. M. "High Yield Olefination of a Wide Scope of Aryl Chlorides Catalyzed by the Phosphinito Palladium PCP Pincer Complex: [PdCl{$C_6H_3(OPPri_2)_2$-2,6}]" *Chem. Commun*. **2000**, 1619–1620.
75. Shaw, B. L.; Perera, S. D.; Staley, E. A. "Highly Active, Stable, Catalysts for the Heck Reaction; Further Suggestions on the Mechanism" *Chem. Commun.* **1998**, 1361–1362.
76. Shaw, B. L. "Speculations on New Mechanism for Heck Reactions" *New. J. Chem.* **1998**, 77–79.

77. Gruber, A. S.; Zim, D.; Ebeling, G.; Monteiro, A. L.; Dupont, J. “Sulfur-Containing Palladacycles as Catalyst Precursors for the Heck Reaction” *Org. Lett*. **2000**, *2*, 1287–1290.
78. Miyazaki, F.; Yamaguchi, K.; Shibasaki, M. “The Synthesis of a New Palladacycle Catalyst. Development of a High Performance Catalyst for Heck Reactions” *Tetrahedron Lett*. **1999**, *40*, 7379–7383.
79. Yu, K. Q.; Sommer, W.; Weck, M.; Jones, C. W. “Silica and Polymer-Tethered Pd–SCS-pincer Complexes: Evidence for Precatalyst Decomposition to Form Soluble Catalytic Species in Mizoroki–Heck Chemistry” *J. Catal.* **2004**, *226*, 101–110.
80. Yu, K.; Sommer, W.; Richardson, J. M.; Weck, M.; Jones, C.W. “Evidence that SCS Pincer Pd(II) Complexes are only Precatalysts in Heck Catalysis and the Implications for Catalyst Recovery and Reuse” *Adv. Synth. Catal.* **2005**, *347*, 161–171.
81. Phan, N. T. S.; Van Der Sluys, M.; Jones, C. W. “On the Nature of the Active Species in Palladium Catalyzed Mizoroki–Heck and Suzuki–Miyaura Couplings – Homogeneous or Heterogeneous Catalysis, A Critical Review” *Adv. Synth. Catal.* **2006**, *348*, 609–679.
82. Sommer, W. J.; Yu, K.; Sears, J. S.; Ji, Y.; Zheng, X.; Davis, R. J.; Sherrill, C. D.; Jones, C. W.; Weck, M. “Investigations into the Stability of Tethered Palladium(II) Pincer Complexes during Heck Catalysis” *Organometallics* **2005**, *24*, 4351–4361.
83. Miyaura, N.; Suzuki, A. “Stereoselective Synthesis of Arylated (E)-Alkenes by the Reaction of Alk-1-Enylboranes with Aryl Halides in the Presence of Palladium Catalyst” *Chem. Comm.* **1979**, *19*, 866–867.
84. *Boronic Acids*: *Preparation and Applications in Organic Synthesis, Medicine and Materials*, ed. Hall, D. G., Wiley-VCH, Edmonton, Alberta, **2005**.
85. Jacks, T. E.; Belmont, D. T.; Briggs, C. A.; Horne, N. M.; Kanter, G. D.; Karrick, G. L.; Krikke, J. J.; McCabe, R. J.; Mustakis, J. G.; Nanninga, T. N.; Risedorph, G. S.; Seamans, R. E.; Skeean, R.; Winkle, D. D.; Zennie, T. M. "Development of a Scalable Process for CI-1034, an Endothelin Antagonist" *Org. Process Res. Dev.* **2004**, *8*, 201–212.

86. Banihashemi, A.; Eghbali, M. “Polycondensation of Pyridine-2,6-Dicarboxylic Acid with Some Di- and Tetraamino Compounds” *J. Polym. Sci.* **1976**, *14*, 2658–2664.
87. Hirao, T.; Moriuchi, T.; Mikami, S.; Ikeda, I.; Ohshiro, Y. “A Novel System for Oxygenation. Effect of Multidentate Podand Ligand in Transition Metal Catalyzed Epoxidation with Molecular Oxygen” *Tetrahedron Lett.* **1983**, *34*, 1031–1034.
88. Hirao, T.; Moriuchi, T.; Ishikawa, T.; Nishimura, K.; Mikami, S.; Ohsiro, Y.; Ikeda, I. “A Novel Catalytic System for Oxygenation with Molecular Oxygen Induced by Transition Metal Complexes with a Multidentate *N*-Heterocyclic Podand Ligand” *J. Mol. Catal. A* **1996**, *113*, 117–130.
89. Ray, M.; Ghosh, D.; Shirin, Z.; Mukherjee, R. “Highly Stabilized Low-Spin Iron(III) and Cobalt(III) Complexes of a Tridentate Bis-Amide Ligand 2,6-Bis(*N*-phenylcarbamoyl)pyridine. Novel Nonmacrocyclic Tetraamido-N Coordination and Two Unusually Short Metal-Pyridine Bonds” *Inorg. Chem.* **1997**, *36*, 3568–3572.
90. Patra, A. K.; Mukherjee, R. “Bivalent, Trivalent, and Tetravalent Nickel Complexes with a Common Tridentate Deprotonated Pyridine Bis-Amide Ligand. Molecular Structures of Nickel(II) and Nickel(IV) and Redox Activity” *Inorg. Chem.* **1999**, *38*, 1388–1393.
91. Patra, A. K.; Ray, M.; Mukherjee, R. “Magneto–Structural Studies of Monohydroxo-Bridged Dicopper(II) Complexes M[$Cu_2L_2(OH)$]·$2H_2O$ (M-Na^+(**1**) and K^+(**2**); H_2L-2,6-bis[N-(phenyl)carbamoyl]pyridine). Effect of Cu-OH-Cu Bridge Angle on Antiferromagnetic Coupling” *Polyhedron* **2000**, *19*, 1423–1428.
92. Singh, A. K.; Balamurugan, V.; Mukherjee, R. “Synthesis and Characterization of Low-Spin and Cation Radical Complexes of Ruthenium(III) of a Tridentate Pyridine Bis-Amide Ligand” *Inorg. Chem.* **2003**, *42*, 6497–6502.
93. Kawamoto, T.; Prakash, O.; Ostrander, R.; Rheingold, A.L.; Borovik, A. S. Metallohelices: Effects of Weak Interactions on Helical Morphology” *Inorg. Chem.* **1995**, *34*, 4294–4295.

94. Kawamoto, T.; Hammes, B. S.; Haggerty, B.; Yap, G. P. A.; Rheingold, R. L.; Borovik, A. S. “Synthesis and Structure of Helical Supramolecular Arrays” *J. Am. Chem. Soc*. **1996**, *118*, 285–286.
95. Kawamoto, T.; Hammes, B.S.; Ostrander, R.; Rheingold, R. L.; Borovik, A. S. “Synthesis and Structures of Nickel(II) and Copper(II) Complexes of 2,6-Bis[(2-acetylphenyl)carbamoyl]pyridine: Effects of Molecular Structure on Crystal Lattice Architecture” *Inorg. Chem.* **1998**, *37*, 3424–3427.
96. Shirlin, Z.; Thompson, J.; Liable-Sands, L.; Yap, G. P. A.; Rheingold, A. L.; Borovik, A. S. “C_2-Symmetric ligands containing hydrogen bond donors: synthesis and properties of Cu(II) complexes of 2,6-bis[N,N-(2-carboxamidophenyl)carbamoyl]pyridine” *Dalton Trans.* **2002**, 1714–1720.
97. Huang, D.; Holm, R. H. “Reactions of the Terminal Ni(II)-OH Group in Substitution and Electrophilic Reactions with Carbon Dioxide and Other Substrates: Structural Definition of Binding Modes in an Intramolecular Ni(II)···Fe(II) Bridged Site” *J. Am. Chem. Soc.* **2010**, *132*, 4693–4701.
98. Halvagar, M. R.; Neisen, B.; Tolman, W. B. “Copper-, Palladium-, and Platinum-Containing Complexes of an Asymmetric Dinucleating Ligand” *Inorg. Chem.* **2013**, *52*, 793–799.
99. Donoghue, P. J.; Gupta, A. K.; Boyce, D. W.; Cramer, C. J.; Tolman, W. B. “An Anionic, Tetragonal Copper(II) Superoxide Complex” *J. Am. Chem. Soc.* **2010**, *132*, 15869–15871.
100. Woertink, J. S.; Smeets, P. J.; Groothaert, M. H.; Vance, M. A.; Sels, B. F.; Schoonheydt, R. A.; Solomon, E. I. “A $[Cu_2O]^{2+}$ Core in Cu-ZSM-5, the Active Site in the Oxidation of Methane to Methanol” *Proc. Natl. Acad. Sci. U.S.A.* **2009**, *106*, 18908–18913.
101. Que, L., Jr.; Tolman, W. B. “Biologically Inspired Oxidation Catalysts” *Nature* **2008**, *455*, 333–340.
102. Moriuchi, T.; Bandoh, S.; Miyaji, Y.; Hirao, T. “A Novel Heterobimetallic Complex Composed of the Imide-Bridged [3]Ferrocenophane and the Tridentate Palladium(II) Complex” *J. Organomet. Chem.* **2000**, *599*, 135–142.

103. Moriuchi, T.; Bandoh, S.; Miyaishi, M.; Hirao, T. “A Novel Redox-Active Conjugated Palladium Homobimetallic Complex” *Eur. J. Inorg. Chem.* **2001**, 651–657.
104. Shen, X.; Moriuchi, T.; Hirao, T. “Chirality Induction of Polyaniline Derivatives through Chiral Complexation” *Tetrahedron Lett.* **2004**, 4733–4736.
105. Dell’Amico, D. B.; Calderazzo, F.; Di Colo, F.; Guglielmetti, G.; Labella, L.; Marchetti, F. “Coordination Properties Towards Palladium(II) of a Tridentate Dianionic Ligand Acting as a N- or a N,O-donor” *Inorg. Chim. Acta* **2006**, *359*, 127–135.
106. Machado, K.; Mishra, J.; Suzuki, S.; Mishra, G. S. “Synthesis of Superparamagnetic Carbon nanotubes Immobilized Pt and Pd Pincer Complexes: Highly Active and Selective Catalyst Towards Cyclohexane Oxidation with Dioxygen” *Dalton Trans.* **2014**, *43*, 17475–17482.

Chapter 2

Pd(II) Complexes Based on

Acyclic and Macrocyclic Amide-Based NNN-Pincer Ligands

2.1. *Abstract*

Palladium(II) complexes derived from acyclic and macrocyclic NNN-pincer ligands were investigated. Complexes **2.6a**, **2.7**, **2.8**, **2.9**, **2.11**, and **2.12** are characterized using ^{1}H and ^{13}C nuclear magnetic resonance (NMR) spectroscopy, as well as positive mode high-resolution mass spectrometry electrospray ionization (HRMS-ESI) and X-ray diffraction (XRD) crystallography. Due to the low solubility of complex **2.10**, it is characterized only by XRD crystallography. Employing high temperatures, these complexes are effective catalysts in the Heck reaction between 4-iodotoluene and stryene. Complex **2.11** is the most effective catalyst, with a quantitative conversion to the Heck coupling products observed after 0.25 hours. On the other hand, when complex **2.9** is employed as the catalyst, an induction period of 2.5 hours is observed before the detection of any product. All of the complexes are compared in terms of their stabilities and induction periods. Reasons for the observed differences in catalysis are discussed.

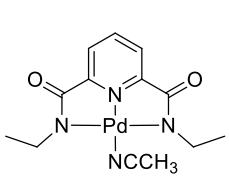

2.6a

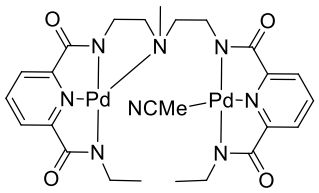

2.7

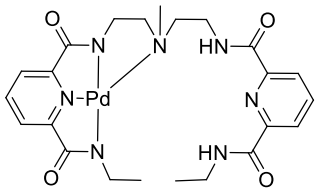

2.8

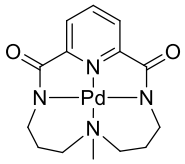

2.9

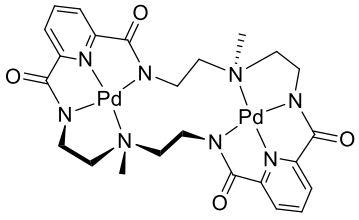

2.10

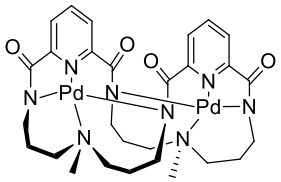

2.11

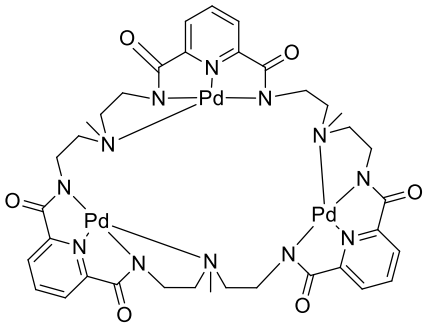

2.12

2.2. *Introduction*

Many enzymes use cooperation between two metals to carry out reactions on unactivated small molecule substrates.[1-3] For example, ureases[4] (Figure 2.1) contain a dinuclear Ni(II) active site in which each metal independently activates the electrophile (urea) or nucleophile (hydroxide ion) in the first step of the hydrolysis of urea. Due to the complex steric and electronic environments in the active sites of enzymes, reactions of small unactivated molecules can be achieved with high efficiency and selectivity. However—for good reason—the strict substrate specificity of enzymes restricts the number and types of substrates that can be used.

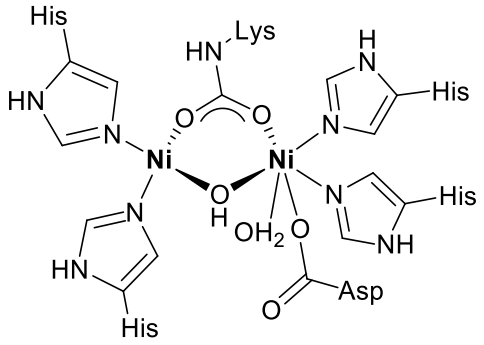

Figure 2.1. ChemDraw representation of the active site of urease containing two Ni(II) centers.[4]

Unlike biological systems, synthetic catalysts can exploit the properties of a broader range of metals and ligands.[5-7] The search for functional analogues of biological systems has grown immensely since the 1990s, and has been driven in part by the solving of the X-ray crystal structures of many bimetallic enzymes.[8] In general, these synthetic bimetallic catalysts can be categorized into two groups: 1) those containing bridging ligands and 2) those containing ligands with isolated nucleating sites (Figure 2.2). Many of the first

synthetic models focused on metals such as Cu(I), Cu(II), Ni(II), Fe(II), Fe(III), and Mn(III).[9,10] However, few cases exist in which the chemistry studied in these model systems has been transferred to a diverse set of organic substrates.

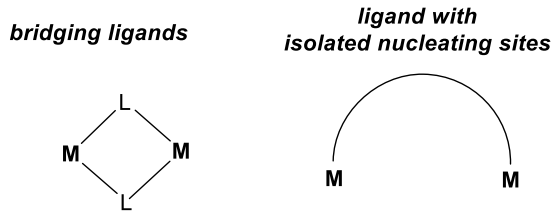

Figure 2.2. Schematic representation of different ligand binding modes of multimetallic complexes.

Alternatively, multinuclear complexes containing metals and ligands that do not naturally occur in enzymes provide new opportunities to develop reactions using diverse substrates. In 1988, Robson and coworkers synthesized a bis[palladium(II)] complex containing bridging sulfur and oxygen atoms between the metal centers that was used to catalyze the hydration of acetonitrile to acetamide (Scheme 2.1).[11] Complete conversion to acetamide was observed after 50 minutes after refluxing in a MeCN/H_2O/THF (5:2:1) solvent mixture using a catalyst concentration of 4 x 10^{-4} M. The acid/base dependence of the hydration in the presence of the bis[palladium(II)] complex led the authors to propose a mechanism in which both metals are necessary to carry out the transformation. In contrast to a previously reported mononuclear Pt(II) complex-mediated nitrile hydration reaction, [12] which involved attack by a free hydroxide nucleophile, the reaction rate was reduced in the presence of one equivalent of a hydroxide ion source. Thus, the authors propose an intermediate complex in which acetonitrile and a hydroxide ion are bound to the Pd(II) metal centers.

Scheme 2.1. Hydration of acetonitrile to acetamide catalyzed by a bis[palladium(II)] complex.[11]

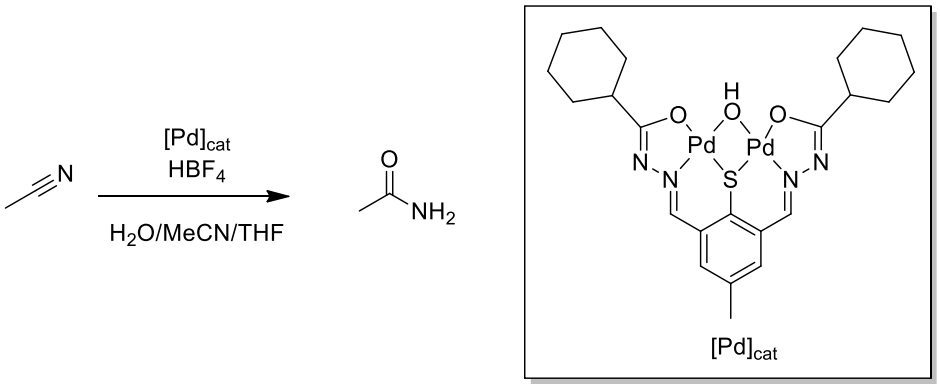

Perhaps one of the most famous examples of a bis[palladium(II)] complex was reported by Herrmann and coworkers in 1997.[13] Aptly named "Herrmann's catalyst," complexes of this type were among the first palladacycles to be investigated in Heck coupling reactions. Using low catalyst loadings, quantitative conversions to the Heck coupling product were observed. For example, the coupling of 4'-bromoacetophenone with butyl acrylate was realized after 24 h using just 0.0001 mol % catalyst loading. Complexes of this type were also found to be good catalysts for the coupling of aryl chlorides with different substituted olefins. An 84% yield was observed in the coupling of 4-chlorobenzaldehyde with butyl acrylate after 24 h using 0.2 mol % catalyst loading. The authors theorized that the perceived air and thermal stability is responsible for the excellent catalytic activity, although they stopped short of proposing a Pd(II)/Pd(IV) catalytic cycle. A mechanistic discussion of the role of palladacycles in the Heck reaction can be found in Chapter 1 (Section 1.2.1) of this dissertation.

Scheme 2.2. Heck coupling of 4'-bromoacetophenone with butyl acrylate using Herrmann's catalyst.[13]

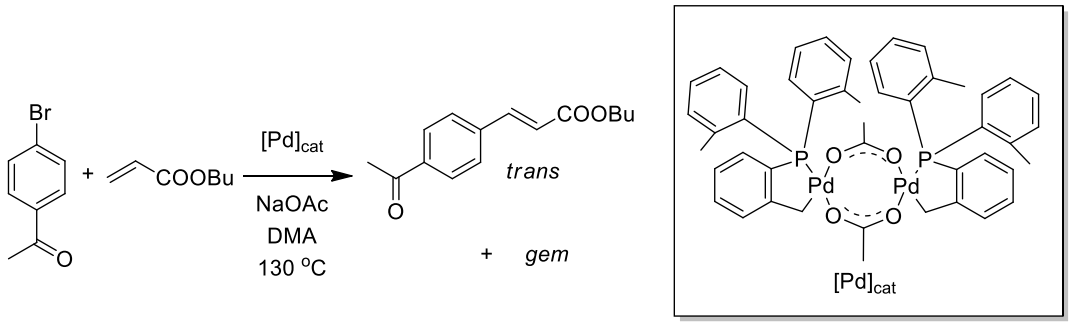

Examples also exist of multimetallic complexes employing isolated pincer nucleating sites within the same ligand. In 2001, van Koten and coworkers reported the design and synthesis of tris(pincer)- and hexakis(pincer)-substituted benzene ligands that coordinate Pd(II).[14] The tris[palladium(II)] complex was investigated in the double Michael reaction between ethyl α-cyanoacetate and methyl vinyl ketone (Scheme 2.3). In a related study, the van Koten group demonstrated that a Pt(II) dendrimer can be efficiently recovered by a MPF-membrane, making these types of systems well suited for catalyst recycling applications.[15]

Scheme 2.3. Double Michael addition catalyzed by a tris[palladium(II)] complex.[14]

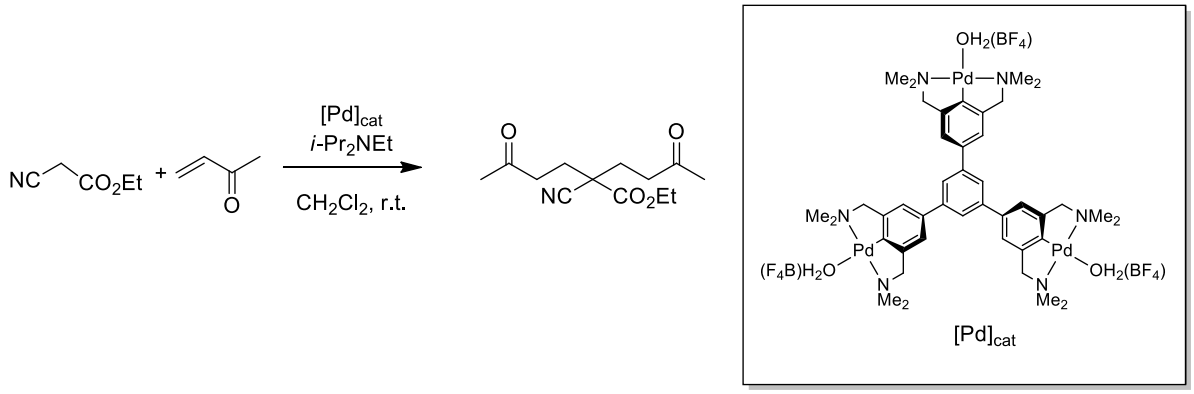

In 2011, Tsukuda and coworkers reported bis[palladium(II)] complexes based on a macrocyclic NCN-bis(pincer) ligand (Scheme 2.4).[16] The conditions in which these complexes are synthesized can be manipulated to isolate either the U- or Z-type isomer of the complex. Both isomers were explored as catalysts in the Heck coupling of iodobenzene with styrene. When the reaction was carried out using 1 x 10^{-3} mol % loading of the Z-type isomer, the reaction yield was 30% after 24 hours. Alternatively, a yield of 94% was obtained after 22 hours using larger catalyst loading (1 x 10^{-2} mol %) of the Z-type isomer. Similar yields were obtained using the U-type isomer.

Scheme 2.4. Heck reaction of iodotoluene and styrene using bis[palladium(II)] complexes.[16]

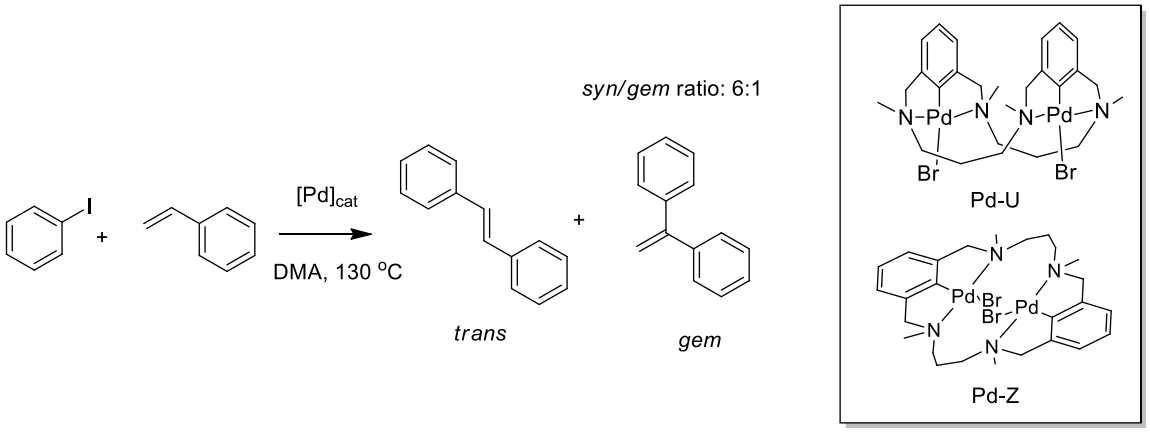

As discussed in Chapter 1, our group has studied the transition metal chemistry of the binucleating macrocyclic ligands illustrated in Figure 2.3.[17,18] In 2004, the Bowman-James group reported the synthesis of a bis[palladium(II)] SCS-pincer complex, which is a capable catalyst for the Heck reaction of 4-iodotoluene and styrene.[17] Three years later, the Bowman-James group reported the homobimetallic structures of Cu(II), Ni(II), Co(III), Fe(III), $Cr_2O_7^{2-}$, and ReO_4^- with a tetraamide-based macrocycle.[18] This work was an

extension of a series of studies that explored the anion recognition properties of tetraamide and tetrathioamide macrocycles.[19-21] This synthetic background and curiosity about multimetallic synthetic catalyst systems represents the basis for the studies presented in this chapter.

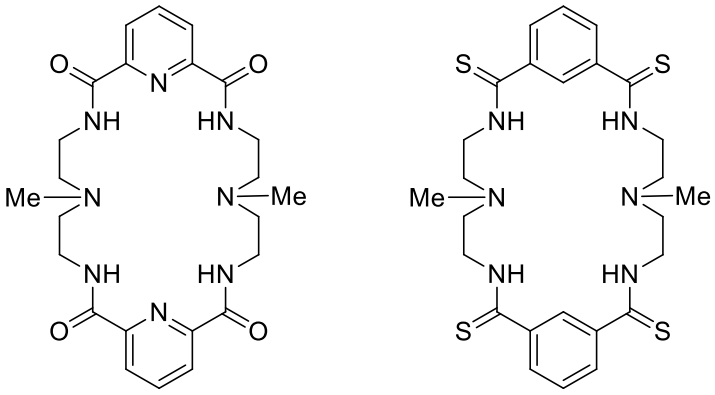

Figure 2.3. Tetraamide and tetrathioamide macrocycles previously investigated by the Bowman-James group for anion recognition and transition metal chelation.[17-21]

2.3 *Results and Discussion*

2.3.1 *Ligand Synthesis*

The ligands addressed in the discussion that follows are illustrated in Figure 2.4. Specifically, compounds **2.2**, **2.3a**, **2.3b**, **2.4**, and **2.5** were initially synthiszed as part of the Bowman-James' group research into supramolecular host-guest chemistry. The following discussion provides a historical perspective of the synthesis of these ligands. In the case of **2.3a**, **2.3b**, and **2.4**, the yields reported are those that I obtained when repeating others' synthetic protocols. Lastly, in order to investigate the coordination chemistry of Pd(II) with a simple acyclic pincer ligand containing aliphatic amide appendages, I synthesized the ethyl-appended NNN-pincer ligand **2.1**.

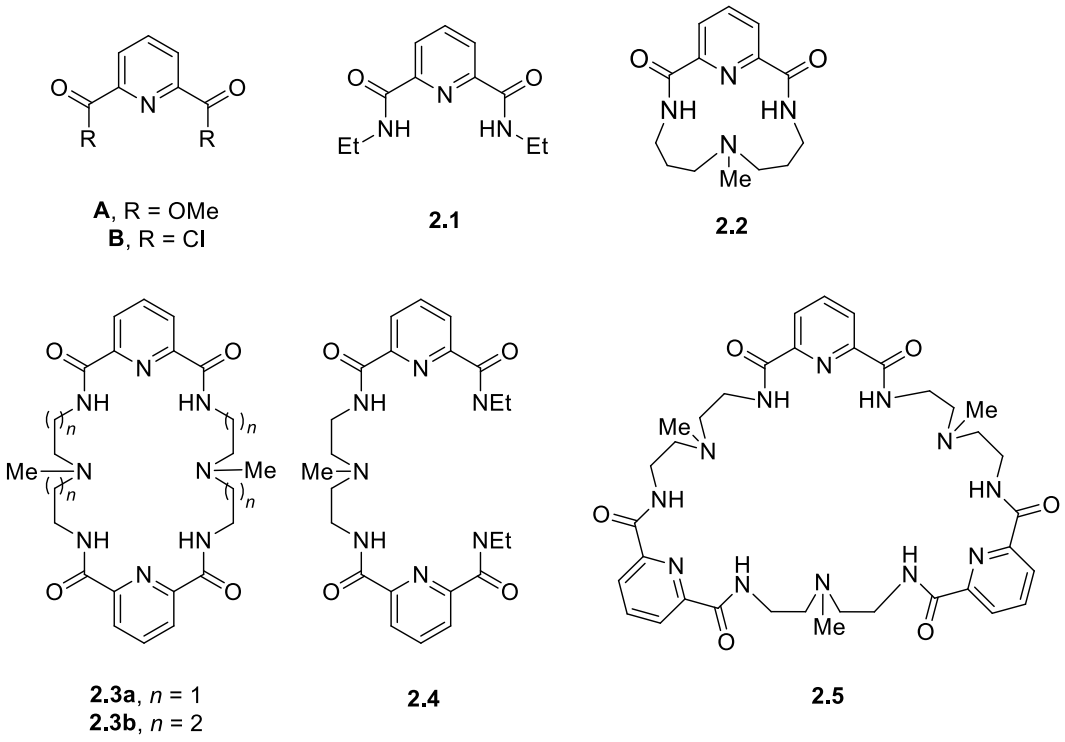

Figure 2.4. Starting materials and ligands investigated in this chapter.

Mononucleating, acyclic NNN-pincer ligands containing aromatic amide appendages were discussed in Chapter 1 (Section 1.3) of this dissertation. The synthesis of these ligands usually involves the reaction of derivatives of aniline with diester **A** or acid chloride **B**. In order to obtain a catalytic and structural foundation for pincer complexes consisting of non-aromatic amide appendages, we synthesized the acyclic NNN-pincer ligand **2.1**, which contains an ethyl amide appendage. Ligand **2.1** was synthesized by bubbling ethylamine (large excess) through a methanolic solution of dimethyl 2,6-pyridinedicarboxylate **A** in a sealed tube at room temperature (Scheme 2.5). After the reaction mixture was stirred for 16 hours, TLC confirmed the consumption of starting material **A**. The solvent was removed *in vacuo* to afford **2.1** as a white solid in 83% yield. Consistent with the formation of **2.1** is the appearance of a signal for the amide proton [H(amide)] (7.80-7.65 ppm), integrating to two protons in the compound's ^{1}H NMR spectrum in $CDCl_3$. Additionally, the positive ion mode ESI mass spectrum of **2.1** in acetonitrile contains a prominent ion peak at *m/z* 244.1038 $[M + Na]^+$.

Scheme 2.5. Synthesis of acyclic ligand **2.1** from dimethyl 2,6-pyridinedicarboxylate **A**.

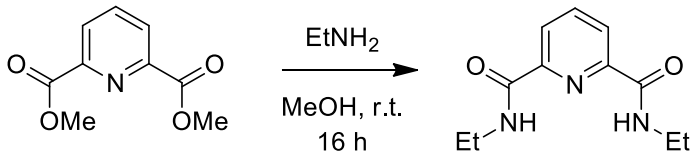

A **2.1** (83%)

Macrocyclic ligand **2.2** has previously been studied for both its metal coordination and anion recognition properties. Wehner and coworkers first used the ligand to coordinate Cu(II) in 1974.[22] Later, Fabbrizzi and coworkers used **2.2** to complex Ni(II), Ni(III), Cu(II), and Cu(III), and investigated the kinetics of metal complex formation.[23] Ligand

2.2 was characterized structurally by Gerald Kut—a Ph.D. student in the Bowman-James group—in 2005,[24] and was reported by Rybak-Akimova in 2006.[25,26] Rybak-Akimova noted that, while large ditopic macrocycles usually coordinate solvent or water molecules, the small monotopic macrocycle is too small and rigid for solvent capture. Additionally, they did not observe any anion recognition properties with **2.2**.

In our group, ligand **2.2** was initially isolated as an unwanted side product by Dr. Kut.[24] More recently, Dr. Rowshan Begum—a postdoctoral fellow in the Bowman-James group—carried out a directed synthesis of **2.2**. Dr. Begum synthesized the ligand by simultaneously adding a solution of 2,6-pyridinedicarbonyl dichloride **B** in methanol and a solution of both 3,3'-diamino-*N*-methyl dipropylamine and triethylamine in methanol dropwise to a flask containing methanol (Scheme 2.6). Following column chromatography, **2.2** was isolated in 13% yield.

Scheme 2.6. Synthesis of macrocyclic ligand **2.2** from 2,6-pyridinedicarbonyl dichloride **B** (carried out by Dr. Begum).

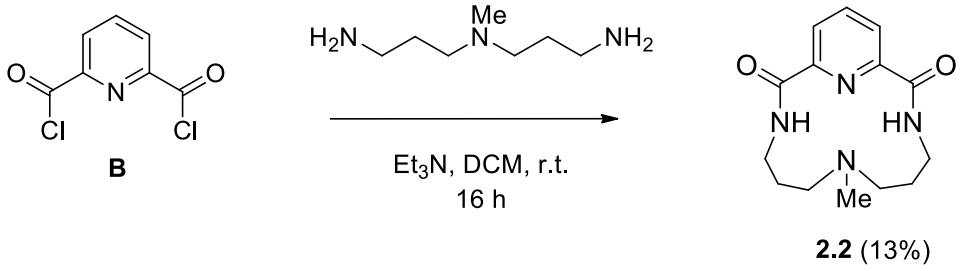

As stated previously, a tetraamide *meta*-xylyl ditopic macrocycle was first reported by our group in 2001.[19] The pyridine analog of this macrocycle with ethylene linkers, compound **2.3a**, was reported two years later by our group.[20] While **2.3a** can be synthesized in one-pot (Scheme 2.7), the one-pot yield (6%) (conducted by Dr. Qi-Qiang

Wang, a postdoctoral fellow in the Bowman-James lab) is considerably lower than that reported in 2001 for the *meta*-xylyl derivative (50 or 55%).[19] Recently, Wang and Bowman-James reported the synthesis of the secondary amine derivative of **2.3a** in 15% yield from the one pot reaction of dimethyl 2,6-pyridine dicarboxylate and *N*-methyl-2-2'-diaminodiethylamine.[27]

Scheme 2.7. One-pot synthesis of 2+2 macrocyclic ligand **2.3a** from 2,6-pyridinedicarbonyl dichloride **B**, carried out by Dr. Wang.

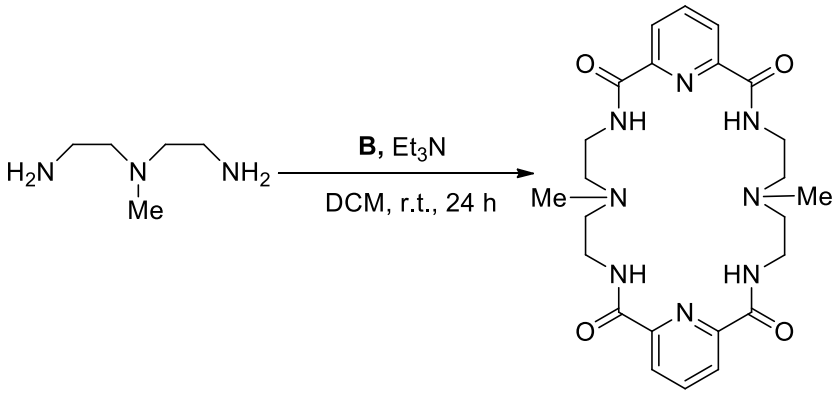

2.3a (6%) WQQ 1-1A

In their efforts to synthesize a mono-*N*-methyl substituted ditopic macrocycle to investigated CO_2 fixation via carbamate formation, Wang and Bowman-James reported the stepwise synthesis of an unsymmetric ligand similar to ethylene-linked macrocyclic ligand **2.3a**.[27] In this protocol, the cyclization step was reduced to a [1+1] reaction, minimizing unwanted adducts and simplifying the workup. Dr. Wang was also able to apply this protocol to the synthesis of **2.3a.** In repeated experiments by Dr. Wang and myself, the two-step yield was higher than that of the one pot reaction. In the first step of the reaction sequence—carried out by myself using Dr. Wang's procedure—a solution of *N*-methyl-2-2'-diaminodiethylamine (1 equiv) in methanol was added dropwise over a period of 2 hours to a refluxing solution of **A** (4 equiv) in methanol, and the reaction mixture was stirred at

reflux for 3 days (Scheme 2.8). Subsequently, the crude products were purified via column chromatography to afford compound **C** as a white powder in 55% yield. In the ring closing step—again, using Dr. Wang's procedure—compound **C** (1 equiv) was added to a solution of *N*-methyl-2-2'-diaminodiethylamine in methanol and the reaction mixture was stirred at reflux for 3 days. Upon cooling, the white precipitate that formed was filtered and dried to afford the desired product, **2.3a**, as a white solid in 45% yield (25% yield over two steps). The positive mode ESI mass spectrum of **2.3a** confirms the formation of the ditopic macrocyclic adduct, with a prominent ion peak at *m/z* 497.2620 $[M + H]^+$. The same procedure leads to formation of propylene-linked macrocyclic ligand **2.3b** via compound **D** if 3-3'-diamino-*N*-methyl dipropylamine is used in both steps of the reaction sequence (compound **D** was synthesized by Thomas Robben—a graduate student in the Bowman-James lab—and was used for the synthesis of **2.3b**) (Scheme 2.8). Conveniently, due to the solubility difference between the desired ditopic macrocyclic adduct and the side products formed during the reaction, no column is necessary in the final step of the synthesis of either **2.3a** or **2.3b**.

Scheme 2.8. Stepwise synthesis of ditopic macrocyclic ligands **2.3a** and **2.3b** via intermediates **C** and **D** respectively.

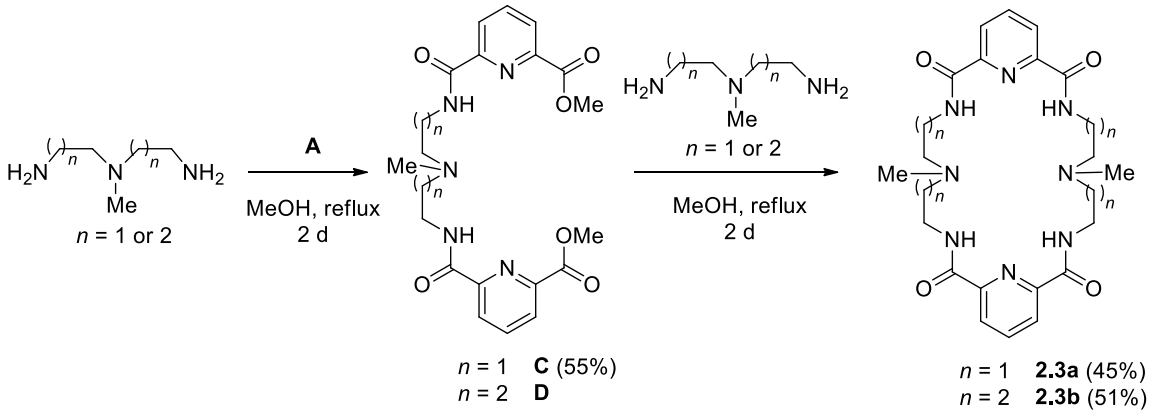

The synthesis of ditopic three-quarter macrocycles can also be achieved from compounds **C** and **D**. Using a modified protocol of one initially developed by Dr. Begum,[28] three-quarter macrocyclic ligand **2.4** was synthesized from **C** by bubbling ethylamine through a solution of **C** in methanol (Scheme 2.9). After stirring at room temperature for 16 hours, the solvent was removed *in vacuo* to afford **2.4** as a colorless oil. Dissolving the oil in acetonitrile, followed by evaporation of the solvent *in vacuo*, led to the isolation of **2.4** as a white solid in 96% yield. Consistent with the formation of an unsymmetric ligand, the ^{1}H NMR spectrum of **2.4** in $CDCl_3$ displays two unique signals for H(amide) at 8.63 and 8.49 ppm. Alternatively, if the ^{1}H NMR spectrum is recorded in DMSO-d_6, no separation between the two amide resonances is observed. Whereas the reaction of the tetraamide of intermediate **D** with $Pd(OAc)_2$ did not afford an isolable product, its chemistry is not reported here. Addition of one or two equivalents of $Pd(OAc)_2$ to the propyl-linked ligand resulted in a dark black solution. No evidence of the formation of a Pd(II) species was observed by mass spectrometry.

Scheme 2.9. Synthesis of three-quarter macrocyclic ligand **2.4** from intermediate **C**.

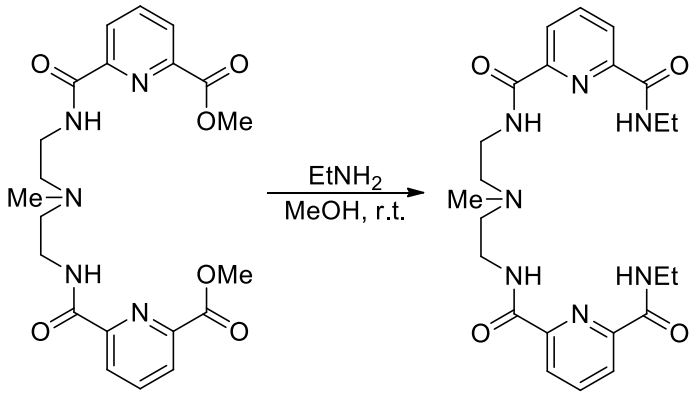

C **2.4** (96%)

Jurczak and coworkers have reported the isolation of tritopic and tetratopic macrocycles during their synthesis of a tetraamide macrocycle from dimethyl 2,6-pyridine dicarboxylate, **A**, and 1,5-diaminopentane.[29,30] Similarly, in 2009 the Bowman-James group reported the isolation of a compound similar to trinucleating tritopic macrocycle **2.5**.[21] In that study, mono-, tri- and tetratopic macrocyclic adducts were isolated via column chromatography during the one-pot synthesis of a Boc-protected ditopic macrocycle in 5%, 10%, and 5% yields, respectively. Recently, in unpublished work, Dr. Wang optimized the directed synthesis of tritopic macrocycle **2.5** in two steps from compound **C** (Scheme 2.10). The positive mode ESI mass spectrum confirmed the formation of the tritopic macrocyclic adduct, with a prominent ion at *m/z* 745.3701 $[M + H]^+$. My attempts to synthesize the propylene-linked derivative of **2.5** were unsuccessful, possibly because the six total additional carbons make the ring-closing step more challenging.

Scheme 2.10. Two-step synthesis of tritopic macrocyclic ligand **2.5** from intermediate **C** (conducted by Dr. Wang).

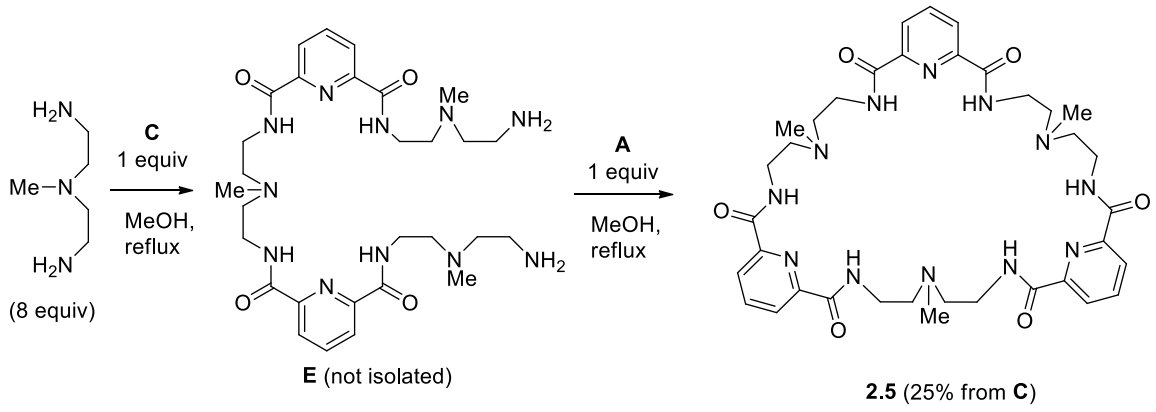

2.3.2 *Synthesis of Pd(II) Complexes*

In a preliminary experiment in 2010, I synthesized Pd(II) NNN-pincer complex **2.6b**[31] (Figure 2.5) and found it to be an efficient precatalyst in the Heck reaction of 4-iodotoluene and styrene. Building on this result, we decided to synthesize a series of Pd(II) complexes based on mono- and multinucleating NNN-pincer ligands (Figure 2.5). Specifically, I synthesized complexes **2.6a**, **2.7**, and **2.8**—which are based on acylic ligands—and complexes **2.10** and **2.11**—which are based on ditopic macrocyclic ligands. To compliment this series of complexes, Dr. Begum synthesized mono[palladium(II)] complex **2.9** and Dr. Wang synthesized tris[palladium(II)] complex **2.12**.

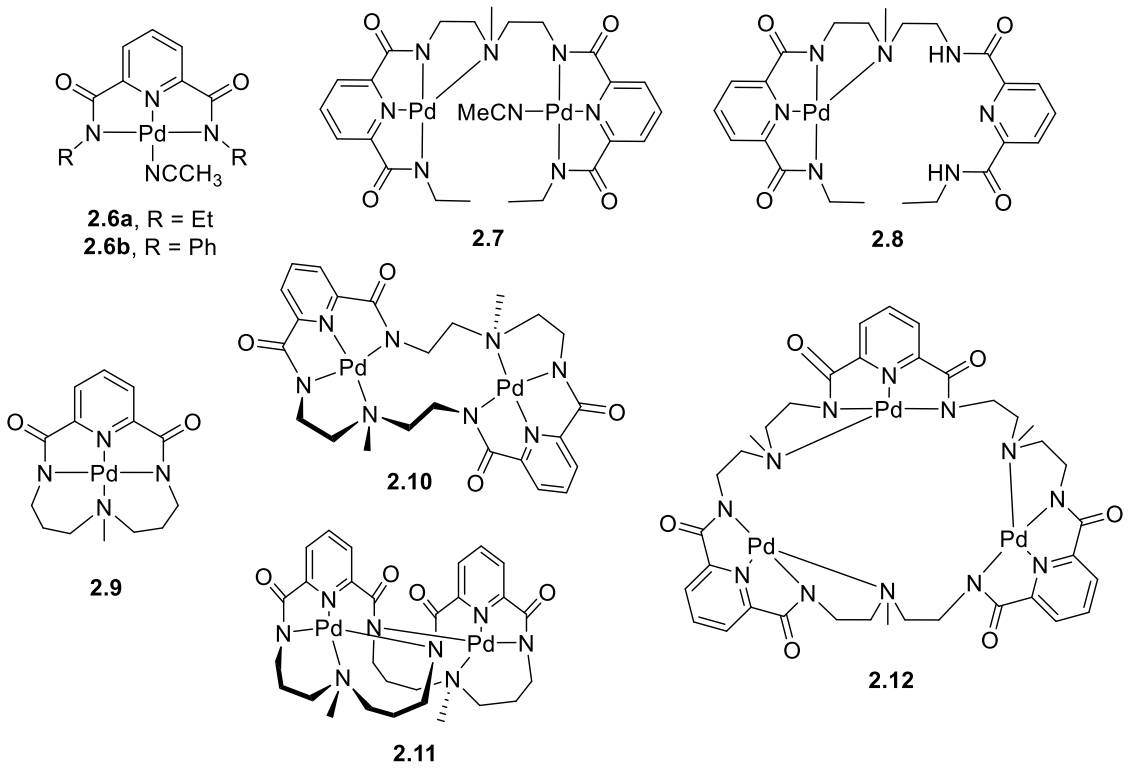

Figure 2.5. Pd(II) NNN-pincer complexes investigated in the Heck reaction by our group.

Synthesis of Pd(II) Complexes from Acyclic Ligands

The Pd(II) NNN-pincer complex **2.6a** was prepared by treatment of a solution of ligand **2.1** in acetonitrile with one equivalent of $Pd(OAc)_2$ (Scheme 2.11). The coordination of Pd(II) was evident from a gradual change in the color of the reaction mixture from maroon to yellow. After 5 hours, the yellow precipitate that formed was filtered and dried to afford **2.6a** as a yellow solid in 60% yield. The ^{1}H NMR data for **2.6a** is consistent with formation of **2.6a**. Most notably, absent from the spectrum is a signal corresponding to H(amide). Further confirmation of the formation of **2.6a** came from the ESI mass spectrum, which contains a prominent ion isotope peak at *m/z* 367.0376 [M + H]$^+$.

Scheme 2.11. Synthesis of Pd(II) NNN-pincer complex **2.6a**.

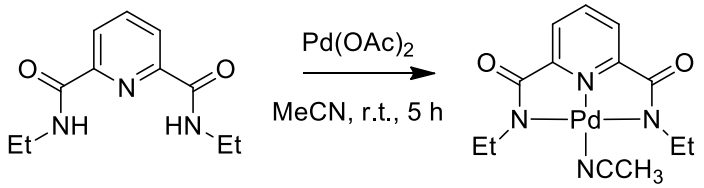

Single crystals of **2.6a** suitable for X-ray diffraction were obtained from a saturated solution of the complex in acetonitrile. The solid state structure of **2.6a** (Figure 2.6) resembles Pd(II) NNN-pincer complexes bearing aromatic amide appendages previously reported by Dell'Amico[31] and Bowman-James.[32-34] The monoclinic unit cell contains a dimer pair in which the molecules are oriented *anti* to each other, with a Pd···Pd distance of 4.247 Å (see Figure A.2.24 in the Appendix). The molecular structure of **2.6a** confirms the NNN-pincer coordination of Pd(II). The N1-Pd-N1S angle is 175.86°, while the N2-Pd-N3 angle is 161.22°. Similar distortion for this N(amide)-Pd-N(amide) angle is common in amide-based Pd(II) NNN-pincer complexes.[31-34] Each of the Pd–N(amide)

bonds are slightly longer than the Pd–N(pyridine) bond (Pd–N3 2.0278 Å; Pd–N2 2.0298 Å; Pd–N1 = 1.9202 Å). The pyridine ring is almost coplanar with the average Pd(II) coordination plane (interplane angle is 6.26°). As expected, the fourth coordination site of Pd(II) is occupied by a molecule of acetonitrile.

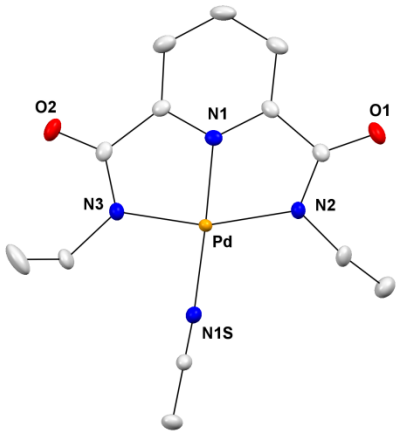

Figure 2.6. Representation of the X-ray crystal structure of complex **2.6a** showing all non-hydrogen atoms as 50% thermal ellipsoids.

The coordination chemistry of the ditopic three-quarter macrocyclic ligand **2.4** was initially studied using two equivalents of $Pd(OAc)_2$ (Scheme 2.12). Ligand **2.4** was added to a solution of $Pd(OAc)_2$ (2 equiv) in acetonitrile, and the reaction mixture was stirred at room temperature for 16 hours. The resulting yellow solution was filtered and triturated with diethyl ether. Over the course of one hour, single crystals emerged from the solution. The solvent was decanted and the crystals were dried to afford bis[palladium(II)] complex **2.7** as a yellow solid in 62% yield. Consistent with the coordination of two Pd(II) atoms was the disappearance of all four proton signals for H(amide) in the ^{1}H NMR spectrum. Further, the aromatic region of the ^{1}H NMR spectrum contains two triplets (which coalesce to form a multiplet) and four doublet of doublets, suggesting that the two Pd(II) atoms are nonequivalent. These data correspond with the tertiary amine coordination of one of the

Pd(II) atoms. Analysis of **2.7** by positive mode ESI-MS confirmed the presence of a bis[palladium(II)] species, with a prominent ion at *m/z* 721.0515 $[M + H]^+$.

Scheme 2.12. Synthesis of Pd(II) complexes **2.7** and **2.8**.

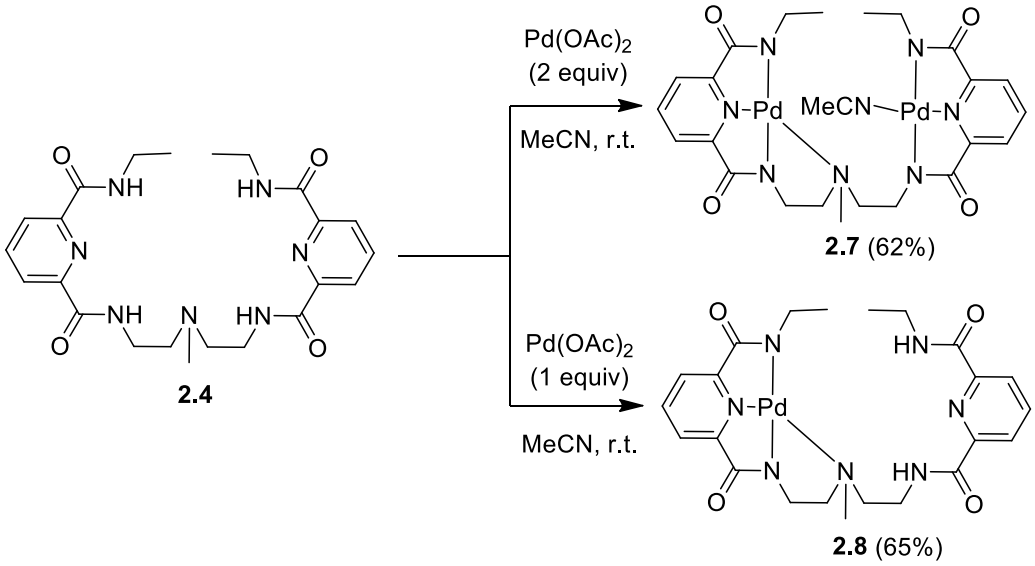

The molecular structure of **2.7** unambiguously confirmed the coordination of two nonequivalent Pd(II) atoms. The relative orientation of the two metal coordination planes observed in the solid state structure for **2.7** closely resembles that of previously reported dinuclear Cu(II) and Ni(II) complexes derived from ditopic macrocyclic ligands (see Scheme 1.21 in Chapter 1).[18] Accordingly, the Pd1···Pd2 distance is close (3.360 Å) to the M···M distance observed in the dinuclear Cu(II) and Ni(II) complexes (3.303 Å and 3.516 Å, respectively). However, in the case of **2.7**, the reason for this U-shape folding is not immediately clear. Despite the relatively short Pd···Pd distance, the distance between the pyridine ring centroids (5.370 Å) is much greater than the analogous distance in the aforementioned Cu(II) and Ni(II) complexes (3.631 Å and 3.719 Å, respectively), which are held together by "face-to-face" π–π stacking interactions. The angle formed between the two pyridine planes is relatively large (20.48°) compared to that of the dinuclear Cu(II)

(13.85°) and Ni(II) (13.21°) complexes. Alternatively, one possible explanation for this folding is that it allows for the electron deficient pyridine rings to interact with the electron rich amide nitrogen or oxygen atom of the opposing pincer site (see Figure A.2.25 in the Appendix); interestingly, the N2···pyridine centroid distance is just 3.538 Å. There is a considerable amount of distortion about Pd1; both the N3-Pd1-N1 (160.94°) and N2-Pd1-N4 (165.26°) angles are much smaller than the expected 180° for an idealized square-planar geometry. Due to the the unsymmetrical coordination of Pd1, the two Pd1–N(amide) distances are different from each other, with the Pd1–N2 bond distance being the shorter of the two by 0.112 Å. Alternatively, the N-Pd-N angles and Pd–N bond distances for Pd2 are similar to those observed in the solid state structure of **2.6a** (*vide supra*).

Another interesting aspect of **2.7** is that all of the molecules in the crystal lattice have the same chirality. The intermolecular pyridine centroid···Pd1 distance is only 3.577 Å. However, the distance between the pyridine centroids of adjacent molecules is 5.440 Å, which is longer than the suggested upper limit of 3.8 Å for parallel-displaced π–π stacking interactions.[35] The adjacent molecules in the crystal lattice of **2.7** form an extended left-handed helix that extends to the adjacent cells. This is evident from the perspective view illustrated in Figure A.2.26 in the Appendix.

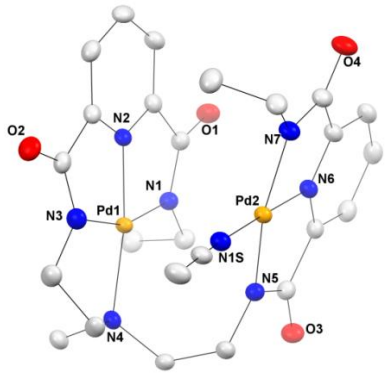

Figure 2.7. Representation of the X-ray crystal structure of complex **2.7** showing all non-hydrogen atoms as 50% thermal ellipsoids.

Whereas the coordination mode of the ligand differs for both of the Pd(II) atoms in bis[palladium(II)] complex **2.10**, we theorized that the tetradentate ligand binds Pd(II) first due to the chelate effect. Thus, we investigated the addition of two equivalents of $Pd(OAc)_2$ to ligand **2.4** on an small scale in DMSO-d_6, and monitored the progress of the reaction by ^{1}H NMR spectroscopy (Figure 2.8). Indeed, after the addition, the ^{1}H NMR spectrum of the reaction mixture showed two signals integrating to one proton each corresponding to H(amide), indicating the formation of a mono[palladium(II)] species. After three hours, the bis[palladium(II)] complex was formed.

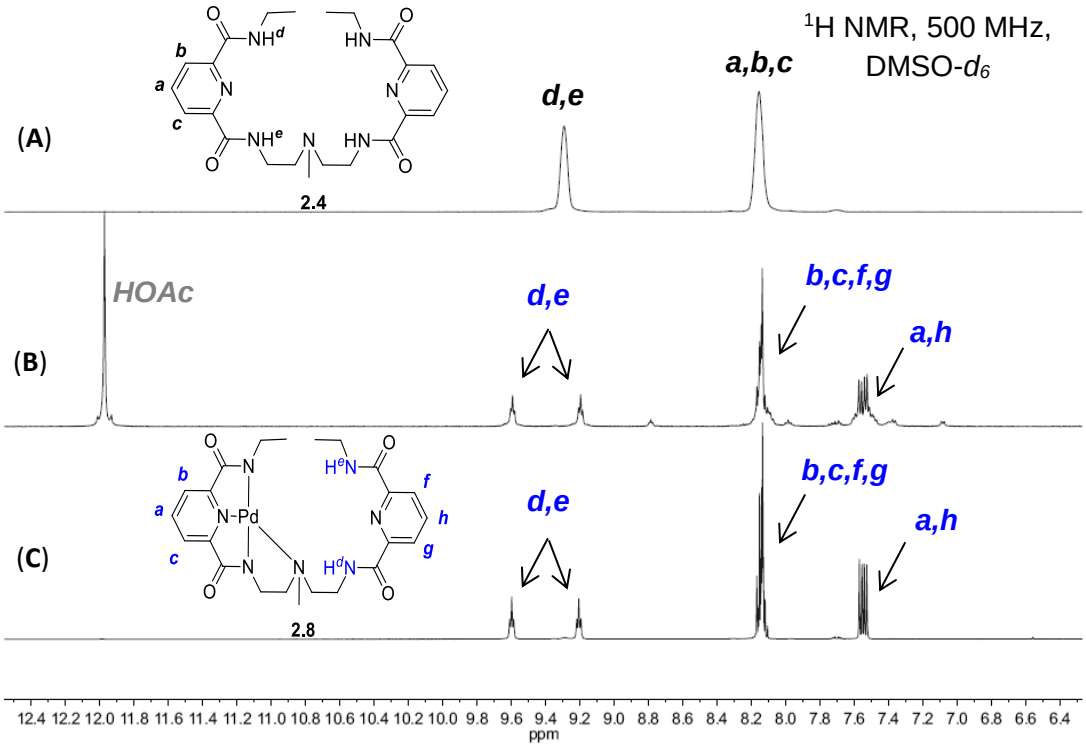

Figure 2.8. ^{1}H NMR spectra of (**A**) three-quarter macrocycle ligand **2.4**, (**B**) addition of $Pd(OAc)_2$ (2 equiv) to **2.4** (5 min after addition), and (**C**) isolated mono[palladium(II)] complex **2.8**.

Based on this result, the synthesis and isolation of the mono[palladium(II)] complex based on ligand **2.4** was attempted. One equivalent of $Pd(OAc)_2$ was added to a solution of **2.4** in acetonitrile**.** After evaporation of the volatiles *in vacuo*, the resulting oil was washed with acetonitrile to give the mono[palladium(II)] complex **2.8** in 65% yield (Scheme 2.12). The relative integrations of the amide (2H) and pyridine (6H) proton signals in the ^{1}H NMR spectrum of **2.8** (Figure 2.8C) correspond to those observed in Figure 2.8B. Further evidence of the formation of **2.8** was a prominent ion peak at *m/z* 574.1385 (Figure 2.9) in the positive mode ESI mass spectrum of the complex,

corresponding to $[M + H]^+$. Furthermore, no ion peak was present corresponding to the bis[palladium(II)] species.

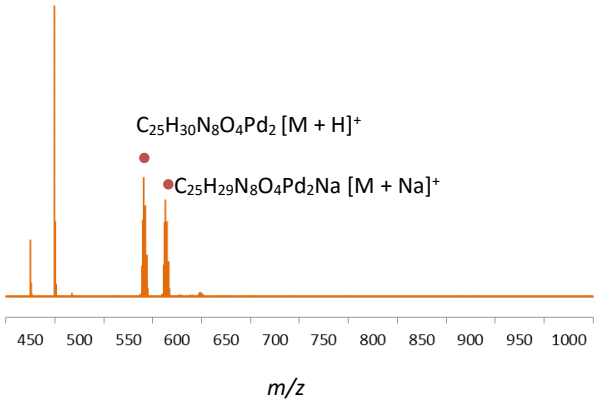

Figure 2.9. Positive mode ESI mass spectrum of complex **2.8**.

Single crystals of **2.8** suitable for X-ray diffraction were grown from slow evaporation of a solution of the complex in acetonitrile. The solid state structure of **2.8** confirms the formation of a mono[palladium(II)] species (Figure 2.10). The intramolecular pyridine ring centroid distance in **2.8** (4.096 Å) is 1.274 Å shorter than the analogous distance in **2.7**. The angle between the two pyridine planes in **2.8** is just 11.68° (compared to 20.48° for the analogous angle in **2.7**). While the Pd–N(amide) distances are shorter than those in **2.7**, the Pd–N(pyridine) distance is slightly longer than the corresponding distance in **2.8**. The Pd–N(amine) distances in **2.7** and **2.8** are within 0.034 Å of each other. Not surprisingly, the extended helical packing that was observed in the crystal lattice for **2.7** is not present in the crystal lattice for **2.8**.

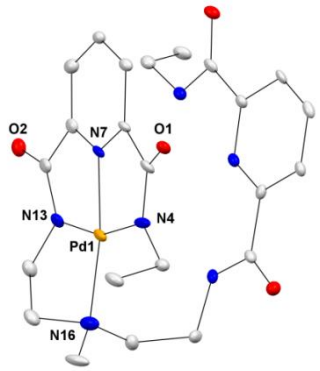

Figure 2.10. Representation of the X-ray crystal structure of complex **2.8** showing all non-hydrogen atoms as 50% thermal ellipsoids.

Synthesis of Pd(II) Complexes from Macrocyclic Ligands

The coordination chemistry of macrocyclic NNN-pincer ligand **2.2** with Pd(II) was first investigated by Dr. Begum. Dr. Begum synthesized complex **2.9** by adding one equivalent of $Pd(OAc)_2$ to an acetonitrile solution of ligand **2.2**. In the X-ray crystal structure of **2.9** (obtained by Dr. Begum), the fourth coordination site is occupied by the N4 tertiary amine (Figure 2.11). While the Pd–N(pyridine) bond distance is similar to the analogous distance in **2.6a**, the average of the two Pd–N(amide) bond distances (2.011 Å) is shorter than that of **2.6a** (2.029 Å). When I repeated the synthesis of **2.9**, the complex was isolated as a yellow powder in 77% yield (Scheme 2.13).

Scheme 2.13. Synthesis of Pd(II) pincer complex **2.9** (first described by Dr. Begum).

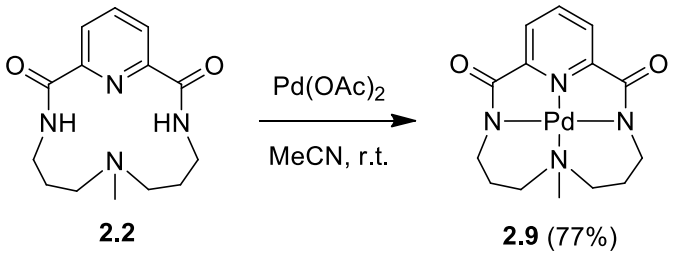

2.2 **2.9** (77%)

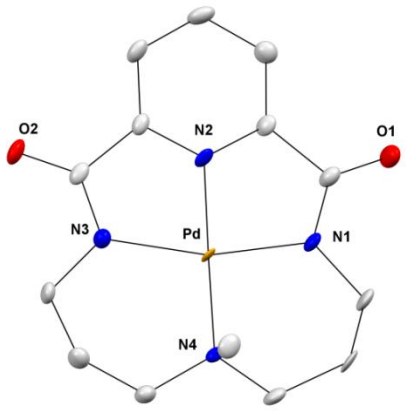

Figure 2.11. Representation of the X-ray crystal structure of complex **2.9** showing all non-hydrogen atoms as 75% thermal ellipsoids.

The bis[palladium(II)] macrocyclic complex **2.10** was synthesized by treating an acetonitrile suspension of ethylene-linked ditopic macrocyclic ligand **2.3a** with two equivalents of $Pd(OAc)_2$ (Scheme 2.14). Over the course of the reaction, a yellow precipitate formed, which was filtered and dried to afford **2.10** in 88% yield. Complex **2.10** is not soluble at room temperature in deuterated organic solvents ($CDCl_3$, CD_3CN, MeOD, DMSO-d_6) or in D_2O, which made characterization by NMR spectroscopy impossible. Due to this low solubility of the complex, analysis by mass spectrometry also was unsuccessful.

Scheme 2.14. Synthesis of bis[palladium(II)] complexes **2.10** and **2.11** from ditopic ligands **2.3a** and **2.3b**.

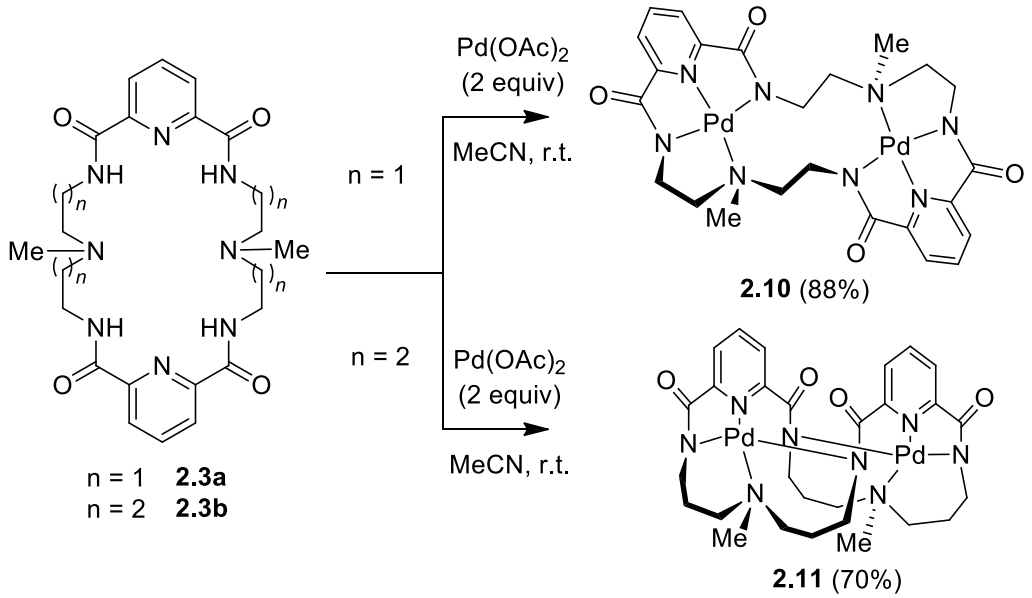

Attempts to crystallize **2.10** from refluxing solutions of DMSO or MeCN did not afford crystals. Surprisingly, when the complex was heated in $CHCl_3$, single crystals suitable for X-ray diffraction were formed while slowly cooling the cloudy suspension to room temperature. The solid state asymmetric unit contains a dimer pair (see Figure A.2.27 in the Appendix), with each molecule having an inversion center. The individual molecules fold in a chair-like conformation (Figure 2.12), similar to the folding of the (*Z*)-bis(palladium) macrocyclic complex reported by Tsukuda and coworkers (Figure 2.3, *vide supra*).[14] In addition to the N1-Pd-N3 distortion also observed in complexes **2.6a**, **2.7**, **2.8**, and **2.9**, the N2-Pd-N4 angle (162.6°) is considerably distorted from idealized square planar geometry. An analogous distortion was observed in complexes **2.7** and **2.8** for the unsymmetrically-coordinated Pd(II) atom. The intramolecular Pd···Pd distance of 5.577 Å is greater than that of bimetallic complex **2.7**, which folds in a U-shape. Complex **2.10**

stacks with channels of chloroform molecules of solvation in between dimer pairs of the complex (see Figure A.2.28 in the Appendix).

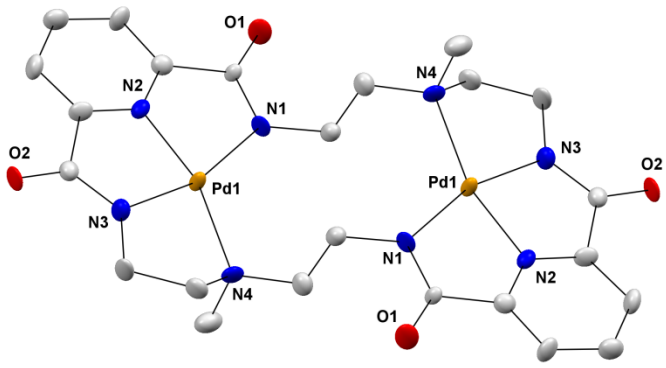

Figure 2.12. Representation of the X-ray crystal structure of **2.10**, showing all non-hydrogen atoms as 50% thermal ellipsoids.

In order to synthesize the propylene-linked ditopic Pd(II) NNN-pincer complex **2.11**, two equivalents of $Pd(OAc)_2$ were added to an acetonitrile solution of ligand **2.3b** (Scheme 2.14). Unlike ethylene-linked complex **2.10**, **2.11** did not precipitate from the crude reaction mixture. Instead, evaporation of the solvent afforded **2.11** as a yellow solid in 70% yield. The aromatic region of ^{1}H NMR spectrum of **2.11** consists of one triplet and two doublet of doublets corresponding to the pyridine protons. The presence of two palladium atoms was supported by the positive mode ESI mass spectrum, which displays a prominent ion peak at *m/z* 763.1010 $[M + H]^+$.

Crystals of complex **2.11** were obtained from slow evaporation of a saturated solution of the complex in acetonitrile. While the X-ray crystal structure of **2.11** (Figure 2.13) confirmed the presence of two Pd(II) atoms, we were surprised to find the Pd(II) atoms were not coordinated in the same manner as those in **2.10**. Each Pd(II) atom is coordinated to a pyridine and amide nitrogen from one pincer site, an amide nitrogen from

the opposite pincer site, and a tertiary amine. This unique coordination results in a relatively twisted molecule; the angle that the average Pd(II) coordination plane forms with the coordinated pyridine (18.29°) is greater than the analogous angles in complexes **2.10** and **2.6a** (12.19° and 6.26°, respectively). Despite the unique conformation of the molecule, the two Pd(II) atoms in **2.11** lie in a considerably less distorted square planar environment compared to those in bimetallic complex **2.10** (for **2.11**: N1-Pd-N4 170.9°; N2-Pd-N3 171.0°). Another distinctive feature of **2.11** is that the Pd–N(pyridine) bond distances in **2.11** are greater than those observed in any other complex reported in this Chapter (for a comprehensive list of the coordinated ligand distances for each complex, see Tables A.2.3 through A.2.9 in the Appendix). The Pd···Pd distance in **2.11** of 5.314 Å is shorter in **2.11** than the analogous distance in **2.10** (5.577 Å). Despite the relatively short intramolecular pyridine···pyridine centroid distance of 3.928 Å, the angle formed between the two pyridine planes is too large (36.47°) for face-to-face or edge-to-face π–π stacking interactions to be considered driving force for the folding observed in **2.11**.

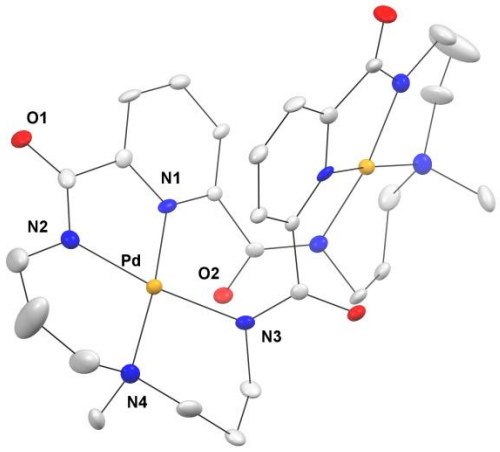

Figure 2.13. Representation of the X-ray crystal structure of complex **2.11** showing all non-hydrogen atoms as 50% thermal ellipsoids.

To complement the series of monotopic and ditopic macrocycles, Dr. Wang investigated the coordination chemistry of tritopic macrocyclic ligand **2.5** with Pd(II). Dr. Wang synthesized complex **2.12** by adding three equivalents of $Pd(OAc)_2$ to an acetonitrile solution of ligand **2.5**. Crystals of complex **2.12** suitable for X-ray analysis were obtained by Dr. Wang from a concentrated solution of the complex in DMF. The X-ray crystal structure of **2.12** (Figure 2.14) confirms the presence of three palladium atoms, all of which contain the same hybrid pincer/amine tetradentate coordination of the ligand. The asymmetric unit contains two crystallographically-independent trinuclear molecules with virtually identical conformations (see Figure A.2.29 in the Appendix). As opposed to bimetallic complexes **2.10** and **2.11**, complex **2.12** does not contain a crystallographic center of inversion; for example, the Pd–N(pyridine) distances differ for each of the three Pd(II) atoms (1.937, 1.918, and 1.926 Å). The angle formed between pyridine ring and the average coordination plane of Pd3B (6.14°) is relatively small compared to that of bimetallic complexes **2.10** (12.19°) and **2.11** (18.29°), and comparable to that of monometallic complex **2.6a** (6.26°).

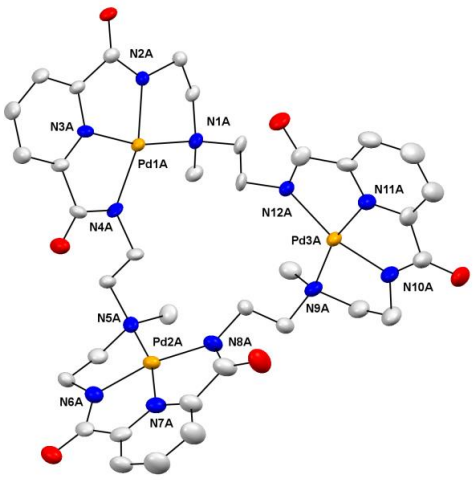

Figure 2.14. Representation of the X-ray crystal structure of complex **2.12**, showing all non-hydrogen atoms as 50% thermal ellipsoids.

2.3.4 *Catalysis Studies*

The catalytic activity of these complexes was evaluated in the Heck reaction of 4-iodotoluene and styrene. After the complexes were recrystallized and dried, they were dissolved in *N*,*N*-dimethylacetamide (DMA) and the corresponding amount of catalyst was added to a DMA (5 mL) solution of 4-iodotoluene (1 equiv), NaOAc (1.1 equiv), tetrabutylammonium bromide (0.2 equiv) in a 25 mL three-necked flask. Once the temperature of the oil bath reached 165 ^{o}C, neat styrene (1.4 equiv) was added, and aliquots were removed every 15 minutes and analyzed by ^{1}H NMR spectroscopy. The reaction products are *trans* and *geminal* 4-methylstilbene. The ratio of the two products is the same, regardless of the catalyst used (ratio of *trans* to *gem* 4-methylstilbene = 5.25:1). The results of these catalytic studies are summarized in Table 2.1.

Complete conversion to 4-methylstilbene was observed after one hour with monometallic complex **2.6a** (Table 2.1, entry 1) and 0.5 h with bimetallic complex **2.7** (Table 2.1, entry 2). Figure 2.15 shows the time course of the Heck reaction using complexes **2.6a**, **2.7**, and **2.8**, which are derived from acyclic ligands. The most prominent induction period was observed with **2.8** (2.48 h), which contains just one Pd(II) atom that chelates a tetradentate ligand (Table 2.1, entry 3). The induction period observed with **2.8** can be attributed to the increased chelate effect imparted by the tetradentate pincer ligand relative to the chelate effect of the tridentate pincer ligand alone in complex **2.6a** and **2.7**. Whereas **2.7** contains a Pd(II) atom that is bound by a tridentate ligand, it would be expected to decompose first and is likely responsible for the observed catalytic activity. Together, the observation of induction periods and the varience in induction periods using complexes with tridentate or tetradentate ligands support the proposed mechanism of the

Table 2.1. Heck coupling of 4-iodotoluene with styrene using complexes **2.6a**, **2.7**, **2.8**, **2.9**, **2.10**, **2.11**, and **2.12**.[a]

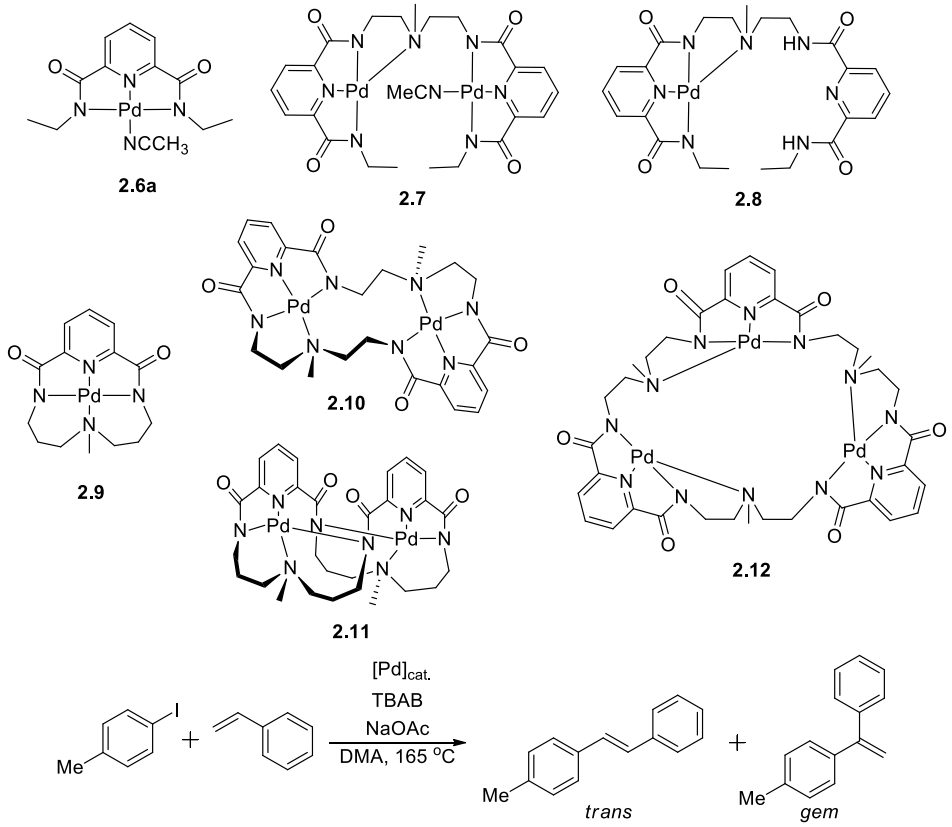

Catalyst	Time (h)	Induction (h)	Conversion (*trans*+*gem*)[b]
2.6a	1	0.46	>99%
2.7	0.75	--	>99%
2.8	3	2.48	>99%
2.9	48	2.86	95%
2.10	0.5	--	>99%
2.11	0.25	--	>99%
2.12	0.75	0.19	>99%

[a]Reaction conditions: styrene (1.4 equiv), NaOAc (1.1 equiv), *n*-Bu_4NBr (20 mol %), 1 x 10^{-1} mol % Pd, DMA, 165 °C. [b]^1H NMR conversion by comparing the relative integrations for of *trans* and *gem*-methylstilbene to the starting material, 4-iodotoluene.

Heck reaction, which involves decomposition of the Pd(II) pincer complex to form catalytically active Pd(0) (see Chapter 1), and is in line with the observation by Eberhard that catalytic activity is proportional to complex stability.[36]

Figure 2.16 shows the time course of the Heck reaction using complexes **2.9**, **2.10**, **2.11**, and **2.12**, which are derived from macrocyclic ligands. The coupling reaction took 48 h to reach 95% conversion to 4-methylstilbene using **2.9** (Table 2.1, entry 4). The long induction period observed with complex **2.9** (2.86 h) can be explained by the multiple juxtopositional fixedness of the monotopic macrocyclic tetradentate ligand, which helps to stabilize the resulting Pd(II) complex via the "macrocyclic effect." Conversely, complexes **2.10**, **2.11**, and **2.12**—which are based on multitopic macroycles—exhibited catalytic activities more similar to that of the acyclic complexes derived from tridentate pincer ligands. These floppy macrocyclic ligands do not have the same level of prearrangement as that seen with the monotopic ligand and thus would not be expected to benefit from the macrocyclic effect. Notably, the Pd–N4 (tertiary amine) bond distance in **2.9** (2.054 Å) is shorter than the corresponding distance in **2.10** (2.120 Å), **2.11** (2.085 Å), and **2.12** (average = 2.086 Å), suggesting that the Pd–N4 bonds in the latter complexes are more prone to substitution compared to the Pd–N4 bond in **2.9**.

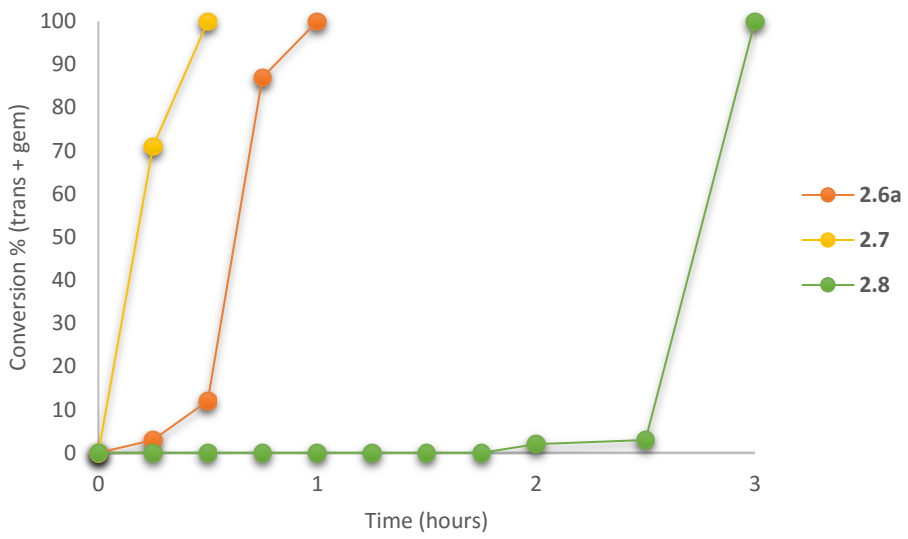

Figure 2.15. Time course showing the formation of *trans*- and *gem*-stilbene for acycles **2.6a, 2.7,** and **2.8.**

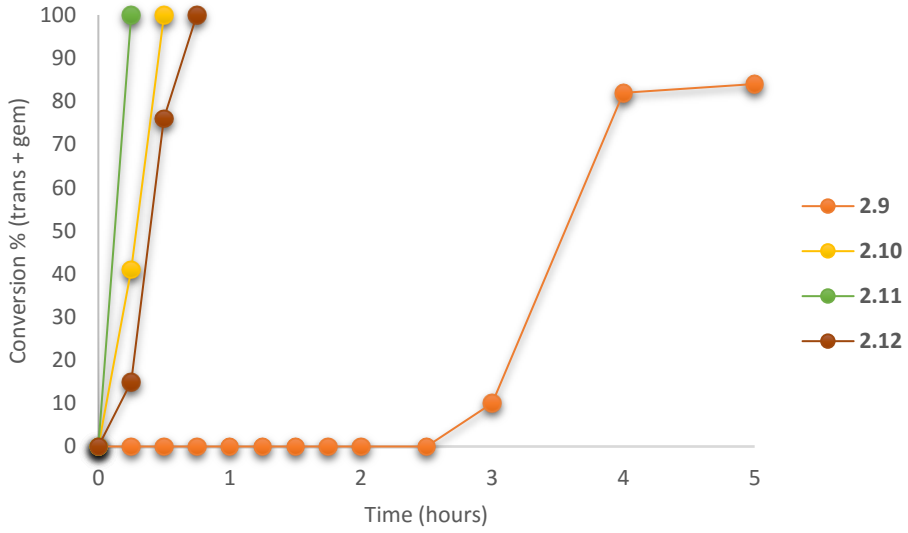

Figure 2.16. Time course showing the formation *trans*- and *gem*-stilbene for macrocycles **2.9, 2.10, 2.11,** and **2.12**.

Palladium black was observed in all catalytic runs. Thus, we performed experiments using **2.6a** or **2.9** in DMA in the absence of the Heck reagents (4-iodotolune, styrene, NaOAc, and TBAB) to verify that the visual detection of palladium black was due to the Pd(II) pincer source. The visual detection of Pd black—as indicated by a color change of the solution from yellow to dark grey/black—was observed after two hours in the case of **2.6a**, but was not observed for 48 hours with **2.9**. Compared with the catalysis results, these data further suggest that the catalytic activity of these complexes is a function of their stabilities.

Intramolecular Heck Reaction in 1,4-dioxane

The potential for developing a tandem one-pot RCM/Heck reaction was studied by attempting the intramolecular Heck reaction of **2.13** in 1,4-dioxane (Scheme 2.15), which we have found in preliminary studies to be a suitable solvent for the RCM reaction in the synthesis of **2.13**. Although the use of 1,4-dioxane in metathesis reactions is rare, similar ethereal solvents are known to be suitable for RCM reactions.[37] Conversely, there is no precedent for a Pd(II) pincer complex-mediated cross coupling reaction in 1,4-dioxane. These reactions were performed on a 0.25 mmol scale with respect to **2.14**. Substrate **2.14** (1 equiv), NaOAc (1.1 equiv), tetrabutylammonium bromide (0.2 equiv), and either **2.6a** or **2.6b** (10 mol %) were dissolved in 1,4-dioxane (2.5 mL) in a sealed tube and the mixture was stirred at 165 ^{o}C for 6 h. Following evaporation of the solvent from the reaction mixture, the crude products were purified via silica gel flash column chromatography to afford the expected product **2.14** in 73% yield. When **2.6b** was employed as the catalyst, a 55% yield was obtained.

Scheme 2.15. The intramolecular Heck reaction of compound **4.2** using Pd(II) NNN-pincer complexes **2.6a** and **2.6b**. [a]Isolated yields.

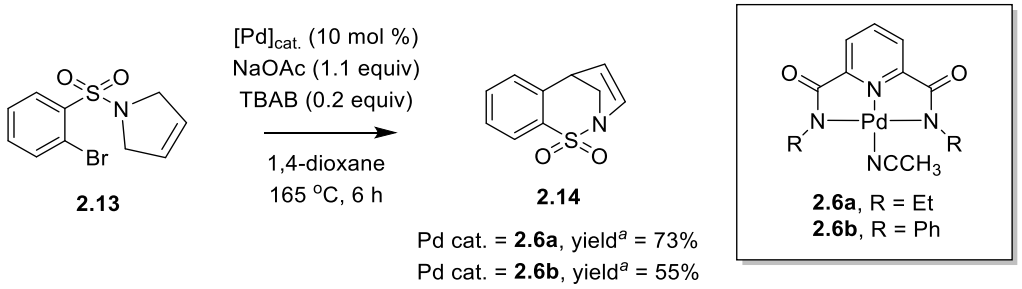

2.4 *Concluding Remarks*

In this chapter, the chemistry of Pd(II) complexes synthesized from acyclic and macrocyclic amide-based NNN-pincer ligands was discussed. In the simplest case, tridentate NNN-pincer ligand **2.1** deprotonates to form the distorted square-planar Pd(II) complex **2.6a**. Alternatively, if an amine functional group is tethered one or both of the amides, the donor ligand coordinates Pd(II) in a tetradentate fashion, as seen in complexes **2.7**–**2.12**. The catalytic activities of these complexes were evaluated in the Mizoroki-Heck reaction of 4-iodotoluene and styrene. To the best of our knowledge, this work represents the first examples of amide-based Pd(II) NNN-pincer complexes being investigated in the Heck reaction. Pincer complexes synthesized from acyclic tridentate pincer ligands did not show an induction period on our sampling time scale. Induction periods were observed using complexes **2.8**—which is stabilized by a chelate effect—and **2.9—**which is stabilized by the macrocyclic effect. Together, these results support earlier work on PCP- and SCS-pincer complexes[36] which suggests that Pd(II) pincer complexes decompose under the harsh conditions employed for Heck reaction to generate catalytically active Pd(0). On the other hand, multimetallic complexes **2.10**, **2.11**, and **2.12**—which were synthesized from floppy macrocyclic ligands—do not benefit from the mmacrocyclic effect and were thus were much more efficient in generating the active catalyst. Pd(II) pincer complexes **2.6a** and **2.6b** were demonstrated to mediate the intramolecular Heck reaction of **2.13** in 1,4-dioxane. Whereas the pincer-ligated Pd(II) complex prevents undesired interferences between Ru(II) (in the form of Grubbs catalyst)

and Pd(II), studies are currently underway to apply this reaction to a one-pot RCM/Heck protocol.

2.5 *Materials and Methods*

2.5.1 *General*

$Pd(OAc)_2$ was purchased from Aldrich. Other chemicals were reagent grade and were used as received without further purification. Pd(II) complex **2.6b**[31] were synthesized using previously described procedure. The starting material for intramolecular Heck reactions (**2.13**) was prepared in two steps from *N*,*N*-Diallyl-2-bromobenzenesulfonamide according to a previously described procedure.[38] All reactions were carried out under ambient conditions. Flash column chromatography was performed using 32-63 mm silica gel (Sorbent). Nuclear magnetic resonance (NMR) spectra were recorded on a Bruker Avance 400 spectrometer or a Bruker Avance 500 spectrometer. Chemical shifts of the ^{1}H and ^{13}C resonances are expressed in ppm, and referenced to the residual solvent signal. Mass spectral data were obtained from the Mass Spectrometry Laboratory at the University of Kansas on a LCT Premier Mass spectrometer. Single-crystal XRD data were obtained at the Small-Molecule X-ray Crystallography Laboratory at the University of Kansas by Dr. Victor Day.

2.5.2 *Synthesis of Ligands*

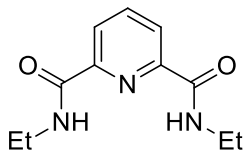

2.1

Ligand 2.1. To a solution of dimethyl 2,6-pyridinedicarboxylate (0.390 g, 2 mmol) in 15 mL methanol was bubbled ethylamine for one minute and the reaction was stirred at room temperature. After 16 h, the starting material was consumed, as indicated by TLC. Solvent was evaporated *in vacuo* and product was dried to afford **2.1** as a white solid (0.369 g,

1.665 mmol, 83%). ^{1}H NMR (500 MHz, $CDCl_3$) δ 8.36 (d, J = 7.8 Hz, 2H), 8.02 (t, J = 7.7 Hz, 1H), 7.80 – 7.65 (br, 2H), 3.59 – 3.54 (m, 4H), 1.30 (t, J = 7.3 Hz, 6H); ^{13}C NMR (126 MHz, $CDCl_3$) δ 163.6, 149.1, 139.2, 125.1, 34.7, 15.2; HRMS (ESI^+) *m/z:* $[M + Na]^+$ calculated for $C_{11}H_{15}N_3NaO_2$ 244.1057; found 244.1038.

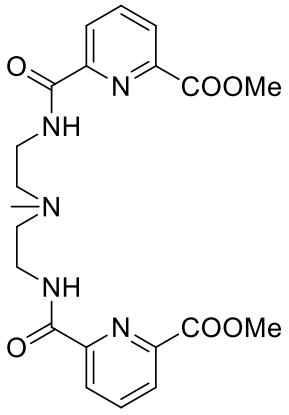

C

Intermediate C. Using a procedure previously reported by Dr. Wang,[27] a solution of *N*-methyl-2,2'-diamino diethylamine (3.51 g, 3.86 mL, 30 mmol) in MeOH (100 mL) was added dropwise over 2h to a solution of dimethyl 2,6-pyridinedicarboxylate (23.4 g, 120 mmol) in MeOH (150 mL) and stirred at reflux for 3 d. Unreacted dimethyl-2,6-pyridinedicarboxylate was collected after gravity filtration and the filtrate was concentrated and purified via flash chromatography using 90:10 DCM-MeOH to afford **C** as a white solid (7.36 g, 16.6 mmol, 55%). ^{1}H NMR (500 MHz, CD_3OD) δ 8.07 (dd, J = 7.7, 1.1 Hz, 1H), 8.02 (dd, J = 7.8, 1.1 Hz, 1H), 7.94 (t, J = 7.8 Hz, 1H), 3.86 (s, 3H), 3.47 (t, J = 6.4 Hz, 4H), 2.65 (t, J = 6.4 Hz, 4H), 2.34 (s, 3H); ^{13}C NMR (126 MHz, MeOD) δ 166.7,

165.8, 151.6, 147.6, 140.4, 128.6, 126.5, 57.0, 53.8, 42.8, 38.5; HRMS (ESI^+) *m/z:* $[M + H]^+$ calculated for $C_{21}H_{26}N_5O_6$ 444.1878; found 444.1898.

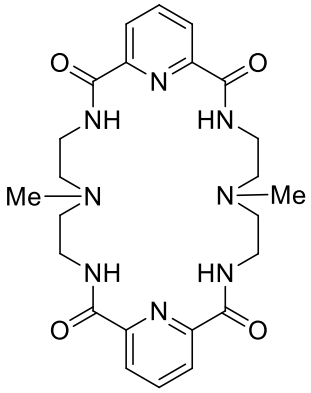

2.3a

Ligand 2.3a. Using a procedure previously reported by Dr. Wang,[27] compound **C** (0.886 g, 2 mmol) was added to a methanolic solution of *N*-methyl-2,2'-diaminodipropylamine (0.234g, 2 mmol) and the resulting solution was refluxed for 3 d. Upon cooling, a white precipitate formed, which was filtered and dried to afford the product as a white solid (0.456 g, 0.918 mmol, 45%). ^1H NMR (500 MHz, CD_3OD) δ 8.00 (d, J = 7.24 Hz, 4H), 7.92 (t, J = 8.52 Hz, 2H), 3.56 (t, J = 5.38 Hz, 8H), 2.81 (t, J = 5.33 Hz, 8H), 2.49 (s, 6H); ^{13}C NMR (126 MHz, CD_3OD) δ 165.6, 149.8, 140.3, 125.4, 57.0, 42.5, 38.6; HRMS (ESI^+) *m/z:* $[M + H]^+$ calculated for $C_{24}H_{33}N_8O_4$ 497.2625; found 497.2620.

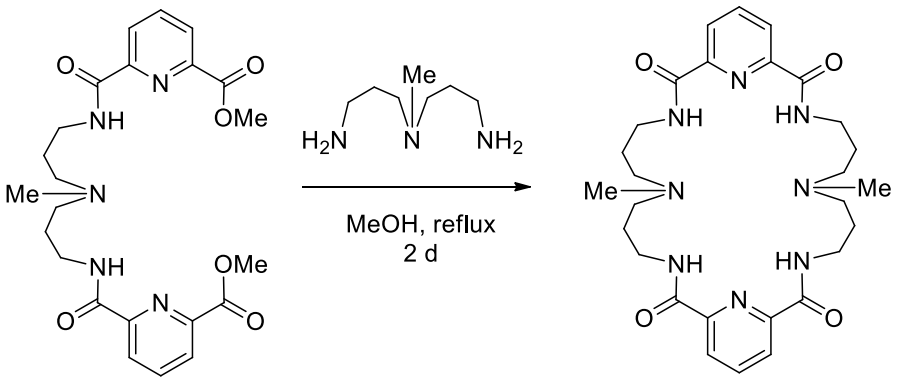

Ligand 2.3b. This ligand was prepared from compound **D** (provided by Thomas Robben) in the same manner as ligand **2.3a** (0.597 g, 1.080 mmol, 51%). ^{1}H NMR (500 MHz, $CDCl_3$) δ 8.67 – 8.56 (br, 4H), 8.27 (d, J = 7.8, 4H), 7.98 (t, J = 7.8, 2H), 3.55 (q, J = 6.5, 8H), 2.57 – 2.43 (br, 8H), 2.25 (s, 6H), 1.93 – 1.82 (br, 8H); ^{13}C NMR (126 MHz, CD_3OD) δ 164.2, 149.3, 139.0, 125.0, 56.7, 42.3, 38.9, 27.1; HRMS (ESI$^+$) *m/z*: $[M + H]^+$ calculated for $C_{28}H_{41}N_8O_4$ 553.3246; found 553.3250.

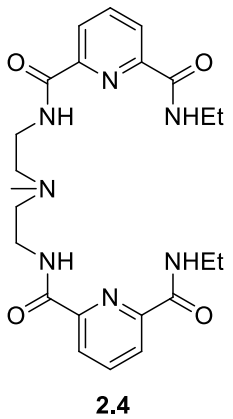

2.4

Ligand 2.4. Using a modified protocol of one initially developed by Dr. Begum,[28] a sealed tube was charged with **C** (223 mg, 0.5 mmol), which was dissolved in methanol, and $EtNH_2$ was bubbled through the solution for one minute and stirred at room temperature. After 16 h, the solvent was evaporated *in vacuo* to give a clear oil. After dissolving the oil in

MeCN and evaporating 3x, the desired product was obtained as a hygroscopic white powder (0.224 g, 0.477 mmol, 96%). ^{1}H NMR (500 MHz, $CDCl_3$) δ 8.63 (t, J = 5.8, 2H), 8.49 (t, J = 5.9, 2H), 8.22 (dd, J = 7.8, 1.1 Hz, 2H), 8.16 (dd, J = 7.8, 1.1 Hz, 2H), 7.89 (t, J = 7.8 Hz, 2H), 3.52 (q, J = 6.1, 4H), 3.41 (quint, J = 7.2, 4H), 2.60 (t, J = 6.1, 4H), 2.32 (s, 3H), 1.16 (t, J = 7.3, 6H); ^{13}C NMR (126 MHz, $CDCl_3$) δ 164.3, 163.6, 149.1, 148.6, 139.0, 125.0, 124.6, 56.4, 43.1, 37.6, 34.6, 14.9; HRMS (ESI^+) *m/z:* $[M + H]^+$ calculated for $C_{23}H_{32}N_7O_4$ 470.2511; found 470.2490.

2.5.3 *Synthesis of Complexes*

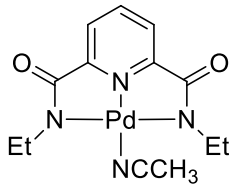

2.6a

Complex 2.6a. Ligand **2.1** (0.056 g, 0.25 mmol, 1 equiv) and $Pd(OAc)_2$ (0.056 g, 0.25 mmol, 1 equiv) were dissolved in acetonitrile (10 mL) and the mixture was stirred for 5 h. The resulting precipitate was filtered to afford the product as a crystalline yellow solid (0.056 g, 0.15 mmol, 60%). This solid was recrystallized from acetonitrile to yield large yellow crystals which were used for XRD and catalysis studies. ^{1}H NMR (500 MHz, DMSO-d_6) δ 8.15 (t, J = 7.8 Hz, 1H), 7.54 (d, J = 7.8 Hz, 2H), 3.07 (q, J = 7.0 Hz, 4H), 1.07 (t, J = 7.0 Hz, 6H); ^{13}C NMR (126 MHz, DMSO-d_6) 168.8, 152.8, 141.3, 123.7, 39.5, 15.5; HRMS (ESI^+) *m/z*: $[M + H]^+$ calculated for $C_{13}H_{17}N_4O_2Pd$ 367.0386; found 367.0376.

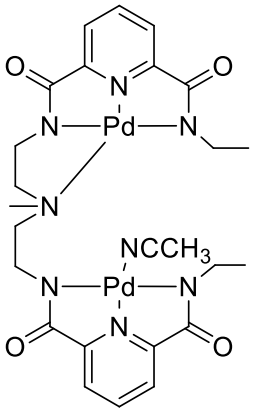

2.7

Complex 2.7. Ligand **2.4** (0.024 g, 0.050 mmol, 1 equiv) was added to a solution of $Pd(OAc)_2$ (0.022 g, 0.10 mmol, 2 equiv) in acetonitrile (5 mL), and the reaction mixture was stirred for 16 h. The resulting yellow solution was filtered through a pipette containing celite. Diethyl ether was added to the filtrate, which formed a crystalline solid suitable for XRD studies over the course of 1 h (0.056 g, 0.077 mmol, 62%). ^{1}H NMR (500 MHz, MeCN-d_3) δ 8.03 – 7.96 (m, 1H), 7.52 (dd, J = 7.8, 1.2 Hz, 1H), 7.44 (dd, J = 7.8, 1.0 Hz, 1H), 7.37 (dd, J = 7.8, 1.2 Hz, 1H), 7.32 (dd, J = 7.8, 1.0 Hz, 1H), 4.04 – 4.01 (m, 1H), 3.56 – 3.44 (m, 4H), 3.30 – 3.26 (m, 1H), 3.19 – 3.06 (m, 2H), 2.93 (s, 3H), 2.86 – 2.79 (m, 2H), 2.45 – 2.37 (m, 2H), 0.98 (t, J = 7.1 Hz, 3H), 0.89 (t, J = 7.1 Hz, 3H); ^{13}C NMR (126 MHz, MeCN-d_3) δ 170.7, 169.0, 168.8, 166.8, 154.6, 152.8, 152.1, 142.0, 141.3, 124.2, 124.1, 123.7, 66.1, 61.3, 49.0, 43.6, 43.3, 41.2, 40.6, 15.5, 15.4; HRMS (ESI$^+$) *m/z*: $[M + H]^+$ calculated for $C_{25}H_{31}N_8O_4Pd_2$ 721.0537; found 721.0515.

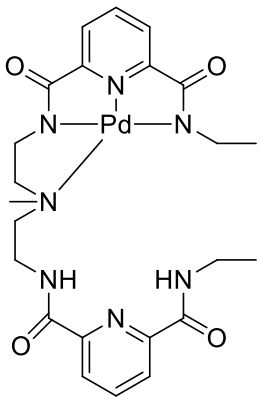

2.8

Complex 2.8. A solution of ligand **2.4** (0.114 g, 0.25 mmol, 1 equiv) in acetonitrile (20 mL) was slowly added to a solution of $Pd(OAc)_2$ (0.056 g, 0.25 mmol) in acetonitrile (10 mL). After stirring for 5 min, the solution became yellow. The reaction mixture was allowed to stir for an additional 16 h, at which a yellow precipitate was observed. The solvent was evaporated and the resulting yellow oil was washed with acetonitrile to afford the product as a yellow powder (0.083 g, 0.16 mmol, 65%). Recrystallization from acetonitrile afforded crystals suitable for XRD studies. ^{1}H NMR (500 MHz, DMSO-d_6) δ 9.60 (t, J = 5.9, 1H), 9.21 (t, J = 6.1, 1H), 8.17 – 8.12 (m, 4H), 7.56 (dd, J = 7.9, 1.1 Hz, 1H), 7.53 (dd, J = 7.8, 1.1 Hz, 1H), 3.99 – 3.94 (m, 2H), 3.58 – 3.52 (m, 2H), 3.47 – 3.40 (m, 2H), 3.28 – 3.17 (m, 2H), 2.91 (s, 3H), 2.88 – 2.82 (m, 4H) 1.16 (t, J = 7.2 Hz, 3H), 1.06, (t, J = 7.0 Hz, 3H); ^{13}C NMR (126 MHz, DMSO-d_6) δ 169.3, 166.1, 163.4, 162.6, 154.0, 152.3, 148.6, 148.2, 141.6, 140.0, 124.1, 124.0, 123.5, 67.6, 58.6, 48.4, 42.9, 41.1, 36.8, 33.6, 15.6, 15.0; HRMS (ESI$^+$) *m/z*: $[M + H]^+$ calculated for $C_{23}H_{30}N_7O_4Pd$ 574.1389; found 574.1385.

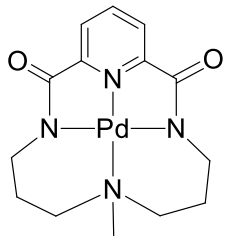

2.9

Complex 2.9. Using a procedure first carried out by Dr. Begum, ligand **2.2** (39 mg, 0.139 mmol, 1 equiv) was added to a solution of $Pd(OAc)_2$ (31 mg, 0.139 mmol, 1 equiv) in acetonitrile (5 mL). The orange mixture was stirred at r.t. for 16 h. The volatiles were evaporated *in vacuo*, and the crude product was washed with diethyl ether (3 x 5 mL) to afford **2.9** as a yellow solid (41 mg, 0.107 mmol, 77%). ^{1}H NMR (500 MHz, DMSO-d_6) δ 8.15 (t, J = 7.9 Hz, 1H), 7.61 (d, J = 7.8 Hz, 2H), 3.65 – 3.60 (m, 2H), 3.38 – 3.30 (m, 2H), 3.12 (t, J = 12.4 Hz, 2H), 3.01 – 2.94 (m, 2H), 2.69 (s, 3H), 2.12 – 2.04 (m, 2H), 1.83 (d, J = 16.5 Hz, 2H); ^{13}C NMR (126 MHz, DMSO-d_6) δ 169.7, 151.8, 141.5, 123.3, 60.4, 43.8, 43.1, 25.7; HRMS (ESI$^+$) *m/z* [M + H]$^+$ calculated for $C_{14}H_{19}N_4O_2Pd$ 381.0538; found 381.0529.

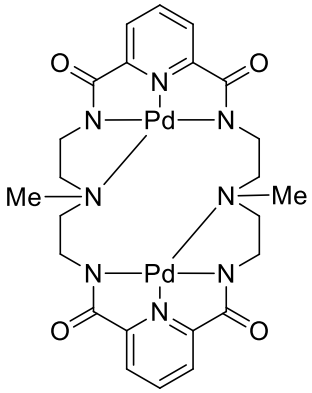

2.10

Complex 2.10. Ligand **2.3a** (0.098 g, 0.2 mmol, 1 equiv) was added to an acetonitrile (20 mL) solution of $Pd(OAc)_2$ (0.088 g, 0.4 mmol, 2 equiv). The resulting yellow mixture was stirred for 1 d. The solvent was removed *in vacuo* to give the product as a yellow solid (0.125 g, 0.176 mmol, 88%). Crystals suitable for XRD analysis were grown from a saturated solution of the complex in $CHCl_3$. Due to the low solubility of the complex in a number of solvents, including $CDCl_3$, CD_3CN, DMSO-d_6, DMF, and D_2O, however, NMR and mass spectrometric data were unable to be obtained.

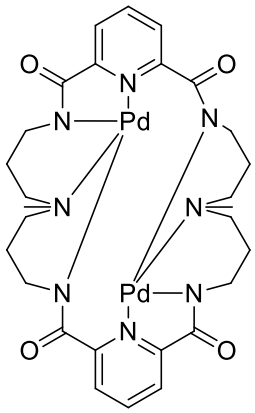

2.11

Complex 2.11. Ligand **2.3b** (0.053 g, 0.096 mmol, 1 equiv) and $Pd(OAc)_2$ (0.043 g, 0.192 mmol, 2 equiv) were suspended in acetonitrile (10 mL) and the reaction mixture was stirred for 16 h at r.t. The solvent was concentrated and the resulting yellow solution was filtered

through a small pipette containing celite. Yellow crystals of the product were obtained from slow evaporation of this acetonitrile solution (0.050 g, 0.067 mmol, 70%). ^{1}H NMR (500 MHz, DMSO-d_6) δ 8.15 (t, J = 7.8 Hz, 2H), 7.61 (dd, J = 7.8, 1.2 Hz, 2H), 7.58 (dd, J = 7.7, 1.2 Hz, 2H), 3.93 – 3.89 (m, 2H), 3.49 – 3.46 (m, 2H), 3.22 – 3.17 (m, 2H), 2.82 (s, 3H), 2.69 – 2.59 (m, 2H), 2.40 – 2.33 (m, 2H), 1.83 – 1.72 (m, 2H); ^{13}C NMR (126 MHz, DMSO-d_6) δ 170.4, 169.5, 151.1, 151.0, 141.6, 123.9, 123.4, 60.6, 48.2, 44.1, 43.3, 27.1, 26.3, 22.5; HRMS (ESI$^+$) *m/z*: $[M + H]^+$ calculated for $C_{28}H_{37}N_8O_4Pd_2$ 763.1007; found 763.1010.

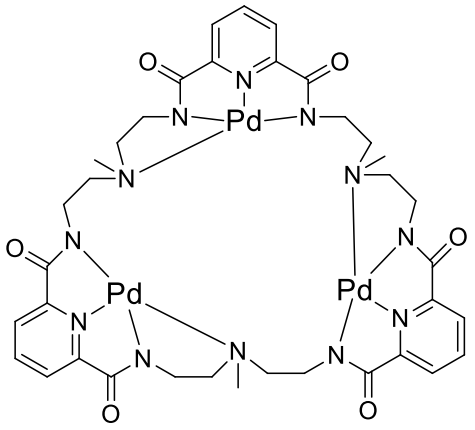

2.12

Complex 2.12. Using a procedure first carried out by Dr. Wang, ligand **2.5** was added to a solution of $Pd(OAc)_2$ in DMF (5 mL). After 1 d, a yellow precipitate was observed. This precipitate was filtered and washed with diethyl ether and MeCN and dried to afford **2.12** as a yellow solid (48 mg, 0.046 mmol, 68% yield). HRMS (ESI$^+$) *m/z* for $C_{37}H_{46}N_{12}O_7Pd_3$ $[M + MeOH]^+$ 1088.0717, found: 1088.0659. Parts-per-million error = (1.0 x 10^6 |observed mass – theoretical mass|)/(theoretical mass) = (1.0 x 10^6 |1088.0659 – 1088.0717|)/(1088.0717) = 1.0 x 10^6 x 5.33 x 10^{-6} = 5.33 ppm.

2.5.4 *Catalysis Studies*

All chemicals—4-iodotoluene, NaOAc, TBAB, and DMA—were purchased from Sigma Aldrich and used without further purification. All reactions were performed under air. 4-iodotoluene (2 mmol, 436 mg), NaOAc (2.2 mmol, 180 mg), TBAB (0.4 mmol, 129 mg), and Pd(II) NNN-pincer complex (2 x 10^{-3} mmol/Pd) were added to a 25 mL three-necked round bottom flask equipped with a reflux condenser and placed in an oil bath. DMA (5 mL) was added to the flask and the temperature of the oil bath was raised to 165 ^{o}C. Styrene (2.8 mmol, 234 μL) was added when the solvent began to reflux (T = 0). The reaction was monitored via TLC and aliquots were taken every 15 minutes for NMR analysis. The samples were analyzed via ^{1}H NMR spectroscopy on a Bruker Avance 500 spectrometer. The yield was calculated by comparing the integration of the olefinic doublet proton signal (2H) of the *trans*-methylstilbene product and the olefinic doublet proton signal (1H) of the *gem*-methylstilbene product to the aromatic doublet proton signal (2H) for the 2-carbon of 4-iodotoluene.

2.5.5 *Intramolecular Heck Reactions in 1,4-dioxane*

To a solution of compound **2.13** (72 mg, 0.25 mmol, 1 equiv) in 1,4-dioxane (2.5 mL) in a 15 mL sealed tube was added NaOAc (23 mg, 0.275 mmol, 1.1 equiv), TBAB (16 mg, 0.05 mmol, 0.2 equiv), and complex **2.6a** (9 mg, 0.025 mmol, 0.1 equiv) or **2.6b** (11mg, 0.025 mmol, 0.1 equiv). The mixture was stirred at 165 ^{o}C for 6 h. Subsequently, the reaction vessel was cooled to 25 ^{o}C and 1,3,5-mesitylene (30 mg, 34.7 µl, 0.25 mmol, 1 equiv) was added. A 0.2 mL aliquot was withdrawn from the crude reaction mixture (containing internal standard) and added to a vial containing 0.5 mL of $CDCl_3$. The samples were analyzed via ^{1}H NMR spectroscopy on a Bruker Avance 500 spectrometer. Following analysis via ^{1}H NMR spectroscopy, the contents of the NMR tube was returned to the crude reaction mixture, and the solvents were evaporated *in vacuo*. The crude products were purified via column chromatography (5:1 to 5:4 hexanes/ethyl acetate) to afford compound **2.14** as a white solid (0.038 g, 0.18 mmol, 73% yield using **2.6a**; 0.028 g, 0.14 mmol, 55% yield using **2.6b**). ^{1}H NMR (500 MHz, $CDCl_3$) δ 7.70 (d, J = 7.73 Hz, 1H), 7.46 (t, J = 7.75 Hz, 1H), 7.38 (t, J = 7.61 Hz, 1H), 7.13 (d, J = 7.58 Hz, 1H), 6.59 (t, J = 3.45 Hz, 1H), 6.44 (d, J = 3.69 Hz, 1H), 4.51 (d, J = 11.9 Hz, 1H), 4.07 (dd, J = 11.9, 4.1, 1H), 3.30 (t, J = 3.7, 1H); ^{13}C NMR (126 MHz, DMSO-d_6) δ 139.9, 135.4, 134.8, 134.4, 131.9, 130.1, 127.6, 125.7, 63.3, 42.5.

2.6 *References*

1. Dismukes, G. C. “Manganese Enzymes with Binuclear Active Sites” *Chem. Rev.* **1996**, *96*, 2909–2926.
2. Urbach, F, L. “The Properties of Binuclear Copper Centres in Model and Natural Compounds” from Metal Ions in Biological Systems, Sigel, H., Ed.; Dekker: New York, vol. 13, **1981**.
3. Vigato, P. A.; Tamburini S.; Fenton, D. E. “The Activation of Small Molecules by Dinuclear Complexes of Copper and Other Metals” *Coord. Chem. Rev*. **1990**, *106*, 25–170.
4. Krajewska, B. “Ureases I. Functional, catalytic and kinetic properties: A review” *J. Mol. Cat. B: Enzymatic* **2009**, *59*, 9–21.
5. Benini S.; Rypniewski W. R.; Wilson K. S.; Miletti S.; Ciurli S.; Mangani S. “A new proposal for urease mechanism based on the crystal structures of the native and inhibited enzyme from Bacillus pasteurii: why urea hydrolysis costs two nickels” *Structure* **1999**, *7*, 205–16.
6. Van den Beuken, E. K.; Feringa, B. L. “Bimetallic Catalysis by Late Transition Metal Complexes” *Tetrahedron*, **1998**, *54*, 12985–13011.
7. Gavrilova, A. L.; Bosnich, B. “Principles of Mononucleating and Binucleating Ligand Design” *Chem. Rev.* **2004**, *104*, 349–383.
8. Tard, C.; Pickett, C. J. “Structural and Functional Analogues of the Active Sites of [Fe]-, [NiFe]-, and [FeFe]-Hydrogenases” *Chem. Rev*. **2009**, *109*, 2245–2274.
9. Kim, E.; Chufá, E. E.; Kamaraj, K.; Karlin, K. D. “Synthetic Models for Heme-Copper Oxidases” *Chem. Rev.* **2004**, *104*, 1077–1134.
10. Wiester, M. J.; Ulmann, P. A.; Mirkin, C. A. “Enzyme Mimics Based Upon Supramolecular Coordination Chemistry” *Angew. Chem. Int. Ed.* **2010**, *50*, 114–137.
11. McKenzie, C. J.; Robson, R. “High Turnover Catalysis at Bimetallic Sites of the Hydration of Nitriles to Carboxamides Co-catalysed by Acid. Highly Specific Hydration of Acrylonitrile to Acrylamide” *J. Chem. Soc. Chem. Commun*. **1988**, 112–114.

12. Bennett, M. A.; Yoshida, T. “Homogeneously Catalyzed Hydration of Nitriles to Carboxamides” *J. Am. Chem. Soc*. **1973**, *95*, 3030–3031.
13. Herrmann, W. A.; Brossmer, C.; Reisinger, C-. P. Riermeier, T. H.; Öfele, K.; Beller, M. “Palladacycles: Efficient New Catalysts for the Heck Vinylation of Aryl Halides” *Chem. Eur. J.* **1997**, *3*, 1357–1364.
14. Dijkstra, H. P.; Meijer, M. D.; Patel, J.; Kreiter, R.; van Klink, G. P. M.; Lutz, M.; Spek, A. L.; Canty, A. J.; van Koten, G. “Design and Performance of Rigid Nanosize Multimetallic Cartwheel Pincer Compounds as Lewis-Acid Catalysts” *Organometallics*, **2001**, *20*, 3159–3168.
15. Van Klink, G. P. M.; Dijkstra, H. P.; van Koten, G. “Recyclable Nanosize Homogeneous Catalysts” *C. R. Chimie* **2003**, *6*, 1079–1085.
16. Tsubomura, T.; Chiba, M.; Nagai, S.; Ishihira, M.; Matsumoto, K.; Tsukuda, T. “Dinuclear Macrocyclic Palladium Complexes having Pincer Coordinating Groups and their Catalytic Properties in Mizoroki-Heck Reactions” *J. Organomet. Chem*. **2011**, *696*, 3657–3661.
17. Hossain, Md. A.; Lucarini, S.; Powell, D.; Bowman-James, K. “Ditopic Double Pincer Palladacycle Catalyst for C-C Coupling” *Inorg. Chem*. **2004**, *43*, 7275–7277.
18. Ghosh, S.; Roehm, B.; Begum, R. A.; Kut, J.; Hossain, M. A.; Day, V. W.; Bowman-James, K. “Versatile Host for Metallo Anions and Cations” *Inorg. Chem*. **2007**, *46*, 9519–9521.
19. Hossain, M. A.; Llinares, J. M.; Powell, D.; Bowman-James, K. “Multiple Hydrogen Bond Stabilization of a Sandwich Complex of Sulfate between Two Macrocyclic Tetraamides” *Inorg. Chem.* **2001**, *40*, 2936–2937.
20. Hossain, M. A.; Kang, S. O.; Llinares, J. M.; Powell, D.; Bowman-James, K. “Elite New Anion Ligands: Polythioamide Macrocycles” *Inorg. Chem.* **2003**, *42*, 5043–5045.
21. Kang, S. O.; Day, V. W.; Bowman-James, K. “The Influence of Amine Functionalities on Anion Binding in Polyamide-Containing Macrocycles” *Org. Lett.* **2009**, *11*, 3654–3657.

22. Voegtle, F.; Weber, E.; Wehner, W.; Naetscher, R.; Gruetze, J. “Heavy Metal Complexes with New Cyclic Ligands” *Chemiker-Zeitung* **1974**, *98*, 562–563.
23. Fabbrizzi, L.; Kaden, T. A.; Perottie, A.; Seghi, B.; Siegfried, L. “Complexation of Divalent and Trivalent Nickel and Copper Ions by Rigid and Flexible Dioxo Tetraaza Macrocycles” *Inorg. Chem*. **1986**, *25*, 321–327.
24. Gerald A. Kut, Ph.D. Dissertation, Synthesis and Characterization of New Classes of Polyamine and Polyamide Anion Receptors, University of Kansas, **2005**.
25. Korendovych, I. V.; Cho, M.; Butler, P. L.; Staples, R. J.; Rybak-Akimova, E. V. *Org. Lett*. **2006**, *8*, 3171–3174.
26. Korendovych, I. V.; Cho, M.; Makhlynets, O. V.; Butler, P. L.; Staples, R. J.; Rybak-Akimova, E. V. “Anion and Carboxylic Acid Binding to Monotopic and Ditopic Amidopyridine Macrocycles” *J. Org. Chem*. **2008**, *73*, 4771–4782
27. Wang, Q-. Q.; Day, V. W.; Bowman-James, K. “Macrocyclic Influences in CO_2 Uptake and Stabilization” *Org. Lett.* **2014**, *16*, 3982–3985.
28. Jia, C.; Wang, Q-. Q.; Begum, R. A.; Day, V .W.; Bowman-James, K. “Chelate Effects in Sulfate Binding by Amide/Urea-Based Ligands” *Org. Biomol. Chem.* **2015**, *13*, 6953–6957.
29. Chmielewski, M. J.; Jurczak, J. “Anion Recognition by Neutral Macrocyclic Amides” *Chem. Eur. J.* **2005**, *11*, 6080–6094.
30. Chmielewski, M. J.; Jurczak, J. “Anion Binding versus Intramolecular Hydrogen Bonding in Neutral Macrocyclic Amides” *Chem. Eur. J.* **2006**, *12*, 7652–7667.
31. Dell’Amico, D. B.; Calderazzo, F.; Di Colo, F.; Guglielmetti, G.; Labella, L.; Marchetti, F. “Coordination Properties Towards Palladium(II) of a Tridentate Dianionic Ligand Acting as a N- or a N,O-donor” *Inorg. Chim. Acta* **2006**, *359*, 127–135.
32. Wang, Q.-Q.; Day, V. W.; Bowman-James, K. “Hexagonal Molecular ‘Palladawheel’” *Chem. Commun*. **2013**, *49*, 8042–8044.
33. Wang, Q.-Q.; Begum, R. A.; Day, V. W.; Bowman-James, K. “Molecular Thioamide⇔Iminothiolate Switches for Sulfur Mustards” *Inorg. Chem*. **2012**, *51*, 760–762.

34. Wang, Q.-Q.; Begum, R.A.; Day, V.W.; Bowman-James, K. “Chemical Mustard Containment Using Simple Palladium Pincer Complexes: The Influence of Molecular Walls” *J. Am. Chem. Soc*. **2013**, *135*, 17193–17199.
35. Janiak, C. “A Critical Account on π–π Stacking in Metal Complexes with Aromatic Nitrogen-Containing Ligands” *J. Chem. Soc., Dalton Trans.* **2000**, 3885–3896.
36. Eberhard, M. R. “Insights into the Heck Reaction with PCP Pincer Palladium(II) Complexes” *Org. Lett.* **2005**, *6*, 2125–2128.
37. Ashworth, I. W.; Nelson, D. J.; Percy, J. M. “Solvent Effects on Grubbs’ Pre-Catalyst Initiation Rates” *Dalton Trans*. **2013**, 42, 4110–4113.
38. Evans, P.; McCabe, T.; Morgan, B. S.; Reau, S. “Double Reduction of Cyclic Aromatic Sulfonamides: A Novel Method for the Synthesis of 2- and 3-Aryl-Substituted Cyclic Amines” *Org. Lett.* **2005**, *43*, 43–46.

Chapter 3

Novel Route to Heterobimetallic Palladium(II)–Silver(I) and –Gold(I) Complexes with NHC-Tethered Pincer Ligands

3.1 *Abstract*

Novel *N*-heterocyclic carbene (NHC)-tethered palladium(II) NNN-pincer complexes containing either silver(I) or gold(I) have been synthesized. Treatment of dimethyl 2,6-pyridinedicarboxylate with 1-(3-aminopropyl) imidazole, followed by single or double alkylation with methyl iodide, gives hybrid NNN-pincer/imidazolium NHC precursor ligands **3.3** and **3.5**, respectively. Palladation of the NNN-pincer site of these two ligands proceeds to give unsymmetrically substituted Pd(II) complex **3.6** and symmetrically substituted Pd(II) complex **3.10**. Complex **3.10** was converted to Pd(II) NNN-pincer/NHC complex **3.11** in the presence of AgOAc, leaving an imidazolium NHC precursor available to coordinate other metals. The ability of **3.11** to form a heterobimetallic complex was demonstrated by the reaction that occurs with Ag_2O to form Pd(II)/Ag(I) complex **3.12**. The formation of **3.12** was observed using ^{1}H, ^{13}C, and ^{13}C DEPT NMR spectroscopies and positive mode ESI mass spectrometry. However, the structure could not be unambiguously confirmed due to crystallization difficulties. Preliminary catalytic investigations indicate that complexes **3.6**, **3.7**, **3.10**, and **3.11** are efficient catalysts for the Heck coupling reaction of 4-iodotoluene and styrene; though longer reaction times are observed when either complex **3.7** or **3.11**—both of which contain tetradentate ligands—are employed as the Pd-catalyst. This study provides a new platform from which to build heterobimetallic complexes containing Pd(II).

3.2 *Introduction*

Catalysis typically involves lowering the activation energy, E_a, of a chemical transformation by lowering the HOMO-LUMO gap between two substrates in order to promote a desired reaction. Over the last half-century, most of the efforts in catalyst development have focused on the activation of only one of the substrates—either the nucleophile or electrophile—in a given reaction. In practice, this has led to the development of very useful reactions (e.g. carbon–carbon bond formation, polymerization reactions, hydrogenation reactions) that have garnered widespread use in industry and earned multiple Nobel Prizes.[1] However, catalytic systems that contain two independent catalysts in solution can have the added advantage of activating two separate substrates, which in turn results in a two-pronged approach to lowering the HOMO-LUMO gap.[2] Ito and coworkers have described a two-component catalyst system involving $Rh(acac)(CO)_2$ and $Pd(Cp)(\pi\text{-}C_3H_5)$ to construct optically active compounds from activated nitriles (Scheme 3.1).[3] Synergy was achieved by combining two known interactions; whereas α-cyano esters undergo Michael and aldol reactions in the presence of catalytic amounts of $RhH(CO)(PPh_3)_3$, allylic carbonates are activated in the presence of Pd to form electrophilic π-allylpalladium(II) complexes. Notably, in the absence of the Pd-catalyst, no product formation was observed. Alternatively, in the absence of the Rh-catalyst, the yield was high (97%), but the product of the reaction was completely racemic. When used together, these two catalysts propel the nucleophilic attack of a π-allylpalladium(II) complex via a Rh(I)-activated enolate complex. Under the optimized conditions in which both catalysts were employed, the product was formed in 93% yield with excellent enantioselectivity (99% ee). Similar approaches have been utilized for Pd(0)- and Cu(I)-

catalyzed triazole formation[4] and, most famously, the Pd(0)- and Cu(I)-catalyzed Sonogashira cross-coupling reaction.[5] Alternatively, catalysts having multiple active sites in the same molecule can be used to achieve different goals that can assist in cooperative, regenerative, and sequential catalysis.[6] These heterobimetallic systems have the potential benefit of achieving synergy via proximity.

Scheme 3.1. Pd(II)/Rh(I) two-component catalyst system employed for the alkylation of nitriles.[3]

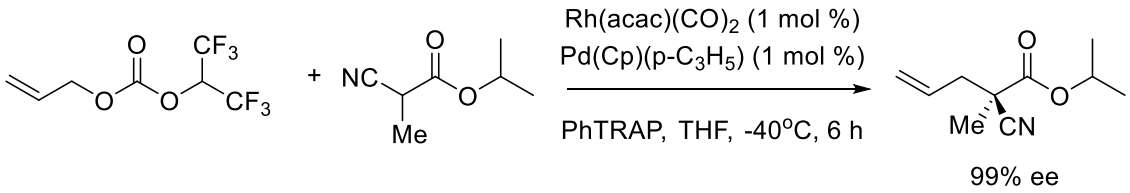

In 2002, Brown and van Koten described heterobimetallic complexes which were synthesized by reacting 3-bis(diphosphinomethyl)ferrocene with $[(C_2H_4)_2RhCl]_2$ to afford a hybrid ferrocene/Rh(I) PCP-pincer complex (Scheme 3.2A).[7] Since then, examples in which ferrocene and ruthenocene-type complexes are incorporated to the backbone of PCP and SCS pincer ligands have been extensively studied.[8,9] For example, complexes incorporating both Pd(II) and Ru(II) in the same molecule have proved to be competent catalysts in the cross coupling reaction of *trans*-2-phenylvinylboronic acid with vinyl epoxide (Scheme 3.2B). Interestingly, the catalytic activity of the heterobimetallic Pd(II)/Ru(II) complex (GC yield after 10 h = 86-95%) is higher than that of the related monometallic Pd(II) SCS pincer (GC yield after 10 h = 13%). As the authors suggest, this enhancement is likely due to the decreased electron density on the Pd(II) metal center in the heterobimetallic complex, which results in faster transmetalation from boron derivatives during the rate determining step of the catalytic cycle.

Scheme 3.2. (**A**) Synthesis of a ferrocene-derived Rh(II) PCP-pincer complex[7] and (**B**) cross-coupling reaction between *trans*-2-phenylvinylboronic acid and vinyl epoxide using a heterobimetallic Pd(II)/Ru(II) catalyst.[9]

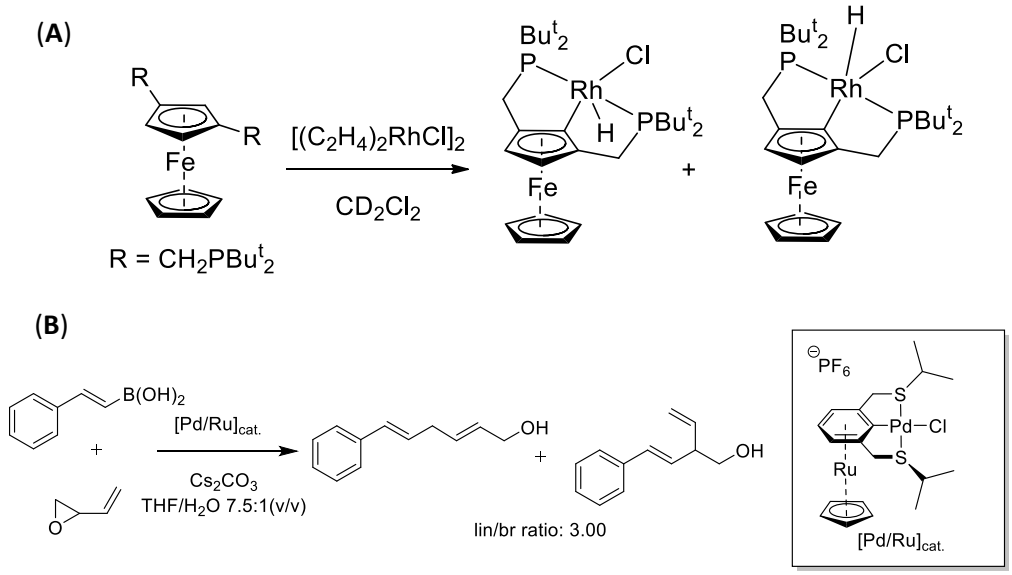

In their efforts to develop new oxidation catalysts, amide-based NNN-pincer complexes have recently been studied as mimics for carbon monoxide dehydrogenase by Holm,[10] and in later reports by Tolman.[11,12] In 2010, Holm reported the use of a binucleating macrocycle to selectively bind two metals with bridging ligands (Figure 3.1). The binucleating ligand binds Ni(II) at the pincer site and Fe(II) at the triamine site to afford complexes with Ni···Fe distances ranging from 3.7 to 4.8 Å, depending on the bridging ligand. To gain insight into biological oxidation mechanisms, these complexes were used as carbon monoxide dehydrogenase enzyme mimics. In 2013, Tolman reported bimetallic Cu(II), and heterobimetallic Cu(II)/Pd(II) and Cu(II)/Pt(II) complexes with the same ligand (Figure 3.1).[11,12]

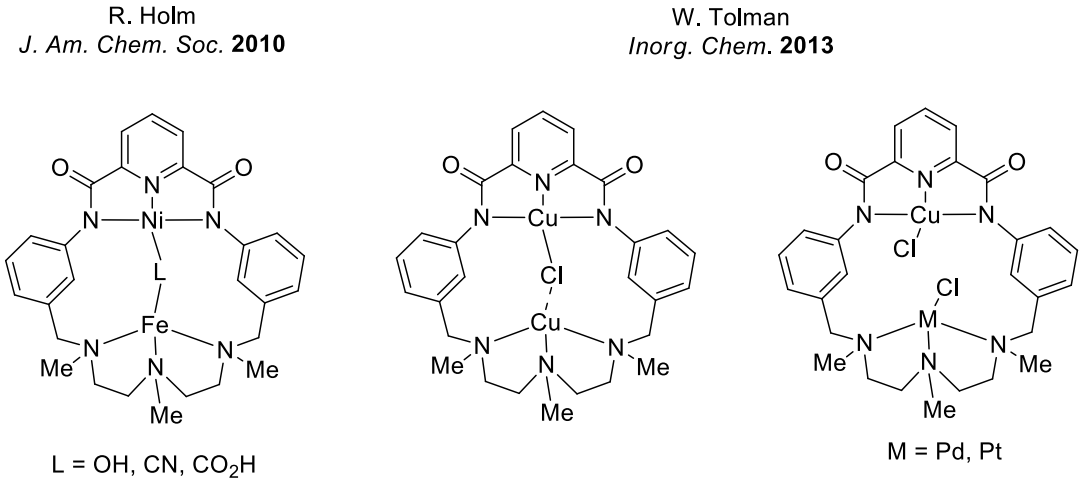

Figure 3.1. Examples of homo- and heterobimetallic complexes with macrocyclic NNN-pincer ligands.[10-12]

Another efficient method of synthesizing heterobimetallic complexes is to utilize the unique binding properties of *N*-heterocyclic carbene (NHC) ligands, as they form stable complexes with a variety of catalytically-relevant transition metals. The synthesis of NHC metal complexes is discussed at the beginning of Section 4.3.2 of this Chapter. Although NHC ligands are strong σ-donors, they are weak π-acceptors compared to traditional carbenes (Figure 3.2), and thus the metal–ligand bond is denoted by a single bond. Also, in contrast to traditional carbenes, NHCs usually act as spectator ligands for transition metals and thus do not partake in chemical reactions.

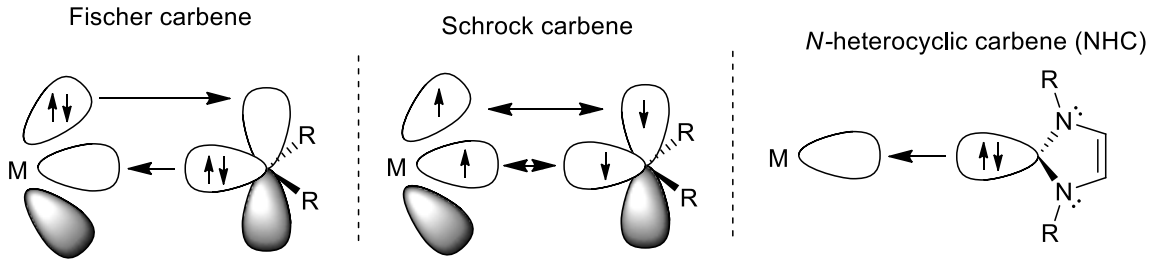

Figure 3.2. Comparison of the bonding orbitals in Fischer, Schrock, and *N*-heterocyclic carbene metal complexes. Adapted from Frenking *et al.*[13]

The Peris group has used a unique triazolyl ligand, 1,2,4-trimethyltriazolyl-diylidene (ditz), to investigate the properties of its complexes with Rh(I), Ir(I), Ir(III), Pd(II), and Ru(II).[14-16] Heterobimetallic complexes containing Rh(I) and Ir(III) were found to catalyze a tandem reaction sequence involving the oxidative cyclization of 2-aminophenyl ethyl alcohol, followed by alkylation of the resulting indole.[15] However, this tandem reaction sequence was also carried out using a homobimetallic Ir(I) catalyst based on the ditz ligand. In 2009, Peris and coworkers investigated a Pd(II)/Ir(I) catalyst for its use in a tandem reaction sequence employing an Ir(I)-catalyzed dehalogenation/hydrogen transfer to form 1-phenylethanol (Scheme 3.3).[16] In this case, the heterobimetallic Pd(II)/Ir(I) complexes are more active (GC yield = >99%) than their homobimetallic counterparts (GC yield = 0% for bispalladium(II) and bisiridium(I) complexes with the ditz ligand).

Scheme 3.3. Tandem dehydrogenation/cross coupling reactions catalyzed by a Pd(II)/Ir(III) complex.[16]

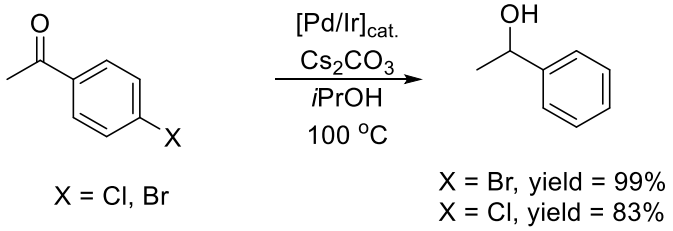

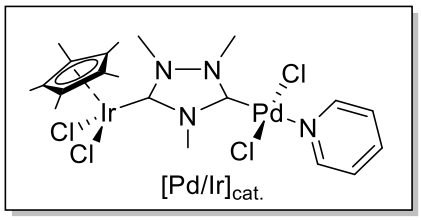

Straub and coworkers have also used NHCs for the synthesis of heterobimetallic complexes (Scheme 3.4).[17] Metal-NHC complexes were synthesized by selective deprotonation at the thiol-functionalized triazoline ligand, followed by the addition of

$PdCl_2$ to give the Pd(II)-NHC complex as a mixture of two diastereomers. They were able to synthesize a heterobimetallic Au(I)/Pd(II) complex as a mixture of two diastereomers by using a strong base (NaOMe). Additionally, they synthesized a heterobimetallic Cu(I)/Pd(II) complex and isolated it as a single isomer. The solid-state structure of the Pd(II)/Cu(I) complex was solved and the Pd···Cu distance was found to be 3.41 Å.

Scheme 3.4. Synthesis of a thiol-functionalized Pd/Cu Complex via stepwise deprotonation (purple ball = Cu; orange ball = Pd).[17]

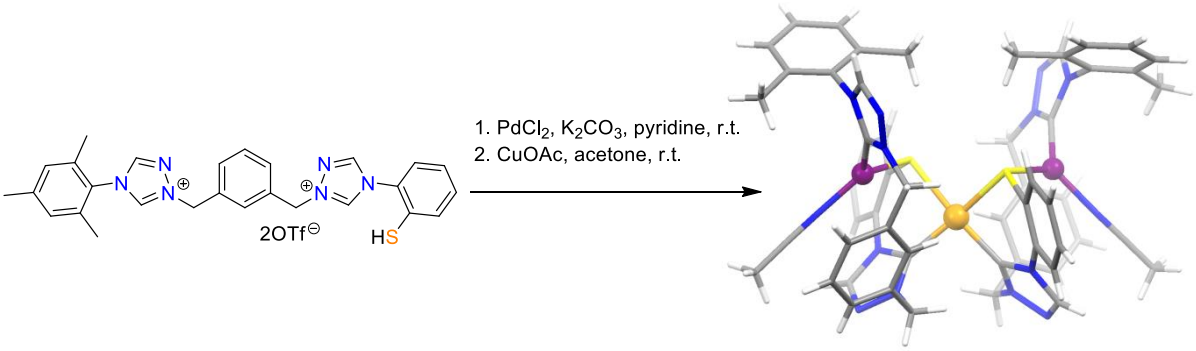

NHC ligands have also been combined with other multidentate ligands to allow selective incorporation of metals. A chiral Ni(II)/Pd(II) salen/NHC-complex has been reported by Peters.[18,19] In the first step of the synthesis, the introduction the metals into these hybrid ligands proceeds via the selective incorporation of Pd(II) or Ni(II) into the salen ligand site. Formation of a Ag(I)-NHC complex was followed by the transmetalation of Ag(I) with other metals to form heterobimetallic complexes. It was shown that the heterobimetallic Ni(II)/Pd(II) complexes were efficient catalysts in the 1,4-addition of oxindole to *trans*-nitrostyrene (Scheme 3.5). Although quantitative conversion of the oxindole was observed, each of the diastereomers were formed as racemic mixtures.[18] Aiming to enhance the rigidity of the complex and decrease the M···M distances, Peters and coworkers have investigated the coordination chemistry of macrocyclic derivatives of these ligands for asymmetric catalysis applications.[19] Kato and coworkers have

investigated similar homobimetallic Mn(III) salen-based complexes and observed asymmetry transfer.[20]

Scheme 3.5. The 1,4-addition of oxindole to *trans*-nitrostyrene catalyzed by a heterobimetallic Pd(II)/Ni(II) complex.[18]

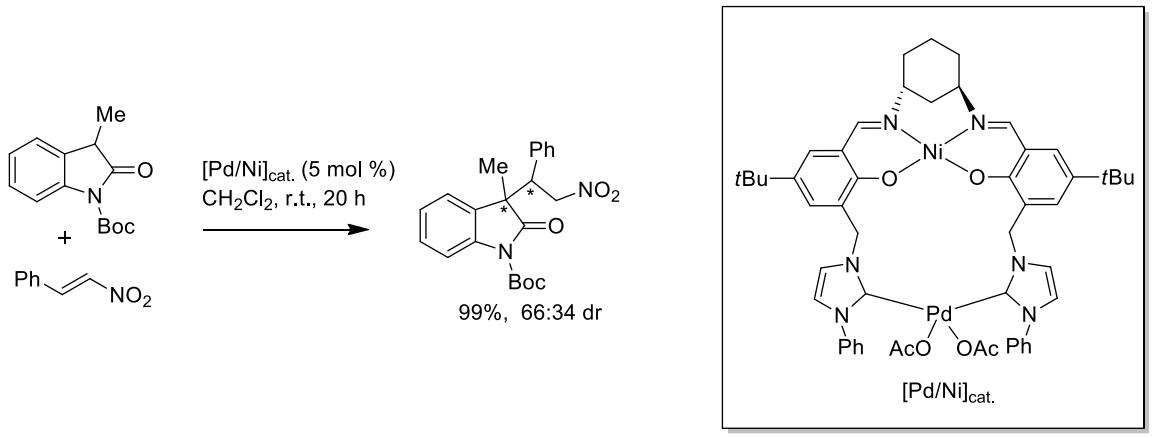

Earlier this year, Huynh and coworkers reported the synthesis of digold(I) and Co(III)/Au(I) complexes using a hybrid NNN-pincer/NHC-precursor ligand similar to those described in this chapter.[21] In the first step of their synthesis, the ligand was metallated using Ag_2O to give a Ag(I)-biscarbene complex (Scheme 3.6). This complex was treated with [AuCl(tht)] (tht = tetrahydrothiophene) in the presence of a noncoordinating solvent (dichloromethane) to afford mononuclear and dinuclear Au(I)-biscarbene complexes. The metallacycle architecture of the dinuclear complex results in the strong coordination of a BF_4^- anion, as evidenced by a downfield shift of the NNN-pincer amide proton [H(am)] signals (0.45-0.83 ppm) in the ^1H NMR spectrum of the complex. The association of the anion was also observed in the X-ray molecular structure of the complex, which contains a single BF_4^- ion in the center of the metallocycle, surrounded by eight hydrogen bonds. Addition of $CoCl_2 \cdot 6H_2O$ to the dinuclear Au(I)

complex under oxidative conditions afforded the heterobimetallic Co(III)/Au(I) complex, which exists as a helicate in the solid state.

Scheme 3.6. Synthesis of homobimetallic Au(I) and heterobimetallic Au(I)/Co(III) complexes.[21]

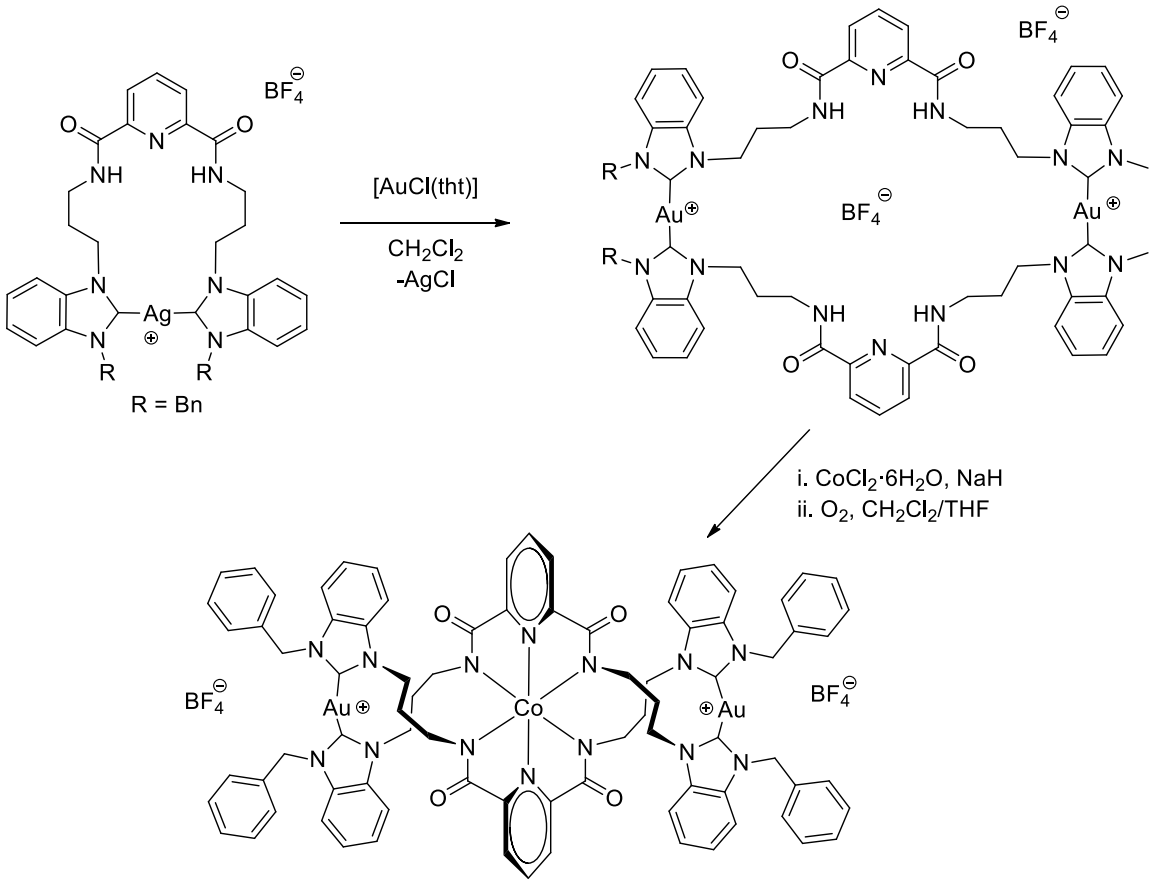

Our group has developed applications for anion recognition and binding using amide and thioamide macrocyclic ligands.[22-27] As an extension of this work, a macrocyclic SCS-pincer Pd(II) complex was synthesized by our group in 2004 (Figure 3.3A) and investigated in the Heck coupling reaction of 4-iodotoluene and styrene to form *trans*- and *gem*-stillbene (Figure 3.3B).[28] In 2006, a series of acyclic thioamide and iminothiolate SCS and SNS Pd(II) and Pt(II) complexes were prepared and the Pd(II) complexes were

used as catalysts for the same Heck reaction.[29] Recently, we found that Pd(II) NNN-pincer complexes can also serve as efficient catalysts in the Heck reaction (Chapter 2), with catalytic activities comparable to those of the aforementioned Pd(II) SCS-pincer complexes. These studies served as an incentive to design derivatives of NNN-pincer ligands capable of binding two separate metals in order to probe modern C–C bond forming reactions.

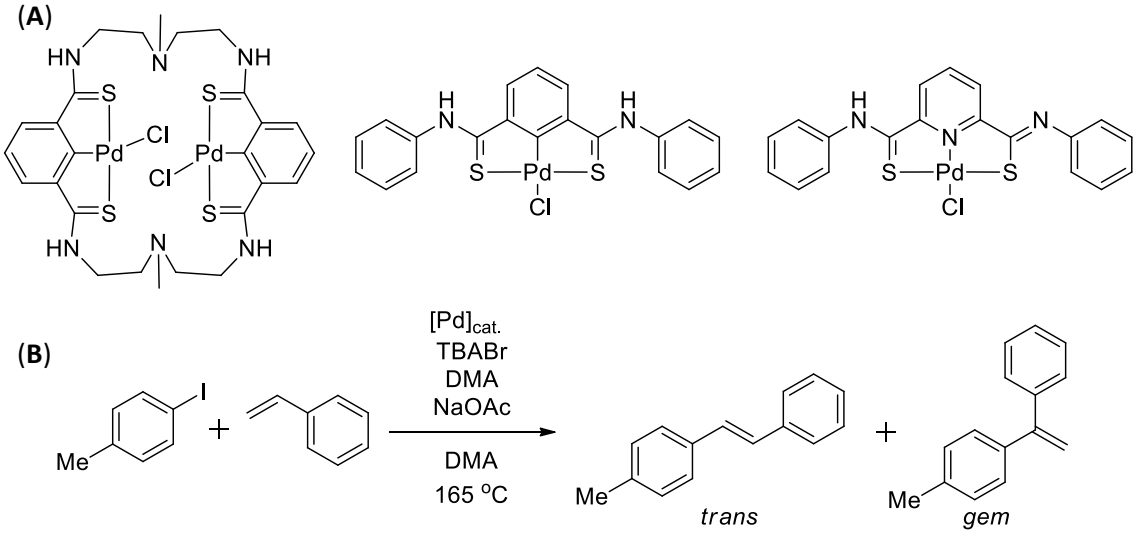

Figure 3.3. (**A**) Macrocyclic and acyclic Pd(II) pincer complexes designed by the Bowman-James group and (**B**) Heck coupling of 4-iodotoluene and styrene.[28,29]

3.3 *Results and Discussion*

3.3.1 *Ligand Synthesis*

Amide-based NNN-pincer ligands and their Pd(II) complexes have been described previously by our group.[30-32] In most cases, the complexes can be synthesized using a two-step protocol starting from dimethyl 2,6-pyridinedicarboxylate. Motivated by the ease with which one can vary the amide appendages in these ligands, we sought to design a platform from which to synthesize heterobimetallic complexes by combining the pincer binding site with another attractive class of ligands: NHCs. The incorporation of both ligands into one molecule should allow for the assembly of multimetallic complexes (Figure 3.4).

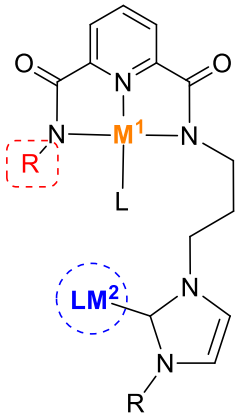

Figure 3.4. Scaffold design of hybrid NNN-pincer/NHC heterobimetallic complexes.

The unsymmetrically substituted hybrid ligand **3.3** was synthesized in two steps from dimethyl 2,6-pyridinedicarboxylate **A** and 1-(3-aminopropyl) imidazole **B** (Scheme 3.7) using a protocol similar to one previously reported by our group for analogous unsymmetrically substituted amide-based NNN-pincer ligands.[33] In the first step, a solution of **B** (1 equiv) was added dropwise to a refluxing solution of **A** (4 equiv) in methanol. The resulting clear solution was stirred at reflux for 3 days. Upon cooling, the

precipitate that was formed was filtered, washed with cold methanol, and dried to provide pure **A** (as determined by ^{1}H NMR spectroscopy), which was recycled for future reactions. Following filtration, removal of the filtrate solvent *in vacuo*, followed by column chromatography—to separate the single and double substitution products—gave the mixed amide ester **3.1** in 37% yield, as confirmed by ^{1}H NMR spectroscopy.

In the second step, ethylamine was bubbled through a solution of **3.1** in methanol at room temperature (Scheme 3.7). The reaction was monitored by TLC and the starting material was consumed after 48 hours. The volatiles were removed and the resulting oily residue was dissolved in acetone and triturated with hexanes to afford a white precipitate. The suspension was filtered, and the resulting white solid was dried to afford unsymmetrically substituted bisamide **3.2** in 82% yield. As expected for an unsymmetrically substituted ligand, the ^{1}H NMR spectrum of **3.2** displays two triplet proton signals corresponding to the nonequivalent amide protons at 8.84 and 8.76 ppm.

Scheme 3.7. Synthesis of unsymmetrically substituted hybrid pincer/NHC-precursor ligand **3.3**.

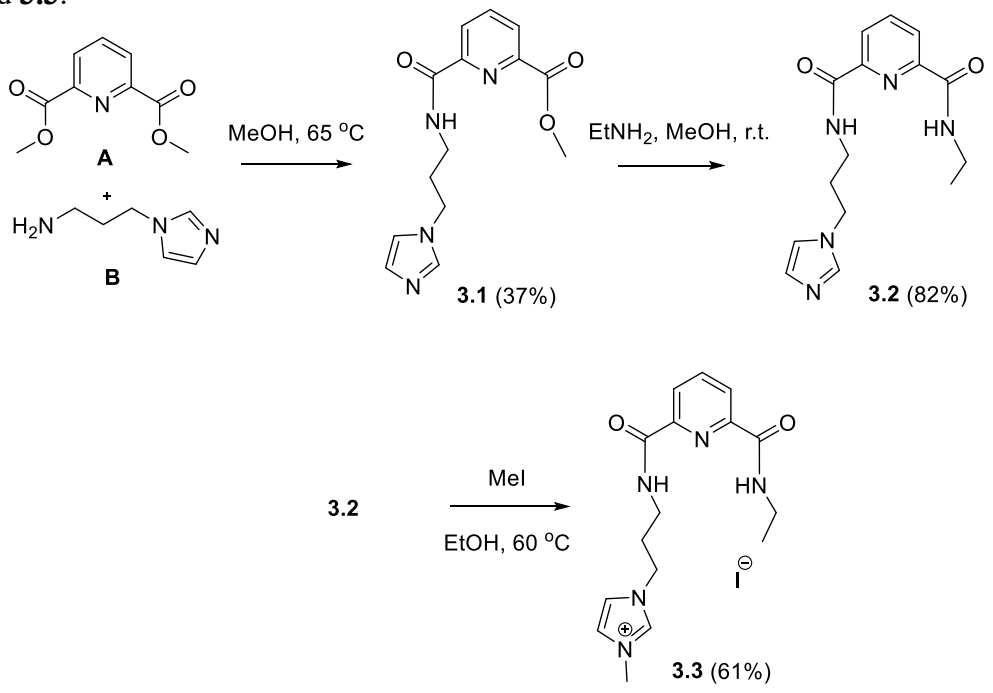

Compound **3.2** was converted to the imidazolium salt by *N*-alkylation of the imidazole moiety with iodomethane. A solution of **3.2** and iodomethane in ethanol was stirred at reflux for 48 hours. After cooling the reaction mixture, the white precipitate that formed was filtered and dried to afford the unsymmetrically substituted hybrid pincer/NHC-precursor ligand **3.3** in 61% yield. Ligand **3.3** was characterized by ^{1}H and ^{13}C NMR spectroscopies, and positive ion mode ESI-MS (in MeCN). Notably, in the ^{1}H NMR spectrum of **3.3** (Figure 3.5), H^{h} is shifted downfield compared to the corresponding proton signal in the ^{1}H NMR spectrum of **3.2**. This shift originates from the deshielding effect of the resonance-stabilized imidazolium cation. The three unique pyridine proton signals (H^{a}, H^{b}, and H^{c}) and two unique amide proton signals (H^{d} and H^{e}) are characteristic of an unsymmetrically substituted ligand.

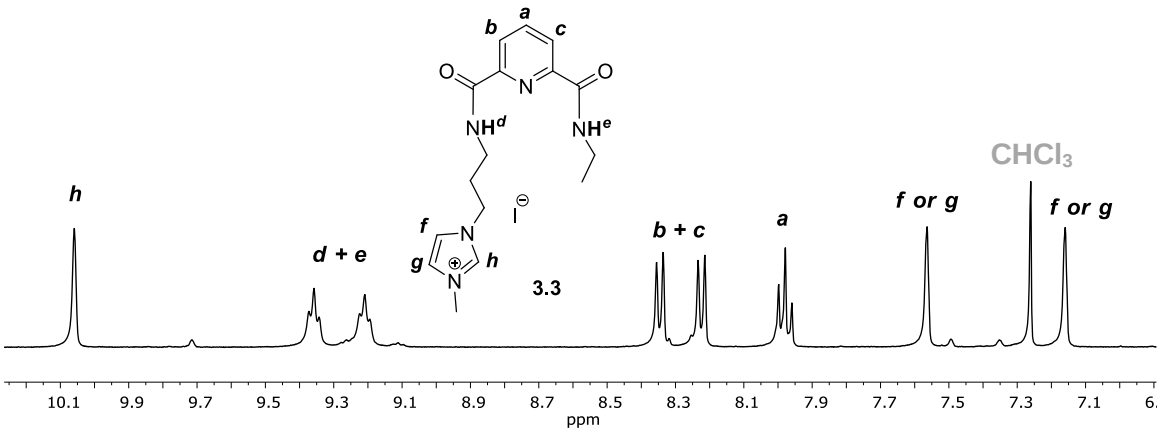

Figure 3.5. Aromatic region of the ^{1}H NMR spectrum (400 MHz, $CDCl_3$) of unsymmetrically substituted hybrid pincer/NHC-precursor ligand **3.3**.

Symmetrically substituted hybrid pincer/NHC-precursor ligand **3.5** was synthesized in 66% yield over two steps (Scheme 3.8) using a similar procedure to the one described for **3.3**. In the first step, **A** (1 equiv) and **B** (2 equiv) were dissolved in methanol

and stirred at reflux for 7 days. Following evaporation of the solvent, the crude products were purified via flash column chromatography on silica to give bisamide **3.4** as a clear oil. The oil was dissolved in acetone and triturated with diethyl ether, which resulted in the formation of a white precipitate. Following filtration of the suspension, **3.4** was recovered as a white solid in 82% yield.

In the second step, *N*-Alkylation of the imidazolium moiety in **3.4** with iodomethane in refluxing ethanol afforded the symmetrically substituted hybrid pincer/NHC ligand **3.5** in 77% yield (Scheme 3.8). An excess of iodomethane (>5 equiv) was necessary to drive the reaction to completion. The ^{1}H NMR spectrum of **3.5** in DMSO-d_6 features a characteristic signal for the acidic imidazolium proton [H(im)] at 9.16 ppm. If the product is not washed with cold acetone, a light-yellow solid is isolated, likely due to iodine impurities from iodomethane. However, no impurities were observed in the ^{1}H NMR spectrum of this light-yellow solid.

Scheme 3.8. Synthesis of symmetrically substituted hybrid pincer/NHC-precursor ligand ligand **3.5**.

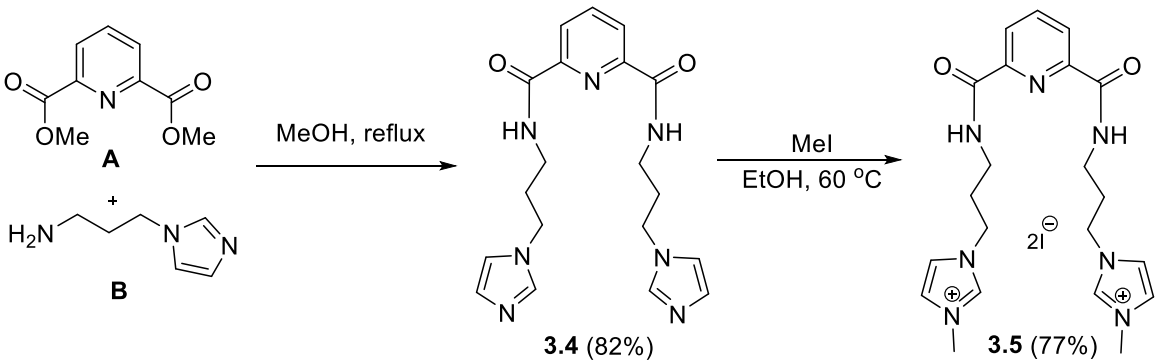

3.3.2 *Synthesis of Pd(II) NNN-Pincer Complexes*

The methods for preparing pincer and NHC complexes with transition metals are similar. NHC-metal complexes are traditionally prepared in one of three ways: 1) from imidazolium salts via a mild internal base (e.g. $Pd(OAc)_2$),[34] 2) via an external base (e.g. NaOAc, Et_3N, KHMDS, NaH) in the presence of a metal halide,[35] or 3) via transmetalation from NHC complexes of Ag(I).[36] Whereas the pK_a values of amide and imidazolium salt protons are similar, a potential problem arises in utilizing these hybrid ligands for selective and sequential formation of heterobimetallic complexes. The pK_a value for an amide proton adjacent to an electron withdrawing substituent, such as pyridine, is estimated to be 21,[37] while the pKa value of the acidic proton in an unsaturated imidazolium salt can range from 18.6 to 24.[37]

The coordination chemistry of the unsymmetrically substituted hybrid pincer/NHC-precursor ligand **3.3** was initially explored with $Pd(OAc)_2$. It was hoped that the tridentate coordination of the NNN-pincer ligand would drive the metalation of the pincer site by virtue of the chelate effect, leaving an available imidazolium NHC precursor to bind other metals. An equimolar solution of **3.3** and $Pd(OAc)_2$ was stirred in acetonitrile for 24 hours at room temperature (Scheme 3.9). Over the course of the reaction, the dark maroon solution eventually yielded a yellow precipitate. This precipitate was filtered, washed with diethyl ether, and dried to afford unsymmetrically substituted Pd(II) NNN-pincer complex **3.6** as a yellow solid in 87% yield. The ^1H NMR spectrum of **3.6** is consistent with the NNN-pincer coordination of Pd(II). Specifically—in line with our previous observations (Chapter 2, *vide supra*)—the disappearance of the two amide proton signals is indicative of the formation of a Pd(II) NNN-pincer complex. Further confirmation of the Pd(II)

species came from the positive mode ESI mass spectrum, which features a prominent ion isotope pattern centered at *m/z* 461.0920 $[M - I + NCCH_3]^+$.

Scheme 3.9. Synthesis of Pd(II) complex **3.6.**

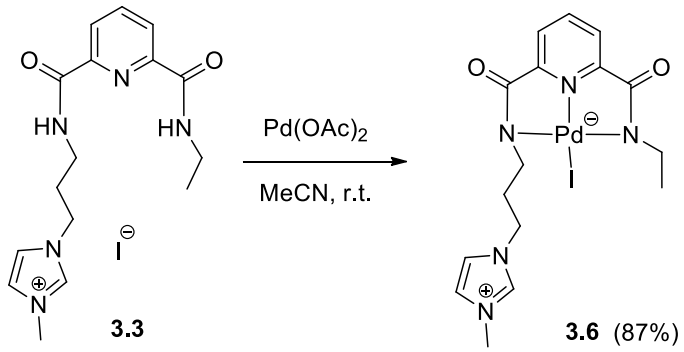

Crystals of **3.6** suitable for single crystal X-ray diffraction were obtained from slow diffusion of diethyl ether into a saturated solution of the complex in acetonitrile at room temperature. The molecular structure of **3.6** (Figure 3.6) supports the NMR and HRMS data, and unequivocally confirms the NNN-pincer coordination of Pd(II). The palladium center in **3.6** has a distorted square planar coordination geometry. Unlike the Pd(II) NNN-pincer complexes we studied in Chapter 2, the fourth coordination site in **3.6** is occupied by an iodide ligand, which the soft Pd(II) center prefers over acetonitrile. The pincer ligand coordinates the metal center through one Pd–N(pyridine) bond (1.943 Å) and two relatively longer Pd–N(amide) bonds (2.057 and 2.046 Å). Consistent with the greater *trans* influence of the iodide ligand compared to acetonitrile, the Pd–N(pyridine) distance in **3.6** (1.943 Å) is slightly longer than that of the ethyl amide appended Pd(II) NNN-pincer complex **2.6a** studied in Chapter 2 (1.920 Å). While the N1-Pd-I bond angle is close to the expected 180° (177.47°), to accommodate the metal ion, the N2-Pd-N3 bond angle is 159.5°. This distortion was also present in previously reported Pd(II) NNN-pincer complexes.[31,32,38] Intermolecular parallel-displaced π–π stacking interactions result in the

formation of dimer pairs in the crystal lattice of **3.6**, which contain an intermolecular pyridine···pyridine centroid distance of 3.582 Å (see Figure A.3.30 in the Appendix).

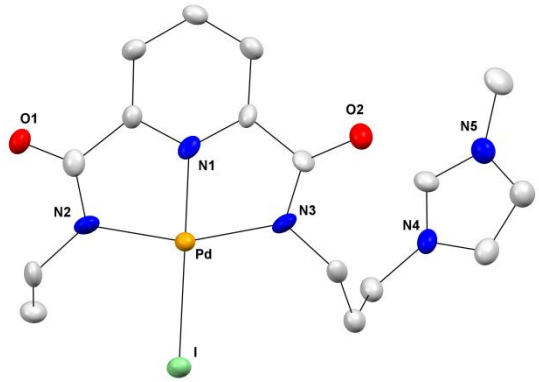

Figure 3.6. Representation of the X-ray crystal structure of complex **3.6** showing all non-hydrogen atoms as 50% thermal ellipsoids.

Ag(I)-NHC complexes can undergo transmetalation with a variety of other metals to generate a variety of NHC complexes.[39,40] Thus, we chose to explore the coordination chemistry of the imidazolium NHC precursor in **3.6** with AgOAc. It was theorized that reaction of **3.6** with AgOAc would provide a Pd(II)/Ag(I) heterobimetallic complex containing a 1:1 metal ratio. Reactions were initially carried out on a small scale in NMR tubes so that the reaction progress could be monitored by ^{1}H NMR spectroscopy. Complex **3.6** (1 equiv) was treated with AgOAc (1 equiv) in DMSO-d_6 at room temperature (Figure 3.7). However, instead of witnessing the disappearance of the signal for the acidic imidazolium proton H(im)—which would result from the formation of a Ag(I)–carbene bond—a reaction product was observed in a roughly 1:1 ratio with **3.6** (Figure 3.7B). The new signal for H(im) 0.22 ppm downfield compared to **3.6** is consistent with the replacement of the iodide ligand with a hydrogen bond acceptor such as acetate, as in the proposed complex **3.6-OAc**. To drive the formation of this new complex, a second equivalent of AgOAc was added to the NMR tube, resulting in the disappearance of all

proton signals for **3.6** (Figure 3.7C). The proposed complex **3.6-OAc** is not stable, however, and when the reaction progress was assessed after 16 hours, a set of signals corresponding to a new reaction product was observed (Figure 3.7D). Interestingly, no signal corresponding to H(im) was present among this new set of signals, suggesting that H(im) was deprotonated and a metal–carbene bond was formed. At this point, an aliquot was withdrawn from the NMR tube and diluted in acetonitrile for ESI-MS analysis. No peak envelope containing Ag(I) was present in the ESI mass spectrum of this reaction product. These results would suggest the formation of a Pd–C bond to form the Pd(II) complex **3.7**, possibly via transmetalation from the proposed complex **3.6**-AgOAc.

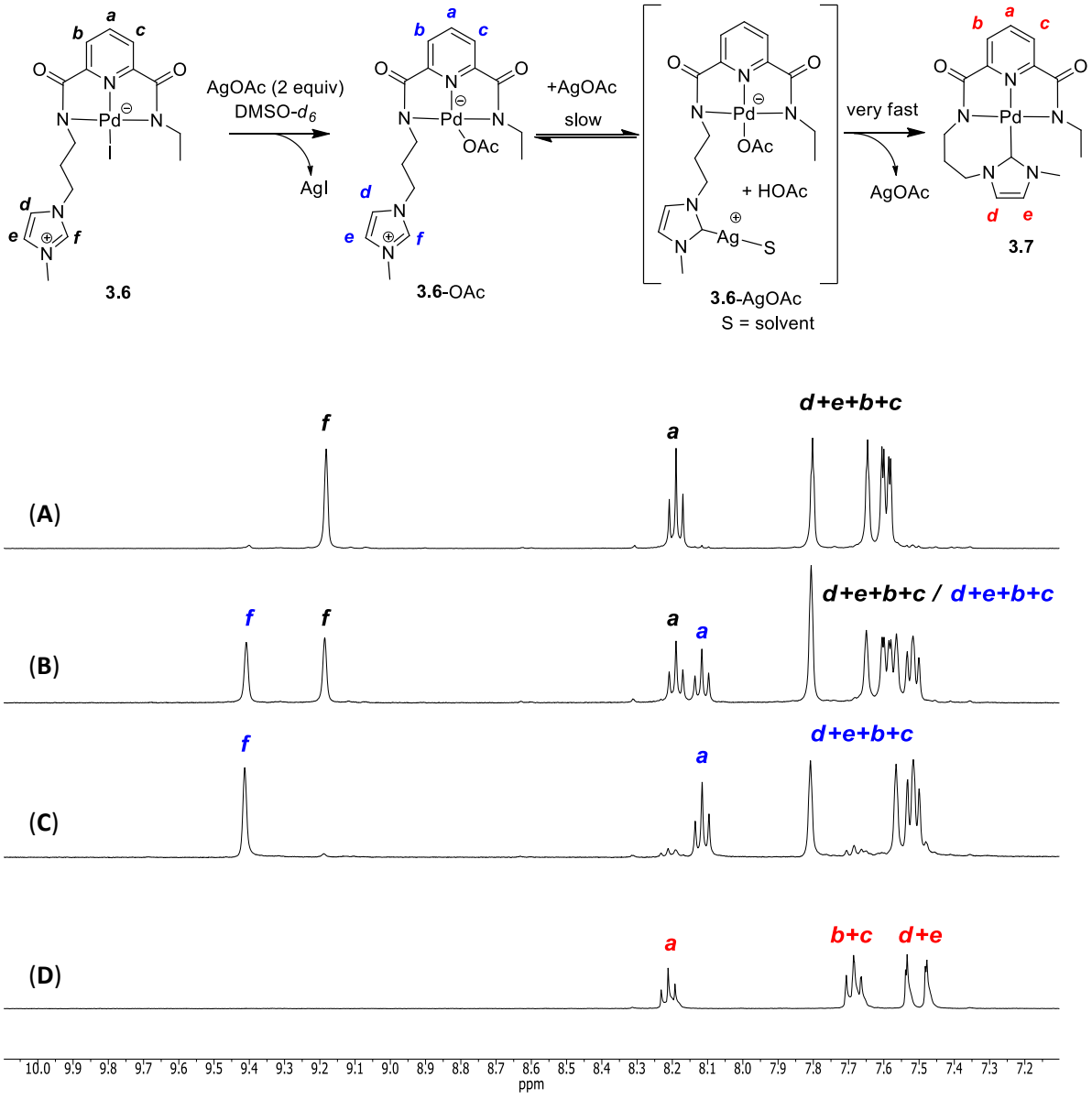

Figure 3.7. Top: schematic representation of the reaction of **3.6** with AgOAc. Bottom: Aromatic region of the ^{1}H NMR spectra (400 MHz) in DMSO-d_6 of (**A**) **3.6**, (**B**) **3.6** plus AgOAc (1 equiv), (**C**) **3.6** plus AgOAc (2 equiv), (**D**) **3.6** plus AgOAc (2 equiv) after 16 h.

On a larger scale, AgOAc (2.1 equiv) was added to a solution of complex **3.6** in acetonitrile, which resulted in the formation of a grey suspension in a yellow solution

(Scheme 3.10). After stirring for 16 hours, the precipitate was filtered, and the solvent was removed *in vacuo* to afford complex **3.7** as a yellow powder in 79% yield. In addition to the disappearance of H(im) in ^{1}H NMR spectrum of **3.7**, the ^{13}C NMR spectrum contains a signal at 166.4 ppm, providing further support for the formation of a Pd–C(carbene) bond.

Scheme 3.10. Synthesis of Pd(II) complex **3.7**.

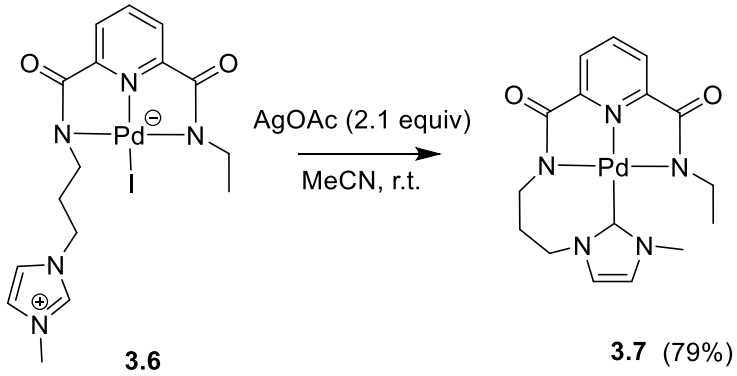

3.6 **3.7** (79%)

Crystals of **3.7** suitable for single crystal X-ray diffraction were obtained from the slow evaporation of an acetonitrile solution of the complex at room temperature. The molecular structure of **3.7** (Figure 3.8) supports our conclusions from the NMR spectroscopic and MS data for the formation of **3.7**. Complex **3.7** contains a relatively long Pd– N1 bond (1.961 Å), which is consistent with the increased *trans* influence of the carbene ligand relative to acetonitrile and iodide (Pd–N1 is 1.920 and 1.943 Å for **2.6a** and **3.6**, respectively). Similar to what was observed for complex **3.6**, the N2-Pd-N3 bond angle in **3.7** (159.85°) is smaller than the idealized angle of 180°. Another distinctive feature of **3.7** is that the plane of the imidazolium ring forms a dihedral angle of 51.38° with the average coordination plane of Pd(II).

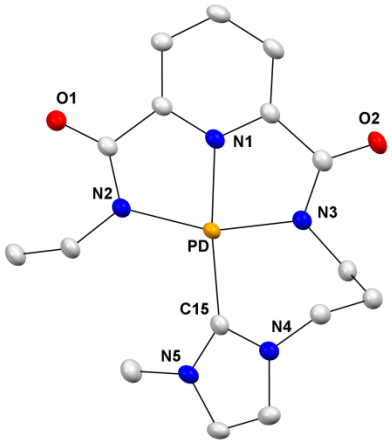

Figure 3.8. Representation of the X-ray crystal structure of complex **3.7** showing all non-hydrogen atoms as 50% thermal ellipsoids.

Unlike Pd(II) NNN-pincer complex **3.6**, the ^{1}H NMR signals for the enantiotopic protons in **3.7** are magnetically nonequivalent. Whereas a resonance similar to 5.06 ppm in the ^{1}H NMR spectrum of **3.7** (Figure 3.9) also appears in the ^{1}H NMR spectra of complexes **3.11**, **3.12**, and **3.13** (see Figures A.3.20, A.3.24, and A.3.27, respectively, in the Appendix), we suspect that this signal corresponds to the proton *gamma* to the amide nitrogen (closest to the NHC). The observed coupling constant for this signal ($^{2}J_{H,H}$ = 13.4 Hz) is consistent with the geminal coupling of aliphatic protons.[41] The two protons *beta* to the amide nitrogen coalesce and appear as a multiplet (1.82 – 1.74 ppm). Of the three remaining protons belonging to the propylene linker, it is not immediately clear which corresponds to the triplet of doublets proton signal at 1.88 ppm. However, due to the fact that the coupling constant ($^{2}J_{H,H}$ = 12.6 Hz) does not match that of the signal at 5.06 ppm, this signal likely represents one of the enantiotopic protons on the carbon *alpha* to the amide nitrogen. The close proximity of this proton to the Pd(II) metal center (see Figure

A.3.31 in the Appendix) may be responsible for the upfield nature of this signal compared to the corresponding triplet proton signal in the ^{1}H NMR spectrum of **3.6** (3.54 ppm).

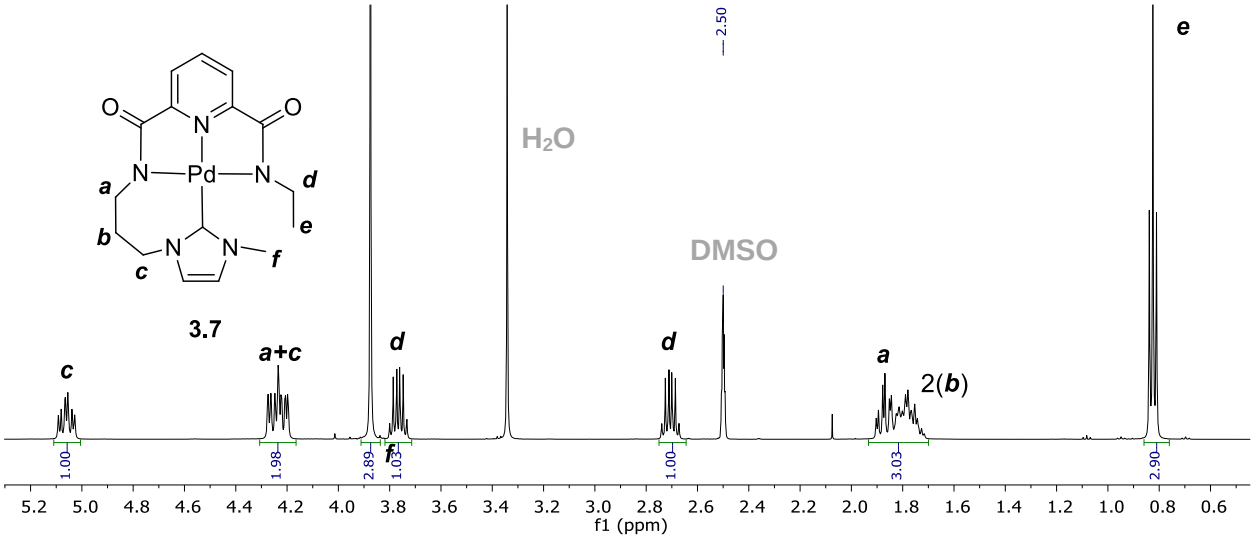

Figure 3.9. Aliphatic region of the ^{1}H NMR spectrum (500 MHz, DMSO-d_6) of complex **3.7**.

With the synthesis and characterization of the unsymmetrically substituted Pd(II) complex **3.7** in hand, we speculated that submitting the symmetrically substituted hybrid pincer/NHC-precursor ligand **3.5** to a similar protocol would result in an available imidazolium NHC precursor to coordinate additional metals. Toward this goal, we monitored the addition of one equivalent of $Pd(OAc)_2$ to a solution of **3.5** in CD_3CN (Figure 3.10). The reaction was conducted in an NMR tube and monitored by ^{1}H NMR spectroscopy. However, rather than selectively forming the desired product, three different species were observed, distinguishable by the presence of three singlet H(im) resonances (9.26, 8.92, and 8.85 ppm) (Figure 3.10A). Additionally, the presence of the triplet proton signal for H(amide) at 9.31 ppm indicated that the starting material, **3.5**, had not been consumed. We suspected the two new H(im) signals in the ^{1}H NMR spectrum of the

reaction mixture corresponded to reaction products involving Pd(II) coordination to the pincer site, as they were not accompanied by an additional amide resonance. The positive mode ESI mass spectrum of an aliquot of the NMR-scale reaction—diluted in acetonitrile—confirmed the formation of a new Pd(II) species. However, attempts to obtain crystals of the new Pd(II) species were unsuccessful, resulting in the isolation of a dark red oil.

To determine whether the distribution of singlet H(im) resonances in Figure 3.10A was due to the coordination of different counterions in the fourth coordination site of the new pincer complex, we added an excess of tetrabutylammonium acetate (TBAOAc) to a solution of $Pd(OAc)_2$ (1.2 equiv) and ligand **3.5** (1 equiv) in DMSO-d_6. The ^{1}H NMR spectrum of this reaction showed the formation of one major species, suggesting the formation of acetate-bound Pd(II) complex **3.8** (Figure 3.10B). Comparison of the chemical shift of proton signal for H(im) to the H(im) signals in the crude reaction mixture (Figure 3.10A) revealed that **3.8** is a minor product in the initial reaction. The addition of excess tetrabutylammonium iodide (TBAI) to the same NMR tube resulted in the appearance of a new set of signals resembling that of the major product from the initial reaction, suggesting iodide coordinates palladium to form complex **3.9** (Figure 3.10C). The observation that **3.9** (X = I) as the major product is in line with the formation of **3.6** (X = I) from ligand **3.3**, described earlier.

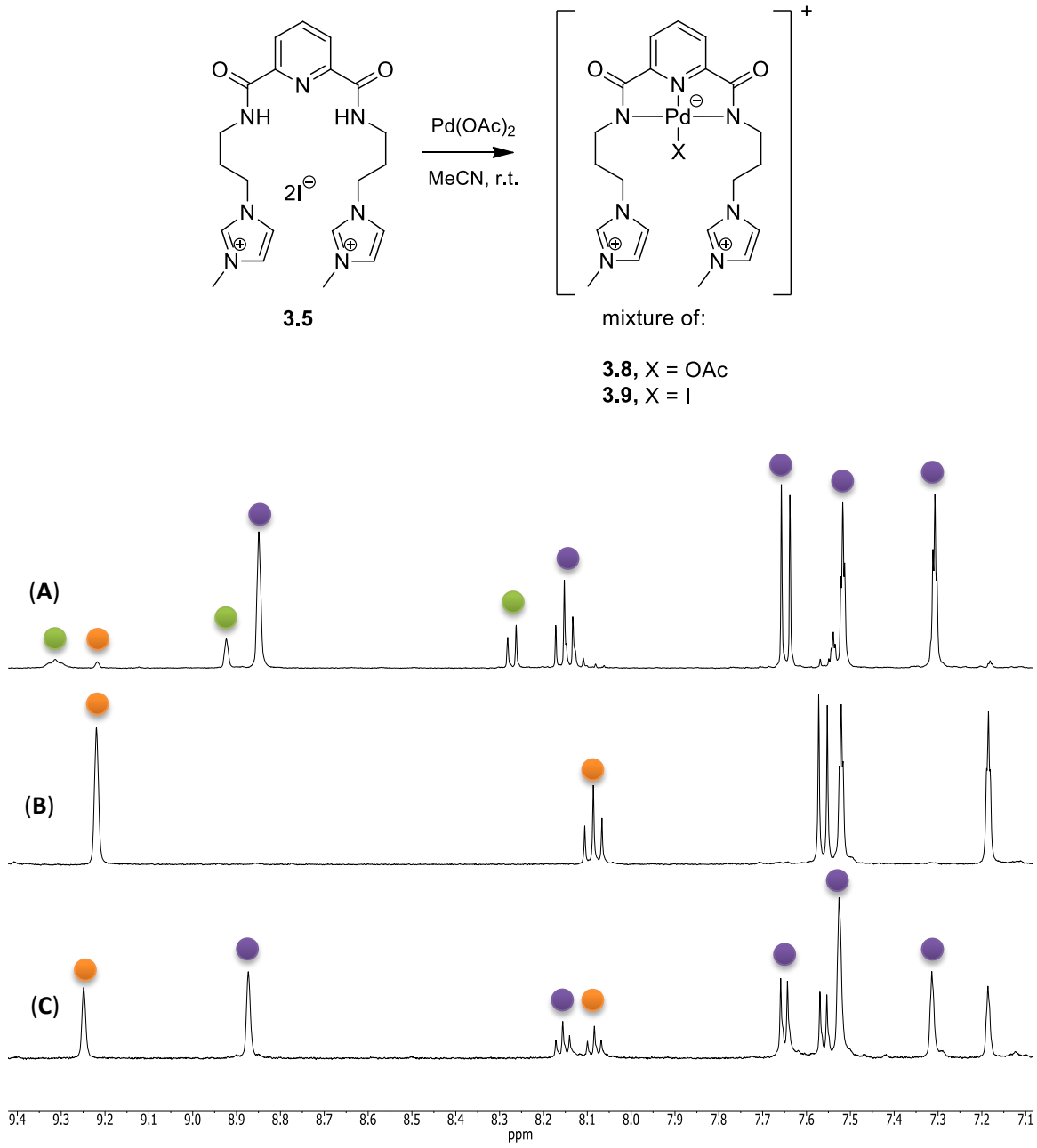

Figure 3.10. Top: schematic illustration of the reaction of **3.5** with $Pd(OAc)_2$. Bottom: Aromatic region of the ^1H NMR spectra in DMSO-d_6 of (**A**) the mixture that results from addition of $Pd(OAc)_2$ to **3.5**, (**B**) the addition of $Pd(OAc)_2$ (1.2 equiv) and TBAOAc (excess) to **3.5** and (**C**) addition of TBAI to the contents of the mixture analyzed in spectra (**B**) (= **3.5**; = **3.8**; = **3.9**).

On a larger scale, TBAI (3 equiv) and $Pd(OAc)_2$ (1 equiv) were added to a solution of ligand **3.5** in acetonitrile, but the work-up proved troublesome and we were unable to crystallize **3.9** out of the reaction mixture. This result was possibly due to the presence of excess iodide, which leads to the consumption of palladium in the form of PdI_2, as indicated by the dark red color of the solution. Attempts to add an excess of $Pd(OAc)_2$ (up to 3 equiv) to **3.5** in acetonitrile also did not lead to an isolable product. Based on these experiments, an alternate route was pursued.

We theorized that exchanging the iodide counter ions in **3.5** with triflate counter ions would help us avoid the complicated mixture of reaction products discussed above. Using this approach, the desired Pd(II) NNN-pincer complex **3.10** was obtained in two steps (in one-pot) from ligand **3.5** (Scheme 3.11). Treatment of **3.5** with AgOTf (2 equiv) in acetonitrile resulted in the formation of a flaky light yellow precipitate—characteristic of silver iodide—which was removed by filtration. The ^1H NMR spectrum of the crude reaction mixture filtrate was similar to that of **3.5** in that the amide and imidazolium salt protons were still intact (Figure 3.11). Following addition of $Pd(OAc)_2$ to the same pot, the solution turned yellow within five minutes. After stirring for three hours, the volatiles were removed *in vacuo* to afford **3.10** as a yellow solid in 89% yield. The ^1H NMR spectrum of **3.10** displays a singlet proton signal at 9.16 ppm for H(im). The signal for the two unbound triflate counterions that appears at 79.13 ppm in the ^{19}F NMR spectrum of **3.10** is in agreement with the reported chemical shift for a free triflate anion.[42]

Scheme 3.11. Synthesis of complex **3.10**.

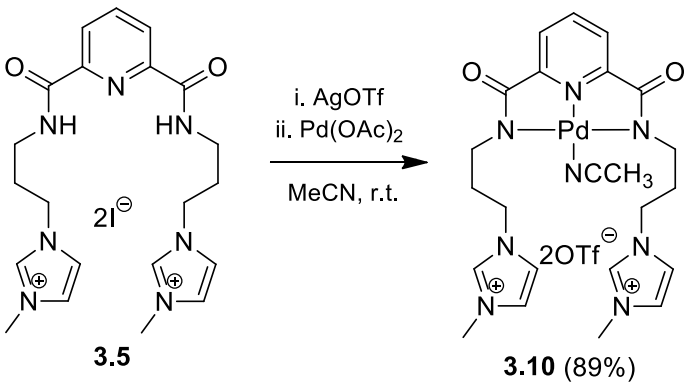

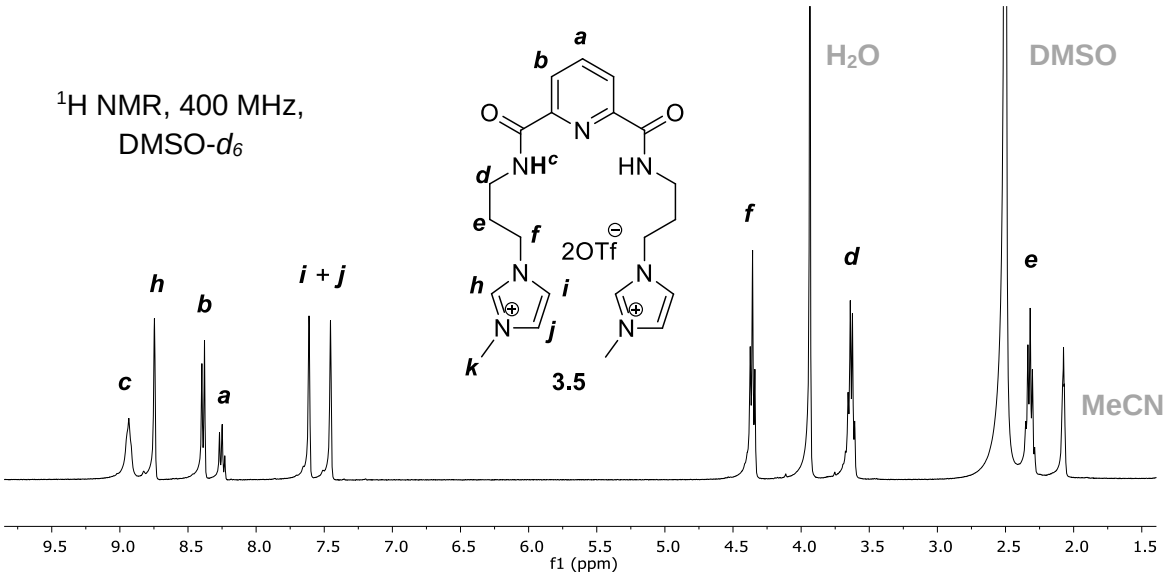

Figure 3.11. The ^{1}H NMR spectrum of the crude reaction mixture of **3.5** after the addition of AgOTf (2 equiv).

Single crystals of **3.10** suitable for X-ray diffraction were obtained by vapor diffusion of diethyl ether into a solution of the complex in acetonitrile. The molecular structure of **3.10** shows the expected NNN-pincer coordination of Pd(II), with a molecule of acetonitrile occupying the fourth coordination site (Figure 3.12). The Pd–N bond

distances are shorter than those observed for **3.6**, but very similar as those observed in **2.6a**, which also features an acetonitrile ligand (Chapter 2, *vide supra*). The N2-Pd-N3 bond angle is distorted (161.26º), although to a lesser extent than the corresponding angle in complexes **3.6** and **3.7**. Whereas the N1-Pd-N1S bond angle is exactly 180º, the molecular structure of **3.10** has a C_2 axis of symmetry along the Pd–N1 bond (see Figure A.3.32A in Appendix). The imidazolium cations stack *anti* to each other on opposite sides of the Pd(II) coordination plane. The crystal lattice of **3.10** contains of a dimer pair of enantiomers (see Figure A.3.32B in Appendix). The presence of two triflate counterions was also confirmed by this solid state structure.

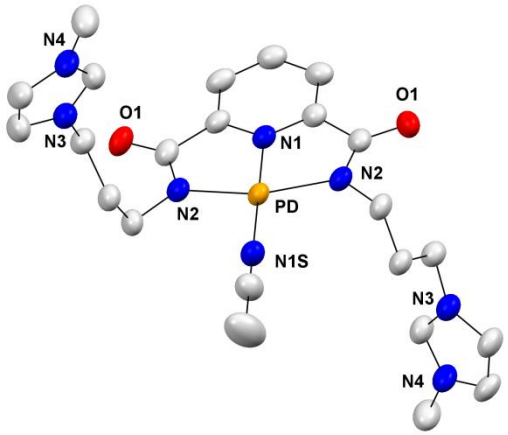

Figure 3.12. Representation of the X-ray crystal structure of Pd(II) complex **3.10** showing all non-hydrogen atoms as 50% thermal ellipsoids. The two triflate counter ions are omitted for clarity.

The symmetrically substituted tetradentate Pd(II) complex **3.11** was prepared in a similar manner to unsymmetrically substituted tetradentate Pd(II) complex **3.7**. An acetonitrile solution of **3.10** was treated with two equivalents of AgOAc, and the reaction mixture was stirred overnight at room temperature (Scheme 3.12). The Ag(I) species slowly decomposed over time to yield a grey precipitate, which was filtered, and the

solvent of the filtrate was removed *in vacuo*. The resulting hygroscopic yellow solid was dissolved in acetonitrile and stirred for 2 hours, after which a yellow precipitate formed. This precipitate was filtered and washed with diethyl ether (3 x 5 mL) to afford **3.11** as a yellow solid in 79% yield.

Scheme 3.12. Synthesis of complex **3.11**.

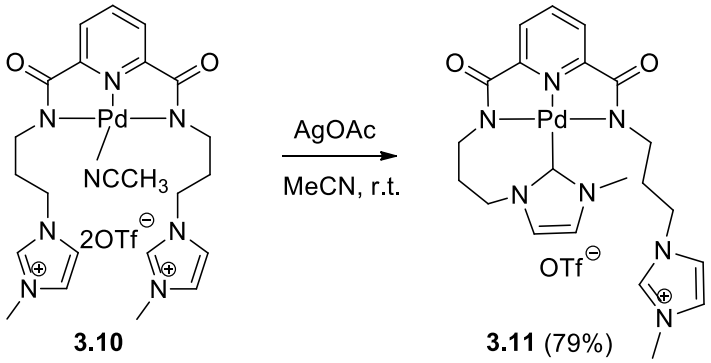

The NMR data are consistent with the formation of **3.11**; most notably, in the ^{1}H NMR spectrum, the ratio of the integration for the proton *para* to pyridine nitrogen relative to H(im) is 1:1 (Figure 3.13), compared to 2:1 for the analogous ratio of protons in **3.10**. Similar to what was observed in the aliphatic region of the ^{1}H NMR spectrum of unsymmetrically substituted tetradentate Pd(II) complex **3.7**, the enantiotopic protons of the propylene linker arm in **3.11** are magnetically nonequivalent. In the ^{13}C NMR spectrum, a new signal appears at 165.7 ppm, which is consistent with the literature value for a carbene bonded to Pd(II)[43] and similar to the signal observed for the carbene in **3.7** (166.4 ppm). The unbound triflate anion appears at 79.13 ppm in the ^{19}F NMR spectrum, also in line with **3.7**. Further confirmation of the formation of **3.11** came from the positive mode ESI mass spectrum (in MeCN), which displays a prominent ion peak at *m/z* 514.1188 $[M - OTf]^{+}$.

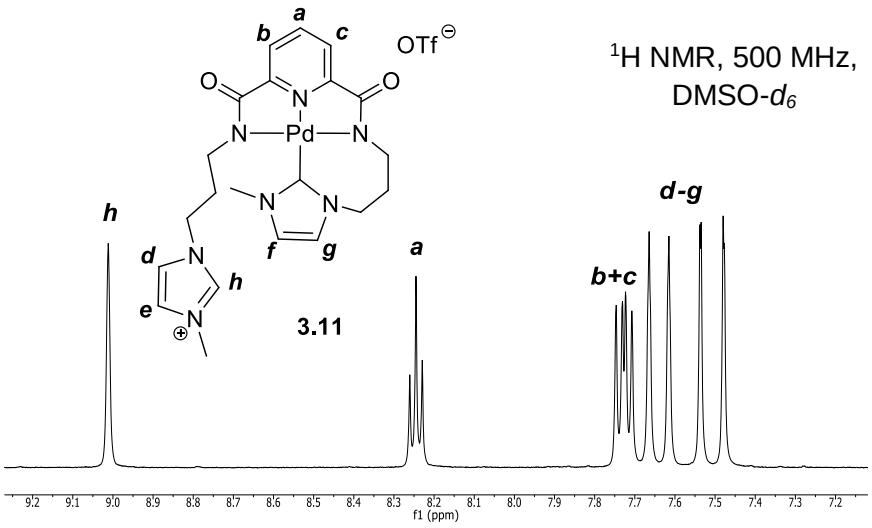

Figure 3.13. Aromatic region of the ^{1}H NMR spectrum of complex **3.11** in DMSO-d_6.

Single crystals of **3.11** suitable for X-ray diffraction were obtained by slow diffusion of diethyl ether into a saturated solution of **3.11** in acetonitrile. The molecular structure of **3.11** (Figure 3.14) confirmed the hybrid NNN-pincer/NHC coordination of Pd(II), as well as the presence of an unbound imidazolium NHC precursor and triflate counterion. The Pd–N bond lengths are very similar to those of **3.7**, but longer than those of complexes **3.6** and **3.10**. The N2-Pd-N3 and N1-Pd-C13 angles are also similar to the corresponding angles in **3.7**. The angle that the Pd(II) coordination plane forms with the imidazolium plane is 53.08°—only slightly larger than the analogous angle in **3.7** (51.38°)—suggesting that the added steric bulk of the opposite amide-appended propylimidazolium arm does not interfere with the Pd–C(carbene) bond formation. The potential influence that the amide-appended propylimidazolium arm has on this angle is obvious from perspective view of **3.11** shown in Figure A.3.33 of the Appendix.

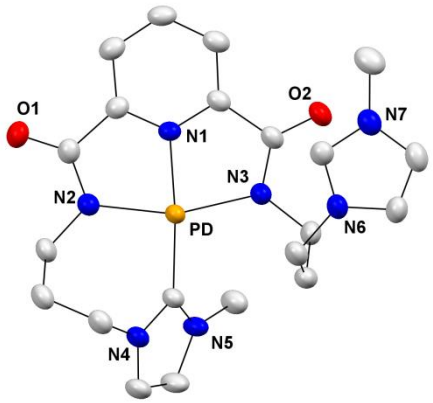

Figure 3.14. Representation of the X-ray crystal structure of Pd(II) complex **3.11** showing all non-hydrogen atoms as 50% thermal ellipsoids. The triflate counter ion is omitted for clarity.

3.3.3 *Synthesis of Heterobimetallic Complexes*

With the intent of developing a protocol that could be used to synthesize heterobimetallic complexes, we investigated the addition of excess (5 – 10 equiv) silver(I) oxide (Ag_2O) to complex **3.11** using deuterated derivatives of well-known solvents for Ag(I)-NHC complex formation.[15,20,21,34,36] The reactions were carried out on a small scale and monitored by ^{1}H NMR spectroscopy. The conversion of **3.11** to the new product was determined by comparing the integrations for the triplet proton signals *para* to the pyridine nitrogens in **3.11** and the reaction product. Based on spectral data, we propose the structure of the reaction product to be the bis-carbene complex, **3.12**. However, as multiple attempts to acquire single crystals for X-ray diffractions were unsuccessful, we were unable to unequivocally confirm the structure of this molecule.

Although the solubility of Ag_2O in water is high compared to that in organic solvents, initial attempts in D_2O at 40°C resulted in trace product formation (Table 3.1, entry 1). Addition of Ag_2O to **3.11** in CD_3CN at room temperature led to the formation of

a new set of aromatic peaks corresponding to the reaction product (Table 3.1, entry 2). Notably, the signals corresponding to this product did not include a signal for H(im), suggesting the new product contains the desired Ag(I)-NHC coordination. Further improvement of the reaction yield was observed at higher temperatures using CD_2Cl_2 or CD_3CN (Table 3.1, entries 3 and 5). Unfortunately, multiple attempts to crystallize the product from the reaction mixture in these solvents were unsuccessful. Although some have reported the synthesis of Ag(I)-NHC complexes in the presence of molecular sieves,[44-46] no improvement in the conversion was observed when the reaction was carried out in the presence of 3Å molecular sieves in CD_3CN. However, when the reaction was carried out in DMSO-d_6, the reaction proceeded almost quantitatively (Table 3.1, entry 6).

Table 3.1. Optimization of silver(I) oxide addition to **3.11**. [a]Yield determined by comparing the signals for the protons *para* to the pyridine nitrogen in **3.11** and **3.12** by ^{1}H NMR spectroscopy.

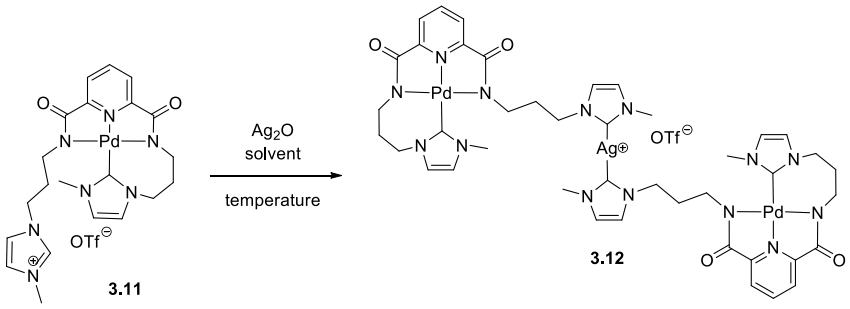

Entry	Solvent	Temperature (^{o}C)	Yield[a]
1	D_2O	40	Trace
2	CD_3CN	25	53
3	CD_3CN	45	78
4	CD_2Cl_2	25	0
5	CD_2Cl_2	40	76
6	DMSO-d_6	25	98

On a larger scale, Ag_2O (4.2 equiv) was added to a solution of **3.11** in DMSO and stirred at room temperature for 24 hours (Scheme 3.13). Subsequently, after the excess Ag_2O (black precipitate) was filtered, the addition of a small amount of acetone to the filtrate enabled it to be miscible with diethyl ether, which was triturated into the filtrate until it became cloudy. The resulting cloudy mixture was stored at 0 ^oC for 24 hours, which resulted in the formation of a yellow crystalline solid. The solvents were decanted, and the solid was dried to afford **3.12** in 30% yield. The ^1H NMR spectrum of **3.12** in DMSO-d_6 was unchanged from that of the *in situ* generated complex. The most convincing evidence for the formation of Ag(I)-biscarbene complex **3.12** came from its ^{13}C NMR spectrum. The signal for the C(carbene) bonded to Ag(I) appears at 177.3 ppm, compared to 141.8 ppm for the analogous carbon in the imidazolium NHC precursor **3.11**. This chemical shift is in line with previously reported values for Ag(I)-biscarbene complexes.[47] Conversely, Ag(I)-monocarbene complexes are known to exhibit a ^{13}C NMR resonance significantly upfield from their biscarbene counterparts.[47,48] The signal for the C(carbene) bonded to Pd(II) appears at 164.8 ppm, which is similar to the chemical shift for the analogous carbon in **3.11** (165.7 ppm). The positive mode ESI mass spectrum also corroborates the formation of **3.12**, with prominent ion isotope patterns for both the monomer (*m/z* 620.0126 [**3.11** – H – OTf + Ag]$^+$) and dimer (*m/z* 1135.1176 [2(**3.11** – H – OTf) + Ag]$^+$) adducts of the Ag(I)-carbene formation (Figure 3.16). Similar ESI-MS observations of both mono- and biscarbene adducts have been reported for Ag(I)-NHC complexes.[39] Attempts to crystallize **3.12** using a variety of solvents (DCM, MeCN, MeOH at r.t. or 0^{o}C) did not yield X-ray quality crystals.

Scheme 3.13. Synthesis of Pd(II)/Ag(I) complex **3.12**.

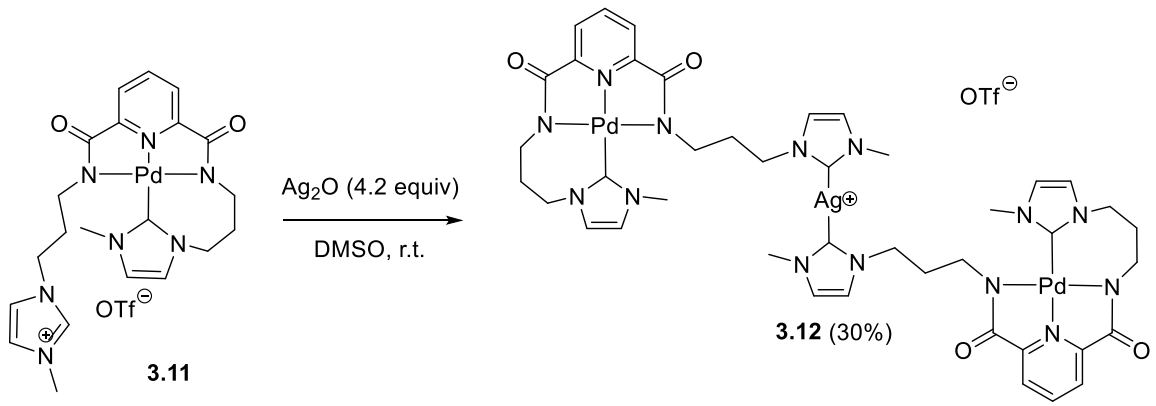

Transmetalation [Ag(I) → Au(I)] was carried out by the addition of $AuClMe_2S$ to a solution of **3.12** in DMSO-d_6 to form **3.13** (Scheme 3.15). Whereas the addition of one equivalent of $AuClMe_2S$ to **3.12** only resulted in partial transmetalation (Figure 3.15B), two equivalents of $AuClMe_2S$ were necessary for the reaction to achieve near completion (Figure 3.15C), as observed by ^{1}H NMR spectroscopy. Akin to **3.12**, both the monomer (*m/z* 710.0745 [**3.11** – H – OTf + Au]$^+$) and dimer (*m/z* 1225.1749 [2(**3.11** – H – OTf) + Au]$^+$) adducts of the Au(I)-NHC complex were observed in the positive mode ESI mass spectrum (Figure 3.16). Complex **3.13** decomposed while attempting recrystallization from a solution of DMSO-d_6 at room temperature. Further studies are necessary to confirm the molecular the structure of **3.13**.

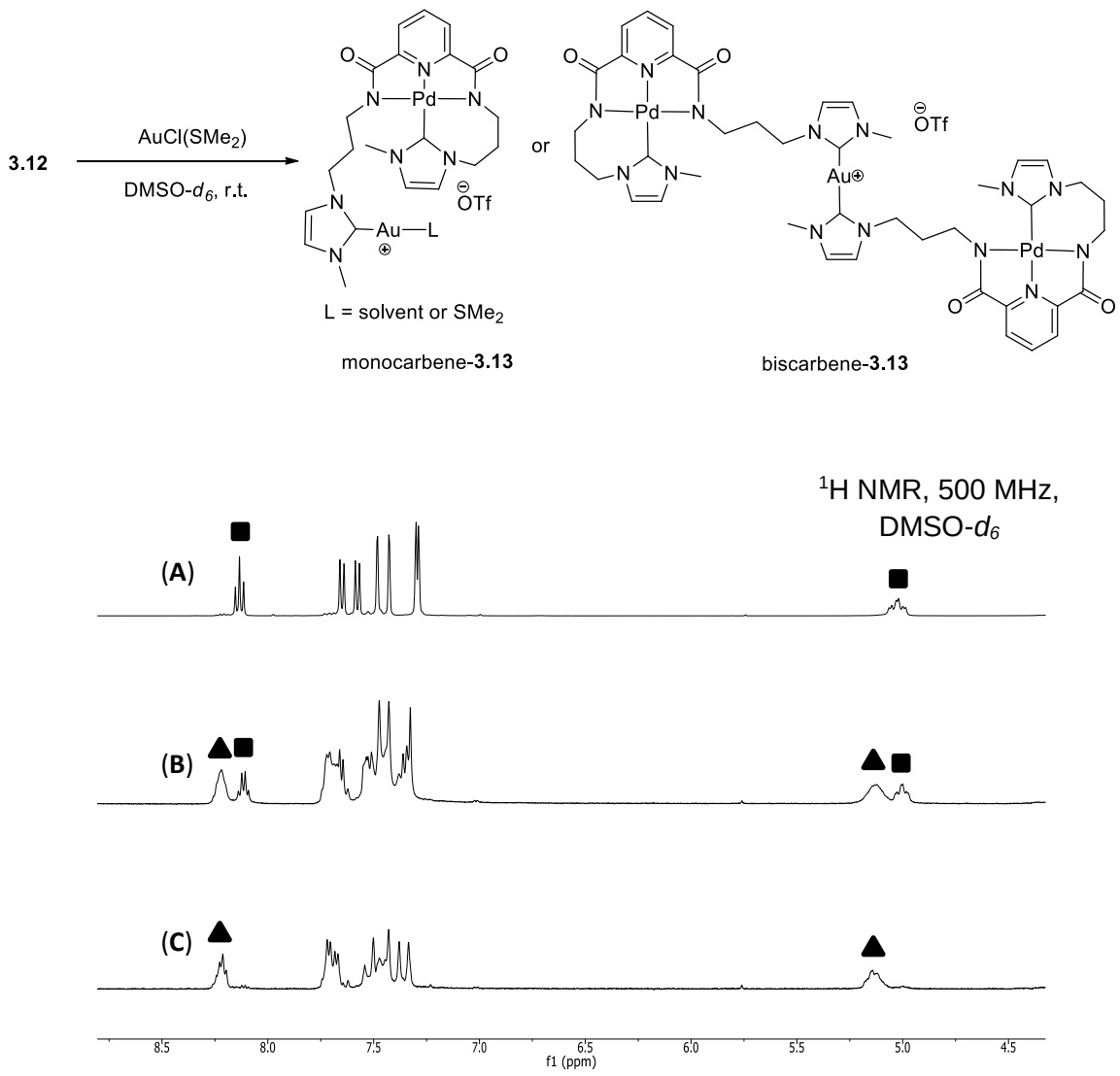

Figure 3.15. Selected region of the ^{1}H NMR spectra of (**A**) complex **3.12**, (**B**) complexes **3.12** + **3.13**, and (**C**) complex **3.13** (■= complex **3.12**; ▲= complex **3.13**).

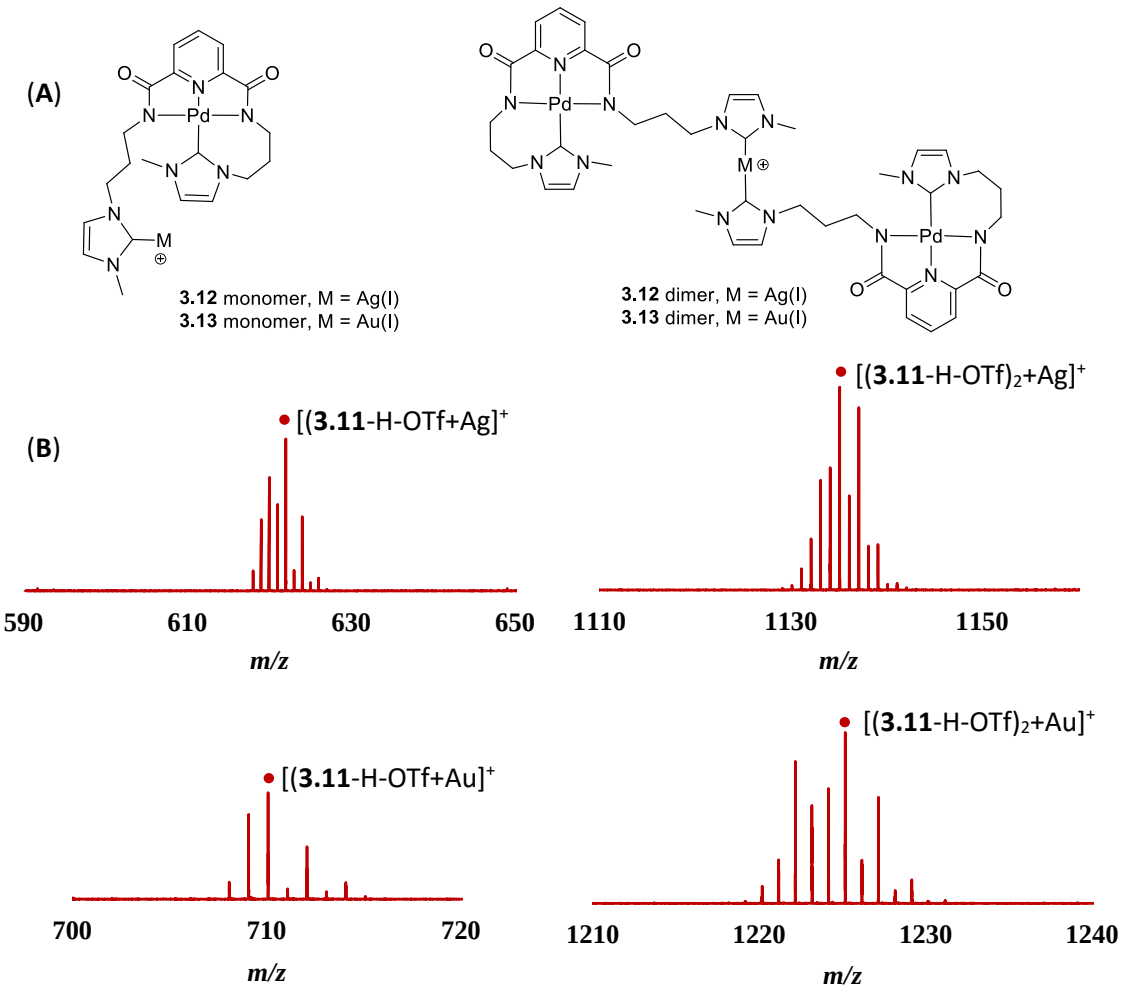

Figure 3.16. (**A**) Chemdraw representations of the monomer and dimer isomers of complexes **3.12** and **3.13** observed in the mass spectrum and (**B**) isotopic patterns observed in the positive mode electrospray ionization mass spectra of **3.12** and **3.13** (in MeCN).

3.3.4 *Application in Heck Catalysis*

In Chapter 2 of this dissertation, we demonstrated that tri- and tetradentate Pd(II) NNN-pincer complexes are efficient catalysts in the Heck coupling reaction of 4-iodotoluene and styrene. Induction periods and longer reaction times were observed when either complex **2.8** or **2.9**—both of which contain a tetradentate ligands—was employed the catalyst (Table 2.1, entries 3 and 4; for induction periods, see Figures 2.15 and 2.16, *vide supra*). Organ and coworkers have proposed a Pd(0)/Pd(II) catalytic cycle for the Heck reaction in which the palladium atom remains coordinated to the NHC throughout the cycle.[49] Additionally, Glorius and coworkers have recently shown that NHCs can stabilize Pd(0) nanoparticles.[50] Thus, we were curious to see whether the presence of a Pd–C (NHC) bond would facilitate—or hinder—the formation of a catalytically active Pd(0) species from tetradentate Pd(II) complexes **3.7** and **3.10**. We again selected the Heck reaction of 4-iodotoluene and styrene for this preliminary investigation. For comparison, we also investigated the Heck coupling reaction using Pd(II) complexes **3.6** and **3.10**, which contatin tridentate pincer ligands. The reactions were performed on a 2.0 mmol scale with respect to 4-iodotoluene. To a 25 mL three-necked flask was added 4-iodotoluene (1 equiv), NaOAc (1.1 equiv), tetrabutylammonium bromide (20 mol %), Pd-catalyst (1×10^{-1} mol %), and *N,N*-dimethylacetamide (DMA, 5 mL), and the mixture was heated to 165 ^{o}C. Once the solvent began to reflux, neat styrene (1.4 equiv) was added (T = 0) and aliquots were removed every 15 minutes thereafter for ^{1}H NMR spectroscopic analysis.

Whereas both *trans*- and *gem*-stilbene isomers were produced during the reaction, the ratio of isomers was the same, regardless of which Pd-catalyst was employed (ratio of *trans*- to *gem*-stilbene = 5.25:1). Quantitative conversion to the stilbene isomers was

observed after only 0.5 h using either **3.6** or **3.10** (Table 3.2, entries 1 and 3, respectively). As expected, based on our previous studies using related aliphatic amide appended Pd(II) NNN-pincer complexes (Chapter 2), no activation period was observed on our sampling time scale using these complexes. Conversely, longer reaction times were observed with complexes **3.7** and **3.11** (Table 3.2, entries 2 and 4, respectively). This was also expected, based on our investigations of Pd(II) complex **2.8**, which also contains a tetradentate ligand. Interestingly, an induction period was only observed on our sampling time scale using complex **3.7** (Figure 3.17). Although the reaction took the longest to reach completion when **3.8** was employed as the catalyst, no induction period was observed. While the reason for this discrepancy is not currently understood, it is plausible that the additional imidazolium salt/NHC precursor ligand aids in stabilizing Pd(0) after complex decomposition, prolonging the formation of a catalytically active species. Thus, further studies are necessary to determine the fate of Pd throughout the catalytic cycle, and ultimately to determine if it remains bound to the carbene ligand during catalysis. Interestingly, when the coupling reaction was carried out with catalyst **3.11** in the presence of Ag_2O (0.2 equiv), quantitative conversion to the coupling products was observed after 0.75 hours (Table 3.2, entry 5), compared to 1.75 hours (Table 3.2, entry 4) when Ag_2O was not used. More work is necessary to determine the reason for this improved catalytic activity.

Table 3.2. Heck coupling of 4-iodotoluene with styrene using complexes **3.6**, **3.7**, **3.10**, and **3.11** as catalysts.[a]

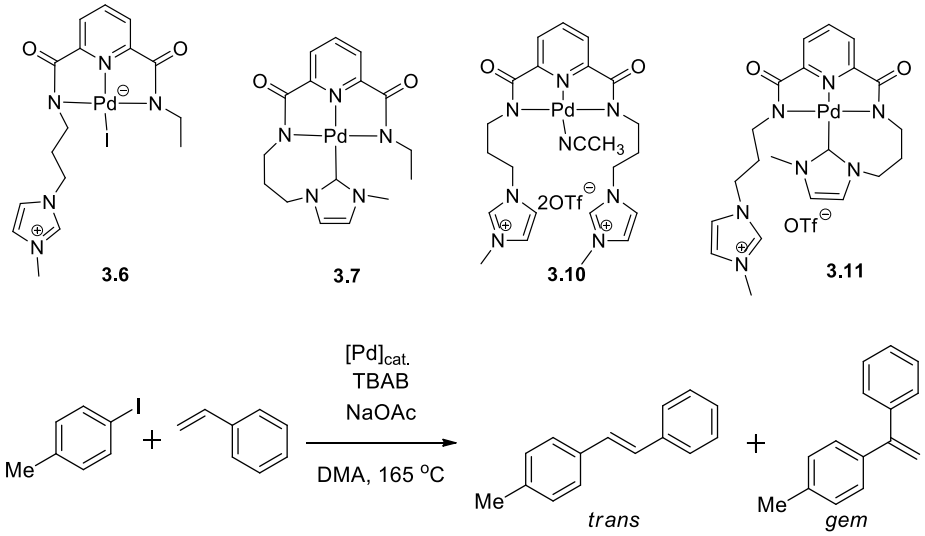

Catalyst	reaction time (h)	Induction (h)	conversion (%) (trans+gem)[b]
3.6	0.5	--	>99
3.7	1.25	0.68	>99
3.10	0.5	--	>99
3.11	1.75	--	98
3.11[c]	0.75	--	>99

[a]Reaction conditions: styrene (1.4 equiv), NaOAc (1.1 equiv), *n*-Bu_4NBr (20 mol %), 1 x 10^{-1} mol % catalyst, DMA, 165 °C. [b]^{1}H NMR conversion obtained by comparing the relative integrations for of *trans* and *gem*-methylstilbene to the starting material, 4-iodotoluene. [c]Plus Ag_2O (0.2 equiv).

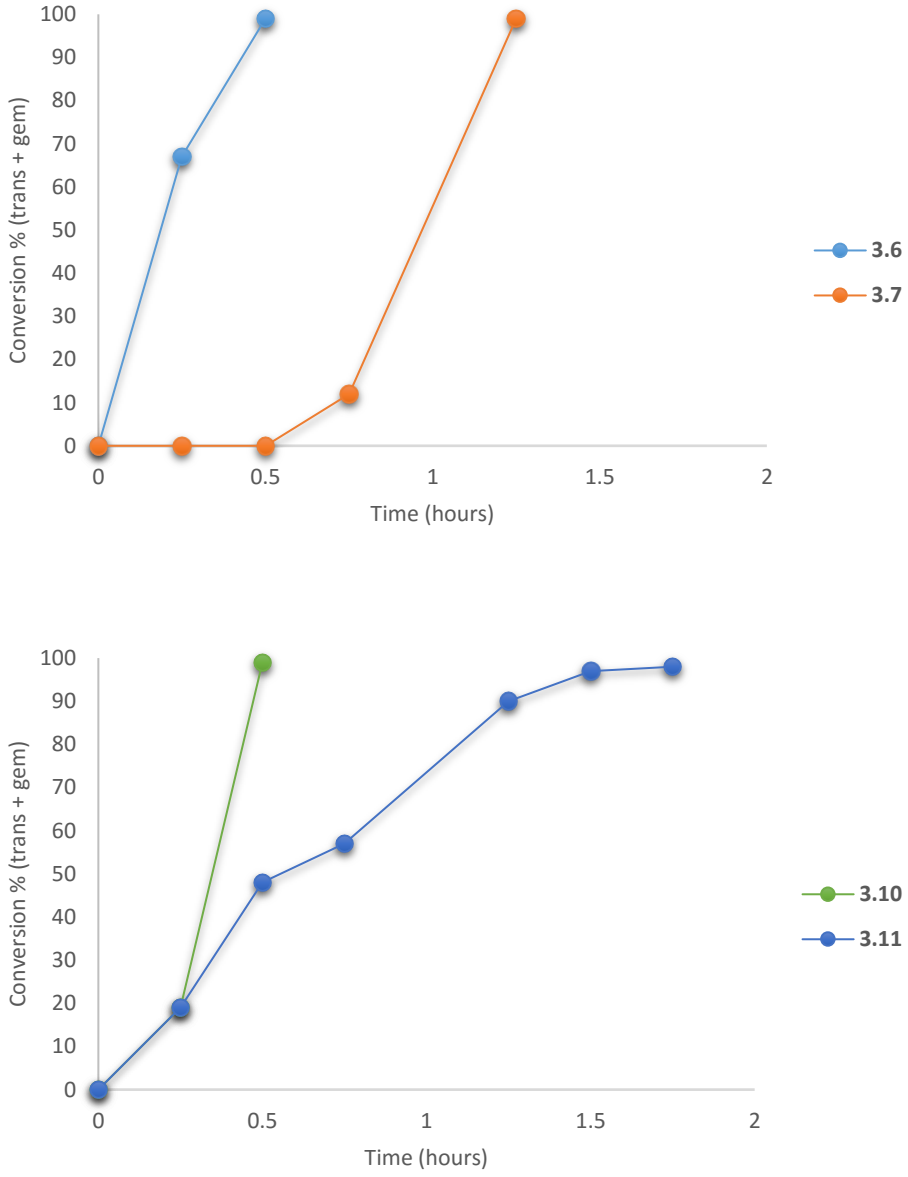

Figure 3.17. Time course of the formation of *trans*- and *gem*-stilbene using catalysts **3.6**, **3.7**, **3.10**, and **3.11**.

3.4 *Concluding Remarks*

Novel hybrid Pd(II) NNN-pincer/NHC complexes containing either Ag(I) or Au(I) have been studied. The formation of the Pd(II) complexes was characterized using ^{1}H, ^{13}C, and ^{13}C DEPT NMR spectroscopies, positive mode HRMS-ESI, and single crystal XRD crystallography. Symmetrically substituted tetradentate Pd(II) complex **3.11**, which contains an available imidazolium NHC precursor, provides a novel platform from which to construct a variety of heterobimetallic complexes. Pd(II)/Ag(I) complex **3.12** and Pd(II)/Au(I) complex **3.13** were characterized by NMR spectroscopy and mass spectrometry. Preliminary catalytic investigations indicate tri- and tetradentate Pd(II) complexes **3.6**, **3.7**, **3.10**, and **3.11** are efficient catalysts for the Heck coupling reaction of 4-iodotoluene and styrene.

Future work will likely focus on establishing the solid state structure of heterobimetallic Pd(II)/Ag(I) complex **3.12**, as well as investigating the scope of metals that can be paired with Pd(II) via transmetallation. Further work could also focus on the synthesis of different unsymmetrically- and symmetrically-substituted ligands, in addition to **3.3** and **3.5**. For example, the incorporation of a benzyl group onto the pendant imidazole (e.g. via *N*-alkylation of the imidazole functional handle in symmetrically substituted compound **3.4** with benzyl bromide) might aid in the synthesis of the subsequent Pd(II) complex, while avoiding the introduction of triflate counter ions into the ligand. Additionally, a pendant benzyl group would be expected to aid in both the stability and crystallization of the subsequent Ag(I)-NHC complex. Ultimately, these types of complexes could be investigated in cooperative catalysis applications.

3.5 *Materials and Methods*

3.5.1 *General*

$Pd(OAc)_2$, Ag_2O, AgOAc, AgOTf, and AuS were purchased from Aldrich. Other chemicals were reagent grade and were used as received without further purification. Nuclear magnetic resonance (NMR) spectra were recorded on a Bruker Avance 400 spectrometer or a Bruker Avance 500 spectrometer. Chemical shifts of the ^{1}H and ^{13}C resonances are expressed in ppm, and referenced to the residual solvent signal. Chemical shifts of the ^{19}F resonances are expressed in ppm and referenced to trifluorobenzene (provided by the KU NMR lab) as an external standard. Mass spectral data were obtained from the Mass Spectrometry Laboratory at the University of Kansas on a LCT Premier Mass spectrometer. Single-crystal XRD data were obtained at the Small-Molecule X-ray Crystallography Laboratory at the University of Kansas by Dr. Victor Day.

3.5.2 *Synthesis of Ligands*

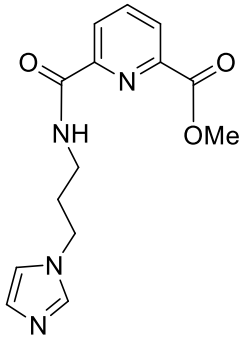

3.1

Methyl 6-((3-(1H-imidazol-1-yl)propyl)carbamoyl)picolinate (**3.1**)**.** To a flask containing a refluxing methanolic (100 mL) solution of dimethyl 2,6-pyridinedicarboxylate (7.48 g, 40 mmol, 4 equiv) was added a methanolic (100 mL) solution of 1-(3-aminopropyl)imidazole (1.25 g, 1.19 mL, 10 mmol, 1 equiv) in a dropwise fashion over 2

h. After 3 d, the solvent was evaporated *in vacuo*, and the crude reaction mixture was purified via column chromatography (90:10 to 80:20 DCM/MeOH) to afford the product as a white powder (1.08 g, 3.7 mmol, 37%). ^{1}H NMR (500 MHz, $CDCl_3$) δ 8.45 – 8.34 (br, 1H), 8.36 (d, J = 7.8 Hz, 1H), 8.22 (d, J = 7.8 Hz, 1H), 8.01 (t, J = 7.8 Hz, 1H), 7.62 (s, 1H), 7.06 (s, 1H), 7.00 (s, 1H), 4.06 (t, J = 7.0 Hz, 2H), 4.01 (s, 3H), 3.50 (q, J = 6.6 Hz, 2H), 2.18 – 2.11 (m, 2H); ^{13}C NMR (126 MHz, $CDCl_3$) δ 165.1, 164.1, 150.1, 146.6, 138.9, 137.3, 129.8, 127.6, 125.6, 119.0, 53.2, 44.7, 36.8, 31.4; HRMS (ESI^+) *m/z*: $[M + H]^+$ calculated for $C_{14}H_{17}N_4O_3$ 289.1290; found 289.1290.

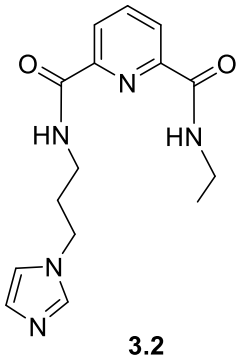

3.2

***N*^{2}-(3-(1H-imidazol-1-yl)propyl)-*N*^{6}-ethylpyridine-2,6-dicarboxamide** (**3.2**). To a sealed tube containing a solution of mixed amide ester **3.1** (0.58 g, 2 mmol) in methanol (10 mL) was bubbled ethyl amine for 2 min. The reaction was stirred at r.t. for 48 h. The solvent was evaporated to afford a clear oil. After 2washing with acetone and hexanes, the product was deposited as a white solid (0.49 g, 1.63 mmol, 82%). ^{1}H NMR (500 MHz, $CDCl_3$) δ 8.84 (t, J = 5.2, 1H), 8.76 (t, J = 5.2, 1H), 8.59 – 8.48 (br, 1H), 8.37 (dd, J = 7.8, 1.2 Hz, 1H), 8.32 (dd, J = 7.8, 1.2 Hz, 1H), 8.02 (t, J = 7.8 Hz, 1H).7.16 – 7.02 (br, 2H), 4.22 (t, J = 6.4, 2H), 3.55 – 3.49 (m, 4H), 2.21 (t, J = 6.3, 2H), 1.24 (t, J = 7.2, 3H); ^{13}C NMR (126 MHz, $CDCl_3$) δ 164.6, 163.8, 149.6, 148.7, 138.9, 125.2, 124.8, 46.2, 36.9,

34.7, 30.6, 15.2; HRMS (ESI$^+$) *m/z*: [M + H]$^+$ calculated for $C_{15}H_{20}N_5O_2$ 302.1612; found 302.1601; [M + Na]$^+$ calculated for $C_{15}H_{19}N_5NaO_2$ 324.1436; found 324.1426.

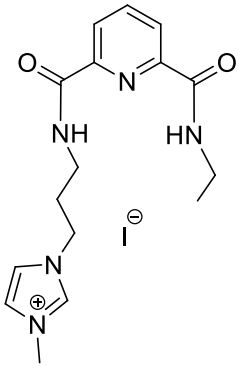

3.3

Ligand 3.3. To an ethanolic (10 mL) solution of unsymmetrically substituted bisamide **3.2** (0.346 g, 1.15 mmol) was added iodomethane (0.185 g, 81 uL, 1.30 mmol) in a sealed tube, and the reaction was sealed and stirred at reflux for 48 h. The white solid that precipitated was filtered and washed with diethyl ether to afford the product as a white solid (0.31 g, 0.53 mmol, 61%). ^{1}H NMR (500 MHz, $CDCl_3$) δ 10.08 (s, 1H), 9.34 (t, J = 6.0 Hz, 1H), 9.19 (t, J = 5.7 Hz, 1H), 8.35 (dd, J = 7.8, 1.1 Hz, 1H), 8.22 (dd, J = 7.7, 1.1 Hz, 1H), 7.98 (t, J = 7.7 Hz, 1H), 7.55 (s, 1H), 7.15 (s, 1H), 4.44 (t, J = 5.6 Hz, 2H), 3.94 (s, 3H), 3.64 – 3.57 (m, 4H), 2.44 (t, J = 5.7 Hz, 2H), 1.28 (t, J = 7.1 Hz, 3H); ^{13}C NMR (126 MHz, $CDCl_3$) δ 165.0, 163.6, 150.1, 148.7, 138.7, 137.9, 125.5, 124.6, 122.9, 122.7, 48.6, 37.0, 36.6, 34.7, 29.1, 15.7; HRMS (ESI$^+$) *m/z*: [M – I]$^+$ calculated for $C_{16}H_{22}N_5O_2$ 316.1768; found 316.1768.

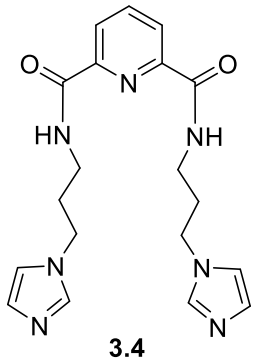

3.4

***N*²,*N*⁶-bis(3-(1H-imidazol-1-yl)propyl)pyridine-2,6-dicarboxamide** (**3.4**). To a solution of dimethyl 2,6-pyridinedicarboxylate (4.7 g, 24 mmol) in methanol (250 mL) was added 1-(3-Aminopropyl)imidazole (6.0 g, 5.72 mL, 48 mmol) and the solution was refluxed for 7 days. Solvent removal *in vacuo* and purification by flash column chromatography (DCM-MeOH; 90:10) gave **3.4** as a clear oil. The oil was taken up in acetone and triturated with diethyl ether to afford a white suspension, which was filtered to give the product as a white solid (7.49 g, 19.6 mmol, 82% yield). ^{1}H NMR (500 MHz, $CDCl_3$) δ 8.89 (t, J = 6.0 Hz, 2H), 8.03 (d, J = 7.7 Hz, 2H), 7.76 (t, J = 7.8 Hz, 1H), 7.30 (s, 2H), 6.75 (s, 2H), 6.73 (s, 2H), 3.79 (t, J = 6.8 Hz, 4H), 3.17 (q, J = 6.5 Hz, 4H), 1.83 (quin, J = 6.7 Hz, 4H); ^{13}C NMR δ (126 MHz, $CDCl_3$) 163.8, 148.3, 138.3, 136.8, 127.8, 124.2, 118.7, 44.2, 36.3, 30.7; HRMS (ESI$^+$) *m/z* $[M + H]^+$ calculated for $C_{19}H_{24}N_7O_2$ 382.1986; found 382.1967; HRMS (ESI$^+$) *m/z* $[M + Na]^+$ calculated for $C_{19}H_{23}N_7NaO_2$ 404.1811; found 404.1767.

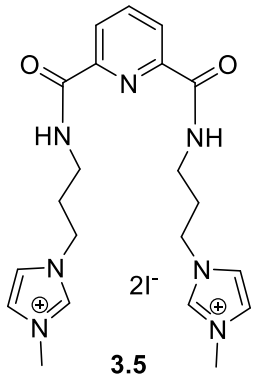

3.5

Ligand 3.5. To an ethanolic (25 mL) solution of symmetrically substituted bisamide **3.4** (0.95 g, 2.5 mmol, 1 equiv) was added iodomethane (1.07 g, 0.467 mL, 7.5 mmol, 3 equiv) in a sealed tube, and the reaction was sealed and stirred at 50 ^{o}C for 48 h. A white solid precipitated out, which was filtered, washed with cold acetone and diethyl ether to afford the product as a white solid (1.28 g, 1.92 mmol, 77%). ^{1}H NMR (500 MHz, DMSO-d$_6$) δ 9.38 (t, J = 6.2 Hz, 2H), 9.16 (s, 2H), 8.23 – 8.19 (m, 3H), 7.83 (s, 2H), 7.71 (s, 2H), 4.26 (t, J = 7.0 Hz, 4H), 3.84 (s, 6H), 3.43 (q, J = 6.4 Hz, 4H), 2.14 (q, J = 6.8 Hz, 4H); ^{13}C NMR (126 MHz, DMSO-d$_6$) δ 163.4, 148.4, 139.6, 136.7, 124.4, 123.5, 122.3, 46.9, 35.8, 35.7, 30.1; HRMS (ESI^{+}) *m/z* [M – I]$^{+}$ calculated for $C_{21}H_{29}IN_7O_2$ 538.1422; found 538.1428.

3.5.3 *Synthesis of Metal Complexes*

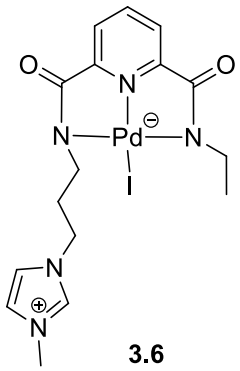

3.6

Complex 3.6. Ligand **3.3** (0.400 g, 0.90 mmol, 1 equiv) was dissolved in an acetonitrile (15 mL) solution of $Pd(OAc)_2$ (0.201 g, 0.90 mmol, 1 equiv) and the reaction was stirred at r.t. for 24 h. The precipitate that formed was filtered and washed with diethyl ether to afford the complex as a dark yellow solid (0.427 g, 0.780 mmol, 87%). ^{1}H NMR (500 MHz, DMSO-d_6) δ 9.19 (s, 1H), 8.18 (t, J = 7.8 Hz, 1H), 7.80 (s, 1H), 7.64 (s, 1H), 7.59 – 7.57 (m, 2H), 4.16 (t, J = 6.7 Hz, 2H), 3.82 (s, 3H), 3.54 (t, J = 6.3 Hz, 2H), 3.49 (q, J = 6.9 Hz, 2H), 2.03 (t, J = 6.5 Hz, 2H), 0.95 (t, J = 6.8 Hz, 3H); ^{13}C NMR (126 MHz, DMSO-d_6) δ 170.6, 169.7, 151.6, 151.0, 140.42, 136.7, 123.8, 123.7, 123.2, 122.5, 47.1, 44.7, 43.0, 35.6, 31.1, 15.8; HRMS (ESI$^+$) *m/z* [M + MeCN – I]$^+$ calculated for $C_{18}H_{23}N_6O_2Pd$ 461.0912; found 461.0920.

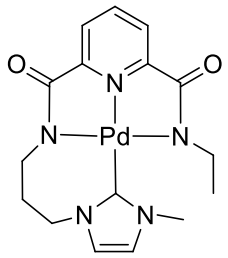

3.7

Complex 3.7. Complex **3.6** (0.104 g, 0.19 mmol, 1 equiv) was dissolved in MeCN (10 mL) and AgOAc (0.066 g, 0.4 mmol, 2.1 equiv) was added. The solution was shaken and allowed to sit without stirring for 16 h. The AgI and colloidal silver that was formed was filtered and to the filtrate was added diethyl ether to precipitate the product as a yellow solid. The complex was recrystallized from slow diethyl ether evaporation into a concentrated solution of the complex in MeCN to afford the complex as a crystalline yellow solid after 2 d (0.069 g, 0.150 mmol, 79%). Notably, **3.7** is stable as a solid in air for at least 18 months, as monitored by ^{1}H NMR spectroscopy in DMSO-d_6. ^{1}H NMR (500 MHz, DMSO-d_6) δ 8.21 (t, J = 7.8 Hz, 1H), 7.69 – 7.65 (m, 2H), 7.53 (d, J = 1.9 Hz, 1H), 7.48 (d, J = 1.8 Hz, 1H), 5.06 (td, J = 13.4, 5.4 Hz, 1H), 4.24 (ddd, J = 18.4, 13.2, 5.2 Hz, 2H), 3.88 (s, 3H), 3.85 – 3.68 (m, 1H), 2.74 – 2.67 (m, 1H), 1.88 (td, J = 12.6, 4.1 Hz, 1H), 1.82 – 1.74 (m, 2H), 0.82 (t, J = 7.0 Hz, 3H); ^{13}C NMR (126 MHz, DMSO-d_6) δ 170.6, 169.8, 166.4, 151.5, 150.8, 141.6, 123.6, 123.5, 122.6, 122.5, 45.9, 43.1, 40.8, 36.2, 29.6, 16.3; HRMS (ESI^{+}) m/z [M + H]$^{+}$ calculated for $C_{16}H_{20}N_5O_2Pd$ 420.0652; found 420.0650.

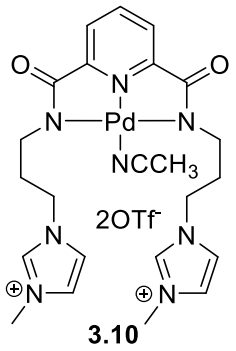

3.10

Complex 3.10. To an acetonitrile (15 mL) solution of ligand **3.5** (1.00 g, 1.5 mmol, 1 equiv) was added AgOTf (0.77 g, 3.0 mmol, 2 equiv). A yellow suspension (AgI) was observed immediately upon addition. The mixture was stirred 5 min before being filtered. To the filtrate was added $Pd(OAc)_2$ (0.336 g, 1.5 mmol, 1 equiv) and the solution was stirred for 16 h. The clear-yellow solution was filtered and the solvent was evaporated *in vacuo* (3x with addition of acetonitrile each time to evaporate the acetic acid) to afford the product as a yellow solid (1.142 g, 1.335 mmol, 89%). Crystals suitable for XRD analysis were grown from slow ether diffusion into concentrated MeCN solution of the complex. ^{1}H NMR (500 MHz, DMSO-d_6) δ 9.16 (s, 2H), 8.22 (t, J = 7.8 Hz, 1H), 7.85 (t, J = 1.7 Hz, 2H), 7.70 (t, J = 1.7 Hz, 2H), 7.63 (d, J = 7.8 Hz, 2H), 4.21 (t, J = 6.9 Hz, 4H), 3.84 (s, 6H), 3.12 (t, J = 6.3 Hz, 4H), 2.08 (s, 3H), 2.02 (t, J = 6.6 Hz, 4H); ^{13}C (126 MHz, DMSO-d_6) δ 169.7, 152.3, 141.7, 136.8, 124.3, 123.5, 122.4, 47.2, 41.1, 35.7, 30.6; ^{19}F NMR (471 MHz, DMSO-d_6) δ -79.13 (s, 6F); HRMS (ESI^+) *m/z* $[M - OTf - MeCN]^+$ calculated for $C_{22}H_{27}F_3N_7O_5PdS$ 664.0776; found 664.0775.

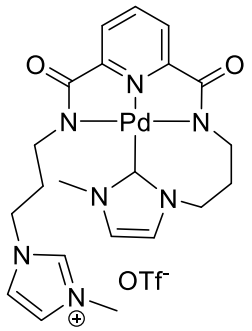

3.11

Complex 3.11. To a solution of complex **3.10** (0.770 g, 0.9 mmol, 1 equiv) in acetonitrile (5 mL) was added AgOAc (0.300 g, 1.8 mmol, 2 equiv) and the reaction was stirred for 16 h. The silver precipitate that formed was filtered and the solvent of the filtrate was concentrated *in vacuo*. After stirring the concentrated solution of crude product in acetonitrile for 2 h, a yellow precipitate formed, which was filtered, washed with diethyl ether (3 x 5 mL) to afford the complex as a yellow powder (0.475 g, 0.715 mmol, 79%). ^{1}H NMR (500 MHz, DMSO-d_6) δ 9.00 (s, 1H), 8.23 (t, J = 7.8 Hz, 1H), 7.72 (m, 2H), 7.65 (s, 1H), 7.60 (s, 1H), 7.53 (d, J = 2.2 Hz, 1H), 7.47 (d, J = 1.5 Hz, 1H), 5.09 (td, J = 13.4, 5.2 Hz, 1H), 4.23 (td, J = 13.7, 13.1, 5.2 Hz, 2H), 4.17 – 3.99 (m, 2H), 3.92 (dt, J = 13.4, 7.2 Hz, 1H), 3.82 (s, 3H), 3.78 (s, 3H), 2.63 (dt, J = 12.4, 5.8 Hz, 1H), 1.93 – 1.71 (m, 4H), 1.62 (dt, J = 13.7, 7.1 Hz, 1H); ^{13}C (126 MHz, DMSO-d_6) δ 171.3, 169.9, 165.7, 151.0, 150.8, 141.8, 136.6, 123.9, 123.7, 123.4, 122.7, 122.2, 122.0, 46.8, 45.9, 43.8, 40.9, 36.8, 35.7, 31.0, 29.6; ^{19}F NMR (471 MHz, DMSO-d_6) δ -79.13 (s, 3F); HRMS (ESI^{+}) m/z [M – OTf]$^{+}$ calculated for $C_{21}H_{26}N_7O_2Pd$ 514.1178; found 514.1188.

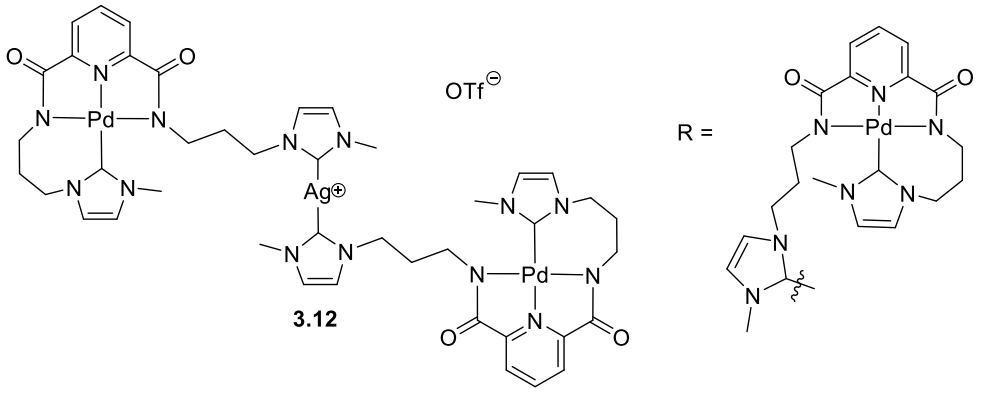

Complex 3.12. Complex **3.11** (0.100 g, 0.151 mmol, 1 equiv) was dissolved in a minimum amount of DMSO and Ag_2O (0.147 g, 0.634 mmol, 4.2 equiv) was added. After stirring for 24 h, the suspension was filtered to remove excess Ag_2O, and to the filtrate was added acetone and diethyl ether. The resulting cloudy solution was cooled to 0 ^oC for 24 h, after which the solvents were decanted to afford a yellow crystalline solid (0.058 g, 0.045 mmol, 30%). ^1H NMR (500 MHz, DMSO-d_6) δ 8.16 (t, J = 7.79 Hz, 2H), 7.68 (d, J = 7.80 Hz, 2H), 7.62 (d, J = 7.78 Hz, 2H), 7.49 (d, J = 1.74 Hz, 2H), 7.43 (d, J = 3.37 Hz, 2H), 7.30 (d, J = 1.48 Hz, 2H), 7.29 (d, J = 1.51, 2H), 5.05 (td, J = 3.02, 13.38, 2H), 4.19 – 4.17 (m, 4H), 4.04 – 3.89 (m, 6H), 3.71 (s, 6H), 3.69 (s, 6H), 2.56 – 2.48 (m, 2H), 1.86 – 1.70 (m, 8H), 1.57 – 1.49 (m, 2H); ^{13}C NMR (126 MHz, DMSO-d_6) δ 177.3, 170.0, 168.7, 164.5, 150.0, 149.5, 140.4, 122.6, 122.6, 122.5, 121.6, 121.4, 120.5, 47.6, 44.7, 42.9, 39.7, 36.9, 35.5, 31.5, 28.4; HRMS (ESI^+) *m/z* $[M - OTf - R]^+$ calculated for $C_{21}H_{25}AgN_7O_2Pd$ 620.0150; found 620.0126; HRMS (ESI^+) *m/z* $[M - OTf]^+$ calculated for $C_{42}H_{50}AgN_{14}O_4Pd_2$ 1135.1259; found 1135.1176. Parts-per-million error = $(1.0 \times 10^6 |\text{observed mass} - \text{theoretical mass}|)/(\text{theoretical mass}) = (1.0 \times 10^6 |1135.1176 - 1135.1259|)/(1135.1259) = 1.0 \times 10^6 \times 7.31 \times 10^{-6} = 7.31$ ppm.

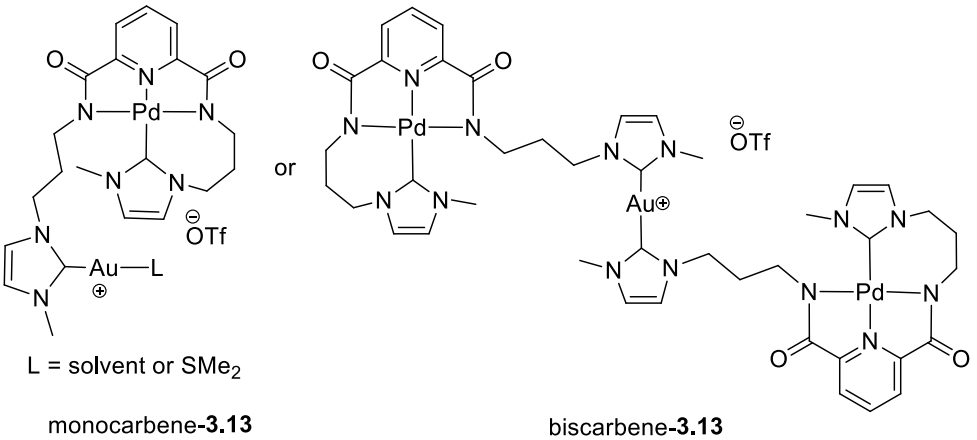

Complex 3.13. To a solution of **3.12** (20 mg, 0.016 mmol) in a minimum amount of DMSO-d_6 was added $AuClMe_2S$ (9 mg, 0.031 mmol, 2 equiv) and the reaction was monitored by ^1H NMR and ESI-MS. ^1H NMR (500 MHz, DMSO-d_6) δ 8.24 – 8.20 (m, 1H), 7.74 – 7.33 (m, 6H), 5.18 – 5.08 (m, 1H), 4.28 – 4.20 (m, 2H), 4.05 – 3.95 (m, 3H), 3.73 (s, 3H), 3.71 (s, 3H), 2.65 – 2.45 (m, 1H), 1.87 – 1.77 (m, 4H), 1.69 – 1.60 (m, 1H); ^{13}C (126 MHz, DMSO-d_6) δ 171.0, 169.8, 168.3, 165.7, 151.1, 150.8, 141.5, 123.7, 123.7, 122.6, 122.3, 121.5, 48.3, 46.0, 44.0, 40.7, 37.7, 36.6, 32.5, 29.4; HRMS (ESI^+) *m/z* $[M - OTf - R]^+$ calculated for $C_{21}H_{25}AuN_7O_2Pd$ 710.0765; found 710.0745; HRMS (ESI^+) *m/z* $[M - OTf]^+$ calculated for $C_{42}H_{50}AuN_{14}O_4Pd_2$ 1225.1874; found 1225.1749. Parts-per-million error = $(1.0 \times 10^6 |\text{observed mass} - \text{theoretical mass}|)/(\text{theoretical mass}) = (1.0 \times 10^6 |1225.1749 - 1225.1874|)/(1225.1874) = 1.0 \times 10^6 \times 1.02 \times 10^{-5} = 10.2$ ppm.

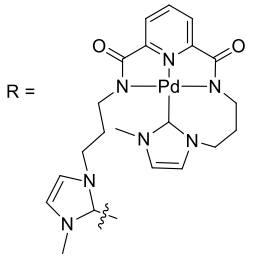

3.5.4 *Heck Reaction General Procedure*

All chemicals—4-iodotoluene, NaOAc, TBAB, and DMA—were purchased from Sigma Aldrich and used without further purification. All reactions were performed under air. 4-iodotoluene (2 mmol, 436 mg), NaOAc (2.2 mmol, 180 mg), TBAB (0.4 mmol, 129 mg), and Pd(II) NNN-pincer complex (2 x 10^{-3} mmol/Pd) were added to a 25 mL three-necked round bottom flask equipped with a reflux condenser and placed in an oil bath. DMA (5 mL) was added to the flask and the temperature of the oil bath was raised to 165 ^{o}C. Styrene (2.8 mmol, 234 μL) was added when the solvent began to reflux (T = 0). The reaction was monitored via TLC and aliquots were taken every 15 minutes for NMR analysis. The samples were analyzed via ^{1}H NMR spectroscopy on a Bruker Avance 500 spectrometer. The yield was calculated by comparing the integration of the olefinic doublet proton signal (2H) of the *trans*-methylstilbene product and the olefinic doublet proton signal (1H) of the *gem*-methylstilbene product to the aromatic doublet proton signal (2H) for 4-iodotoluene.

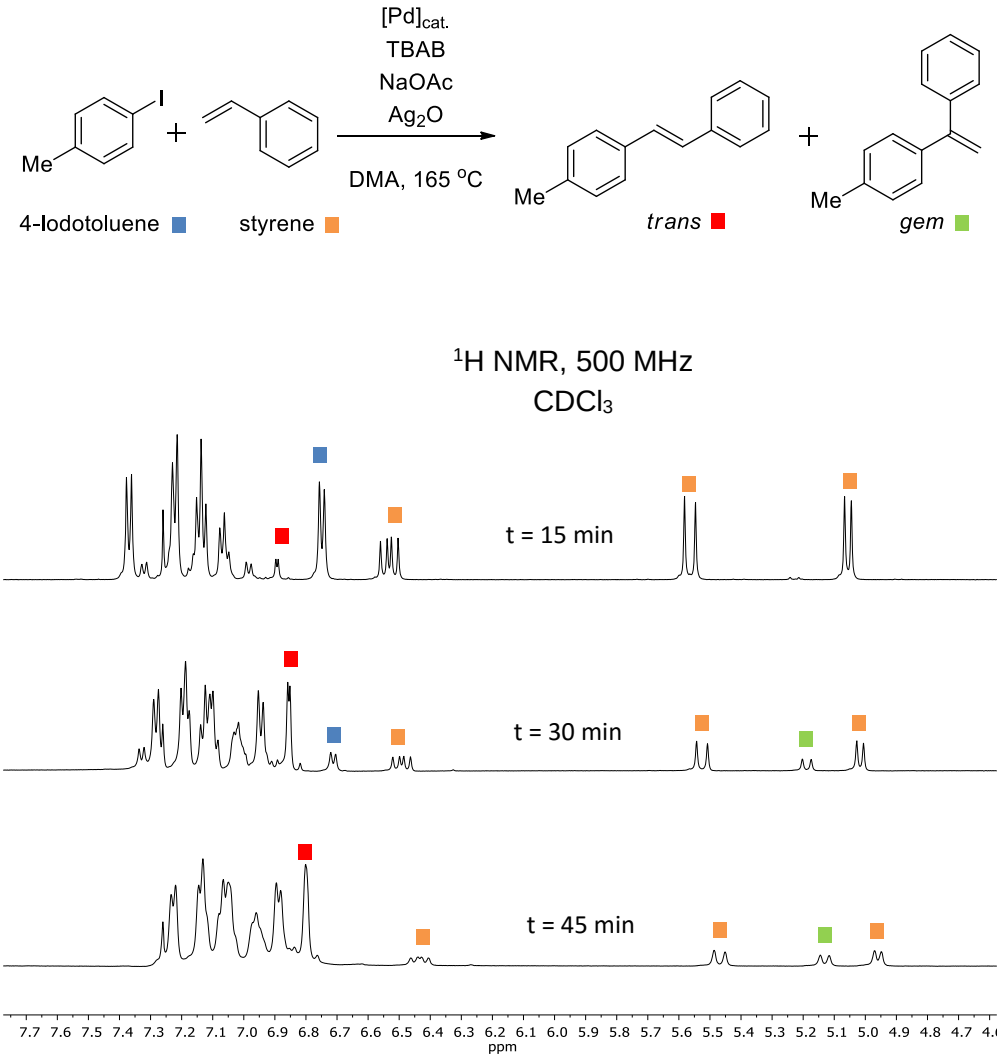

Figure 3.18. Representative ^{1}H NMR spectra in $CDCl_3$ of aliquots taken at 15 minutes, 30 minutes, and 45 minutes after addition of styrene using complex **3.11** (1 x 10^{-1} mol%) as the catalyst and Ag_2O (0.2 eq) as an additive.

3.6 *References*

1. *Note*: 1953, 1963, 1974, 1991, 2000, 2002, and 2005 for polymer chemistry; 2001 asymmetric hydrogenation; 2010 for cross coupling. "All Nobel Prizes in Chemistry" *NobelPrize.Org* Nobel Media AB 2014. Web. 24 Jan, 2015. <http://www.nobelprize.org/nobel_prizes/chemistry/laureates/>
2. Perez-Temprano, M. H.; Casares, J. A.; Espinet, P. "Bimetallic Catalysis using Transition and Group 11 Metals: An Emerging Tool for C–C Coupling and Other Reactions" *Chem. Eur. J.* **2012**, *18*, 1864–1884.
3. Sawamura, M.; Sudoh, M.; Ito, Y. "An Enantioselective Two-Component Catalyst System: Rh-Pd-Catalyzed Allylic Alkylation of Activated Nitriles" *J. Am. Chem. Soc.* **1996**, *118*, 3309–3310.
4. Kamijo, S.; Yamamoto, Y. "A Bimetallic Catalyst and Dual Role Catalyst: Synthesis of *N*-(Alkoxycarbonyl)indoles from 2-(Alkynyl)phenylisocyanates" *J. Org. Chem.* **2003**, *68*, 4764–4771.
5. Sonogashira, K. "Development of Pd-Cu Catalyzed Cross-Coupling of Terminal Acetylenes with sp^2-Carbon Halides" *J. Organomet. Chem.* **2002**, *653*, 46–49.
6. Cooper, B. G.; Napoline, W.; Thomas, C. M. "Catalytic Applications of Early/Late Heterobimetallic Complexes" *Cat. Rev. – Sci. Eng.* **2012**, *54*, 1–40.
7. Farrington, E. J.; Viviente, E. M.; Williams, B. S.; van Koten, G.; Brown, J. M. "Synthesis and Reactivity of a Ferrocene-Derived PCP-pincer Ligand" *Chem. Commun.* **2002**, *4*, 308–309.
8. Koridze, A. A.; Kuklin, S. A.; Sheloumov, A. M.; Dolgushin, F. M.; Lagunova, V. Y.; Petukhova, I. I.; Ezernitskaya, M. G.; Peregudov, A. S.; Petrovskii, P. V.; Vorontsov, E. V.; Baya, M.; Poli, R. "Ferrocene-Based Pincer Complexes of Palladium: Synthesis Structures, and Spectroscopic and Electrochemical Properties" *Organometallics* **2004**, *23*, 4585–4593.
9. Bonnet, S.; Lutz, M.; Spek, A. L.; van Koten, G.; Klein Gebbink, R. J. M. "Bimetallic η6, η1-SCS and PCP-Pincer Ruthenium Palladium Complexes: Synthesis, Structure and Catalytic Activity" *Organometallics* **2010**, *29*, 1157–1167.

10. Huang, D.; Holm, R. H. "Reactions of the Terminal Ni^{II}-OH Group in Substitution and Electrophilic Reactions with Carbon Dioxide and Other Substrates: Structural Definition of Binding Modes in an Intramolecular $Ni^{II}\cdots Fe^{II}$ Bridged Site" *J. Am. Chem. Soc.* **2010**, *132*, 4693–4701.
11. Donoghue, P. J.; Gupta, A. K.; Boyce, D. W.; Cramer, C. J.; Tolman, W. B. "An Anionic, Tetragonal Copper(II) Superoxide Complex" *J. Am. Chem. Soc.* **2010**, *132*, 15869–15871.
12. Halvagar, M. R.; Neisen, B.; Tolman, W. B. "Copper-, Palladium-, and Platinum-Containing Complexes of an Asymmetric Dinucleating Ligand" *Inorg. Chem*. **2013**, *52*, 793–799.
13. Lein, M.; Szabó, A.; Kovács, A.; Frenking, G. "Energy Decomposition Analysis of the Chemical Bond in Main Group and Transition Metal Compounds" *Faraday Discuss*. **2003**, *124*, 365–378.
14. Mas-Marza, E.; Mata, J. A.; Peris, E. "Triazolediylidenes: A Versatile Class of Ligands for the Preparation of Discrete Molecules of Homo- and Hetero-Binuclear Complexes for Improved Catalytic Applications" *Angew. Chem., Int. Ed*. **2007**, *46*, 3729–3731.
15. Zanardi, A.; Corberan, R.; Mata, J. A.; Peris, E. "Homo- and Heterodinuclear Complexes with Triazolyl-diylidene. An Easy Approach to Tandem Catalysts" *Organometallics* **2008**, *27*, 3570–3576.
16. Zanardi, A; Mata, J. A.; Peris, E. "Well-Defined Ir/Pd Complexes with a Triazolyl-diylidene Bridge as Catalysts for Multiple Tandem Reactions" *J. Am. Chem. Soc*. **2009**, *131*, 14531–14537.
17. Seitz, S. C.; Rominger, F; Straub, B. F. "Stepwise Deprotonation of a Thiol-Functionalized Bis(1,2,4-triazolium) Salt as a Selective Route to Heterometallic NHC Complexes" *Organometallics* **2013**, *32*, 2427–2434.
18. Mechler, M.; Latendorf, K.; Frey, W.; Peters, R. "Homo- and Heterobimetallic Pd−, Ag−, and Ni−Hybrid Salen−Bis-NHC Complexes" *Organometallics* **2013**, *32*, 112–130.

19. Mechler, M.; Frey, W.; Peters, R. “Macrocyclic Salen-Bis-NHC Hybrid Ligands and Their Application to the Synthesis of Enantiopure Bi- and Trimetallic Complexes” *Organometallics* **2014**, *33*, 5492–5508.
20. Kato, Y.; Furutachi, M.; Chen, Z.; Mitsunuma, H.; Matsunaga, S. Shibasaki, M. “A Homodinuclear $Mn(III)_2$−Schiff Base Complex for Catalytic Asymmetric 1,4-Additions of Oxindoles to Nitroalkenes” *J. Am. Chem. Soc*. **2009**, *131*, 9168–9169.
21. Teng, Q.; Huynh, H. V. “Controlled Access to a Heterometallic *N*-heterocyclic Carbene Helicate” *Chem. Commun*. **2015**, *51*, 1248–1251.
22. Kang, S.O.; Llinares, J. M.; Day, V. W.; Bowman-James, K. “Cryptand-Like Anion Receptors” *Chem. Soc. Rev.* **2010**, *39*, 3980–4003.
23. Bianchi, A.; Bowman-James, K.; García-España, E. “Aspects of Anion Coordination from Historical and Biological Perspectives” in *Anion Coordination Chemistry*, Bowman-James, K.;Bianchi, A.; García-España, E., Eds., Wiley-Interscience, **2012**, 1–72.
24. Begum, R. A.; Kang, S. O.; Day, V. W.; Bowman-James, K. “Structural Aspects of Anion Coordination Chemistry” in *Anion Coordination Chemistry*, Bowman-James, K.; Bianchi, A.; García-España, E., Eds., Wiley-Interscience, **2012**, 139–223.
25. Taylor, R. W.; Begum, R. A.; Day, V. W.; Bowman-James, K. “Cooperativity and the Chelate, Macrocyclic and Cryptate Effect” in *Supramolecular Chemistry: From Molecules to Nanomaterials* P. A. Gale and J. W. Steed, Eds., John Wiley and Sons, Ltd., **2012**, *1*, 67–93.
26. Wang, Q.-Q.; Begum, R. A.; Day, V. W.; Bowman-James, K. “Alfred Werner’s Expanded Legacy: Anion and Metal Ion Coordination in an Unsymmetrical, Octaamido Cryptand” *Polyhedron*, **2013**, *52*, 515–523.
27. *Anion Coordination Chemistry*, Bowman-James, K.; Bianchi, A.; García-España, E., Eds.; Wiley-VCH: **2012**.
28. Hossain, Md. A.; Lucarini, S.; Powell, D.; Bowman-James, K. “Ditopic Double Pincer Palladacycle Catalyst for C–C Coupling” *Inorg. Chem*. **2004**, *43*, 7275–7277.

29. Begum, R. A.; Powell, D.; Bowman-James, K. "Thioamide Pincer Ligands with Charge Versatility" *Inorg. Chem.*, **2006**, *45*, 964–966.

30. Wang, Q.-Q.; Begum, R. A.; Day, V. W.; Bowman-James, K. "Molecular Thioamide⇔Iminothiolate Switches for Sulfur Mustards" *Inorg. Chem.* **2012**, *51*, 760–762.

31. Wang, Q.-Q.; Begum, R.A.; Day, V.W.; Bowman-James, K. "Chemical Mustard Containment Using Simple Palladium Pincer Complexes: The Influence of Molecular Walls" *J. Am. Chem. Soc*. **2013**, *135*, 17193–17199.

32. Wang, Q.-Q.; Day, V. W.; Bowman-James, K. "Hexagonal Molecular 'Palladawheel'" *Chem. Commun*. **2013**, *49*, 8042–8044.

33. Jia, C.; Wang, Q.-Q.; Begum, R. A.; Day, V. W.; Bowman-James, K. B. "Chelate Effects in Sulfate Binding by Amide/Urea-Based Ligands" *Org. Biomol. Chem.* **2015***, 13*, 6953–6957.

34. Munz, D.; Poethig, A.; Tronnier, A.; Strassner, T. "Ortho-Phenylene Bridged Palladium Bis-*N*-heterocyclic Carbene Complexes: Synthesis, Structure, and Catalysts, *Dalton Trans.* **2013**, *42*, 7297–7304.

35. Fehlhammer, W. P.; Bliss, T.; Kernbach, U.; Brudgam. "Homoleptic Carbene Complexes VI. Bis{1,1′-methylene-3,3′-dialkyl-diimidazoline-2,2′-diylidene} Palladium Chelate Complexes by the Free Carbene Route" *J. Organomet. Chem*. **1995**, *490*, 149–153.

36. Newman, C. P.; Clarkson, G. J.; Rourke, J. P. "Silver(I) *N*-heterocyclic Carbene Complexes: A New Binding Motif" *J. Organomet. Chem*. **2007**, *692*, 4962–4968.

37. "Bordwell pKa Table (Acidity in DMSO)" Web. 24 Jan 2015 www.chem.wisc.edu/areas/reich/pkatable/.

38. Dell'Amico, D. B.; Calderazzo, F.; Di Colo, F.; Guglielmetti, G.; Labella, L.; Marchetti, F. "Coordination Properties Towards Palladium(II) of a Tridentate Dianionic Ligand Acting as a N- or a N,O-donor" *Inorg. Chim. Acta* **2006**, *359*, 127–135.

39. Garrison, J. C.; Youngs, W. J. "Ag(I) *N*-Heterocyclic Carbene Complexes: Synthesis, Structure, and Application" *Chem. Rev.* **2005**, *105*, 3978–4008.

40. Lin, I. J. B.; Vasam, C. S. “Preparation and Application of *N*-Heterocyclic Carbene Complexes of Ag(I)” *Coord. Chem. Rev.* **2007**, *251*, 642–670.

41. Silverstein, R. M.; Webster, F. X.; Kiemle, D. J. “Spectrometric Identification of Organic Compounds” (*7th Edition*); John Wiley & Sons, Inc., 2005.

42. Anderson, D. J.; McDonald, R. Cowie, M. “Carbon–Fluorine Bond Activation in Fluoroolefins: Clear Documentation of Cooperative C–F Bond Activation by Adjacent Metal Centers” *Angew. Chem. Int. Ed.* **2007**, *119*, 3815–3818.

43. Guo, S.; Sivaram, H.; Yuan, D.; Huynh, H. V. “Gold and Palladium Hetero-Bis-NHC Complexes: Characterizations, Correlations, and Ligand Redistributions” *Organometallics* **2013**, *32*, 3685–3696.

44. Larsen, A. O.; Leu, W.; Oberhuber, C. N.; Campbell, J. E.; Hoveyda, A. H. “Bidentate NHC-Based Chiral Ligands for Efficient Cu-Catalyzed Enantioselective Allylic Alkylations: Structure and Activity of an Air-Stable Chiral Cu Complex” *J. Am. Chem. Soc*. **2004**, *126*, 11130–11131.

45. Bonnet, L. G.; Douthwaite, R. E.; Hodgson, R.; Houghton, J.; Kariuki, B. M.; Simonovic, S. “Synthesis, Structure and Reactivity of Palladium(II) Complexes of Chiral *N*-Heterocyclic Carbene–Imine and –Amine Hybrid Ligands” *Dalton Trans*. **2004**, *21*, 3528–3535.

46. Van Veldhuizen, J. J.; Campbell, J. E.; Giudici, R. E.; Hoveyda, A. H. “A Readily Available Chiral Ag-Based *N*-Heterocyclic Carbene Complex for Use in Efficient and Highly Enantioselective Ru-Catalyzed Olefin Metathesis and Cu-Catalyzed Allylic Alkylation Reactions” *J. Am. Chem. Soc*. **2005**, *127*, 6877–6882.

47. Newman, C. P.; Clarkson, G. J.; Rourke, J. P. “Silver(I) *N*-Heterocyclic Carbene Halide Complexes: A New Bonding Motif” *J. Organomet. Chem.* **2007**, *692*, 4962–4968.

48. Arduengo, A. J. III; Dias, H. V. R.; Calabrese, J. C.; Davidson, F. “Homoleptic Carbene-Silver(I) and Carbene-Copper(I)Complexes” *Organometallics* **1993**, *12*, 3405–3409.

49. O’brien, C. J.; Kantchev, E. A. B.; Valente, C.; Hadei, N.; Chass, G. A.; Lough, A.; Hopkinson, A. C.; Organ, M. G. “Easily Prepared Air- and Moisture-Stable

Pd–NHC (NHC=*N*-Heterocyclic Carbene) Complexes: A Reliable, User-Friendly, Highly Active Palladium Precatalyst for the Suzuki–Miyaura Reaction" *Chemistry-Eur. J.* **2006**, *12*, 4743–4748.

50. Richter, C.; Schaepe, K.; Glorius, F.; Ravoo, B. J. "Tailor-Made *N*-Heterocyclic Carbenes for Nanoparticle Stabilization" *Chem. Commun.* **2014**, *50*, 3204–3207.

Chapter 4

Pd(II) Coordination Polymers Based on a

Pyridine-Appended Tetraamide Macrocyclic Ligand

4.1 *Abstract*

A coordination polymer constructed via the self-assembly of pyridine-appended tetraamide macrocycle **4.1** with Pd(II) is studied. The coordination chemistry of Pd(II) when nitrogen donor atoms is investigated using Pd(II) pincer complexes in the presence of pyridine, pyrazine, and 4,4-bipyridine. The structure of the 4,4-bipyridine dimer of phenyl appended amide-based Pd(II) NNN-complex **2.6b** was characterized via X-ray crystallography. Coordination dimers of complexes **2.6a** and **2.6b** with **4.1** were studied with ^{1}H NMR spectroscopy. Coordination dimer **4.6b** (from 2[**2.6b**] + **4.1**) was characterized via X-ray crystallography. Notably, macrocycle **4.1** undergoes a conformational shift upon binding **2.6b** to afford complex **4.6b**. Subsequently, a novel bis[palladium(II)] NNN-dipincer complex was synthesized for future use with **4.1**. The formation of coordination polymers with macrocycle **4.1** was studied using $PdCl_2$ or $Pd(OAc)_2$. Formation of a polymeric species in these cases was evidenced by a significant broadening of the ^{1}H NMR signals corresponding to the macrocycle.

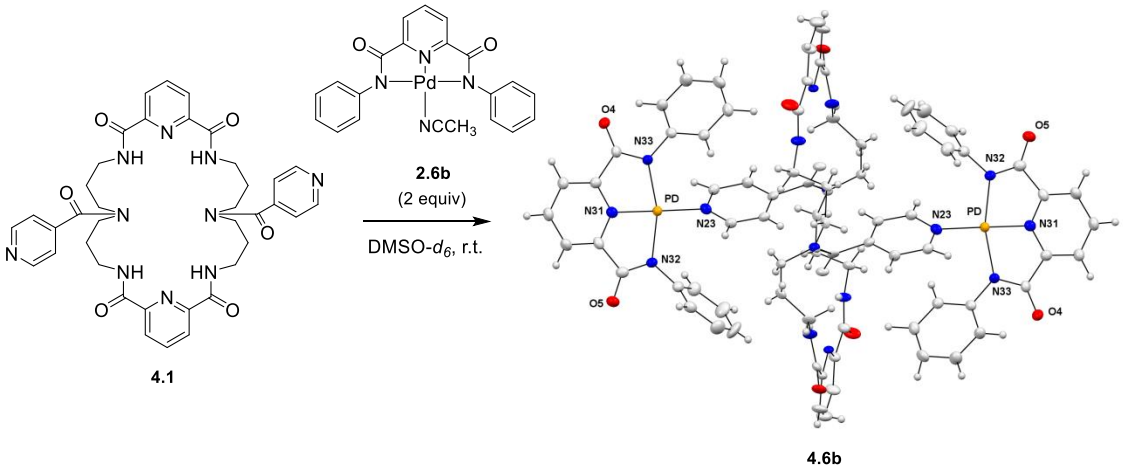

4.2 *Introduction*

The field of supramolecular chemistry is a fast-growing one that ranges from the study of host-guest interactions to the design of polymers that can operate as functional materials.[1] The study of metallo-supramolecular polymers (MSPs) has gained a significant amount of interest over the last two decades.[2] Compared with organic polymers, the reversible nature of MSPs leads to unique functions, such as self-healing, viscosity, and recycling.[3] The type of MSPs based on repeating metal/organic subunits are called metal-organic frameworks (MOF).[4] The structures of MOFs can be one-, two-, or three dimensional, with higher dimensionalities arising from H-bonding or π-π stacking, in addition to metal-ligand coordination. The porous nature of MOFs is typically due to the organic linkers, which can vary in length.[5] This characteristic has led to numerous reports of their use in the storage of gases[6] and other small molecules.[7] Additionally, MOFs have enjoyed applications in heterogenous catalysis,[8] separations,[9] chemical sensing,[10] and biomedicine.[11]

Recently, macrocyclic organic linkers have been employed in MOF synthesis.[12,13] Macrocycles can introduce a second level of porosity into the framework of the MOF, resulting in many interesting properties from the resulting hybrid materials. MOFs employing oxygen-based (crown ether,[14] cyclodextrin,[15] calixarene,[16] cucurbituril,[17] and pillararene[18]) and nitrogen-based (cyclam[19] and porphyrin[20]) macrocycles have been reported. The use of nitrogen-based macrocycles as organic linkers in MOF synthesis has led to many new applications, including selective CO_2 uptake over N_2[21] and as an absorbent for many volatile organic molecules, including methanol, ethanol, acetone, THF, dioxane, and benzene.[22]

Our group has extensively studied the anion recognition properties of various amide and thioamide macrocycles.[23,24a-e] Depending on the size and geometry of the anion guest, a variety of exciting structures can be obtained from these versatile hosts. Our group has also explored the transition metal chemistry with these macrocyclic ligands.[25] Thus, we thought it would be a worthy endeavor to expand our macrocyclic host-guest chemistry to the fast-growing field of coordination polymers.

Recently, Dr. Telikepalli—a postdoc in the Bowman-James group—optimized the synthesis of a small library of macrocycles with urea or amide pendant functionalities, making these macrocycles amenable to the synthesis of coordination polymers. These functionalities can be tailored to access a variety of macrocycles. Due to the ease of synthesis of the propyl-linked macrocycle derivatives, ligands **4.1** and **4.2** were chosen for initial investigations (Figure 4.1).

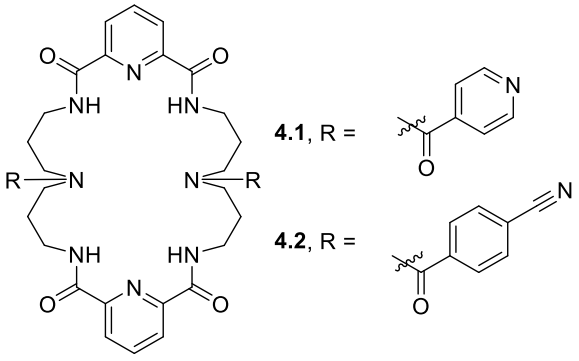

Figure 4.1. Examples of functionalized tetraamide macrocycles synthesized by Dr. Telikepalli.

Of these ligands, **4.1**—which contains an appended pyridine—showed the most promise in initial tests with metal ions. Dr. Telikepalli found that treatment of **4.1** with $AgNO_3$ in DMF afforded coordination polymer **4.3** as a crystalline solid after 3 days

(Scheme 4.1). The two-dimensional network is held together by a series of Ag–N(pyridine) and Ag–O(amide) bonds (Figure 4.2). Pi stacking extends the geometry of this structure over a three-dimensional framework. Interestingly, the tetrahedral arrangement of the Ag metal centers results in a dense, non-porous coordination polymer network. Unfortunately, despite the reproducible crystallization of **4.3** from DMF, no change was observed in solution by ^{1}H NMR (conducted by Dr. Pedro Metola). Thus, we chose to investigate a different approach in order to synthesize stable and predictable coordination polymers from macrocycle **4.1**.

Scheme 4.1.

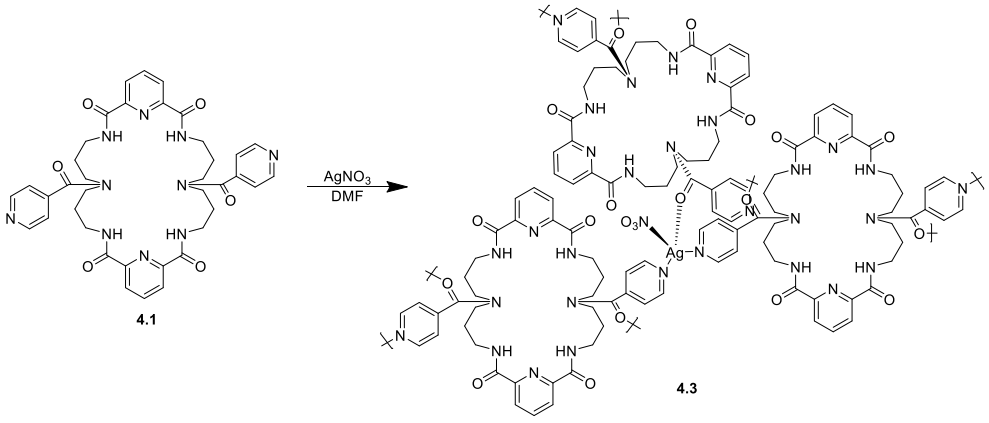

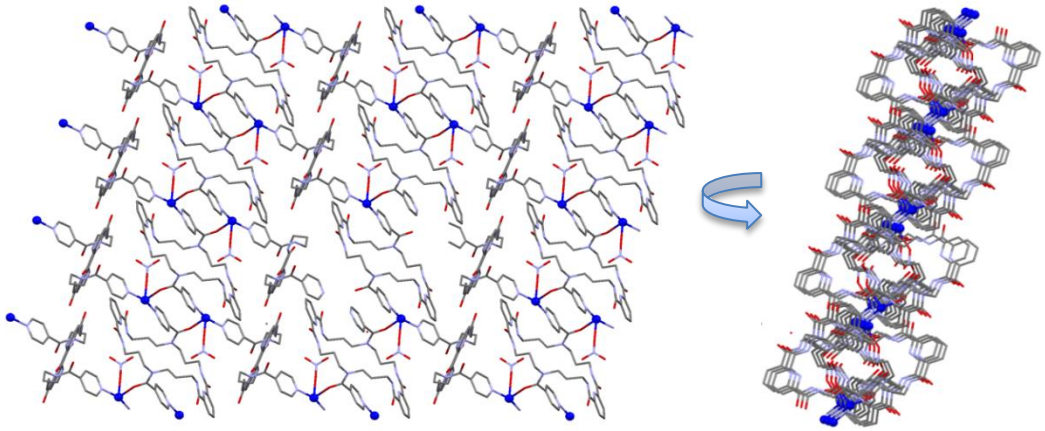

Figure 4.2. Packing diagram of the X-ray crystal structure of **4.3**.

4.3 *Results and Discussion*

The objective of the work presented in this chapter was to synthesize macrocycle-based MOFs to use for anion recognition or small molecule capture. Initial tests probed the binding of Pd(II) NNN-pincer complexes **2.6a** and **2.6b** with pyrazine and 4,4-bipyridine. Subsequently, pyridine-appended tetraamide macrocycle **4.1** was studied for its propensity to form coordination polymers with Pd(II). In order to investigate the effect of different Pd sources on the properties of the resulting supramolecular polymers, we compared the coordination properties of **4.1** with Pd(II) NNN-dipincer complex **4.9** (first approach) or PdX_2 (X = OAc or Cl) (second approach). These two approaches are illustrated in Figure 4.3.

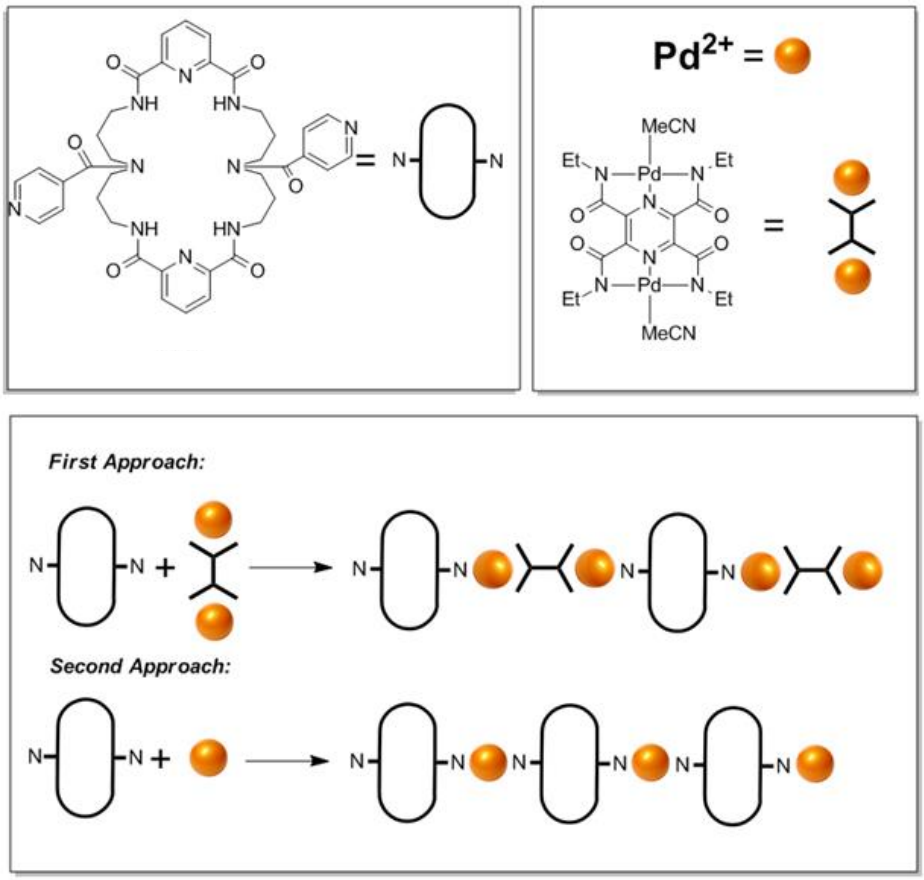

Figure 4.3. Schematic representation of the synthesis of MOFs from macrocycle **4.1**.

4.3.1 *Coordination of Pd(II) NNN-pincer Complexes with Aromatic N-donor Ligands*

The synthesis and catalytic activity of Pd(II) NNN-pincer complexes **2.6a** and **2.6b** were described in Chapter 2 of this dissertation. The formation of coordination dimers with pyrazine or 4,4-bipyridine was studied using **2.6a** and **2.6b** (Scheme 4.2). Upon addition of pyrazine (0.5 equiv) to a yellow solution of **2.6a** (1 equiv) in MeCN-d_3, a yellow precipitate immediately formed. Likewise, a yellow precipitate was observed immediately following the addition of 4,4-bipyridine (0.5 equiv) to a yellow MeCN-d_3 solution of either complex **2.6a** (1 equiv) or complex **2.6b** (1 equiv).

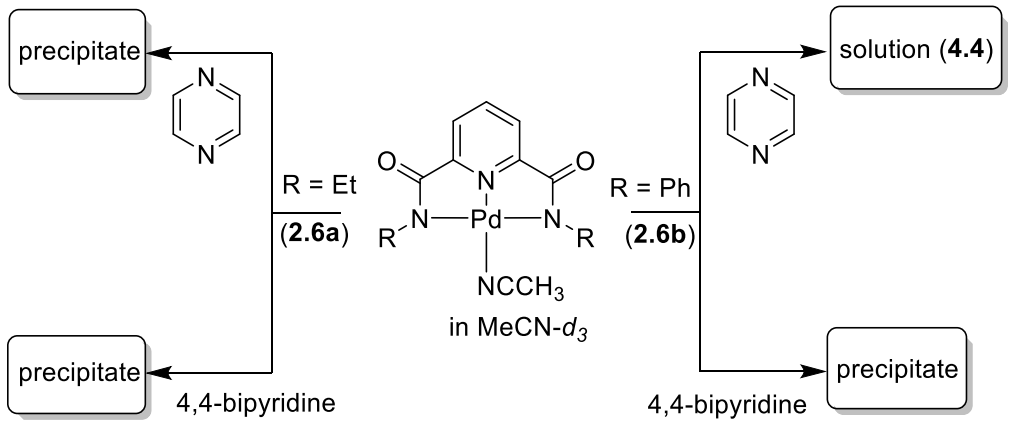

Scheme 4.2. Reaction of **2.6a** and **2.6b** with pyrizine or 4,4-bipyridine.

Conversely, the addition of pyrazine to a solution of **2.6b** in MeCN-d_3 resulted in a yellow solution. The ^{1}H NMR spectrum—recorded immediately after this addition—is shown in Figure 4.4. Upon binding pyrazine, the signals for the aromatic backbone protons C$H^{a\text{-}b}$ of the pincer complex shift downfield. Due to the electron withdrawing effect of pyrazine, this shift is expected. Accordingly, a new set of aromatic signals corresponding to bound pyrazine, C$H^{f\text{-}g}$, appears and overlaps with the signals corresponding to CH^{a}. Such upfield shifts have been observed by our group in a previous study, in which the

binding of a sulfur mustard surrogate, 2-chloroethyl sulphide (CEES), to **2.6b** resulted in an upfield shift of the CEES protons.[26] This shift was attributed to the shielding effect of aromatic amide pendant groups (see Section 1.3.2 in Chapter 1).

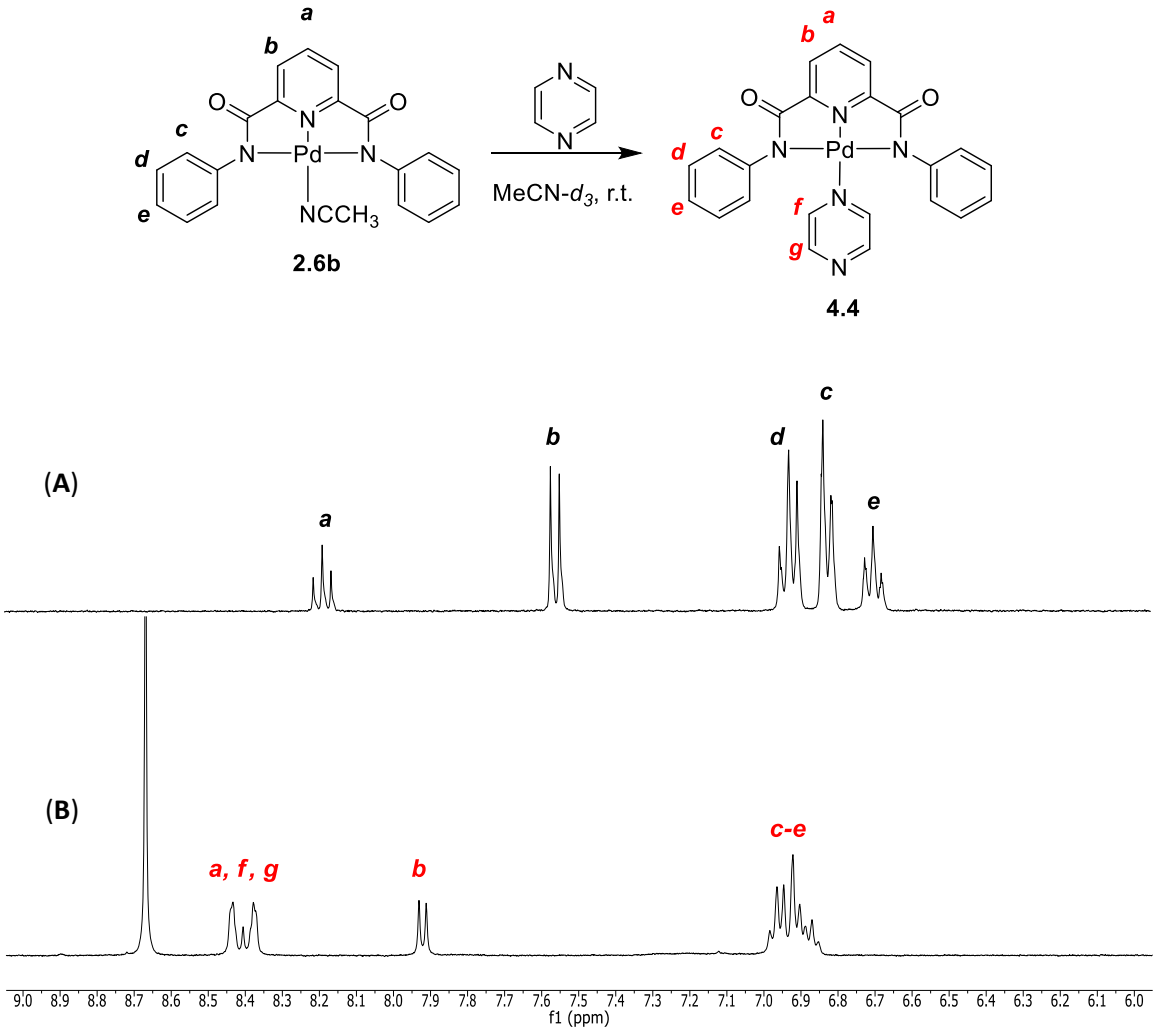

Figure 4.4. Top: reaction of pyrazine with **2.6b** with aromatic proton assignments. Bottom: aromatic region of the ^{1}H NMR spectrum (400 MHz, 298 K, MeCN-d_3) of **2.6b** (**A**) before and (**B**) after the addition of pyrazine.

To elucidate the structure of the precipitates that were observed above, we attempted to grow crystals of **2.6b** in the presence of 4,4-bipyridine. Similar to when the reaction was conducted in MeCN-d_3, the addition of 4,4-bipyridine to a DMF solution of **2.6b** afforded a yellow suspension (Figure 4.5A). Upon heating this suspension to 115 ^{o}C, a yellow solution evolved. Over the course of 1 h, a gradual reduction in the temperature of the oil bath to 25 ^{o}C afforded yellow crystals suitable for X-ray analysis. The X-ray crystal structure confirms the formation of 4,4-bipyridine dimer **4.5** (Figure 4.5B). The Pd–N distances are similar to those we observed for similar NNN-pincer complexes in Chapter 2. Interestingly, the C(12)-C(13)-C(13)-C(12) torsion angle of the 4,4-bipyridine linker is 29.5^{o}, approximately 5^{o} smaller than the reported torsion angle for free 4,4-bipyridine. With intermolecular C···C distances as short as 3.29 Å, parallel-displaced π-π stacking interactions of the phenyl amide substituents results in a very dense packing network (see Figure A.4.10 in the Appendix). Extrapolating this result to the experiments performed above, it is reasonable to assume that dimers were formed in the two other cases in which precipitates were observed (**2.6a** with pyrazine or 4,4-bipyridine; Scheme 4.2, *vide supra*). Presumably, the steric bulk of the phenyl amide substituents in **2.6b** prevents dimerization in the presence of pyrazine.

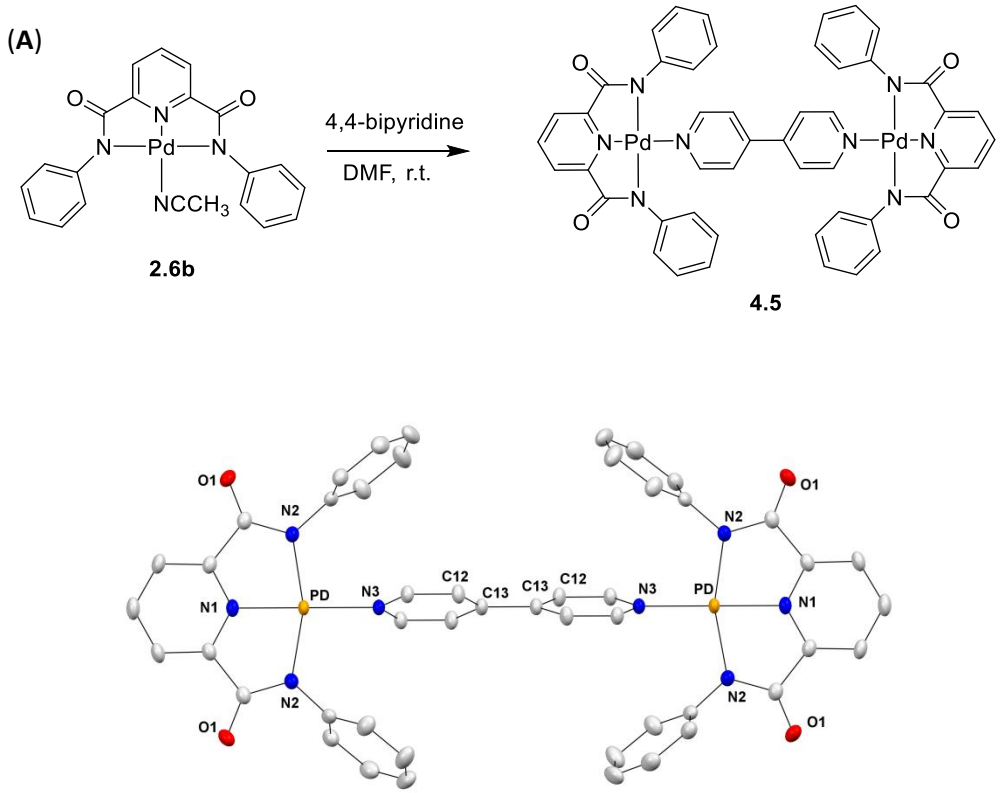

Figure 4.5. (**A**) The reaction of 4,4-bipyridine with complex **2.6b** to form dimer **4.5** and (**B**) X-ray crystal structure of **4.5**.

Dr. Metola investigated the relative ability for anions to coordinate Pd(II) pincer complex **2.6b** in the absence or presence of pyridine (Scheme 4.3). Complex **2.6b** was dissolved in DMSO-d_6, titrated with the corresponding tetrabutylammonium (TBA) salt, and analyzed via ^{1}H NMR spectroscopy. In the absence of pyridine, exchange of the ancillary acetonitrile ligand in **2.6b** with either dihydrogenphosphate or terephthalate anions was observed. However, in the presence of pyridine—which assumes the fourth coordination site—only terephalate displaces the pyridine ligand, as observed by the disappearance of the signal corresponding to bound pyridine. This result was encouraging,

as it suggested that coordination polymers containing Pd–N(pyridine) bonds might be stable in the presence of phosphine anions.

Scheme 4.3. Reaction of **2.6b** with the corresponding TBA salts of either dihydrogenphosphate or terephthalate (carried out by Dr. Metola). The resulting Pd(II) pincer complexes were observed via ^{1}H NMR, but have not been fully characterized.

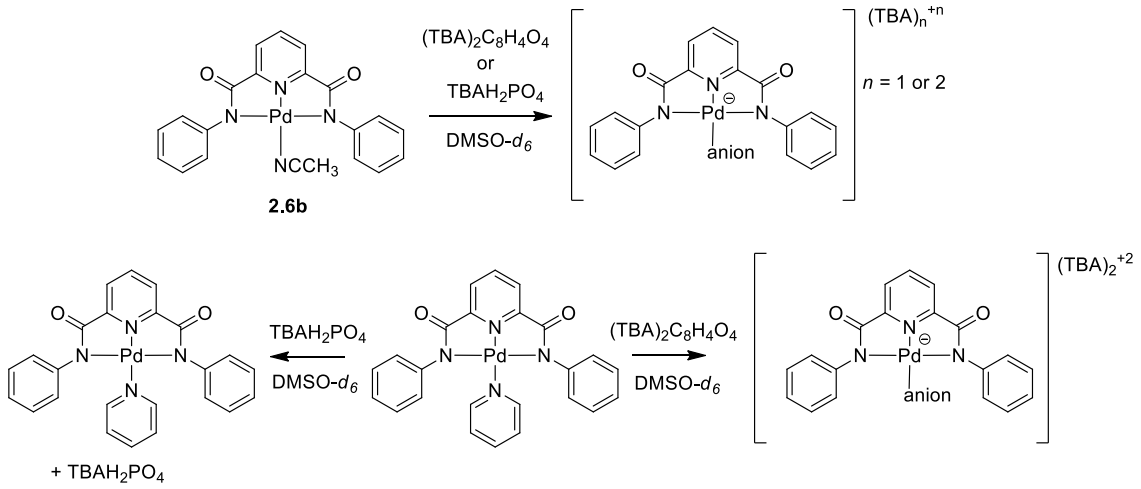

4.3.2 *Coordination of Pd(II) NNN-pincer Complexes **2.6a** and **2.6b** with Macrocyclic Ligand **4.1***

^{1}H NMR studies were employed to investigate the coordination of complexes **2.6a** and **2.6b** with the pendant pyridines in macrocycle **4.1**. Examination of the ^{1}H NMR spectrum upon addition of two equivalents of **2.6a** to a solution of **4.1** in DMSO-d_6 revealed a downfield shift of approximately 0.3 and 0.7 ppm for the pendant pyridine protons, CH^c and CH^d, respectively (Figure 4.6). Further, a slight broadening of proton signals was observed in the aliphatic region of the ^{1}H NMR spectrum. These changes correspond to the binding of **2.6a** to the pendant pyridine of macrocycle **4.1** to afford coordination dimer **4.6a**. Attempts to grow crystals of **4.6a** were unsuccessful.

Likewise, the addition of two equivalents of complex **2.6b** to a solution of macrocycle **4.1** in DMSO-d_6 resulted in a downfield shift of pyridine proton signals in the resulting ^{1}H NMR spectrum, corresponding to the formation of coordination dimer **4.6b** (Figure 4.7). Due to the abundance of aromatic protons in **4.6b**, a precise designation of all peaks was not possible. However, if the integrations of all the aromatic proton signals are summed and normalized to the well-defined amide signals (4H), we get the expected number of protons (44H). Crystals of **4.6b** suitable for X-ray analysis were obtained after crystallization from a MeCN/DMF solvent mixture. For comparison, crystals of **4.1** for X-ray analysis were also grown (crystallization in MeOH). The X-ray crystal structure of **4.6b** reveals that coordination of **2.6b** to **4.1** results in a conformation shift from the chair-like conformation of macrocycle **4.1** (Figure 4.8). The macrocycle in dimeric complex **4.6b** has a flat geometry, with the pendant pyridines pointed *anti* to each other.

Additionally, both pyridines are oriented perpendicular to the plane of the macrocycle to accommodate the sterics imparted by the phenyl appendages of **2.6b**.

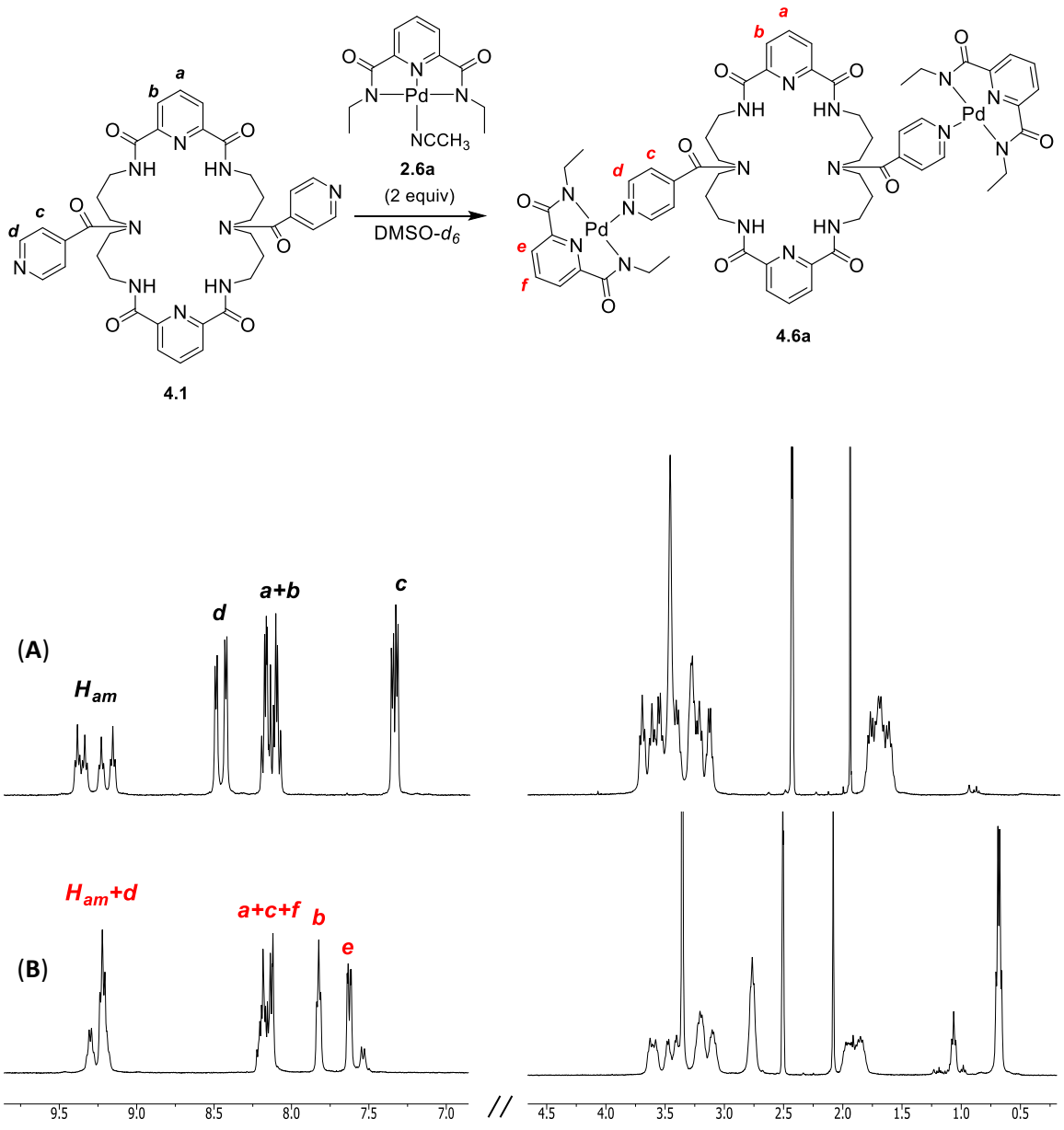

Figure 4.6. Top: Reaction of **2.6a** with **4.1** with assignments for the pendant pyridine protons. Bottom: ^{1}H NMR (500 MHz, 298 K, DMSO-d_6) of **4.1** (**A**) before and (**B**) after adding complex **2.6a** (2 equiv).

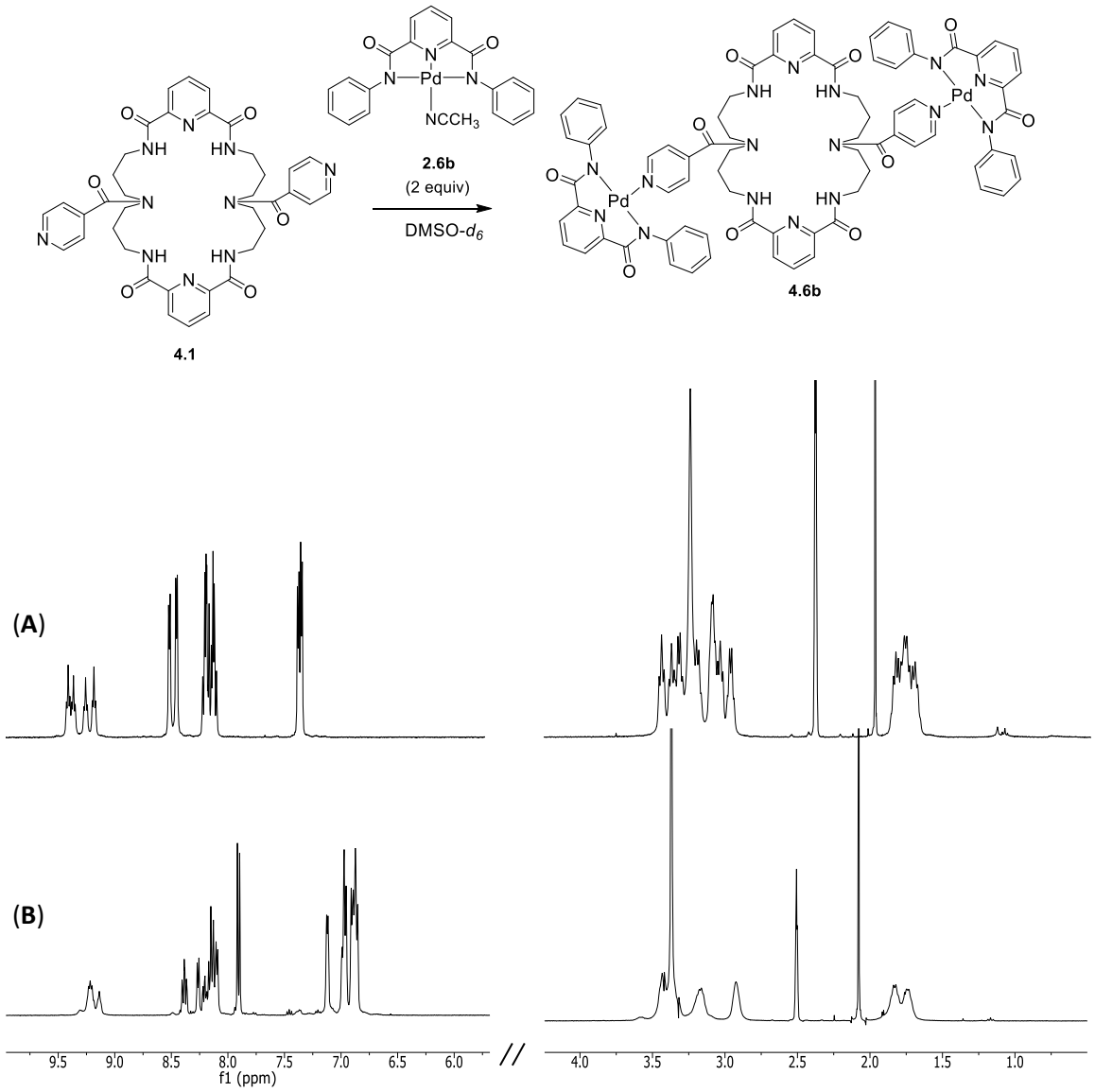

Figure 4.7. Top: Reaction of **2.6b** with **4.1** with assignments for the pendant pyridine protons. Bottom: ^{1}H NMR (500 MHz, 298 K, DMSO-d_6) of **4.1** (**A**) before and (**B**) after adding **2.6b** (2 equiv).

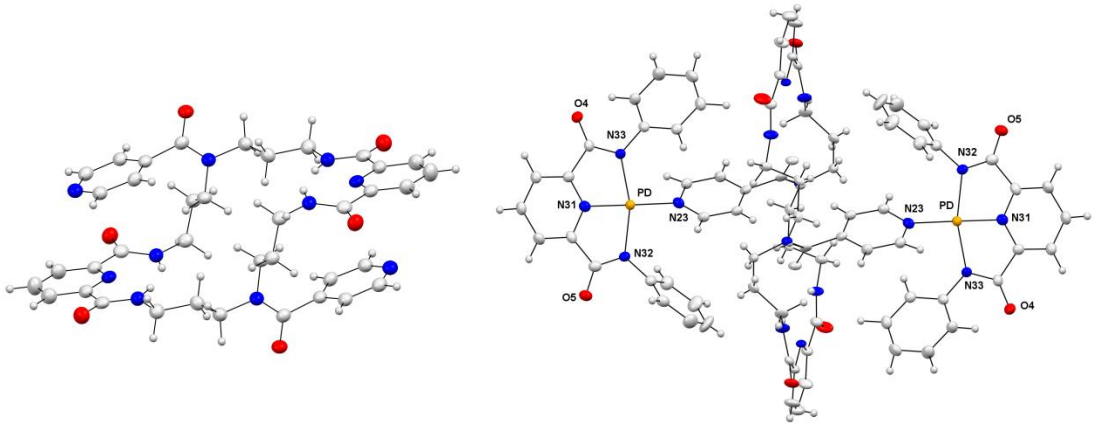

Figure 4.8. X-ray crystal structures of macrocycle **4.1** (left) and coordination dimer **4.6b** (right).

Anion titrations of the coordination dimers **4.6a** and **4.6b** with $TBAH_2PO_4$ and $(TBA)_2C_8H_4O_4$ were performed by Dr. Metola in DMSO-d_6 (Scheme 4.4). The presence of a first order binding curve in the case of $TBAH_2PO_4$ with **4.6b** suggests that **4.6b** is a receptor for phosphate, without compromising the stability of the Pd–N(pyridine) bond. This result agrees with Dr. Metola's earlier observation that phosphate does not displace pyridine in the pyridine-ligated derivative of complex **2.6b** (Scheme 4.3, *vide supra*). Conversely, sigmoidal curves were observed for reaction of **4.6a** with $TBAH_2PO_4$ and **4.6a** or **4.6b** with $(TBA)_2C_8H_4O_4$. The source of irregularities in these binding curves is currently under investigation.

Scheme 4.4.

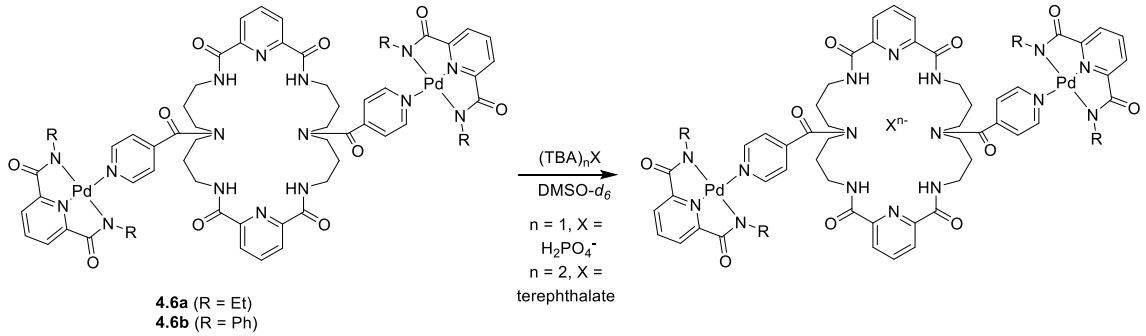

4.3.3 *Self-Assembly of Coordination Polymers: First Approach*

In order to extend the family of metallo-cross linkers to amide-based Pd(II) NNN-pincer complexes—and ultimately to investigate the coordinative crosslinking ability of macrocycle **4.1**—we took on the synthesis of bis[palladium(II)] NNN-dipincer complex **4.9** (Scheme 4.5). Treatment of a methanolic solution of tetramethyl pyrazine-2,3,5,6-tetracarboxylate (**4.7**) with ethyl amine afforded NNN-dipincer ligand **4.8** as a white solid in 52% yield. This compound was characterized by ^{1}H, ^{13}C, and ^{13}C-DEPT NMR spectroscopy, as well as positive ion mode ESI-MS. Treatment of an acetonitrile suspension of **4.8** with two equivalents of $Pd(OAc)_2$ resulted in a maroon solution. After stirring for 16 h, the solvent was evaporated *in vacuo* to afford complex **4.9** as a dark red solid in 86% yield. The ^{1}H NMR spectrum of **4.9** features two signals integrating to two and three protons for the C*H*$_2$ and C*H*$_3$ ethylene protons, respectively. The tridentate coordination of the pincer ligand to Pd(II) was evidenced by a disappearance of the amide NH triplet signal, present at 8.78 ppm in ligand **4.8**. The coordination of acetate in the fourth coordination site was evidenced by a signal at 2.03 ppm in the ^{1}H NMR spectrum and signals at 180.6 and 20.3 ppm in the ^{13}C NMR spectrum. In the negative ion mode

ESI mass spectrum of complex **4.9** in methanol, a prominent ion peak corresponding to [M – H]$^-$ is present at *m/z* 693.0019.

Scheme 4.5.

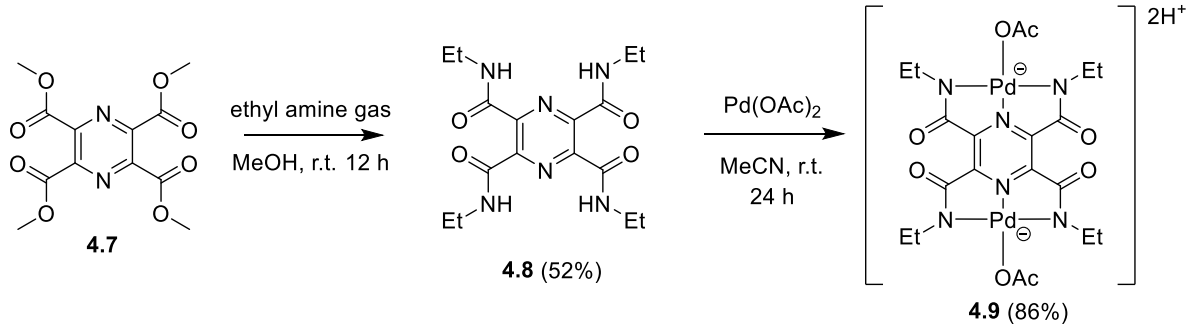

4.7 **4.8** (52%) **4.9** (86%)

Crystals of complex **4.9** for X-ray analysis were obtained from MeOH. The offset array packing observed for **4.9** (see Figure A.4.11 in the Appendix) is similar to the packing of Pd(II) NNN-pincer complex **2.6a**, discussed earlier in this dissertation (see Figure A.2.24 in the Appendix). Both crystallographically-independent Pd centers are disordered, resulting in a partial occupancy of 66/34 and 53/47 for Pd1 and Pd2 respectively. This disorder may be due to the co-crystallization of two different conformations of the complex, or the co-crystallization of molecules with different ligands in the fourth coordination site. Interestingly, the ligand does not appear to be acetonitrile or methanol. In a more recently obtained crystal structure—obtained by Jess Lohrman—the molecule in the fourth coordination site was not disordered and was determined to be acetate. The counter ions in this structure are two protons.

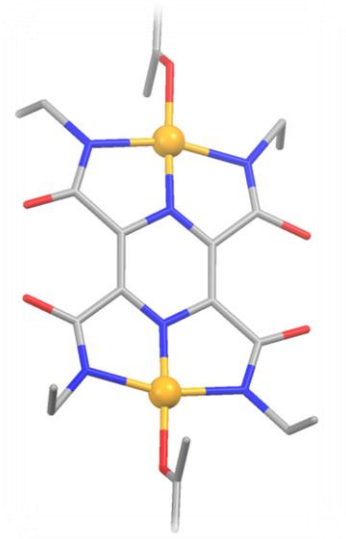

Figure 4.11. Perspective view of the X-ray crystal structure of complex **4.9**.

4.3.4 *Self-Assembly of Coordination Polymers: Second Approach*

As detailed in the introduction, the objective of this approach was to synthesize a coordination polymer containing macrocycle **4.1** and Cl^- or OAc^- salts of Pd(II). We reasoned that the use of a metal with a square-planar coordination geometry might provide a more porous coordination framework relative to the MOF obtained from the reaction of **4.1** with $AgNO_3$, which features a tetradehdral coordination of the metal center, as well as coordination of a carbonyl oxygen, in addition to the pyridine nitrogen, of **4.1**.

Complete conversion to a new species was observed via ^{1}H NMR following the titration of 1.25 equivalents of $PdCl_2$ into a solution of macrocycle **4.1** in DMSO-d_6. Formation of a coordination polymer was evidenced by significant broadening of the macrocyclic signals relative to parent compound **4.1**. Additionally, a significant downfield shift (ca. 0.3 ppm) was observed for signals corresponding the pendant pyridine protons of the proposed coordination polymer, CH^a and CH^b, relative to **4.1.** Based on these results,

we propose the identity of the new species corresponds to MOF **4.11a**, in which $PdCl_2$ is chelated to the pendent pyridine nitrogens (Figure 4.14). Crystal growth of **4.11a** was attempted from slow diffusion of MeOH or MeCN into a 0.027 mM DMSO solution of the complex. After one day, small crystals were observed in the case of the MeOH/DMSO mixture. Although these crystals did not diffract, over the course of a few months thin yellow sheets were formed. Recommendations for further study of this material are provided in the next section.

One concern in employing $Pd(OAc)_2$ to form a coordination polymer with ligand **4.1** was that the acetate ligands might deprotonate the amide hydrogens, resulting in the formation of a Pd(II) NNN-pincer complex with the resulting dianionic ligand. Fortunately, this was not observed. Treatment of a DMSO-d_6 solution of **4.1** with $Pd(OAc)_2$ resulted in a ^{1}H NMR spectrum almost identical to that of **4.11a** (Figure 4.17). In addition to the downfield shifts of C*H*^{a} and C*H*^{b} and overall broadening of the signals, the ratio of integrations for the amide (4H) and pendant pyridine (4H) proton signals remain 1:1, indicating that the Pd(II) atoms coordinate to the pendant pyridine nitrogen to generate coordination polymer **4.11b** rather than forming a pincer complex.

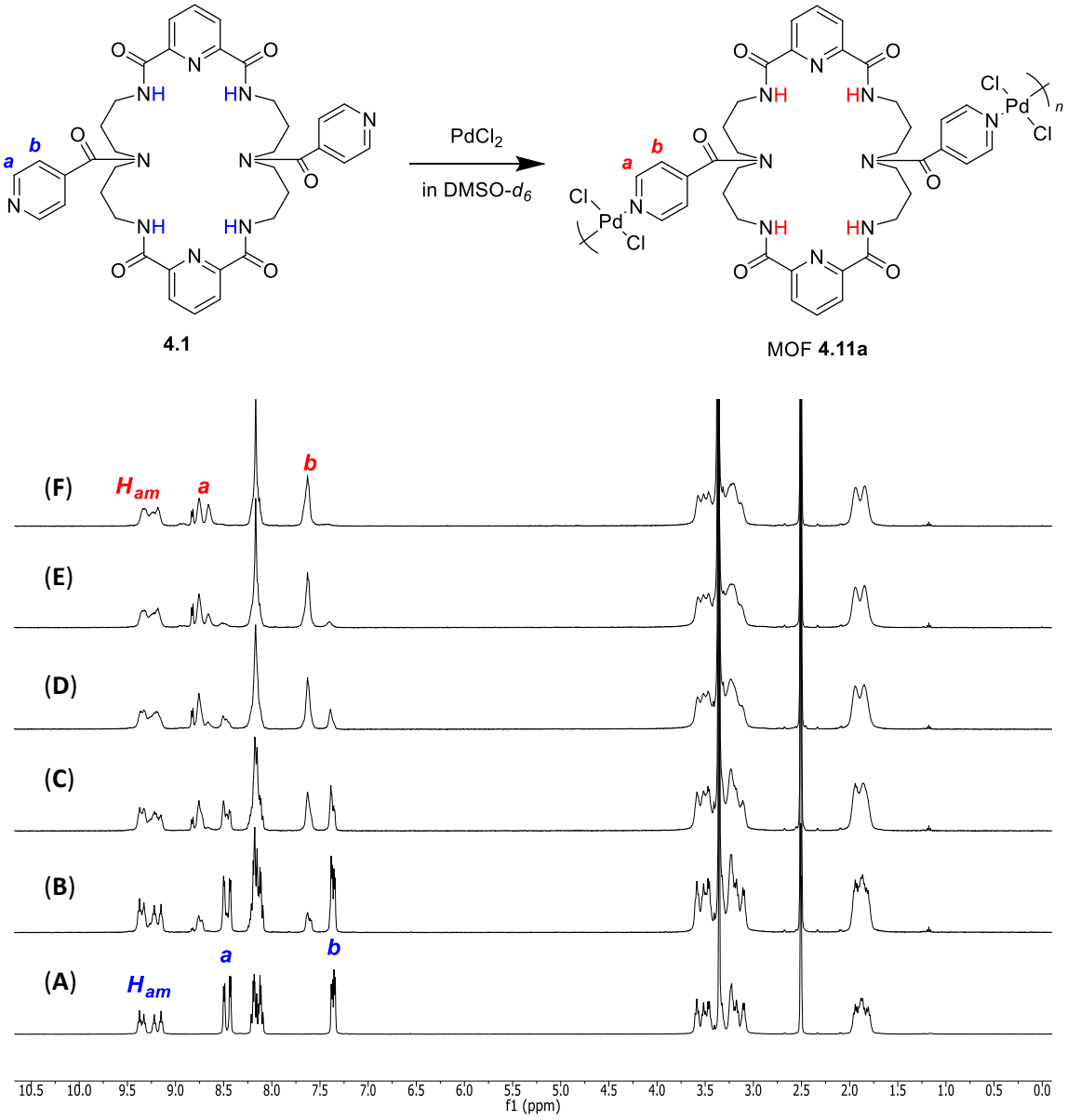

Figure 4.14. Top: Reaction of $PdCl_2$ with **4.1** with assignments for the pendant pyridine protons. Bottom: ^1H NMR (500 MHz, 298 K, DMSO-d_6) of after adding different amounts of $PdCl_2$ to **4.1**. (**A**) 0 equiv, (**B**) 0.25 equiv, (**C**) 0.50 equiv, (**D**), 0.75 equiv, (**E**) 1.00 equiv, and (**F**) 1.25 equiv.

4.4 *Conclusions*

A new family of pyridine-appended tetraamide macrocycles has been studied. Pd(II) pincer complexes **2.6a** or **2.6b**, joined by nitrogen-containing aromatic ligands (pyrazine, 4,4-bipyridine, or macrocycle **4.1**) resulted in stable coordination dimers which were characterized by ^{1}H NMR and X-ray crystallography. In order to apply this methodology to the synthesis of a coordination polymer, we designed and synthesized an NNN-dipincer complex, **4.9**. Current studies are underway to investigate the substitution of the acetate ligand of this dipincer complex with the appended pyridine in **4.1** to form a coordination polymer. We have also demonstrated that the combination of macrocycle **4.1** with PdX_2 (X = Cl or OAc) salts results in a useful method to synthesize coordination polymers, as observed from a significant broadening of the signals the resulting ^{1}H NMR spectra, as well as the formation of flat sheets. The design and study of tetraamide macrocycle-containing coordination polymers could lead to many novel applications resulting from the well-documented separate benefits of both macrocycles and MOFs. The next steps should be aimed at characterizing these coordination polymers (e.g. size exclusion chromatography, atomic force microscopy (AFM), scanning electron microscopy (SEM), and combined X-ray crystallography/molecular modeling) as well as identifying their small molecule absorption properties.

4.5 *Materials and Methods*

4.5.1 *General*

Chemicals and reagents were purchased from Sigma Aldrich Corporation and used without further purification. Macrocycle **4.1** was synthesized and provided by Dr. Telikepalli. Pd(II) NNN-pincer complex **2.6a** was prepared using a procedure reported previously in this dissertation.[27] Pd(II) NNN-pincer complex **2.6b** was prepared using a modified version of a previously reported procedure.[28-30] ^{1}H NMR spectra were recorded on a Bruker DRX 400 MHz NMR spectrometer, 500 MHz Bruker DRX spectrometer equipped with a X-channel broadband observe probe, or a 500 MHz Bruker AVIII spectrometer equipped with a cryogenically-cooled carbon observe probe. Electrospray ionization-mass spectrometry (ESI-MS) was performed on a LCT Premier Mass spectrometer at the Mass Spectrometry Laboratory at the University of Kansas. Single-crystal XRD data were obtained at the Small-Molecule X-ray Crystallography Laboratory at the University of Kansas by Dr. Victor Day.

4.5.2 *Coordination of complexes **2.6a** and **2.6b** with pyrazine and 4,4-bipyridine*

Precipitate tests

A yellow solution of complex **2.6a** (10 mg, 0.027 mmol) or **2.6b** (10 mg, 0.022 mmol) in MeCN-d_3 (3 mL) was treated with pyrazine (0.5 equiv) or 4,4-bipyridine (0.5 equiv). In the case of **2.6a** with pyrazine and 4,4-bipyridine or **2.6b** with 4,4-bipyridine, a yellow precipitate was observed immediately following the addition. Further, upon filtration of the precipitate, a clear filtrate was observed. In the case of **2.6b** with pyrazine,

a yellow solution was observed after addition. Approximately 0.6 mL was taken for ^{1}H NMR analysis on a 400 MHz Bruker NMR spectrometer.

*Crystallization of 4,4-bipyridine dimer **4.5***

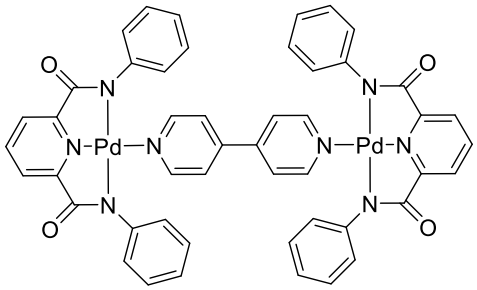

4.5

A 25 mL round bottom flask was charged with dimer complex **4.5** (20 mg, 0.043 mmol) and DMF (5 mL). The resulting suspension was heated to 165 ^{o}C, at which point the temperature was held for 10 min before cooling to r.t. at a rate of ca. 10 ^{o}C every 30 min. While heating, the suspension became a yellow solution at 115 ^{o}C. Upon reaching r.t., the yellow solution was stored for 5 d, affording crystals suitable for X-ray diffraction analysis.

4.5.3 *Crystallization of **4.1***

Macrocycle **4.1** (10 mg, 0.014 mmol)—provided by Dr. Telikepalli—was dissolved in a minimum amount of MeOH (approximately 15 mL) and filtered through a pad of celite. Crystals suitable for X-ray analysis were obtained after 8 weeks.

4.5.4. *^{1}H NMR and crystallization of **4.6a** and **4.6b**.*

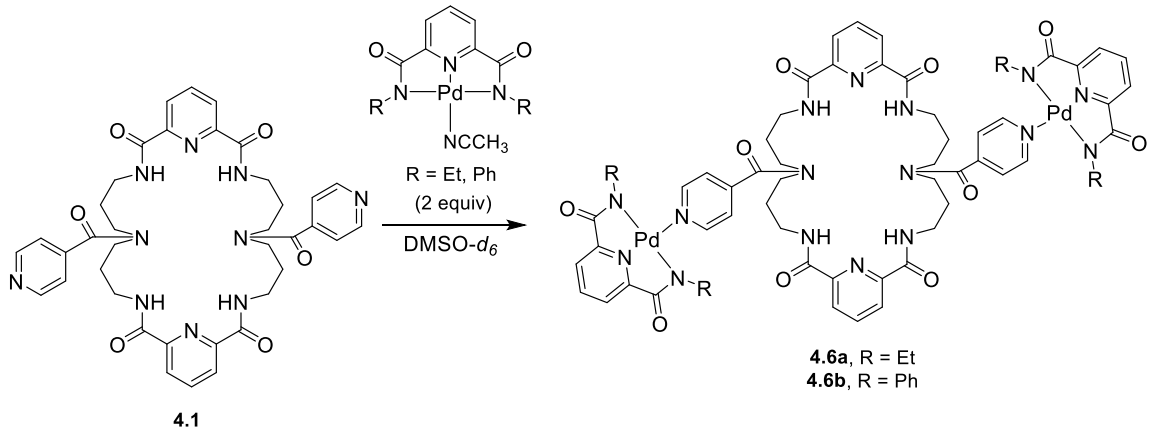

A DMSO-d_6 solution of complex **2.6a** (10.3 mg, 0.028 mmol) or **2.6b** (12.6 mg, 0.110 mmol) was added to a DMSO-d_6 solution of ligand **4.1** (10 mg, 0.014 mmol). ^{1}H NMR studies of the binding were performed on a Bruker NMR spectrometer (500 MHz). For each measurement, a 0.6 mL aliquot of the mixture was taken for ^{1}H NMR analysis. In the case of **4.6b**, crystal growth was induced from addition of a solution of complex **2.6b** (46 mg, 0.099 mmol) in MeCN (10 mL) to a solution of **4.1** (36.5 mg, 0.050 mmol) in DMF (3 mL). Crystals suitable for X-ray crystallographic analysis were obtained overnight.

4.5.5 *Synthesis of NNN-Dipincer Ligand* ***4.8***

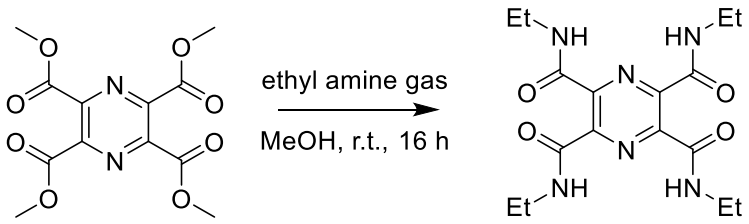

4.7 **4.8** (52%)

To a 15 mL sealed tube containing a suspension of tetramethyl pyrazine-2,3,5,6-tetracarboxylate **4.7** (1 g, 3.00 mmol) in methanol (10 mL) was bubbled ethyl amine for 2 min. The tube was sealed and the mixture was stirred for 16 h. The solvent was evaporated *in vacuo* to afford the product as a white solid (566 mg, 1.56 mmol, 52%). ^{1}H NMR (500 MHz, DMSO-d_6) δ 8.79 (t, J = 5.78 Hz, 4H), 3.36 – 3.30 (m, 8H), 1.16 (t, J = 7.21 Hz, 12H); ^{13}C NMR (126 MHz, DMSO-d_6) δ 163.1, 145.3, 33.8, 14.6; HRMS (ESI^{+}) *m/z* [M + H]$^{+}$ calculated for $C_{16}H_{25}N_6O_4$: 365.1932; found 365.1922.

4.5.6 *Synthesis of Pd(II) NNN-Dipincer Complex* ***4.9***

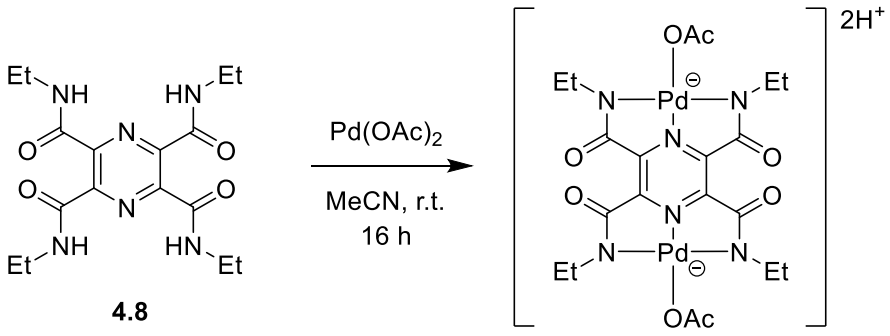

4.8 **4.9**

To a suspension of NNN-pincer ligand **4.8** (300 mg, 0.824 mmol, 1 equiv) in MeCN was added $Pd(OAc)_2$ (369 mg, 1.65 mmol, 2 equiv) and the reaction was stirred at r.t. for

16 h. The solvent was evaporated *in vacuo* and crystals were grown from slow evaporation of a saturated solution of the complex in methanol to afford the product as a dark red crystalline solid (491 mg, 0.709 mmol, 86%). ^{1}H NMR (500 MHz, CD_3OD) 3.24 (br, 8H), 2.03 (s, 6H), 1.19 (t, J = 6.84 Hz, 12H); ^{13}C NMR (126 MHz, CD_3OD) 180.6, 168.1, 149.3, 43.3, 23.0, 14.2; HRMS (ESI^-) *m/z* $[M - H]^-$ calculated for $C_{20}H_{27}N_6O_8Pd_2$: 692.9959, found: 693.0019.

4.5.7 *In situ preparations of **4.11a** and **4.11b***

To a DMSO-d_6 solution of **4.1** (2.7 mM) solution in an NMR tube was added 0.25 equiv portions of a stock DMSO-d_6 solution of $PdCl_2$ (0.1 M). Following each addition, the ^{1}H NMR spectrum of the resulting species was recorded on a Bruker NMR spectrometer at 500 MHz. Complete conversion to a new species was observed following the titration of 1.25 equivalents of $PdCl_2$ into a solution of macrocycle **4.1**. In the case of $Pd(OAc)_2$, 2 equiv was added to 0.5 mL of a 2.7 mM solution of **4.1**.

4.6 *References*

1. Stupp, S. I.; Palmer, L. C. "Supramolecular Chemistry and Self-Assembly in Organic Materials Design" *Chem. Mater.* **2014**, *26*, 507–518.
2. Whittell, G. R.; Hager, M. D.; Schubert, U. S.; Manners, I. "Functional Soft Materials from Metallopolymers and Metallosupramolecular Polymers" *Nature Mat.* **2011**, *10*, 176–188.
3. Herbst, F.; Dohler, D.; Michael, P. Binder, W. H. "Self-Healing Polymers via Supramolecular Forces" *Macromol. Rapid Commun.* **2013**, *34*, 203–220.
4. Zhou, H-. C.; Long, J. R.; Yaghi, O. M. "Introduction to Metal-Organic Frameworks" *Chem. Rev.* **2012**, *112*, 673-674; Zhou, H-. C.; Kitagawa, S. "Metal-Organic Frameworks (MOFs)" *Chem. Soc. Rev.* **2014**, *43*, 5415–5418.
5. Stock, N.; Biswas, S. "Synthesis of Metal-Organic Frameworks (MOFs): Routes to Various MOF Topologies, Morphologies, and Composites" *Chem. Rev.* **2012**, *112*, 933–969.
6. Sumida, K.; Rogow, D. L. Mason, J. A.; McDonald, T. M.; Bloch, E. D.; Herm, Z. R.; Bae, T-. H.; Long, J. R. "Carbon Dioxide Capture in Metal-Organic Frameworks" *Chem. Rev.* **2012**, *112*, 724-781; Suh, M. P.; Park, H. J.; Prasad, T. K.; Lim, D-. W. "Hydrogen Storage in Metal-Organic Frameworks" *Chem. Rev.* **2012**, *112*, 782–835.
7. Wu, H.; Gong, Q.; Olson, D. H.; Li, J. "Commensurate Adsorption of Hydrocarbons and Alcohols in Microporous Metal Organic Frameworks" *Chem. Rev.* **2012**, *112*, 836–868.
8. Lee, J. Y.; Farha, O. K.; Roberts, J.; Scheidt, K. A.; Nguyen, S. T.; Hupp, J. T. "Metal-Organic Framework Materials as Catalysts" *Chem. Soc. Rev.* **2009**, *38*, 1450–1459.
9. Li, J-. R.; Sculley, J.; Zhou, H-.C. "Metal-Organic Frameworks for Separations" *Chem. Rev.* **2012**, *112*, 869–932.
10. Kreno, L. E.; Leong, K.; Farha, O. K.; Allendorf, M.; Van Duyne, R. P.; Hupp, J. T. "Metal-Organic Framework Materials as Chemical Sensors" *Chem. Rev.* **2012**, *112*, 1105–1125.

11. Horcajada, P.; Gref, R.; Baati, T.; Allan, P. K.; Maurin, G.; Couvreur, P.; Ferey, G.; Morris, R. E.; Serre, C. "Metal-Organic Frameworks in Biomedicine" *Chem. Rev.* **2012**, *112*¸ 1232–1268.
12. Zhang, H.; Zou, R.; Zhao, Y. "Macrocycle-Based Metal-Organic Frameworks" *Coord. Chem. Rev.* **2015**, *292*, 74–90.
13. Dong, S.; Zheng, B; Wang, F.; Huang, F. "Supramolecular Polymers Constructed from Macrocycle-Based Host-Guest Molecular Recognition Motifs" *Acc. Chem. Res.* **2014**, *47*, 1982–1994.
14. Zhao, Y. L.; Liu, L.; Zhang, W.; Sue, C. H.; Li, Q.; Miljanic, O. S.; Yaghi, O. M.; Stoddart, J. F. "Rigid-strut-containing crown ethers and [2]catenanes for incorporation into metal-organic frameworks" *Chem. Eur. J.* **2009** *15*, 13356–13380.
15. Smaldone, R. A.; Forgan, R. S.; Furukawa, H.; Gassensmith, J. J.; Slawin, A. M.; Yaghi, O. M.; Stoddart, J. F. "Metal–Organic Frameworks from Edible Natural Products" *Angew. Chem. Int. Ed***. 2010**, *49*, 8630–8634.
16. Liu, L. L.; Ren, Z. G.; Zhu, L. W.; Wang, H. F.; Yan, W. Y.; Lang, J. P. "Temperature-Driven Assembly of Ln(III) (Ln = Nd, Eu, Yb) Coordination Polymers of a Flexible Azo Calix[4]arene Polycarboxylate Ligand" *Cryst. Growth Des.* **2011**, *11*, 3479–3488.
17. Chen, K.; Hu, Y. F.; Xiao, X.; Xue, S. F.; Tao, Z.; Zhang, Y. Q.; Zhu, Q. J.; Liu, J. X. "Homochiral 1D-Helical Coordination Polymers from Achiral Cucurbit[5]uril: Hydroquinone-Induced Spontaneous Resolution" *RSC Adv.* **2012**, *2*, 3217–3220.
18. Strutt, N. L.; Fairen-Jimenez, D.; Iehl, J.; Lalonde, M. B.; Snurr, R. Q.; Farha, O. K.; Hupp, J. T.; Stoddart, J. F. "Incorporation of an A1/A2-Difunctionalized Pillar[5]arene into a Metal–Organic Framework" *J. Am. Chem. Soc.* **2012**, *134*, 17436–17439.
19. Min, K. S.; Suh, M. P. "Self-Assembly and Selective Guest Binding of Three-Dimensional Open-Framework Solids from a Macrocyclic Complex as a Trifunctional Metal Building Block" *Chem. Eur. J.* **2001**, *7*, 303–313.
20. Roznyatovskiy, V. V.; Leeb, C. –H.; Sessler, J. L. "π-Extended Isomeric and Expanded Porphyrins" *Chem. Soc. Rev.*, **2013**, *42*, 1921–1933.

21. Gao, W-. Y.; Niu, Y.; Chen, Y.; Wojtas, L.; Cai, J.; Chen, Y-. S.; Ma, S. "Porous Metal-Organic Framework Based on a Macrocyclic Tetracarboxylate Ligand Exhibiting Selective CO_2 Uptake" *Cryst. Eng. Commun.* **2012**, *14*, 6115–6117.
22. Feng, X.; Chen, K.; Zhang, Y-. Q.; Xue, S-. F.; Zu, Q-. J.; Tao, Z.; Day, A. I. "Stable Cucurbit[5]uril MOF Structures as 'Beaded' Rings Built on a *p*-Hydroxybenzoic Acid Template—a Small Molecule Absorption Material" *Cryst. Eng. Commun.* **2011**, *13*, 5049–5051.
23. Kang, S.O.; Llinares, J. M.; Day, V. W.; Bowman-James, K. "Cryptand-Like Anion Receptors" *Chem. Soc. Rev.* **2010**, *39*, 3980–4003.
24. (a) Bianchi, A.; Bowman-James, K.; García-España, E. "Aspects of Anion Coordination from Historical and Biological Perspectives" in *Anion Coordination Chemistry*, Bowman-James, K.;Bianchi, A.; García-España, E., Eds., Wiley-Interscience, **2012**, 1–72. (b) Begum, R. A.; Kang, S. O.; Day, V. W.; Bowman-James, K. "Structural Aspects of Anion Coordination Chemistry" in *Anion Coordination Chemistry*, Bowman-James, K.; Bianchi, A.; García-España, E., Eds., Wiley-Interscience, **2012**, 139–223. (c) Taylor, R. W.; Begum, R. A.; Day, V. W.; Bowman-James, K. "Cooperativity and the Chelate,Macrocyclic and Cryptate Effect" in *Supramolecular Chemistry: From Molecules toNanomaterials* P. A. Gale and J. W. Steed, Eds., John Wiley and Sons, Ltd., **2012**, *1*, 67–93. (d) Wang, Q.-Q.; Begum, R. A.; Day, V. W.; Bowman-James, K. "Alfred Werner's Expanded Legacy: Anion and Metal Ion Coordination in an Unsymmetrical, Octaamido Cryptand" *Polyhedron*, **2013**, *52*, 515–523. (e) *Anion Coordination Chemistry*, Bowman-James, K.; Bianchi, A.; García-España, E., Eds.; Wiley-VCH: **2012**.
25. (a) Hossain, Md. A.; Lucarini, S.; Powell, D.; Bowman-James, K. "Ditopic Double Pincer Palladacycle Catalyst for C–C Coupling" *Inorg. Chem*. **2004**, *43*, 7275–7277; (b) Ghosh, S.; Roehm, B.; Begum, R. A.; Kut, J.; Hossain, M. A.; Day, V. W.; Bowman-James, K. "Versatile Host for Metallo Anions and Cations" *Inorg. Chem*. **2007**, *46*, 9519–9521.
26. Wang, Q.-Q.; Begum, R.A.; Day, V.W.; Bowman-James, K. "Chemical Mustard Containment Using Simple Palladium Pincer Complexes: The Influence of Molecular Walls" *J. Am. Chem. Soc*. **2013**, *135*, 17193–17199.

27. This compound was prepared according to the protocol described in Chapter 2.
28. Begum, R. A.; Powell, D.; Bowman-James, K. "Thioamide Pincer Ligands with Charge Versatility" *Inorg. Chem.* **2006**, *45*, 964–966.
29. Dell'Amico, D. B.; Calderazzo, F.; Di Colo, F.; Guglielmetti, G.; Labella, L,; Marchetti, F. "Coordination Properties Towards Palladium(II) of a Tridentate Dianionic Ligand Acting as a N- or a N,O-donor" *Inorg. Chim. Acta* **2006**, *359*, 127–135.
30. Wang, Q.-Q.; Begum, R. A.; Day, V. W.; Bowman-James, K. "Molecular Thioamide⇔Iminothiolate Switches for Sulfur Mustards" *Inorg. Chem*. **2012**, *51*, 760−762.

Appendix

A.2 *Supporting Information for Chapter 2*

A.2.1 *NMR Spectra of Ligands*

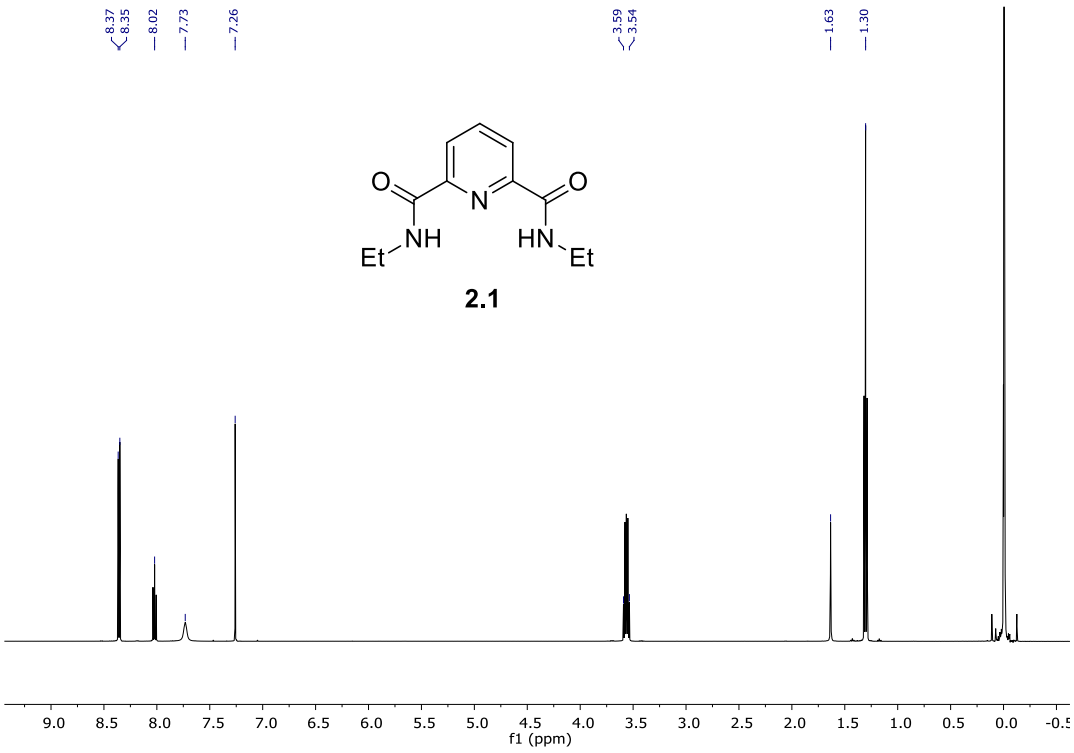

Figure A.2.1. ^{1}H NMR spectrum (500 MHz, $CDCl_3$) of **2.1**.

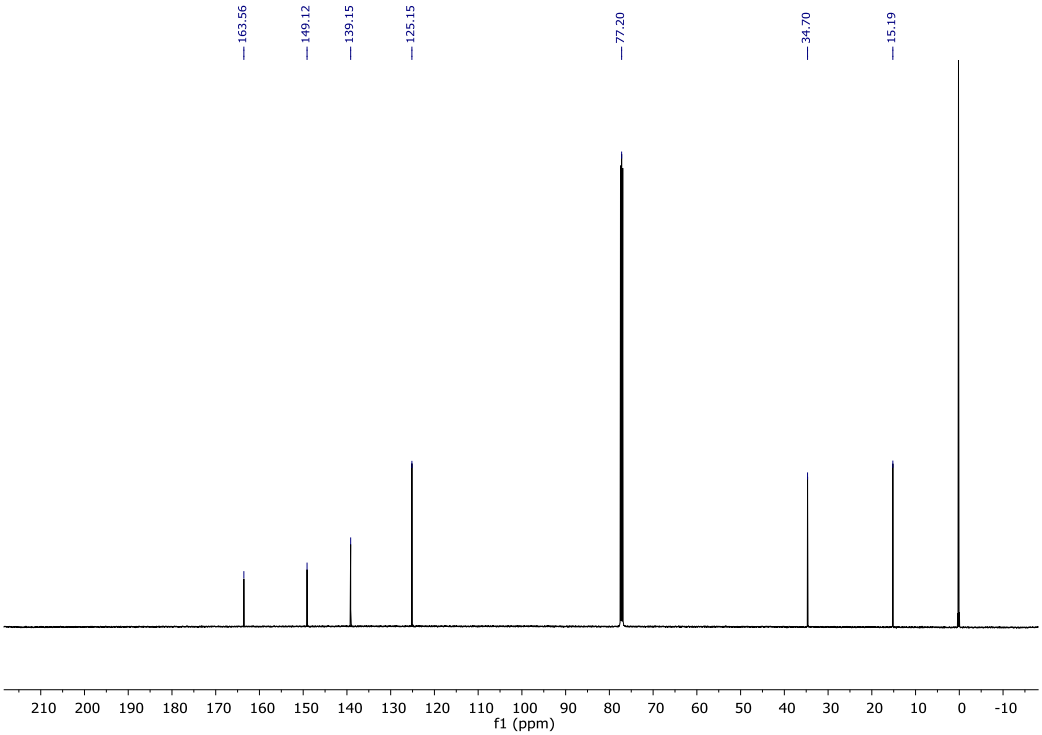

Figure A.2.2. ^{13}C NMR spectrum (126 MHz, $CDCl_3$) of **2.1**.

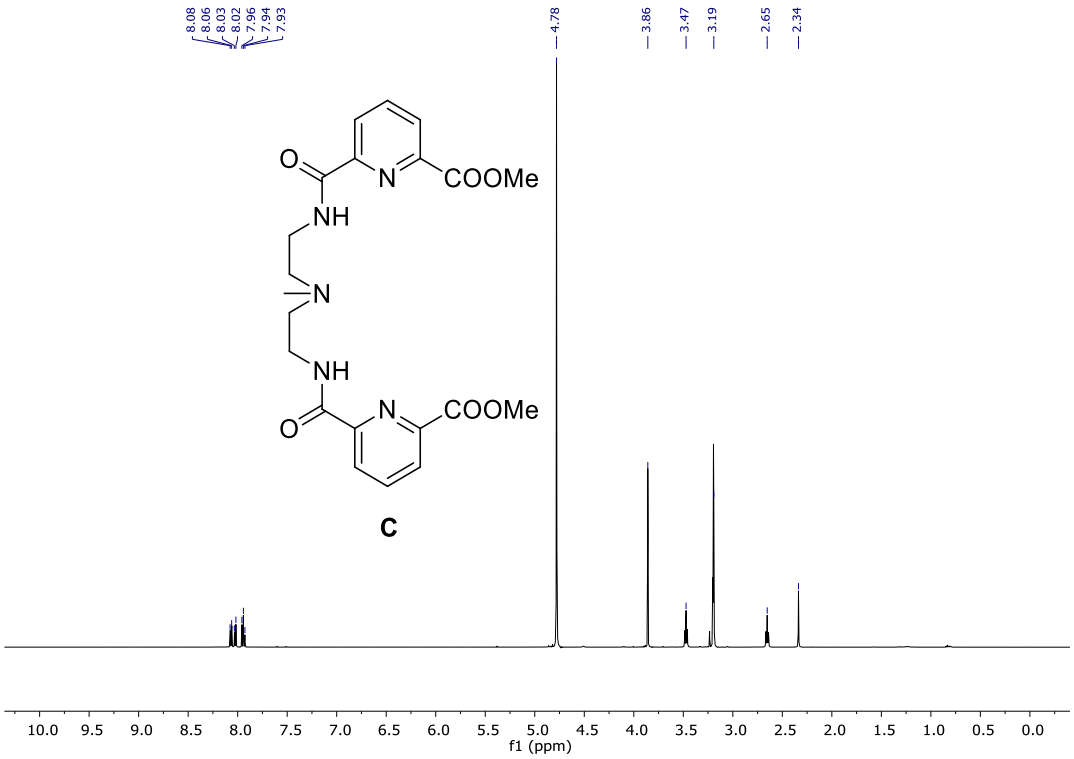

Figure A.2.3. ^{1}H NMR spectrum (500 MHz, CD_3OD) of **C**.

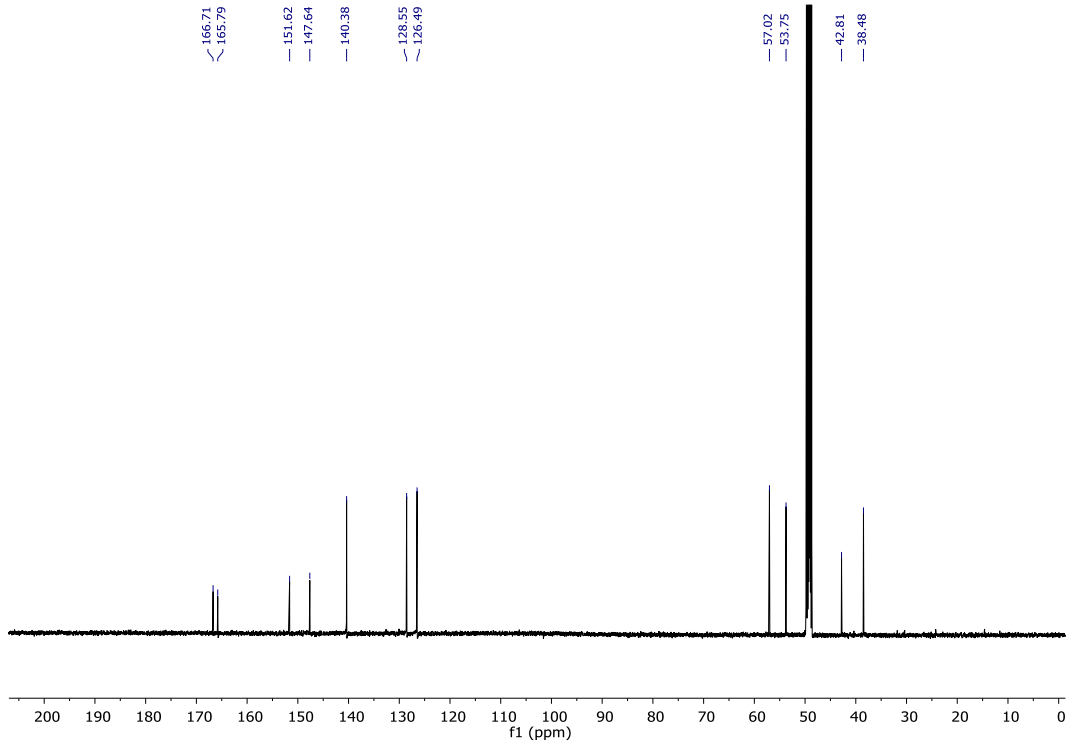

Figure A.2.4. ^{13}C NMR spectrum (126 MHz, CD_3OD) of **C**.

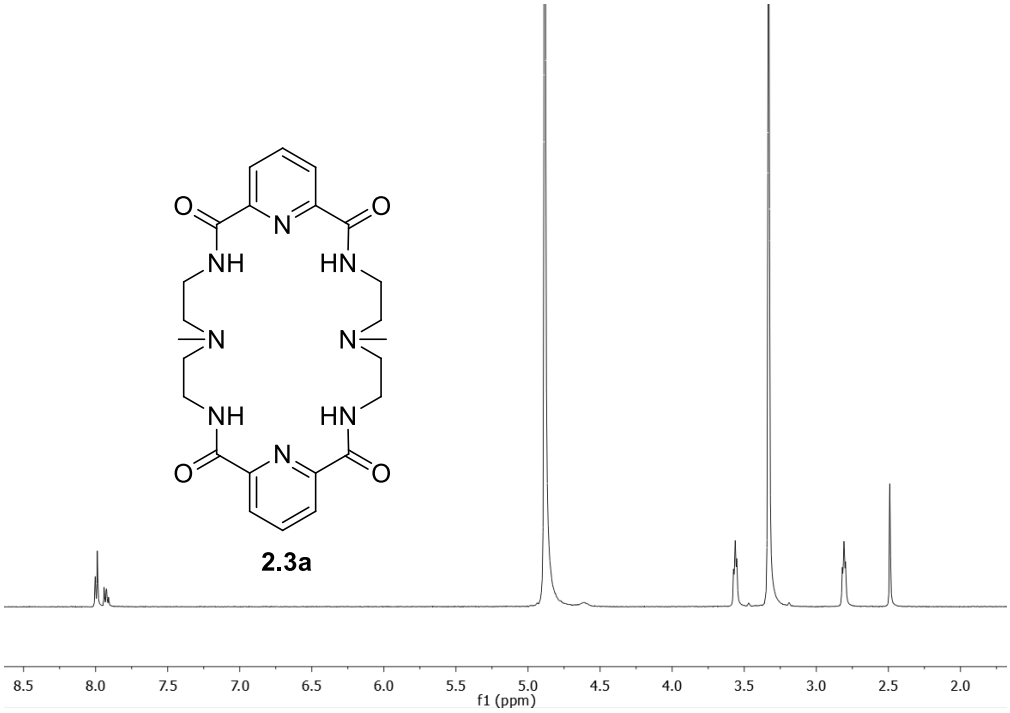

Figure A.2.5. ^{1}H NMR spectrum (500 MHz, CD_3OD) of **2.3a**.

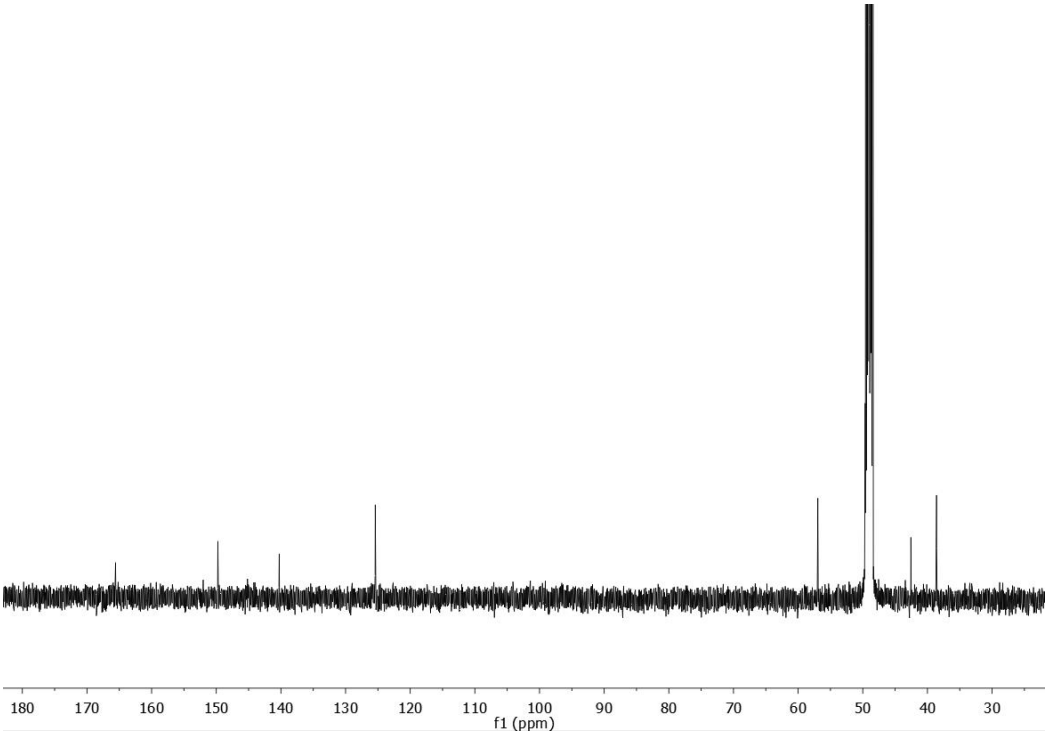

Figure A.2.6. ^{13}C NMR spectrum (126 MHz, CD_3OD) of **2.3a.**

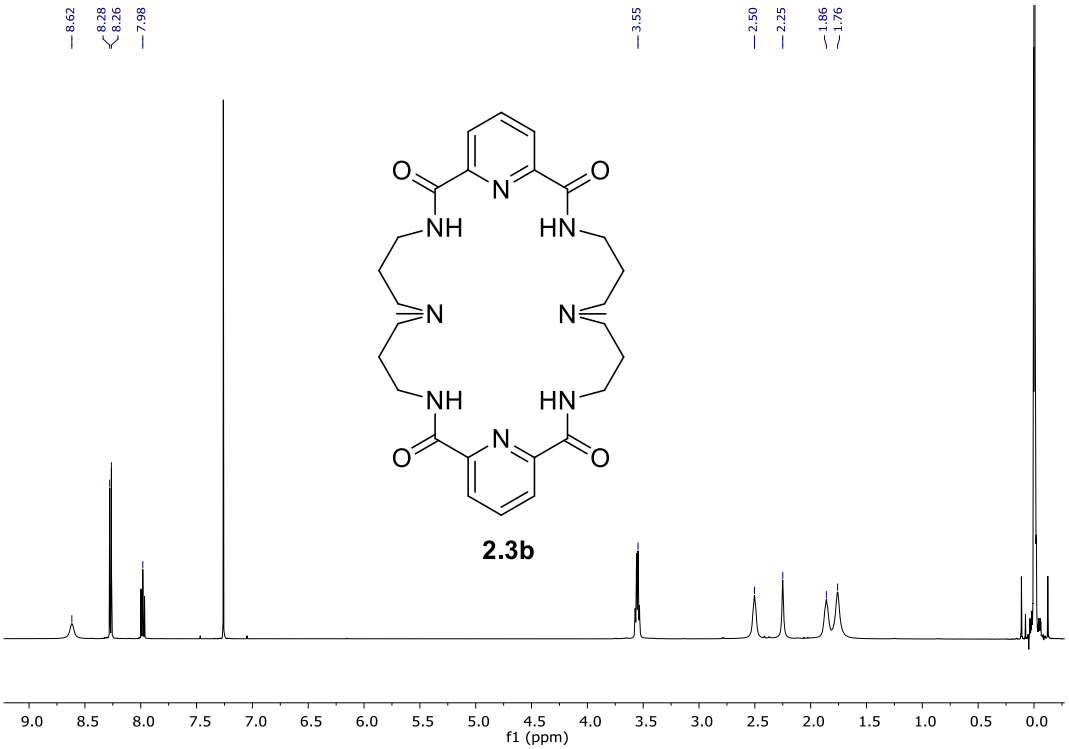

Figure A.2.7. ^{1}H NMR spectrum (500 MHz, $CDCl_3$) of **2.3b**.

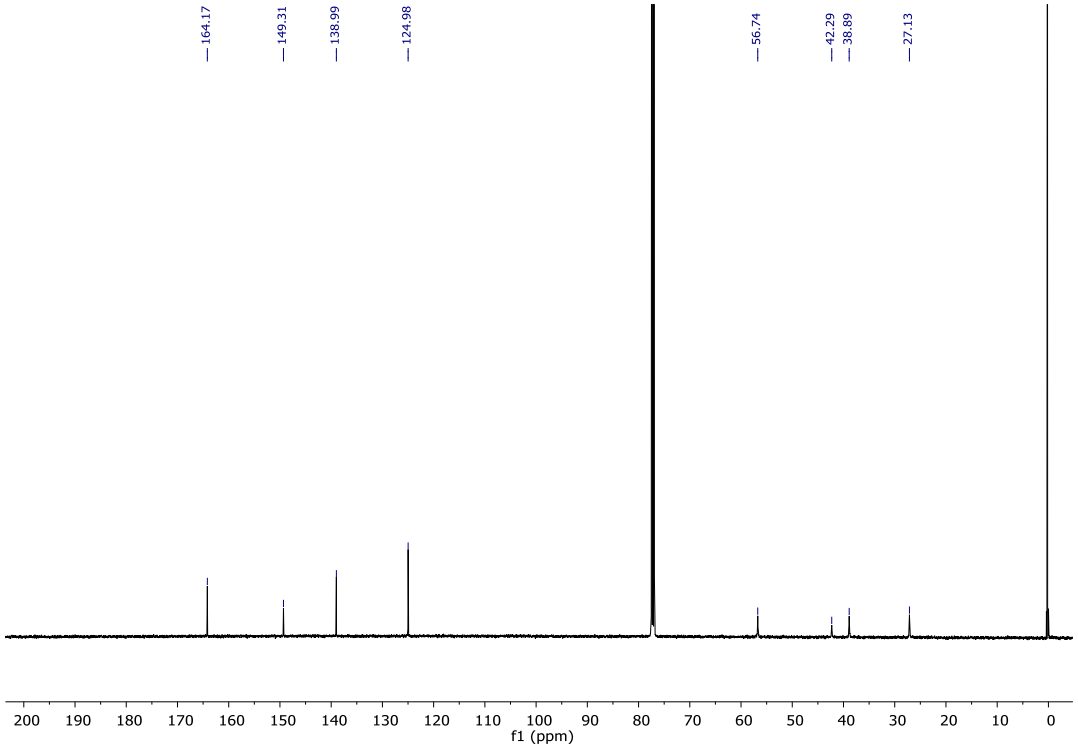

Figure A.2.8. ^{13}C NMR spectrum (126 MHz, $CDCl_3$) of **2.3b**.

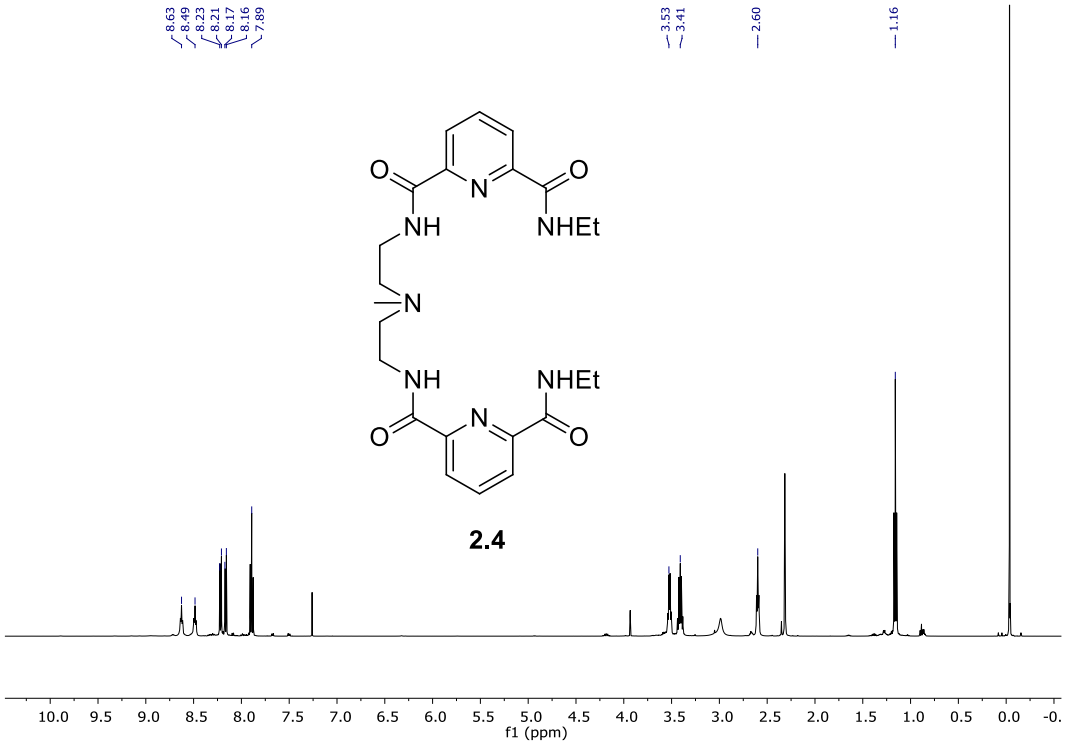

Figure A.2.9. ^{1}H NMR spectrum (500 MHz, $CDCl_3$) of **2.4**.

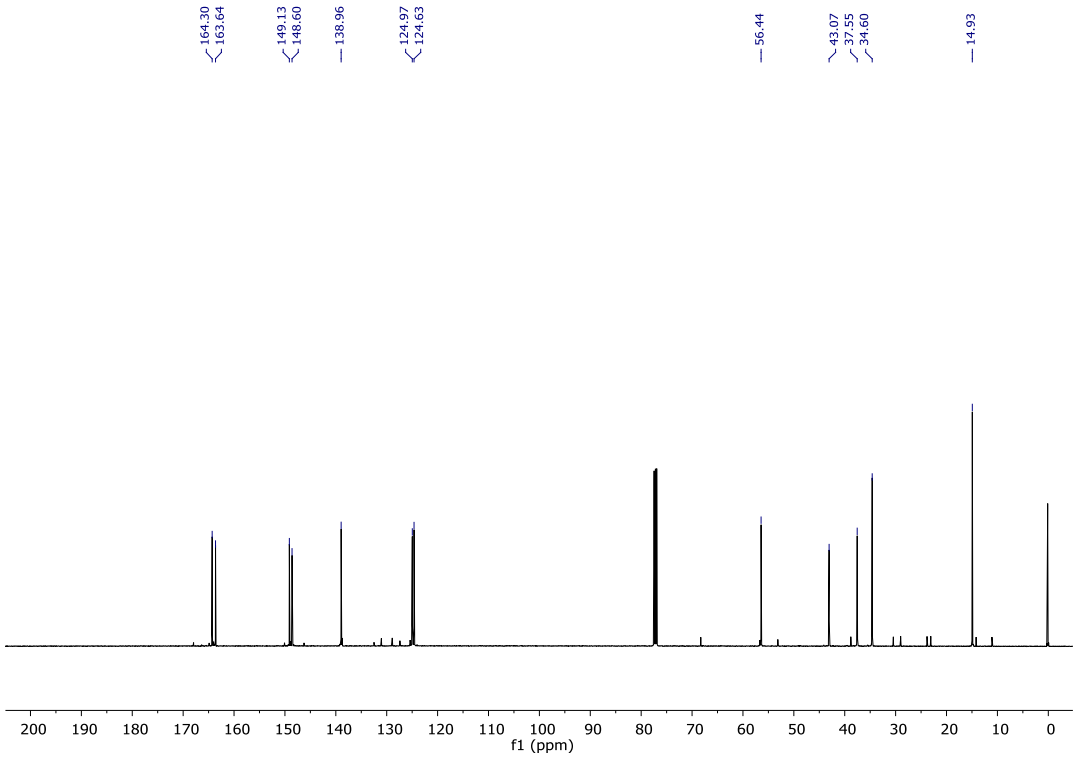

Figure A.2.10. ^{13}C NMR spectrum (126 MHz, $CDCl_3$) of **2.4**.

A.2.2 *NMR Spectra of Metal Complexes*

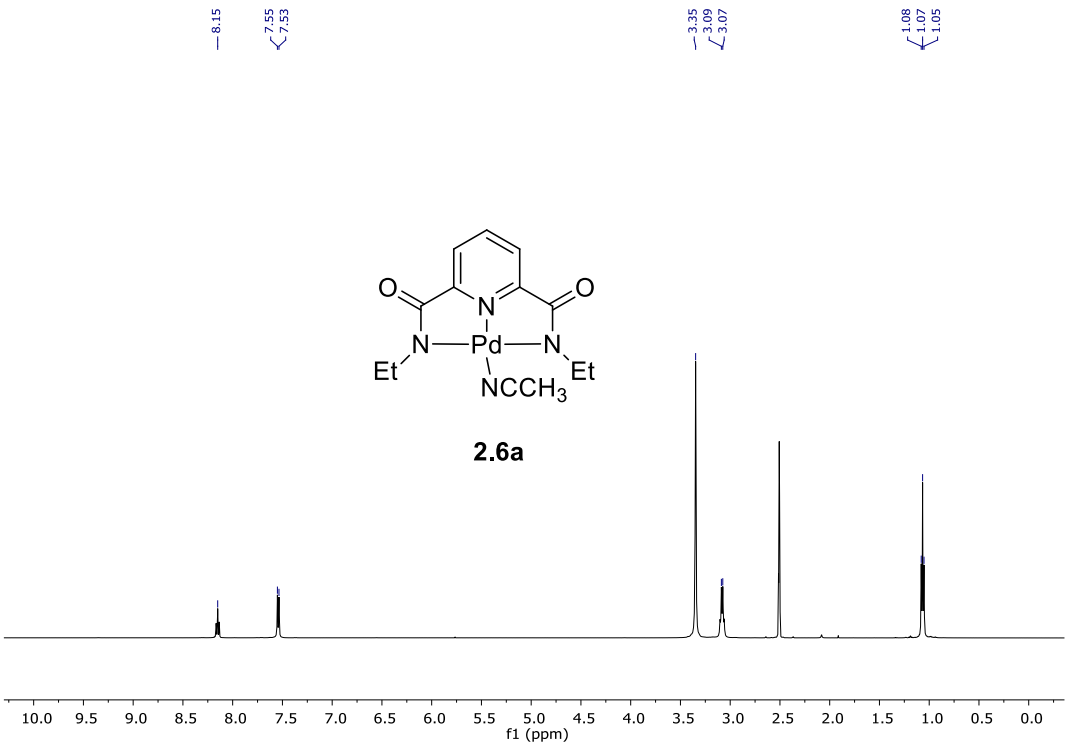

Figure A.2.11. ^{1}H NMR spectrum (500 MHz, DMSO-d_6) of **2.6a**.

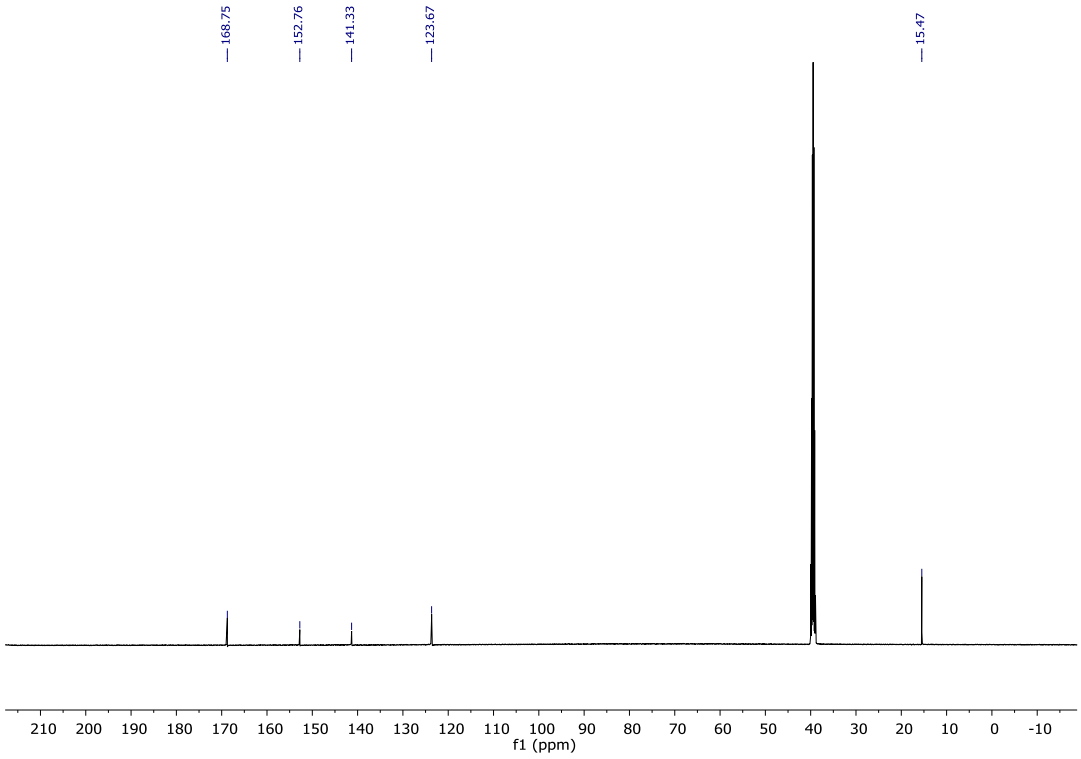

Figure A.2.12. ^{13}C NMR spectrum (126 MHz, DMSO-d_6) of **2.6a**.

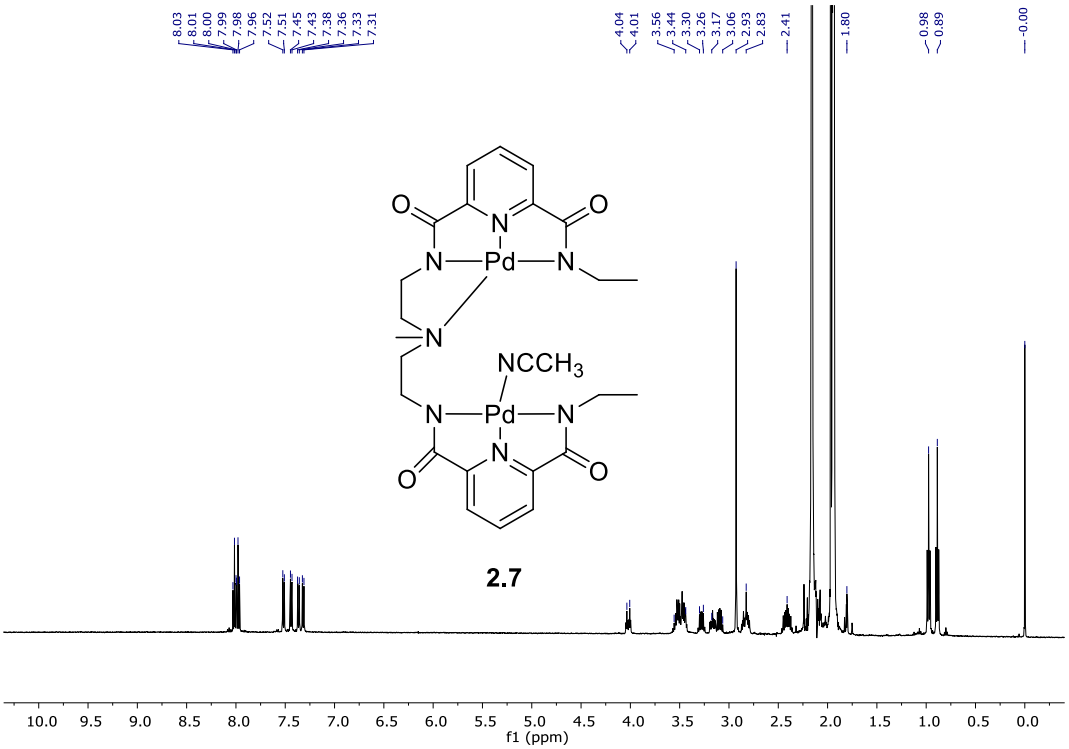

Figure A.2.13. ^{1}H NMR spectrum (500 MHz, MeCN-d_3) of **2.7**.

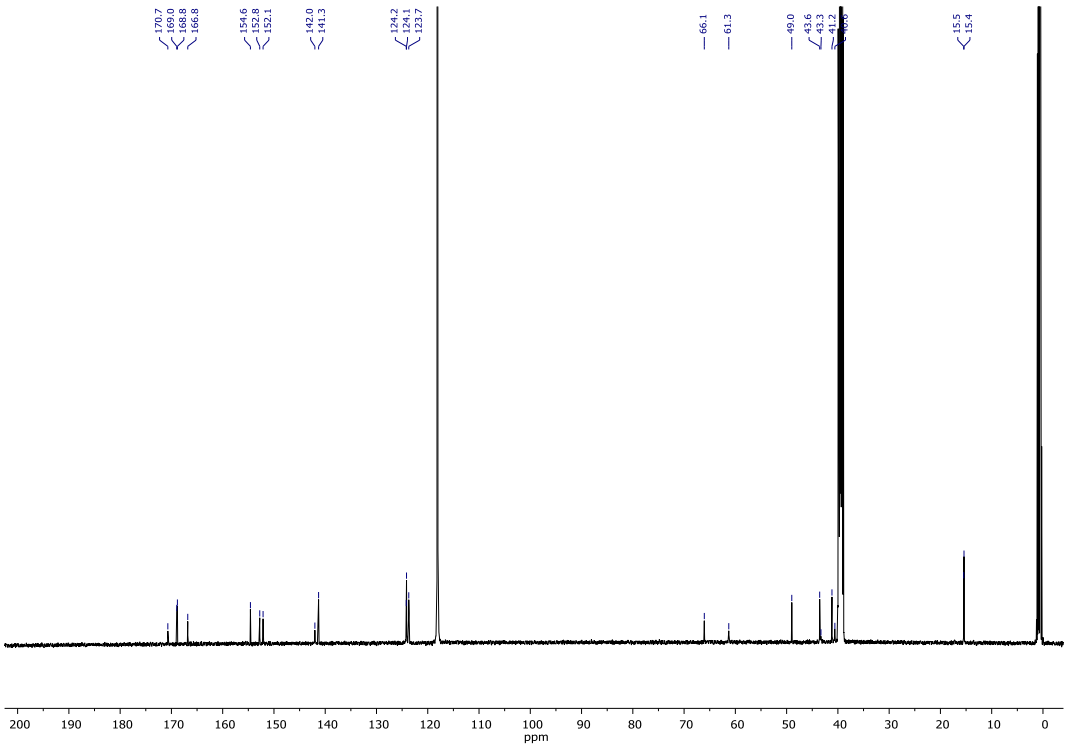

Figure A.2.14. ^{13}C NMR spectrum (126 MHz, MeCN-d_3) of **2.7**.

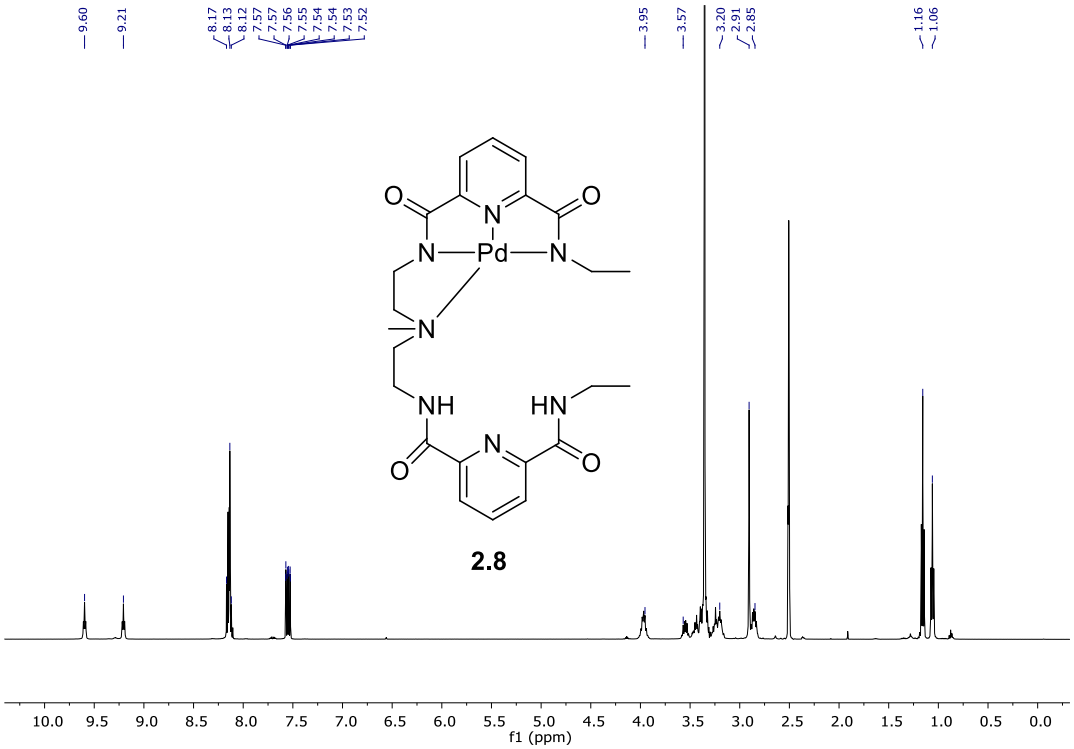

Figure A.2.15. ^{1}H NMR spectrum (500 MHz, DMSO-d_6) of **2.8**.

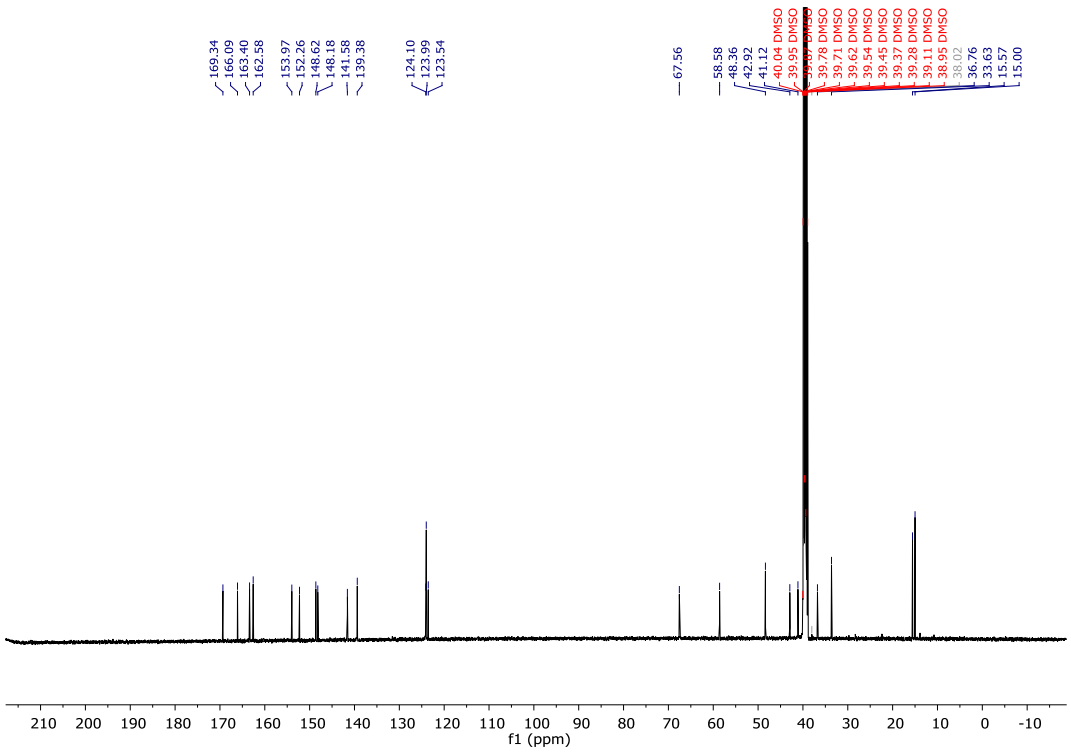

Figure A.2.16. ^{13}C NMR spectrum (126 MHz, DMSO-d_6) of **2.8**.

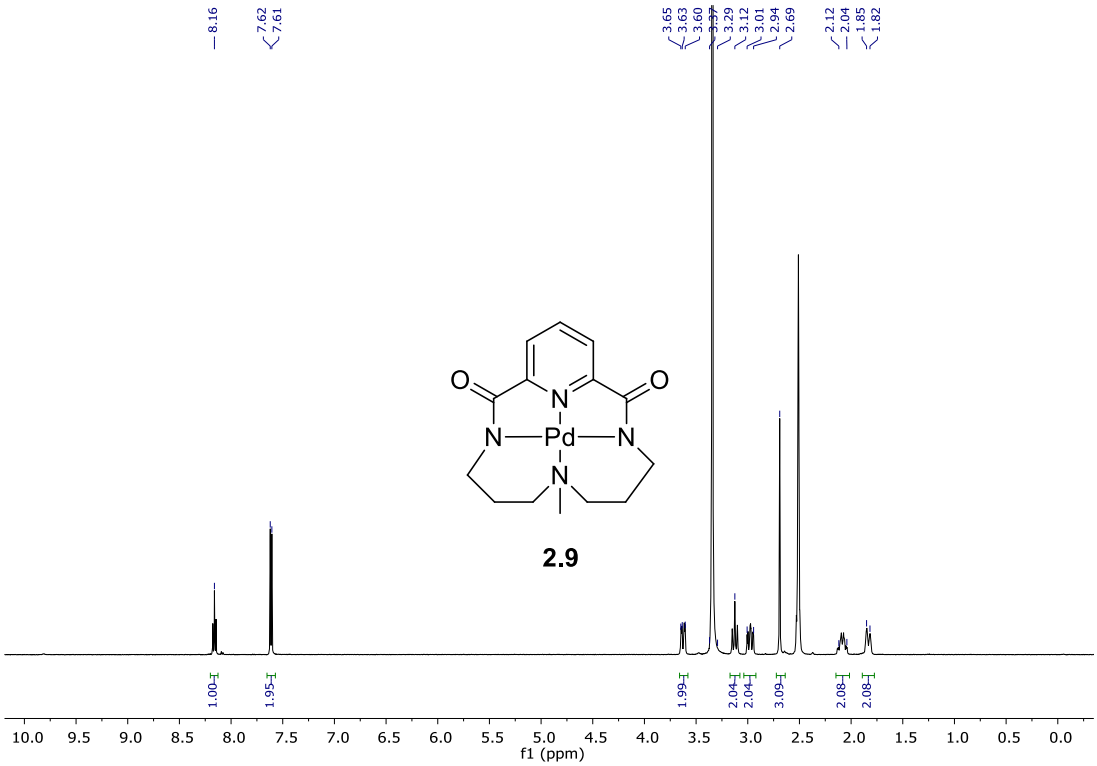

Figure A.2.17. ^{1}H NMR spectrum (500 MHz, DMSO-d_6) of **2.9**.

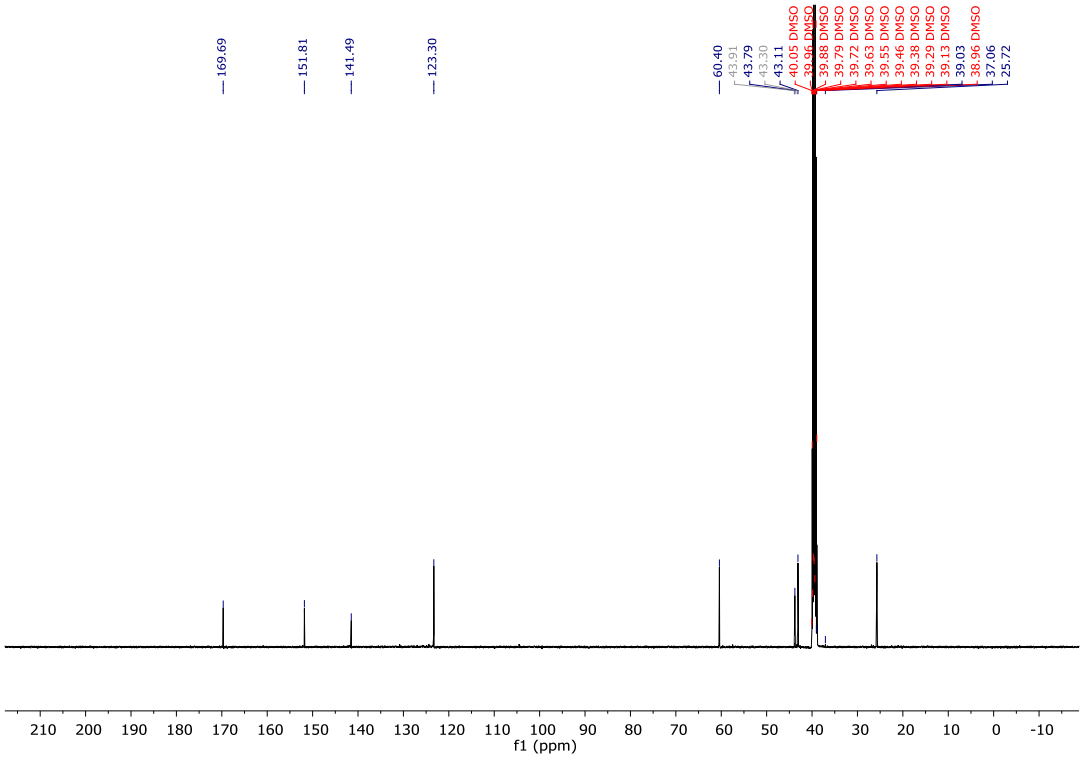

Figure A.2.18. ^{13}C NMR spectrum (126 MHz, DMSO-d_6) of **2.9**.

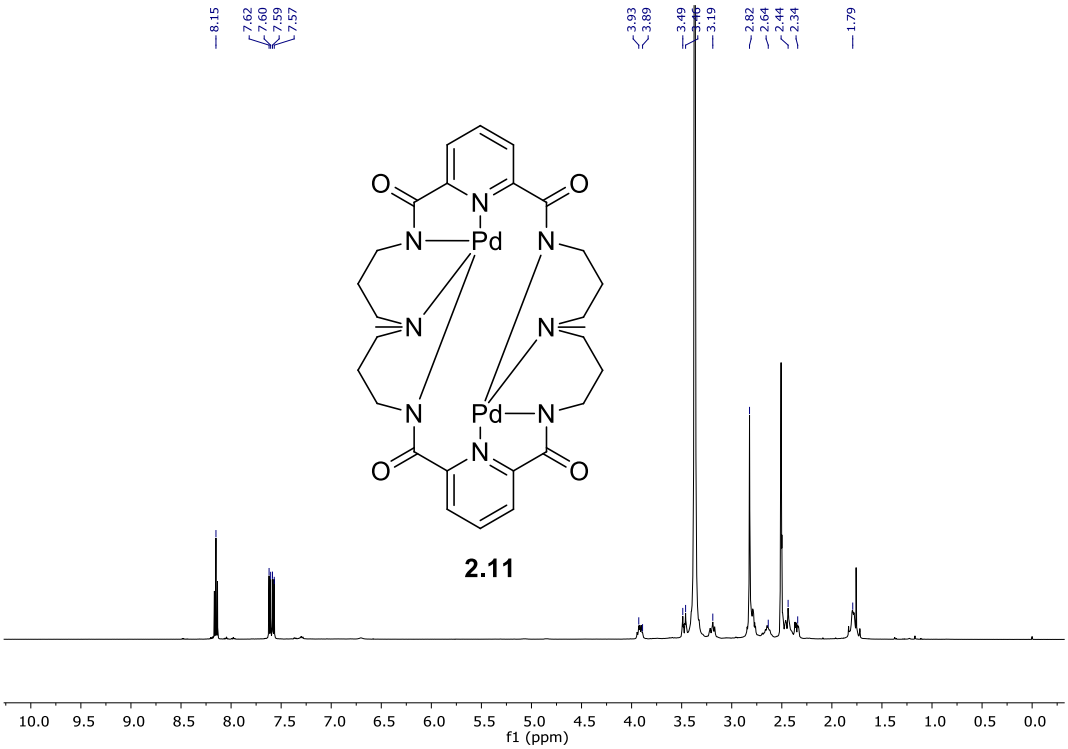

Figure A.2.19. ^{1}H NMR spectrum (500 MHz, DMSO-d_6) of **2.11**.

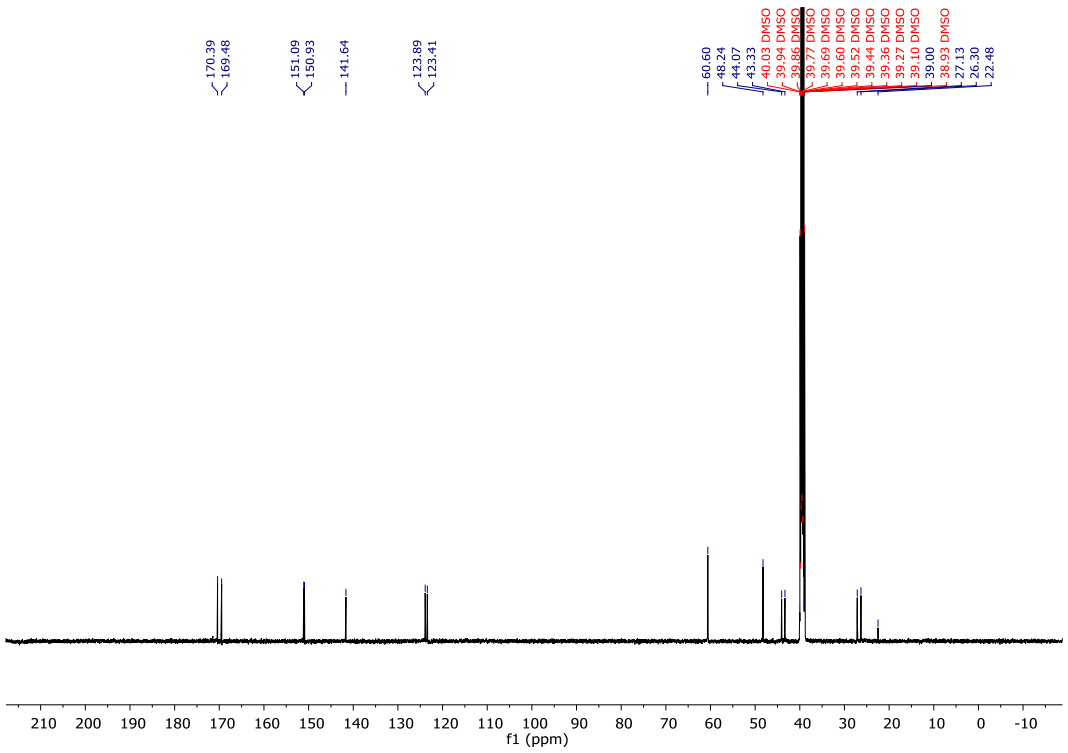

Figure A.2.20. ^{13}C NMR spectrum (126 MHz, DMSO-d_6) of **2.11**.

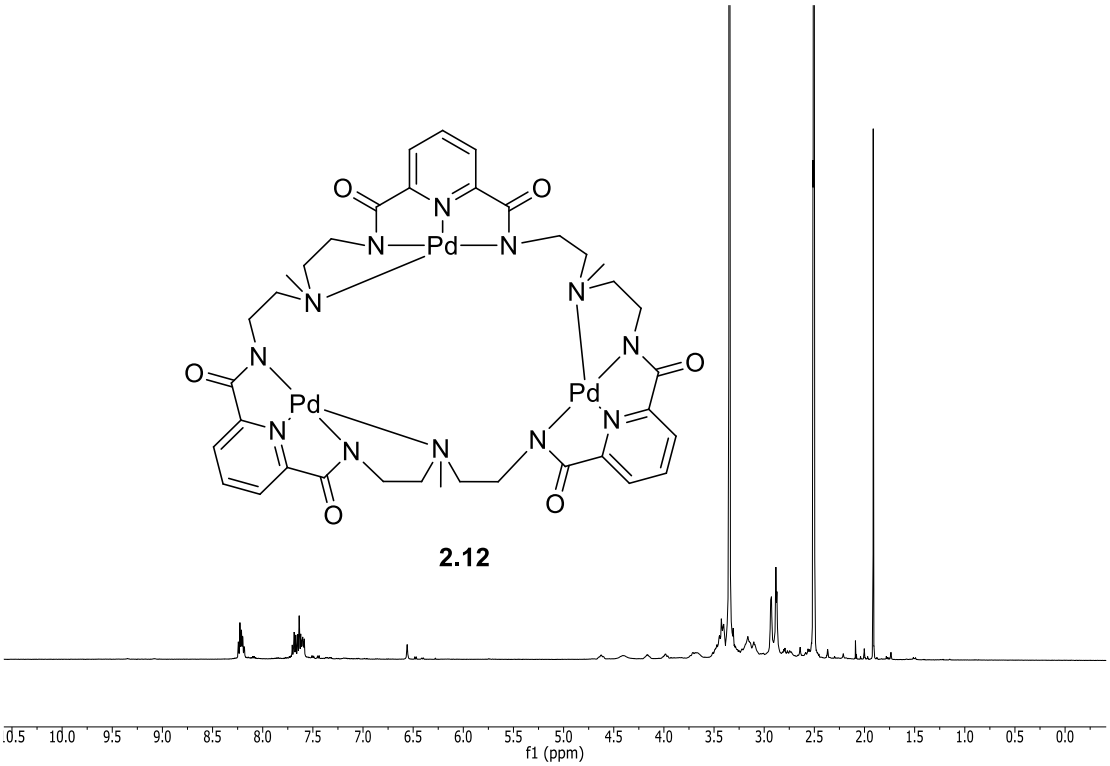

Figure A.2.21. ^{1}H NMR spectrum (500 MHz, DMSO-d_6) of **2.12**.

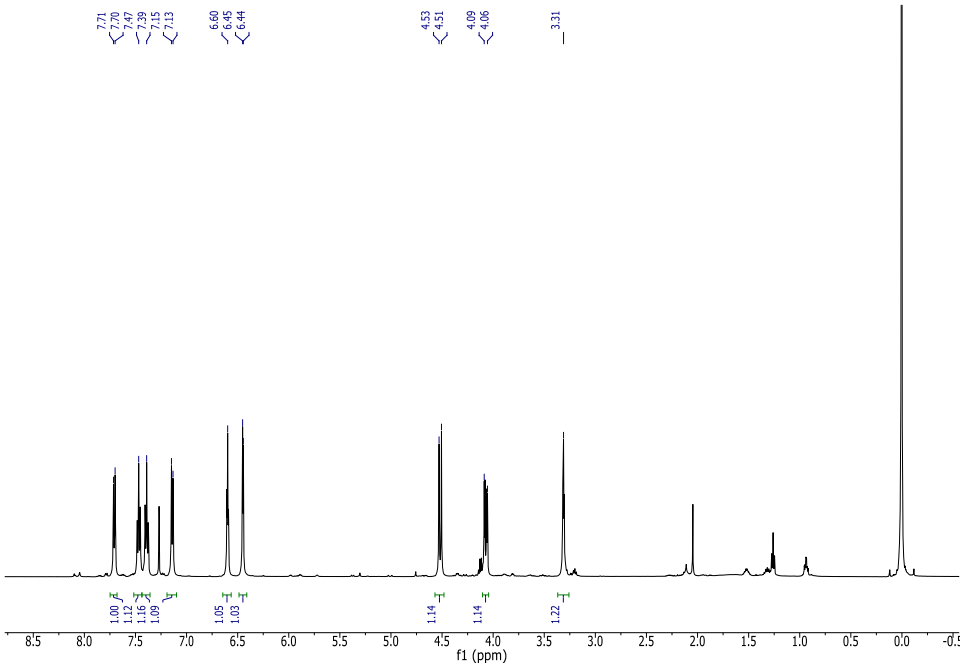

Figure A.2.22. ^{1}H NMR spectrum (500 MHz, $CDCl_3$) of **2.14**.

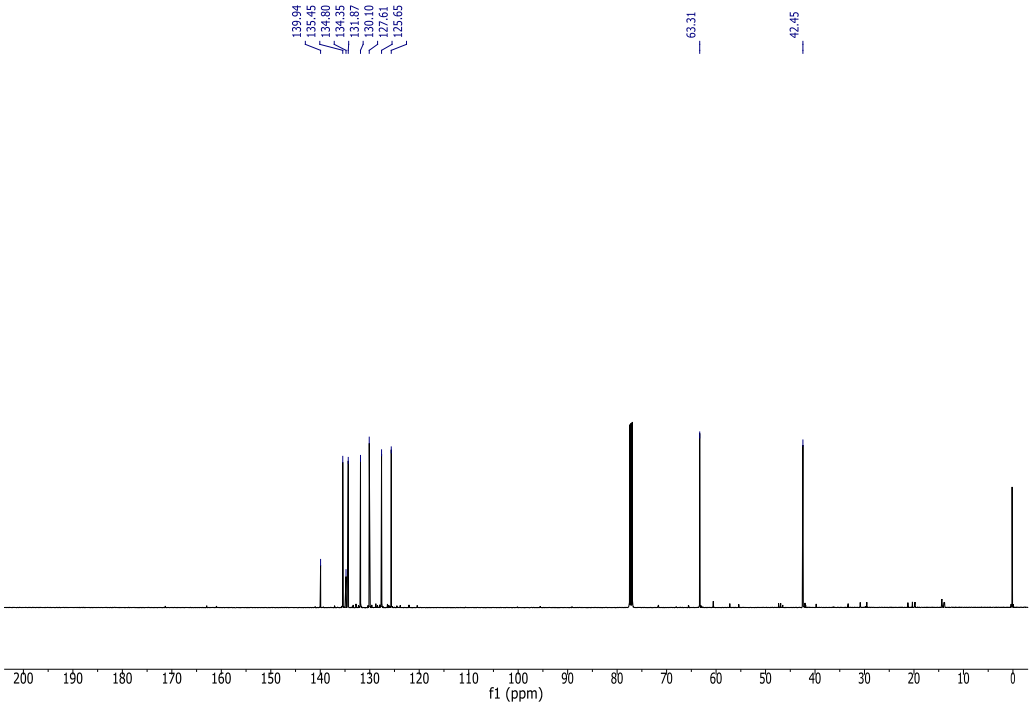

Figure A.2.23. ^{13}C NMR spectrum (126 MHz, $CDCl_3$) of **2.14**.

A.2.3 *Supplementary Information for XRD Studies*

Table A.2.1. Crystallographic data collection and structure refinement for acyclic Pd(II) complexes.

	2.6a	**2.7**	**2.8**
Formula	$C_{13}H_{16}N_4O_2Pd$	$C_{25}H_{32}N_8O_5Pd_2$	$C_{23}H_{31}N_7O_5Pd$
Formula weight	366.70	737.39	591.95
Crystal size (mm^3)	0.10×0.08×0.06	0.05×0.05×0.01	0.05×0.02×0.01
Crystal system	Monoclinic	Monoclinic	Monoclinic
Space group	$P2_1/n$	$P2_1/n$	$P2_1$
a (Å)	10.0785 (3)	9.9325(2)	10.3291(13)
b (Å)	9.5776 (3)	14.5669(3)	16.4812(19)
c (Å)	15.0689 (5)	18.8776(3)	14.8115(18)
α (°)	90	90	90
β (°)	96.622 (1)	97.0880(10)	102.801(10)
γ (°)	90	90	90
V ($Å^3$)	1444.86 (8)	2710.45(9)	2458.5(8)
Z	4	4	4
ρ_{calcd} ($g\ cm^{-3}$)	1.686	1.807	1.599
λ (Å)	1.54178	1.54178	1.54178
T (K)	100(2)	100(2)	100(2)
F(000)	736	1480	1216
μ (mm^{-1})	10.431	11.153	6.510
Abs corr	Multi-scan	Multi-scan	Multi-scan
Max, min trans	1.000, 0.771	1.000, 0.779	1.000, 0.761
θ range (°)	5.02-69.77	3.84-69.37	3.06-69.71
Reflns collected	12677	23541	16832
Indep reflns	2657	4938	6703
R(int)	0.0161	0.0418	0.0609
Data/restr/param	2657 / 0 / 246	4938 / 0 / 384	6703 / 1 / 656
[a] R_1; wR_2	0.0171; 0.0492	0.026; 0.065	0.0707;0.1797
GOF (F^2)	0.990	1.046	1.099
Largest diff. peak and hole (e $Å^{-3}$)	0.35, -0.67	0.088, -1.05	1.770, -1.385

Table A.2.2. Crystallographic data collection and structure refinement for macrocyclic Pd(II) complex **2.11**.

	2.11
Formula	$C_{28}H_{48}N_8O_{11}Pd_2$
Formula weight	885.54
Crystal size (mm^3)	(0.03×0.02×0.01)
Crystal system	Monoclinic
Space group	*C*2/*c*
a (Å)	27.4773(10)
b (Å)	8.1586(3)
c (Å)	14.8972(5)
α (°)	90
β (°)	98.820(3)
γ (°)	90
V ($Å^3$)	3300.1(2)
Z	4
ρ_{calcd} (g cm^{-3})	1.782
λ (Å)	1.54178
T (K)	100(2)
F(000)	1808
μ (mm^{-1})	9.415
Abs corr	Multi-scan
Max, min trans	1.000, 0.845
θ range (°)	3.26-69.78
Reflns collected	13619
Indep reflns	2989
R(int)	0.0493
Data/restr/param	2989 / 38 / 272
[a] R_1; wR_2	0.0598; 0.1384
GOF (F^2)	1.154
Largest diff. peak and hole (e $Å^{-3}$)	3.69, -0.88

Table A.2.3. Coordinated ligand distances (Å) in acyclic Pd(II) complex **2.6a**.

	2.6a
Pd–N(1)	1.920(15)
Pd–N(2)	2.0298(15)
Pd–N(3)	2.0278(15)
Pd–N(1s)	2.011(15)

Table A.2.4. Selected distances (Å) in acyclic Pd(II) complex **2.7**.

	2.7
Pd–N(2)	1.923(2)
Pd–N(3)	1.962(2)
Pd–N(1)	2.074(2)
Pd–N(4)	2.100(2)
Pd(2)–N(6)	1.924(2)
Pd(2)–N(7)	2.015(2)
Pd(2)–N(5)	2.036(2)
Pd(2)–N(1s)	2.012(2)
Pd-Pd(2)	3.360(2)
N(2)-N(6)	4.195(3)

Table A.2.5. Selected distances (Å) in acyclic Pd(II) complex **2.8**.

	2.8
Pd–N(7)	1.938(14)
Pd–N(13)	1.914(12)
Pd–N(4)	1.993(17)
Pd–N(16)	2.134(15)
N(7)-N(22)	3.361(2)

Table A.2.6. Coordinated ligand distances (Å) in macrocyclic Pd(II) complex **2.9**.

	2.9
Pd–N(2)	1.927(2)
Pd–N(3)	2.008(2)
Pd–N(1)	2.013(2)
Pd–N(4)	2.054(2)

Table A.2.7. Selected distances (Å) in macrocyclic Pd(II) complex **2.10**.

	2.10
Pd–N(2)	1.937(7)
Pd–N(3)	1.974(8)
Pd–N(1)	2.052(8)
Pd–N(4)	2.120(10)
Pd–Pd	5.579(2)

Table A.2.8. Selected distances (Å) in macrocyclic Pd(II) complex **2.11**.

	2.11
Pd–N(1)	2.059(6)
Pd–N(2)	2.018(6)
Pd–N(3)	2.022(5)
Pd–N(4)	2.085(16)
Pd–Pd	5.134(7)

Table A.2.9. Selected distances (Å) in macrocyclic Pd(II) complex **2.12**.

	2.12
Pd(1)–N(1)	2.107(8)
Pd(1)–N(2)	1.955(8)
Pd(1)–N(3)	1.933(6)
Pd(1)–N(4)	2.072(6)
Pd(2)–N(7)	1.936(7)
Pd(2)–N(2)	1.951(8)
Pd(2)–N(8)	2.042(8)
Pd(2)–N(5)	2.103(8)
Pd(3)–N(9)	2.087(8)
Pd(3)–N(10)	1.970(1)
Pd(3)–N(11)	1.925(8)
Pd(3)–N(12)	2.084(8)
Pd(1)–Pd(2)	6.422(9)
Pd(1)–Pd(3)	6.548(9)
Pd(2)–Pd(3)	6.356(9)

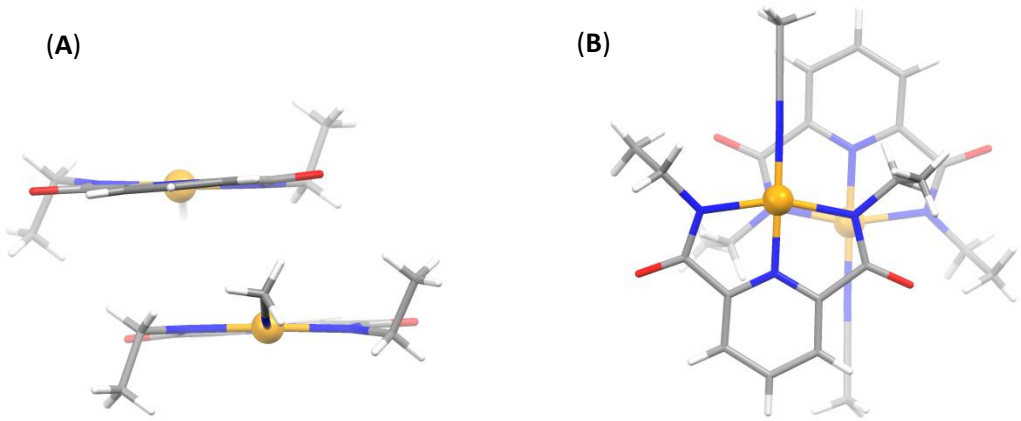

Figure A.2.24. (**A**) Side view and (**B**) top view of the dimer pair of **2.6a** (orange ball = palladium).

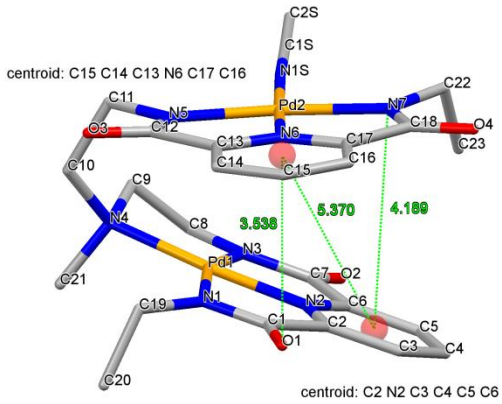

Figure A.2.25. Perspective view of **2.7**, shown approximately along the Pd2-N6 axis (red ball = pyridine centroid).

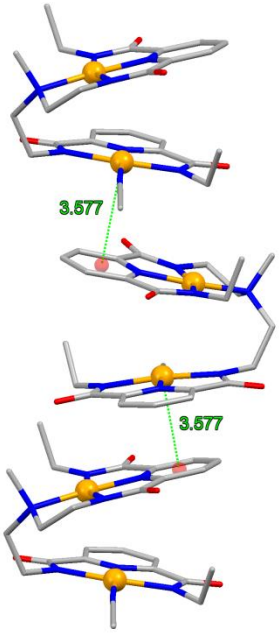

Figure A.2.26. Side view of a portion of the crystal lattice for **2.7** (red ball = N2 pyridine centroid; orange ball = palladium). Intermolecular pyridine centroid–Pd1 distance is 3.577 Å; corresponding interplane angle is 4.27°.

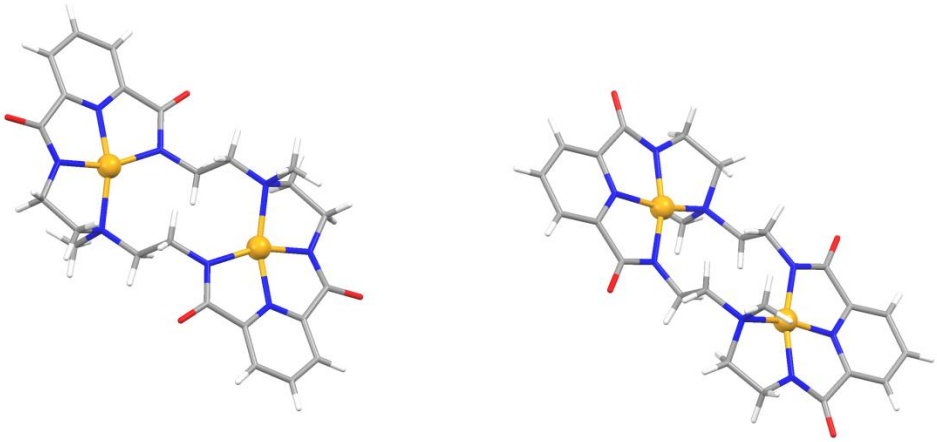

Figure A.2.27. Perspective view of dimer pair of **2.10**.

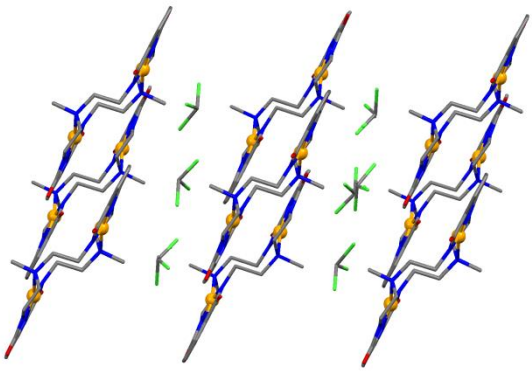

Figure A.2.28. Perspective view of the stacking in complex **2.10.**

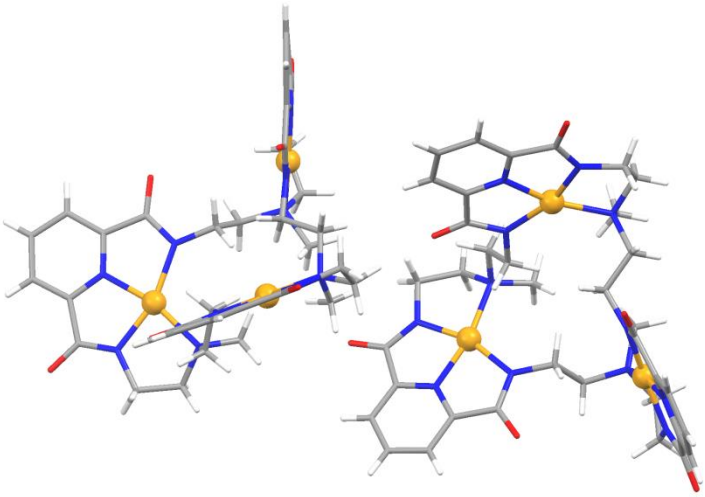

Figure A.2.29. Perspective view of dimer pair of **2.12**.

A.2.4 *Mass Spectra*

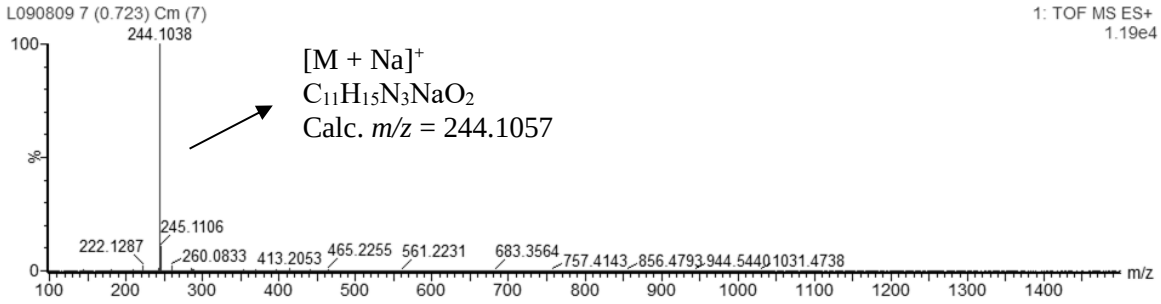

Figure 2.30. HRMS (ESI$^+$) of ligand **2.1**.

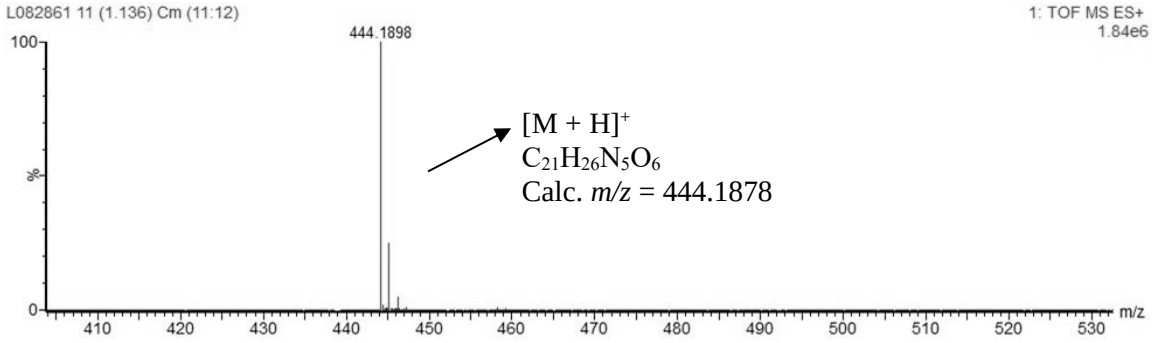

Figure 2.31. HRMS (ESI$^+$) of intermediate **C**.

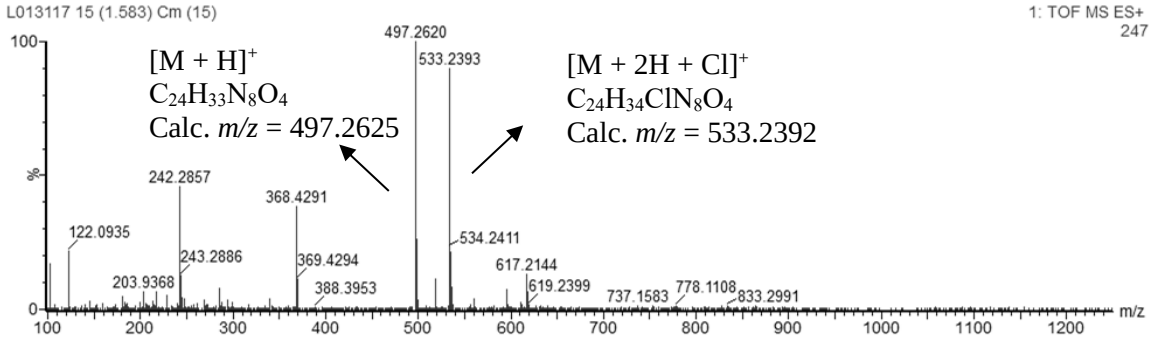

Figure 2.32. HRMS (ESI$^+$) of ligand **2.3a**.

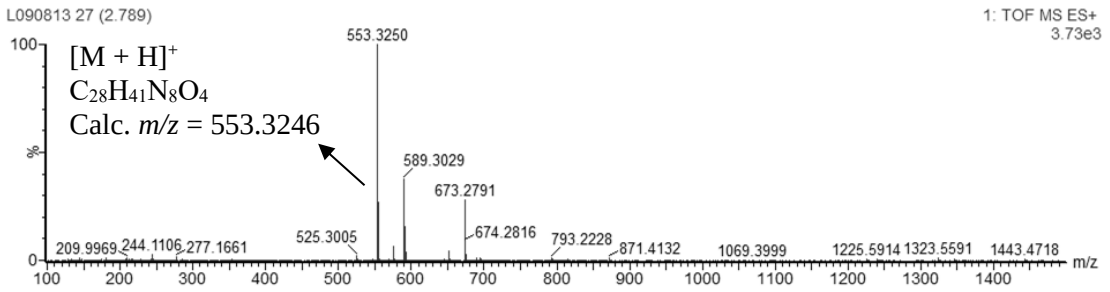

Figure 2.33. HRMS (ESI$^+$) of ligand **2.3b**.

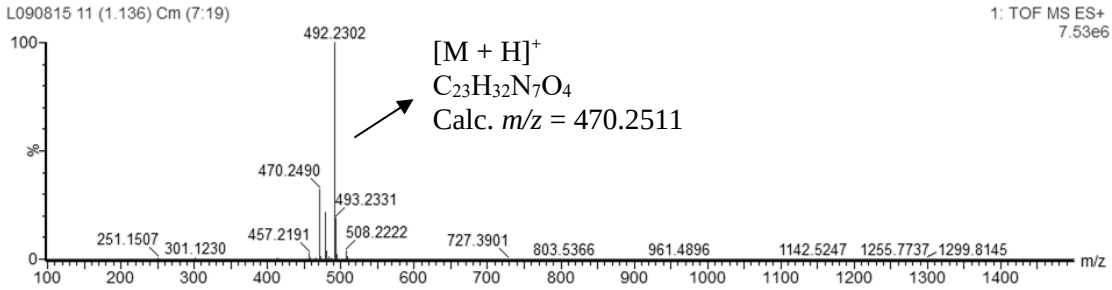

Figure 2.34. HRMS (ESI$^+$) of ligand **2.4**.

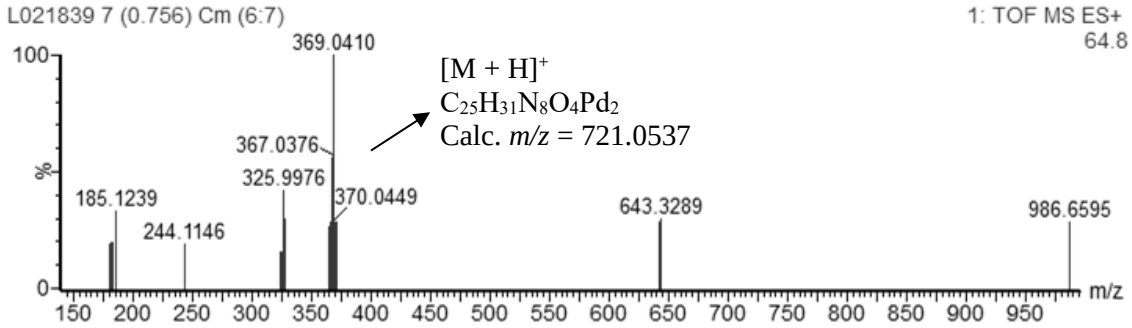

Figure 2.35. HRMS (ESI$^+$) of complex **2.6a**.

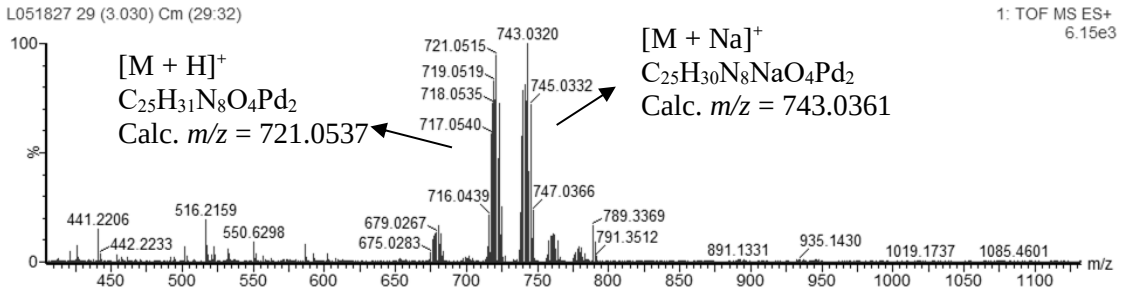

Figure 2.36. HRMS (ESI$^+$) of complex **2.7**.

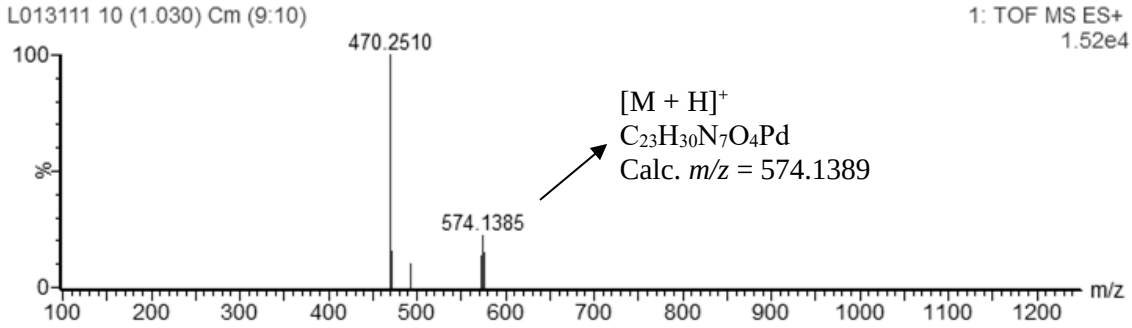

Figure 2.37. HRMS (ESI$^+$) of complex **2.8**.

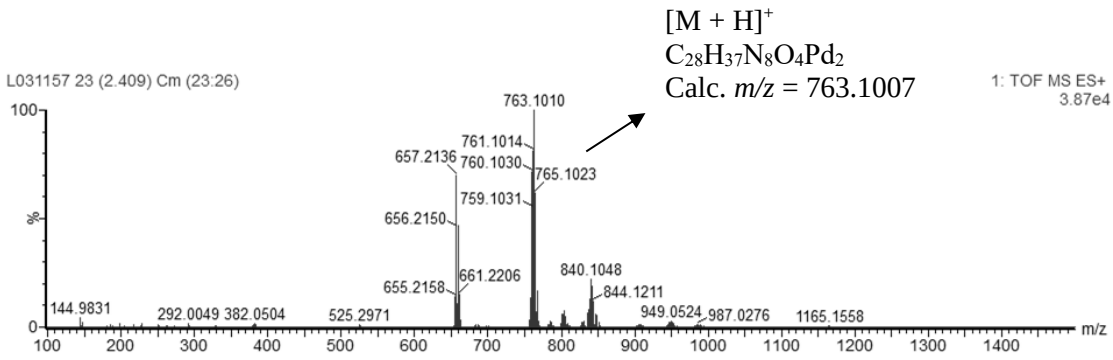

Figure 2.38. HRMS (ESI$^+$) of complex **2.11**.

A.3 *Supporting Information for Chapter 3*

A.3.1 *NMR Spectra of Ligands*

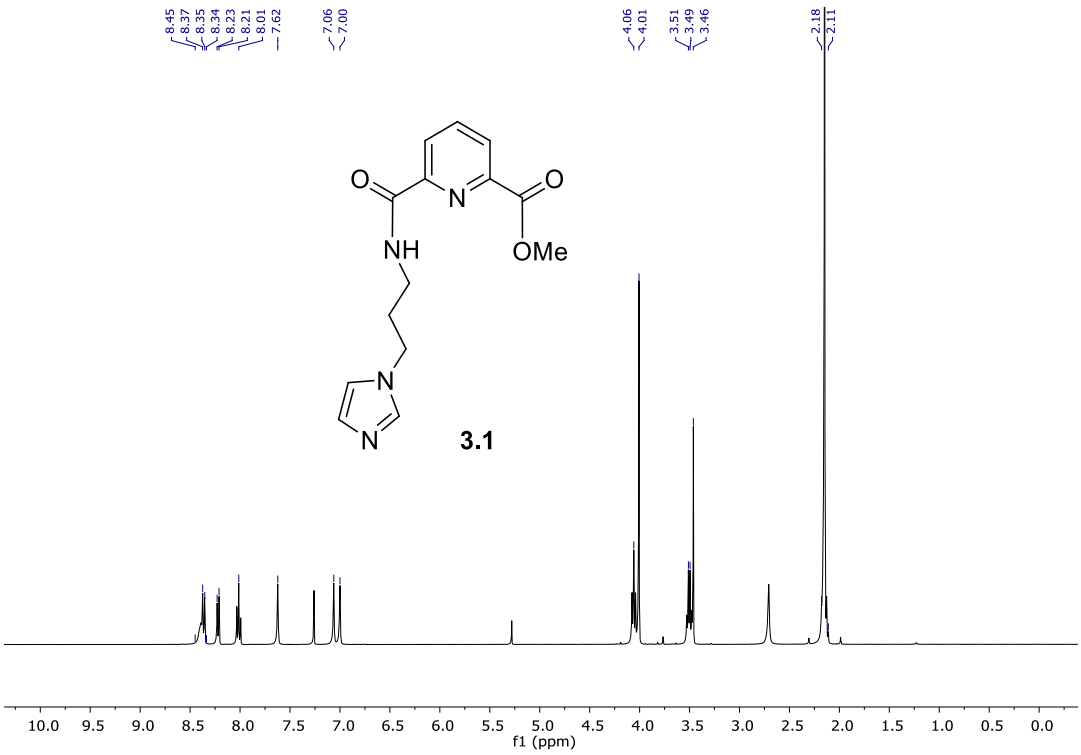

Figure A.3.1. ^{1}H NMR spectrum (500 MHz, $CDCl_3$) of **3.1**.

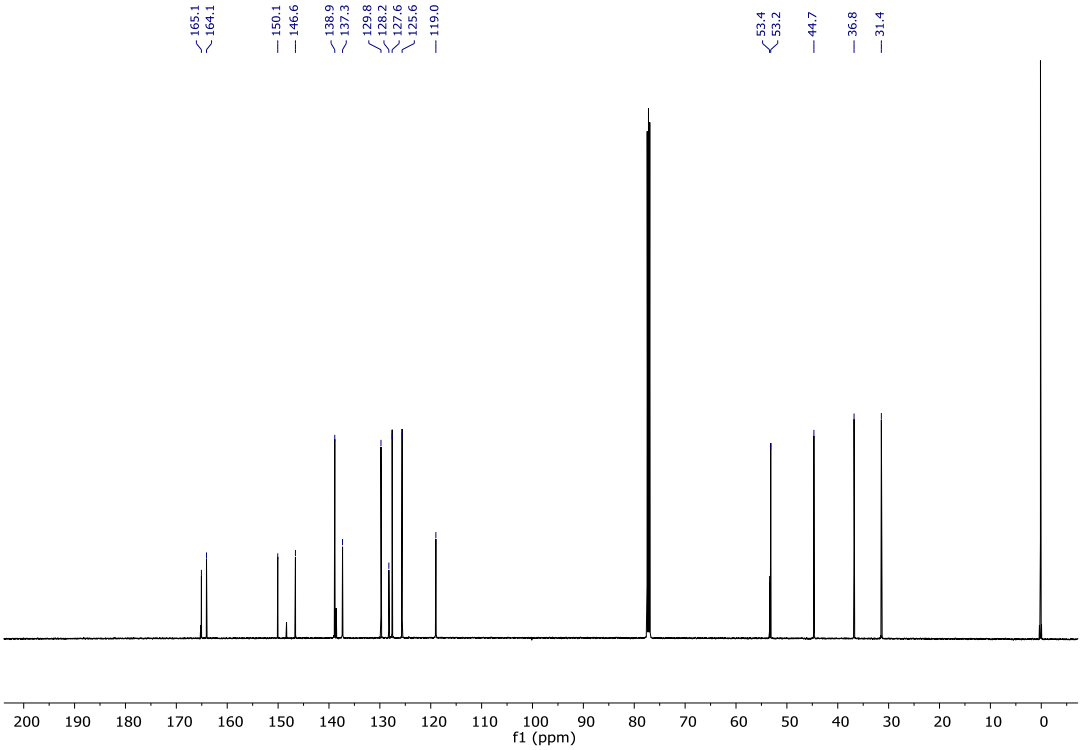

Figure A.3.2. ^{13}C NMR spectrum (126 MHz, $CDCl_3$) of **3.1**.

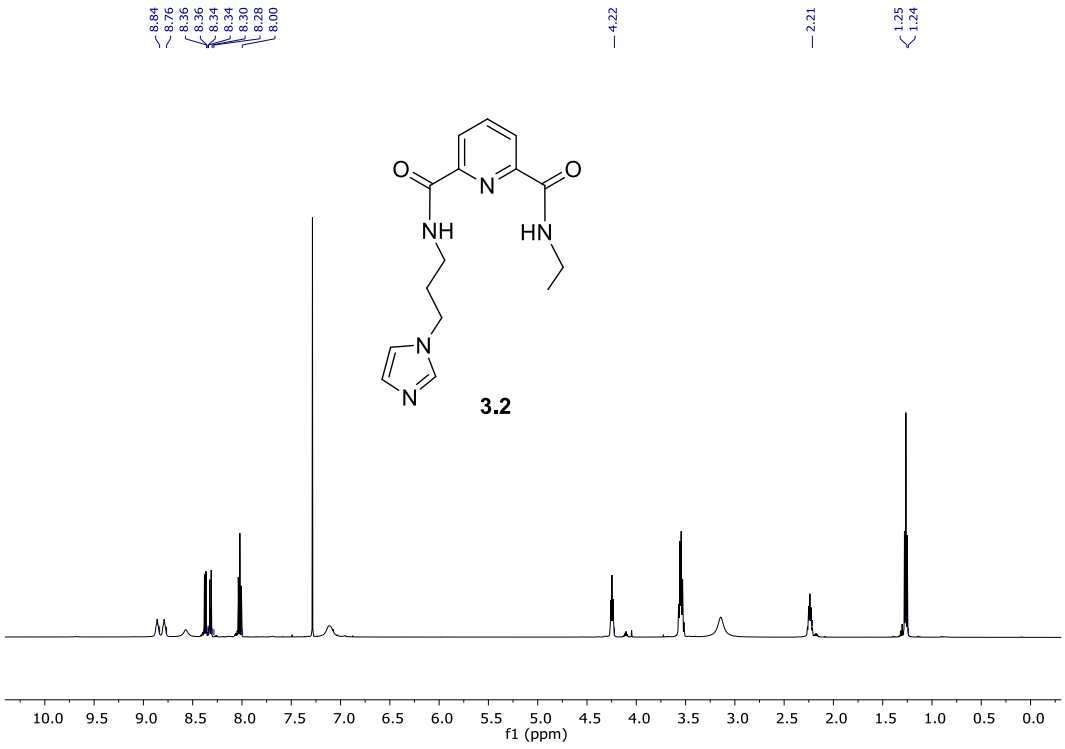

Figure A.3.3. ^{1}H NMR spectrum (500 MHz, $CDCl_3$) of **3.2**.

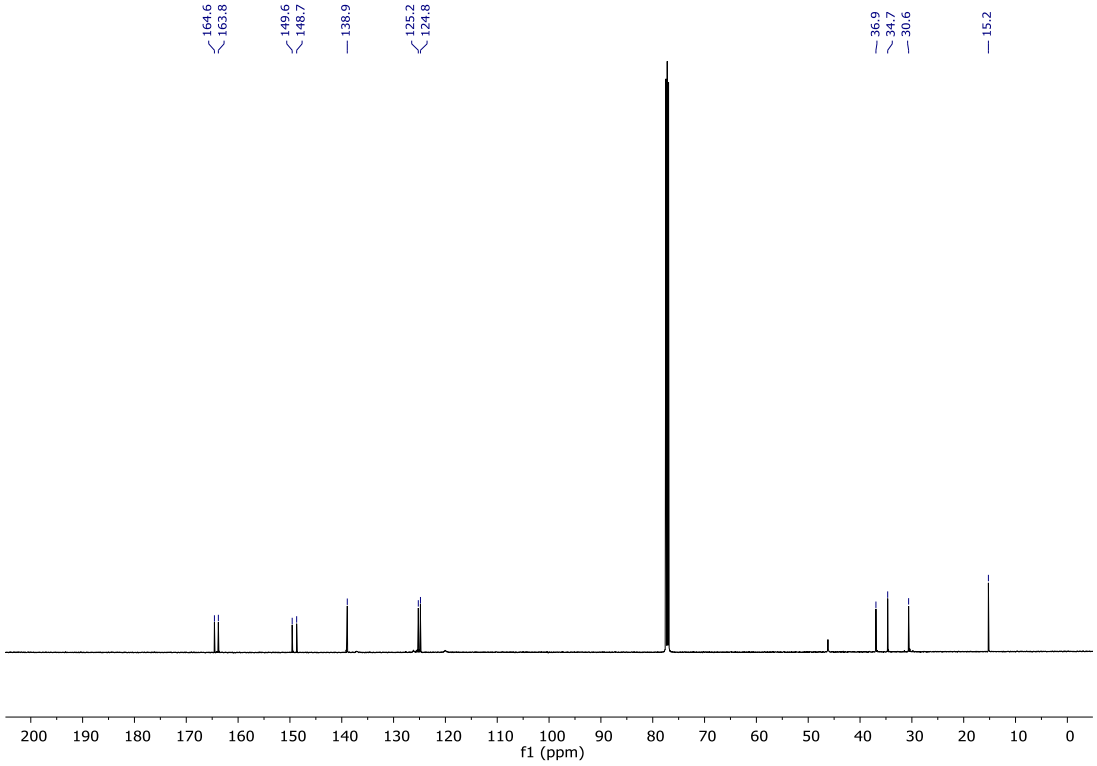

Figure A.3.4. ^{13}C NMR spectrum (126 mHz, $CDCl_3$) of **3.2**.

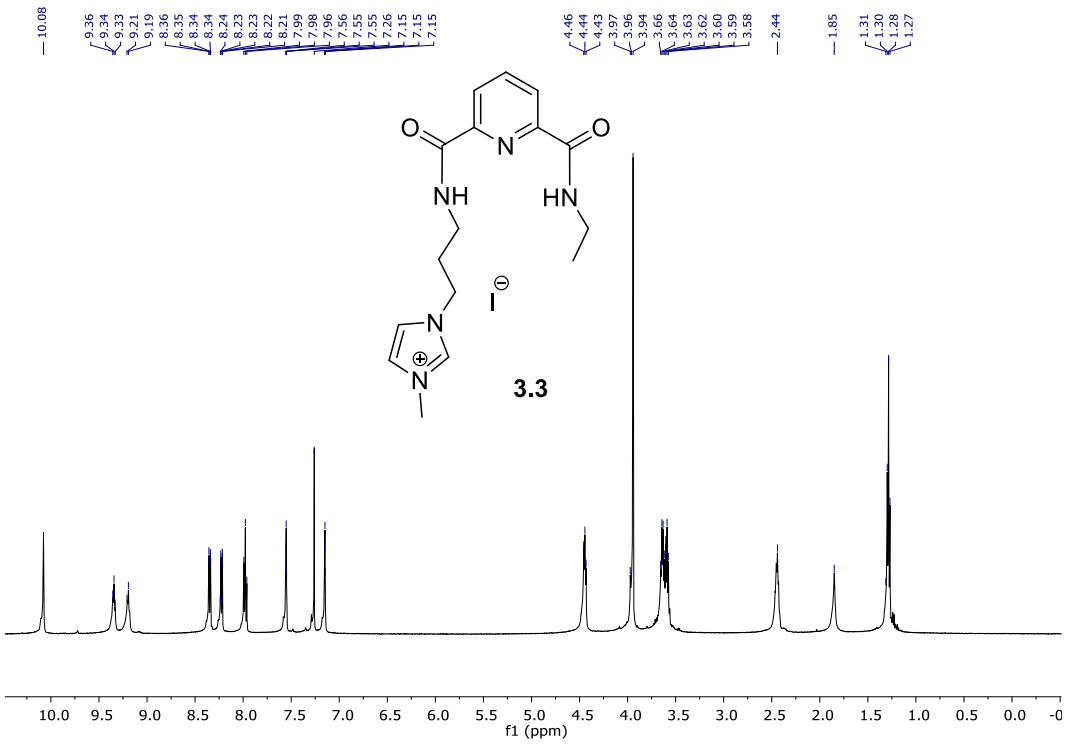

Figure A.3.5. ^{1}H NMR spectrum (500 MHz, $CDCl_3$) of **3.3**.

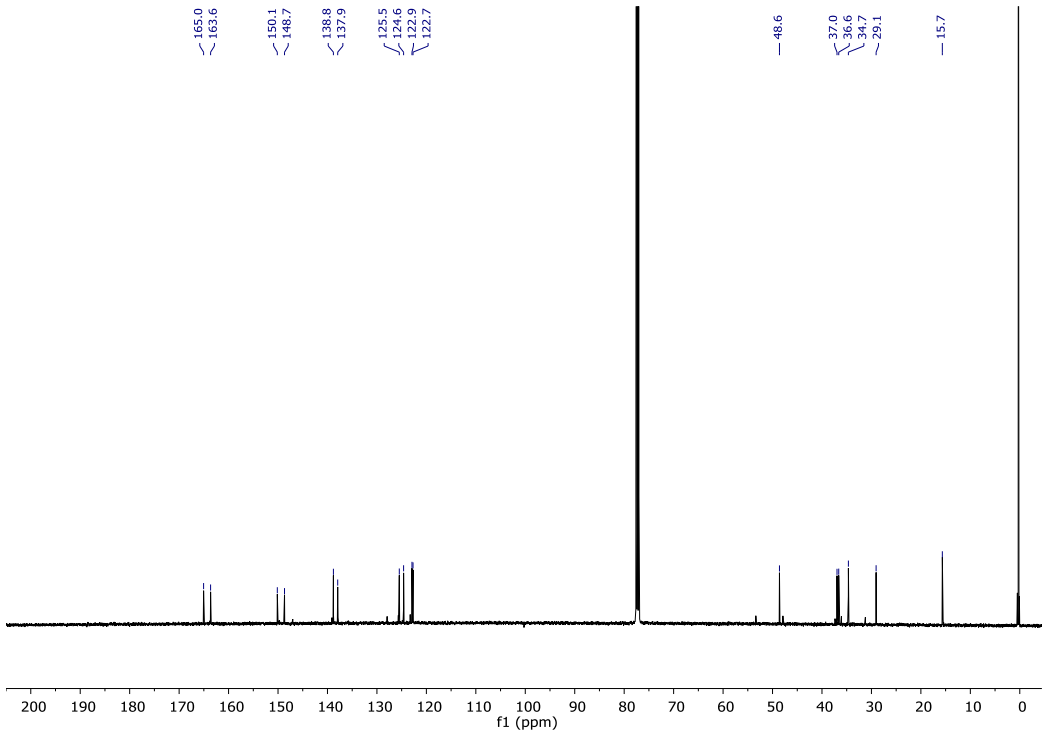

Figure A.3.6. ^{13}C NMR spectrum (126 mHz, $CDCl_3$) of **3.3**.

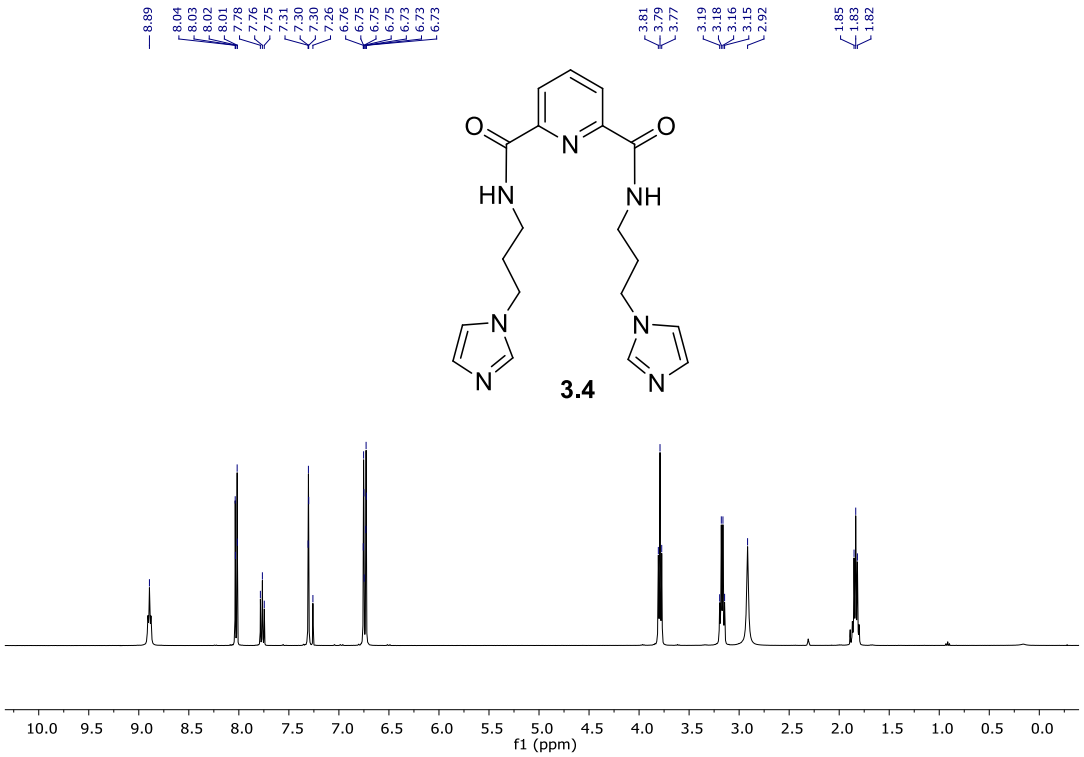

Figure A.3.7. ^{1}H NMR spectrum (500 MHz, $CDCl_3$) of **3.4**.

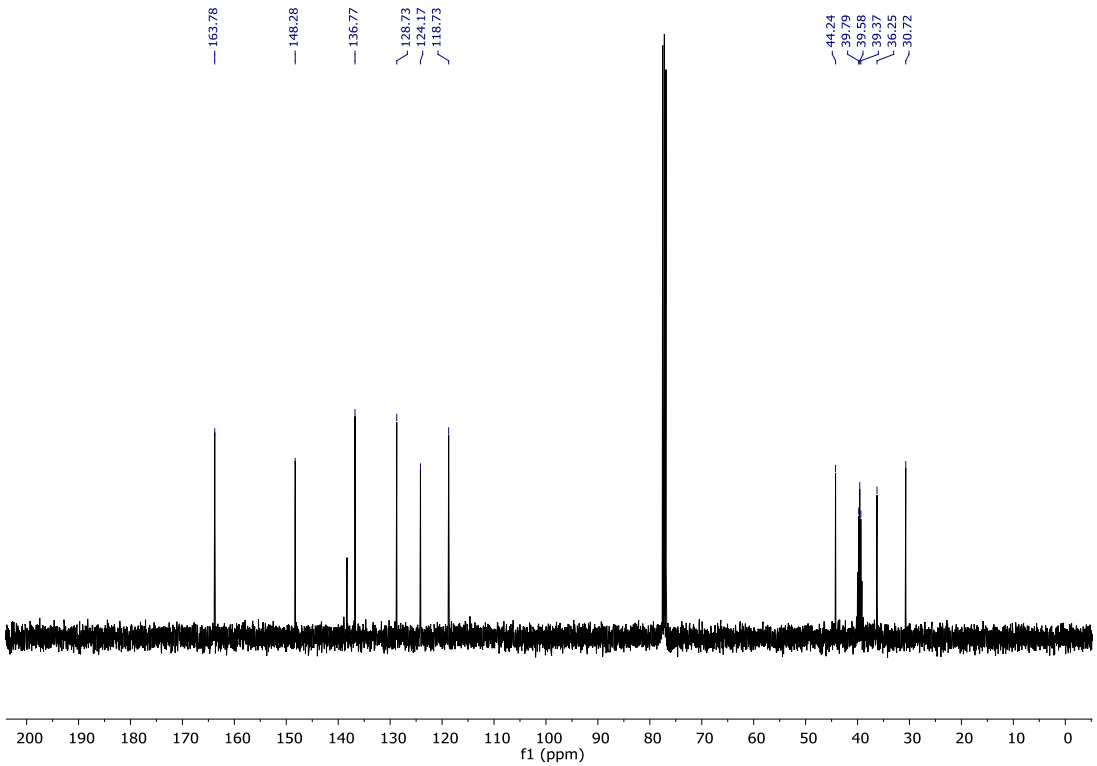

Figure A.3.8. ^{1}H NMR spectrum (126 MHz, $CDCl_3$) of **3.4**.

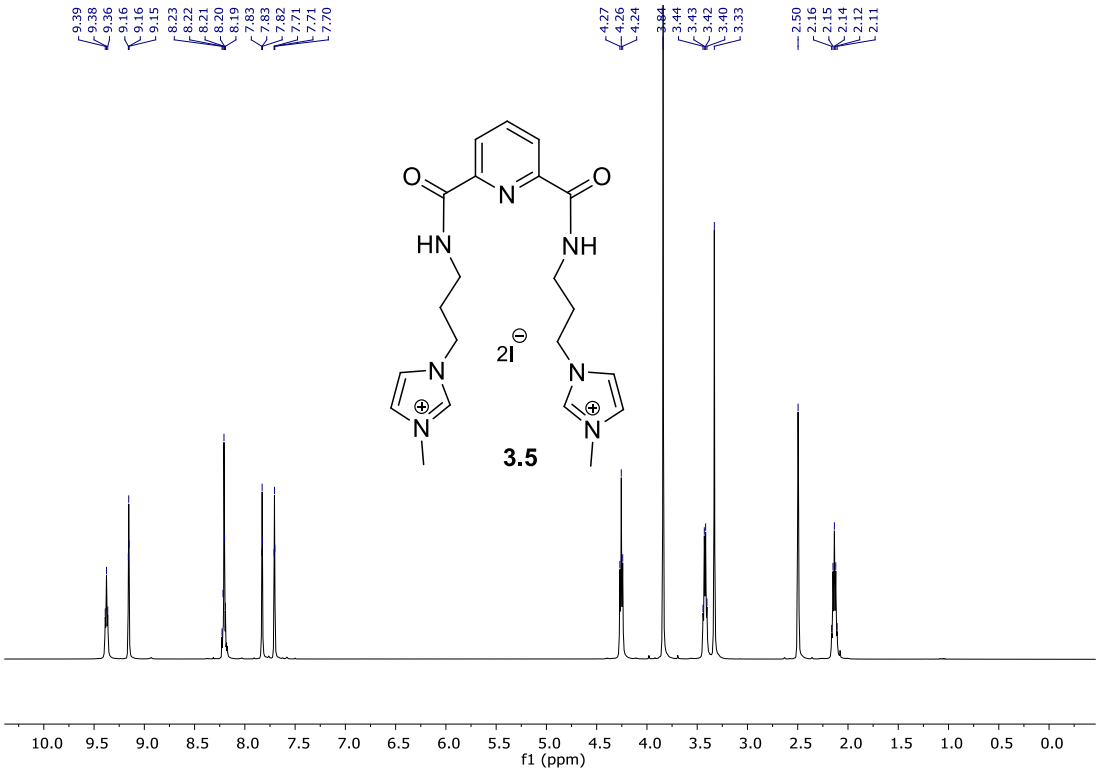

Figure A.3.9. ^{1}H NMR spectrum (500 MHz, DMSO-d_6) of **3.5**.

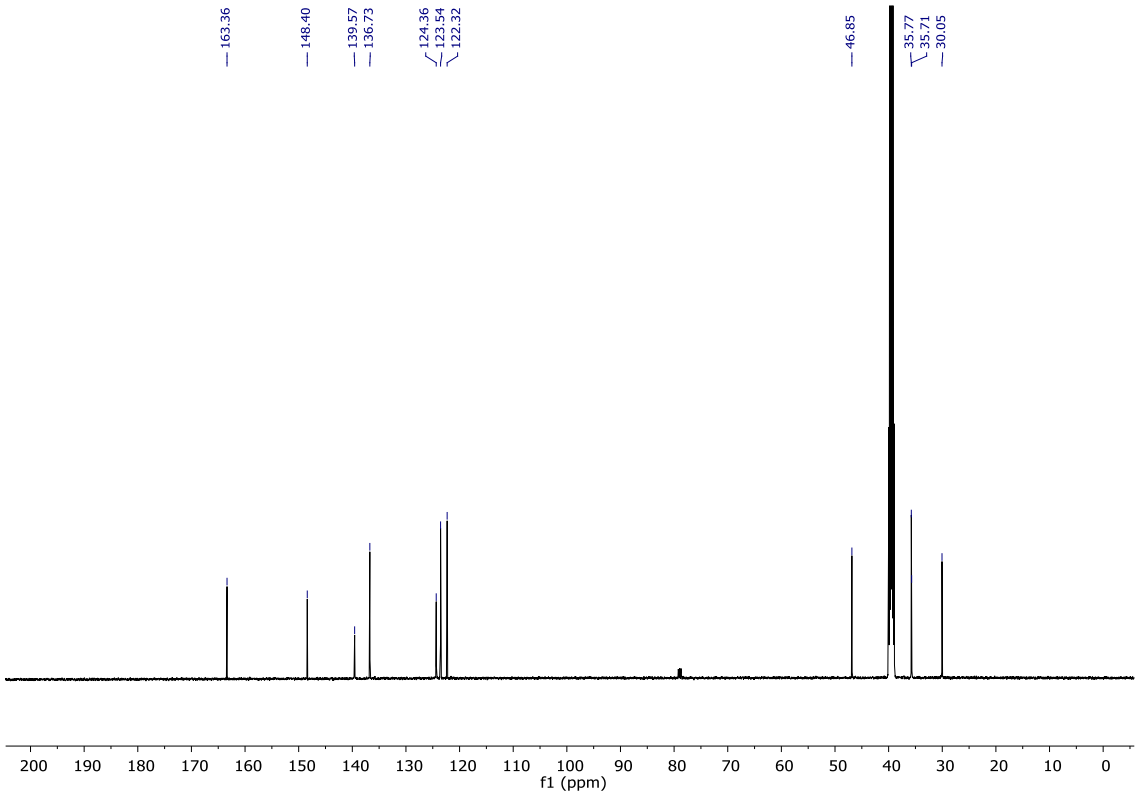

Figure A.3.10. ^{13}C NMR spectrum (126 MHz, DMSO-d_6) of **3.5**.

A.3.2 *NMR Spectra of Metal Complexes*

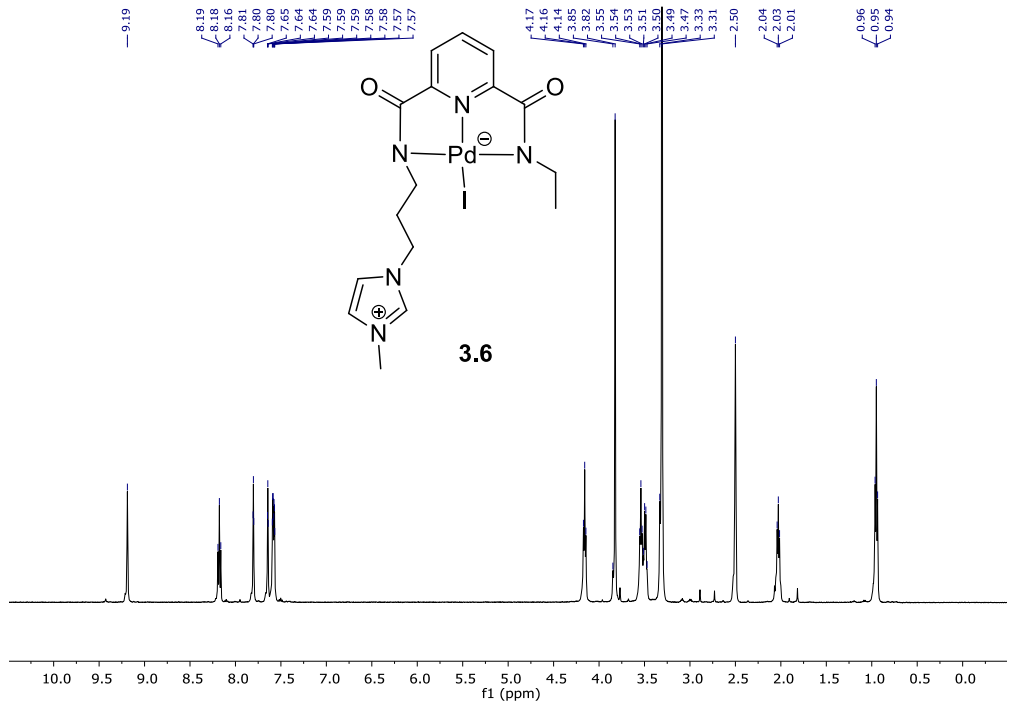

Figure A.3.11. ^{1}H NMR spectrum (500 MHz, DMSO-d_6) of **3.6**.

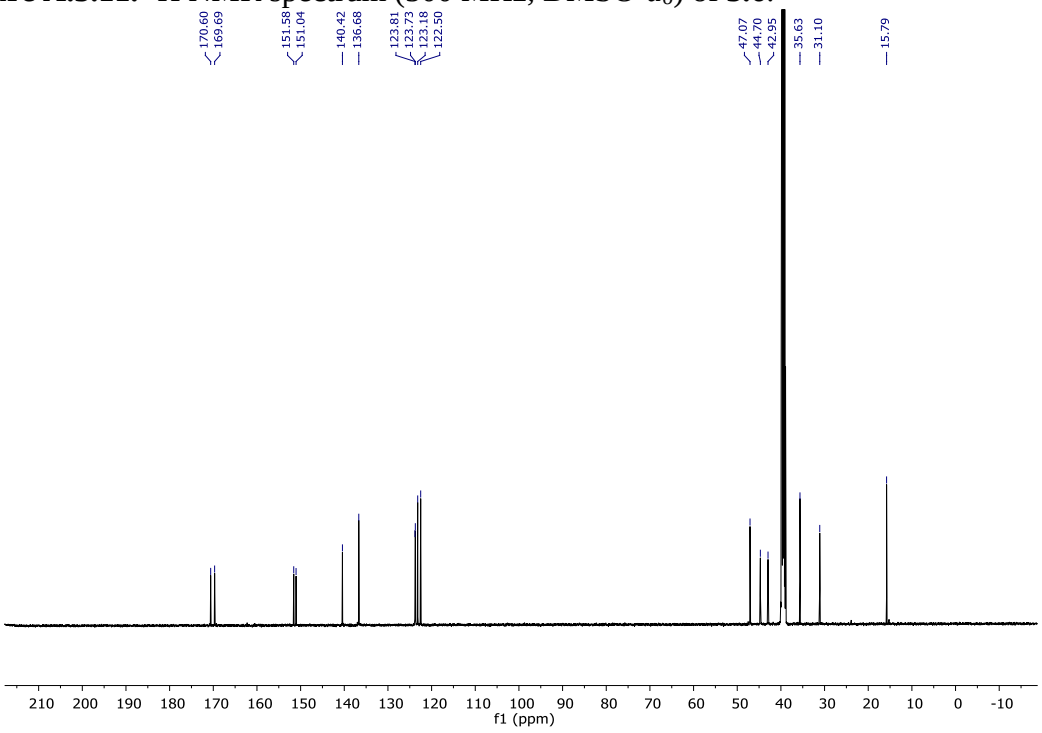

Figure A.3.12. ^{13}C NMR spectrum (126 MHz, DMSO-d_6) of **3.6**.

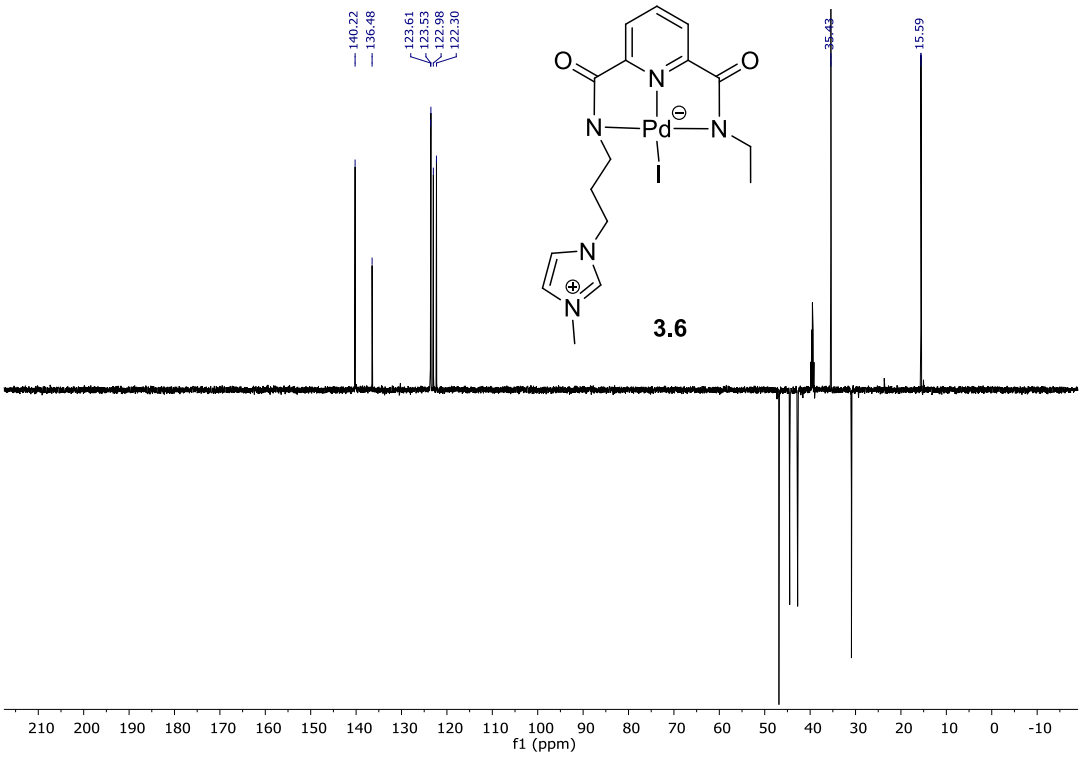

Figure A.3.13. ^{13}C NMR DEPT spectrum (126 MHz, DMSO-d_6) of **3.6**.

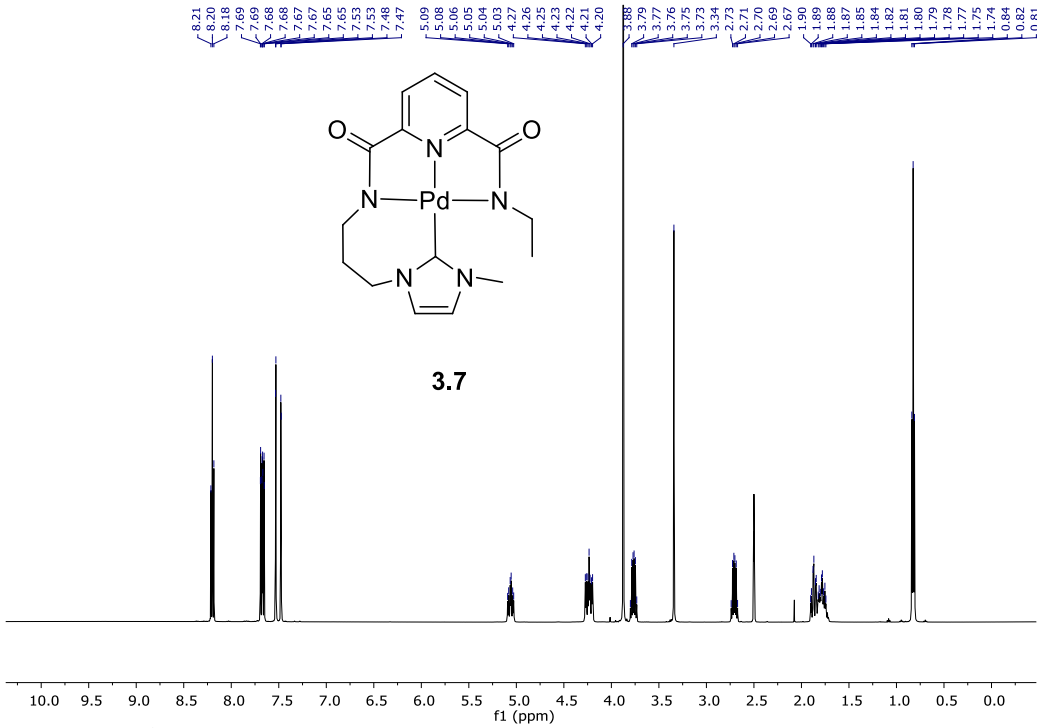

Figure A.3.14. ^{1}H NMR spectrum (500 MHz, DMSO-d_6) of **3.7**.

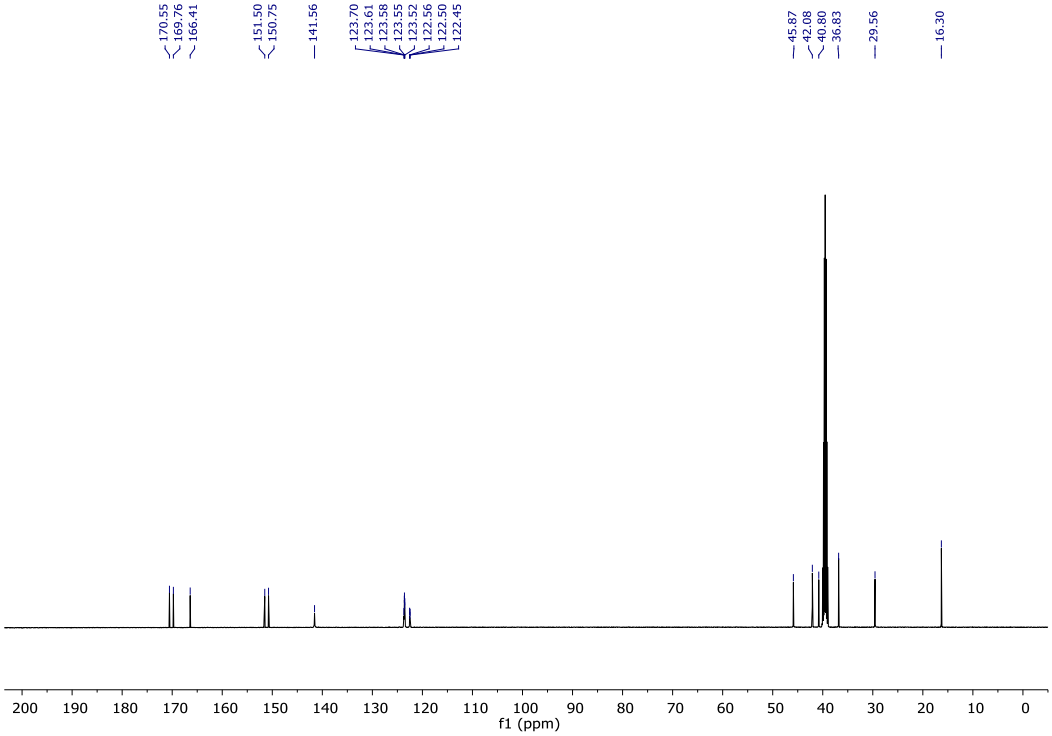

Figure A.3.15. ^{13}C NMR spectrum (126 MHz, DMSO-d_6) of **3.7**.

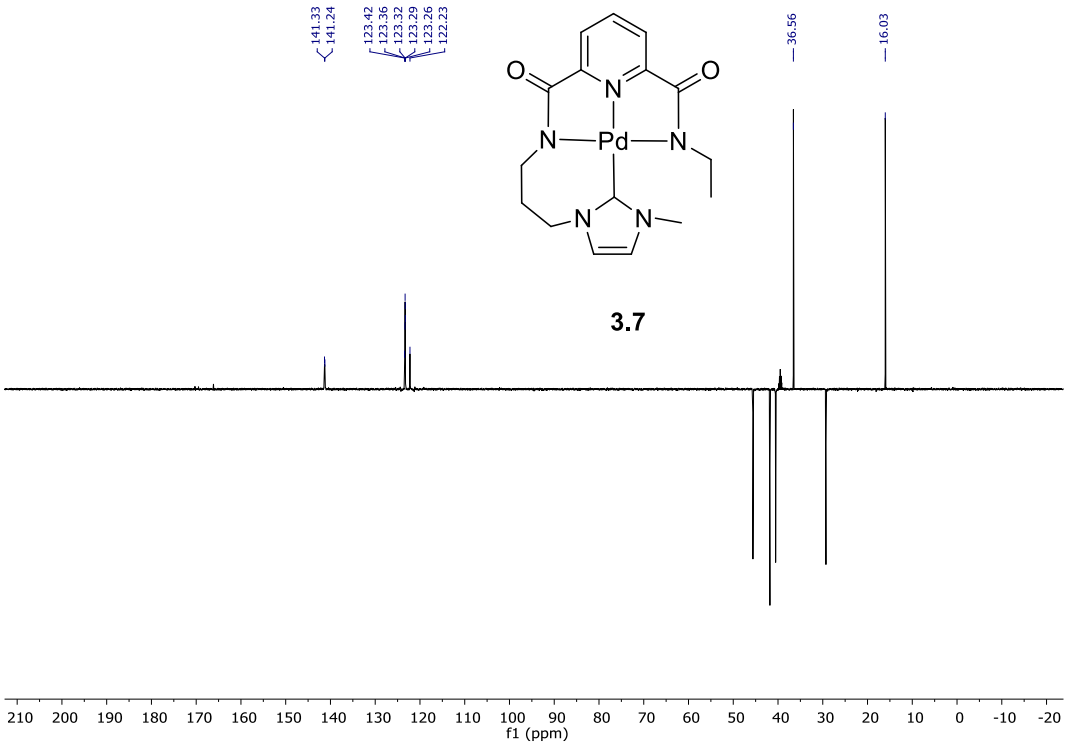

Figure A.3.16. ^{13}C NMR DEPT spectrum (126 MHz, DMSO-d_6) of **3.7**.

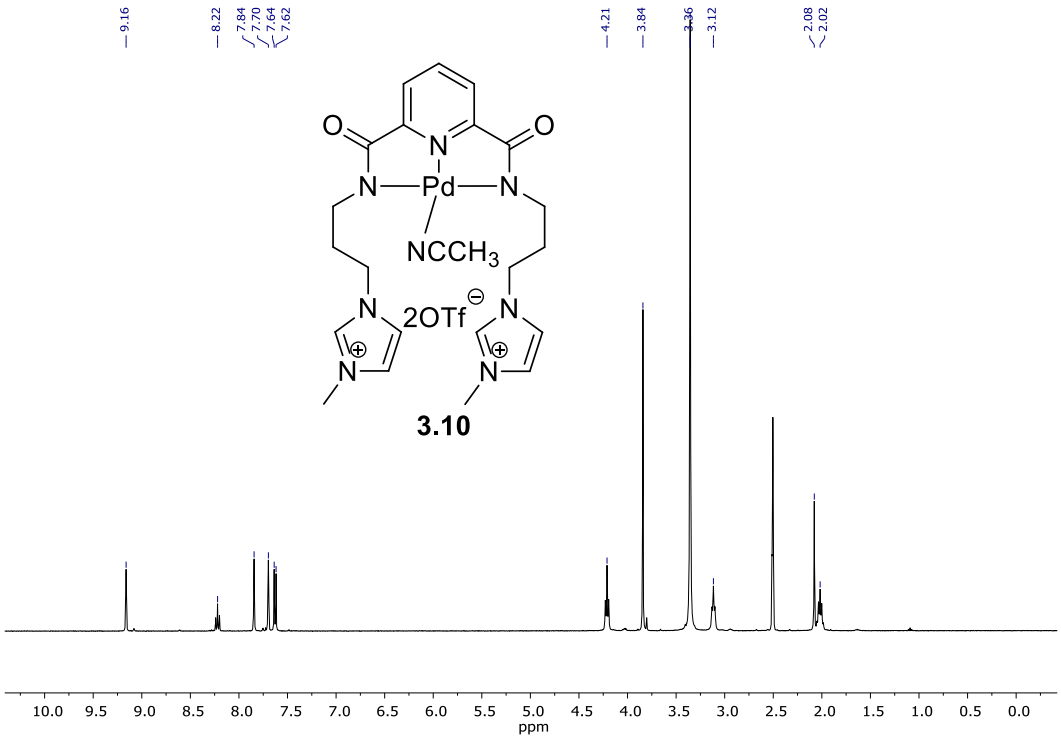

Figure A.3.17. ^{1}H NMR spectrum (500 MHz, DMSO-d_6) of **3.10**.

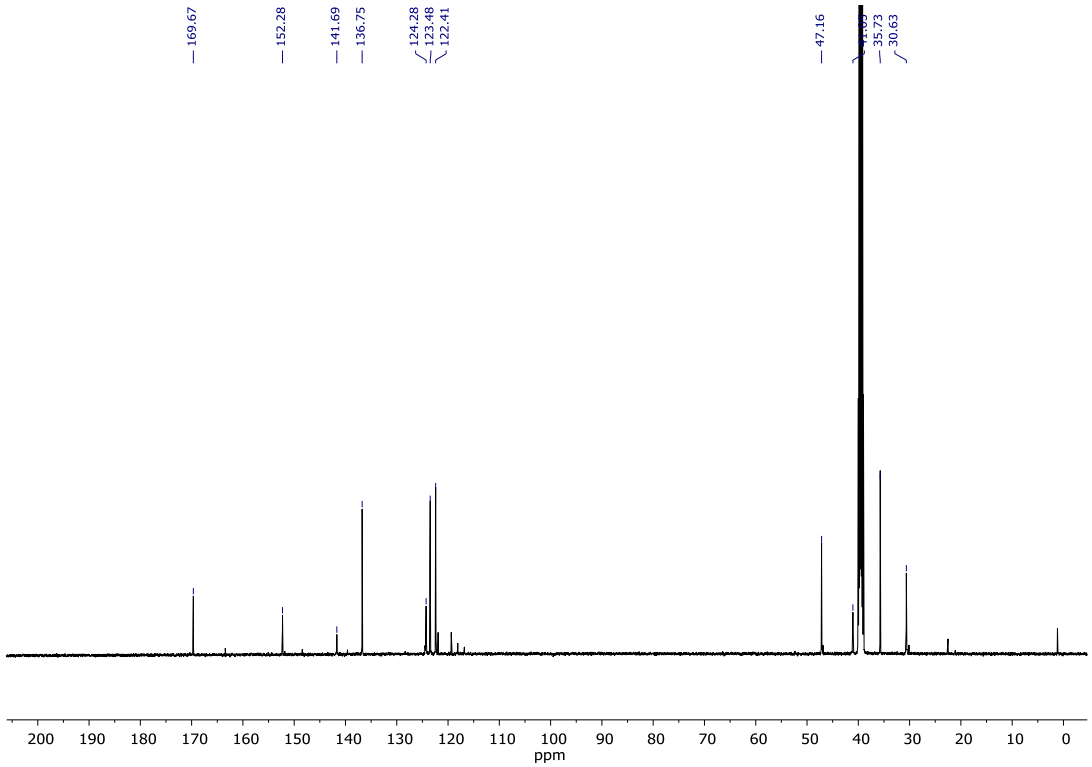

Figure A.3.18. ^{13}C NMR spectrum (126 MHz, DMSO-d_6) of **3.10**.

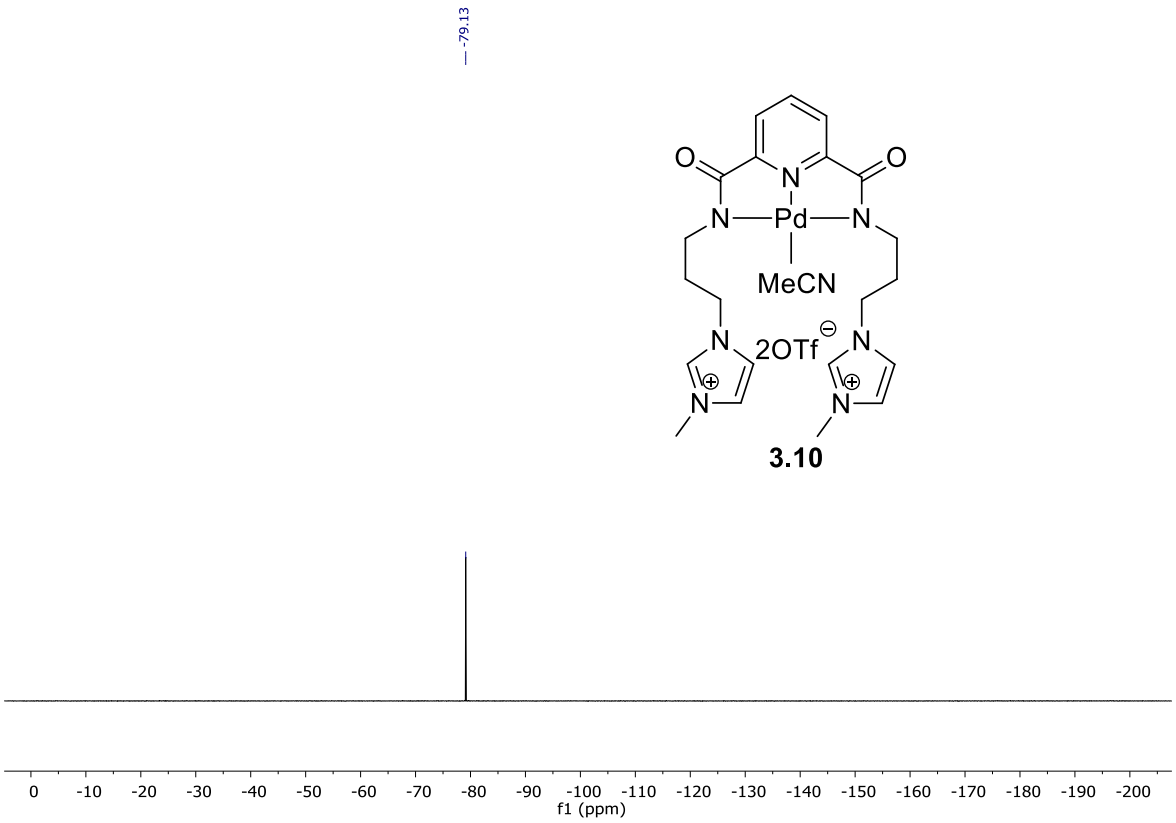

Figure A.3.19. ^{19}F NMR spectrum (471 MHz, DMSO-d_6) of **3.10**.

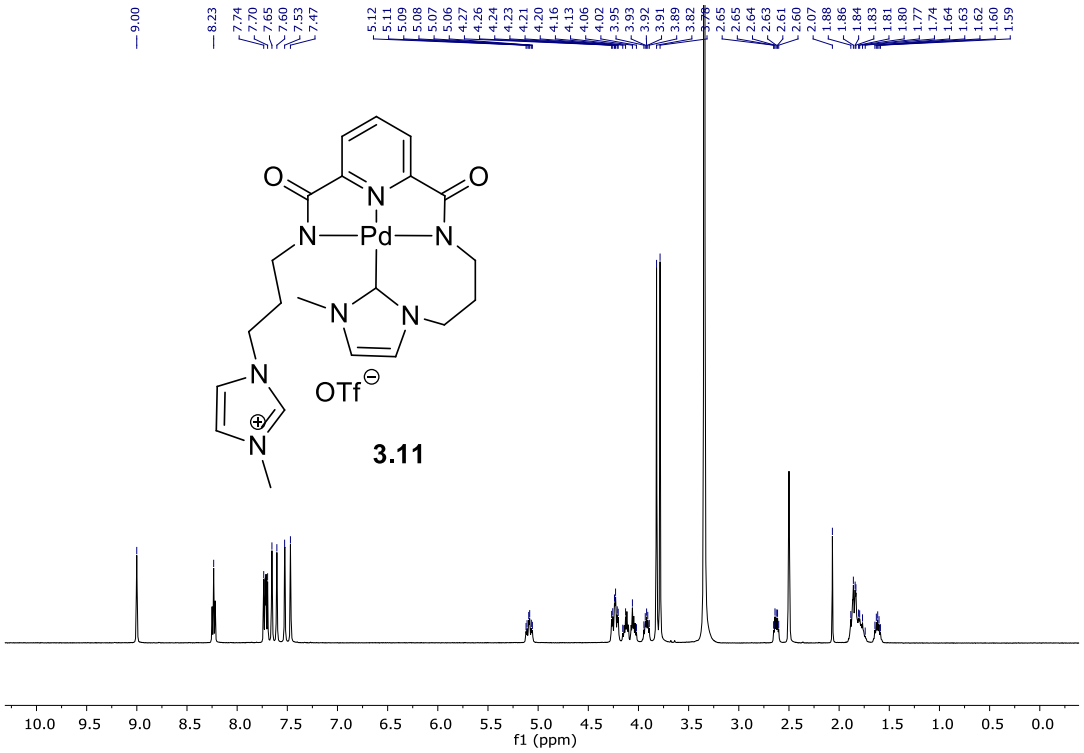

Figure A.3.20. ^{1}H NMR spectrum (500 MHz, DMSO-d_6) of **3.11**.

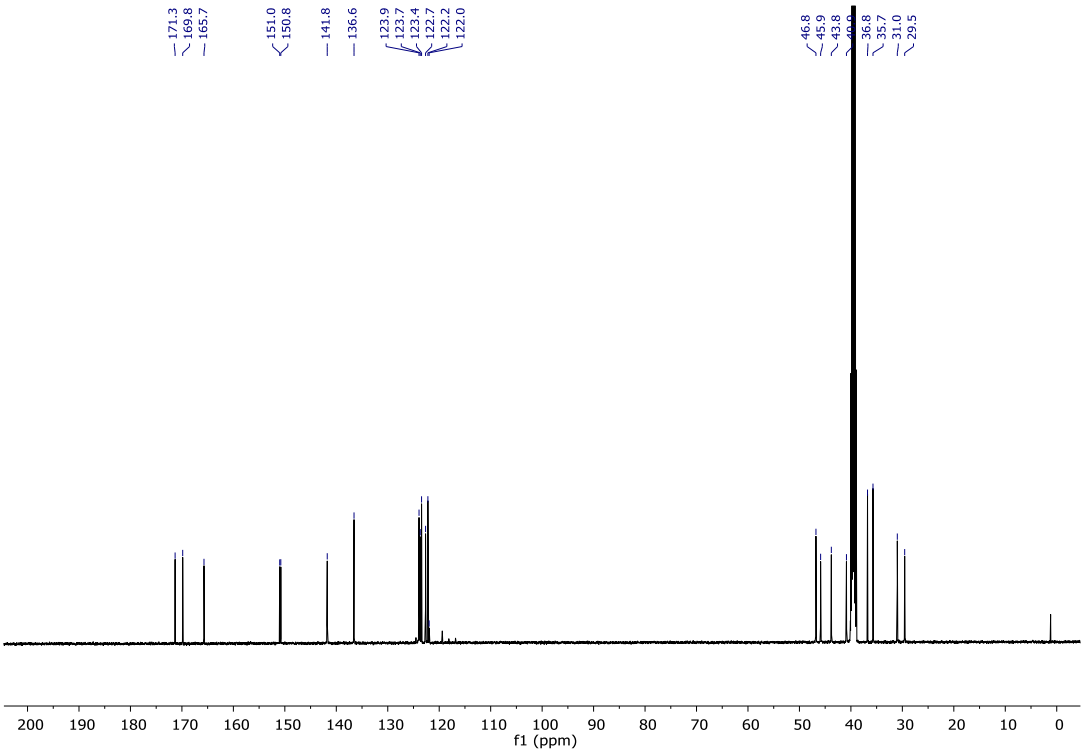

Figure A.3.21. ^{13}C NMR spectrum (126 MHz, DMSO-d_6) of **3.11**.

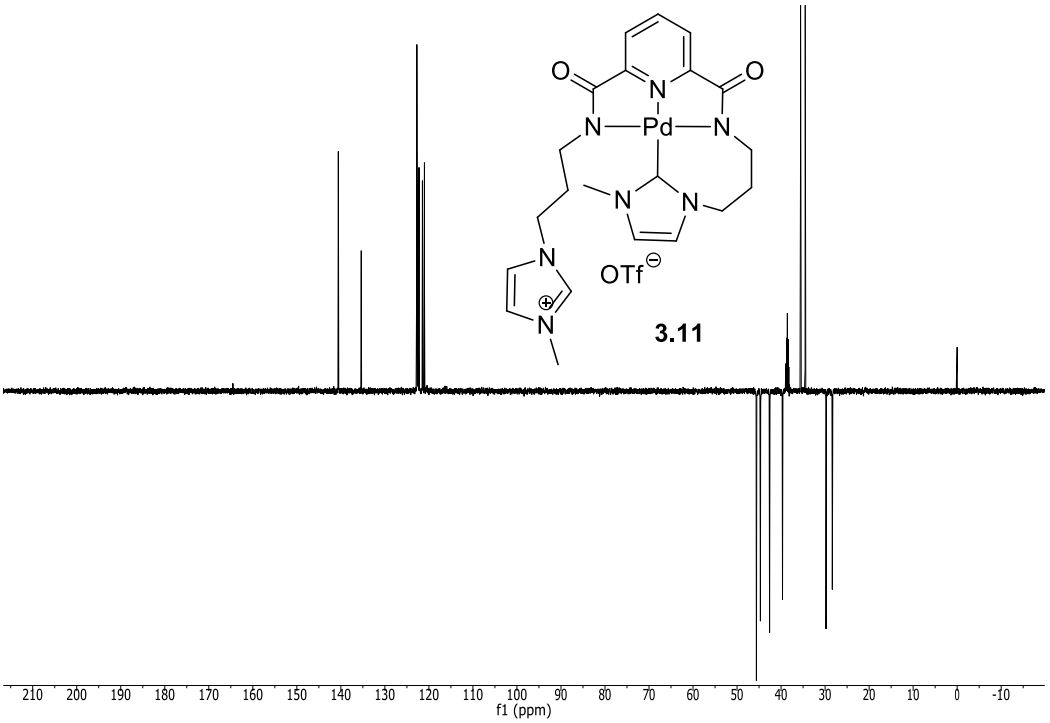

Figure A.3.22. ^{13}C NMR DEPT spectrum (126 MHz, DMSO-d_6) of **3.11**.

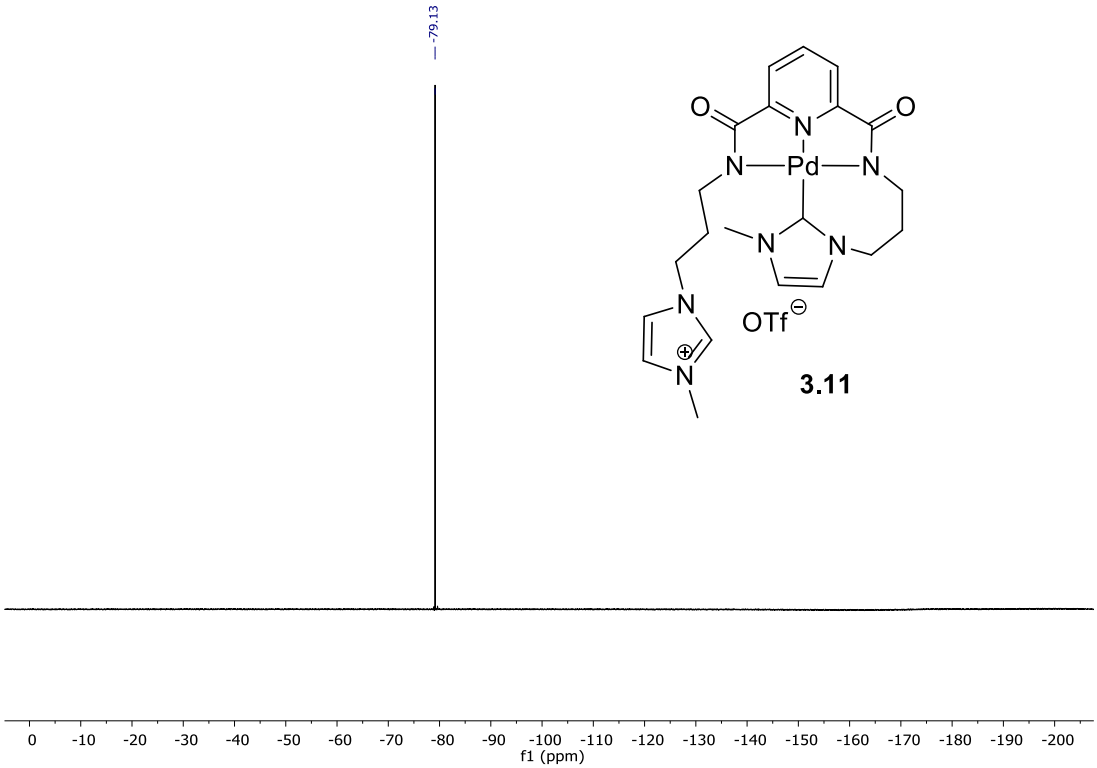

Figure A.3.23. ^{19}F NMR spectrum (471 MHz, DMSO-d_6) of **3.11**.

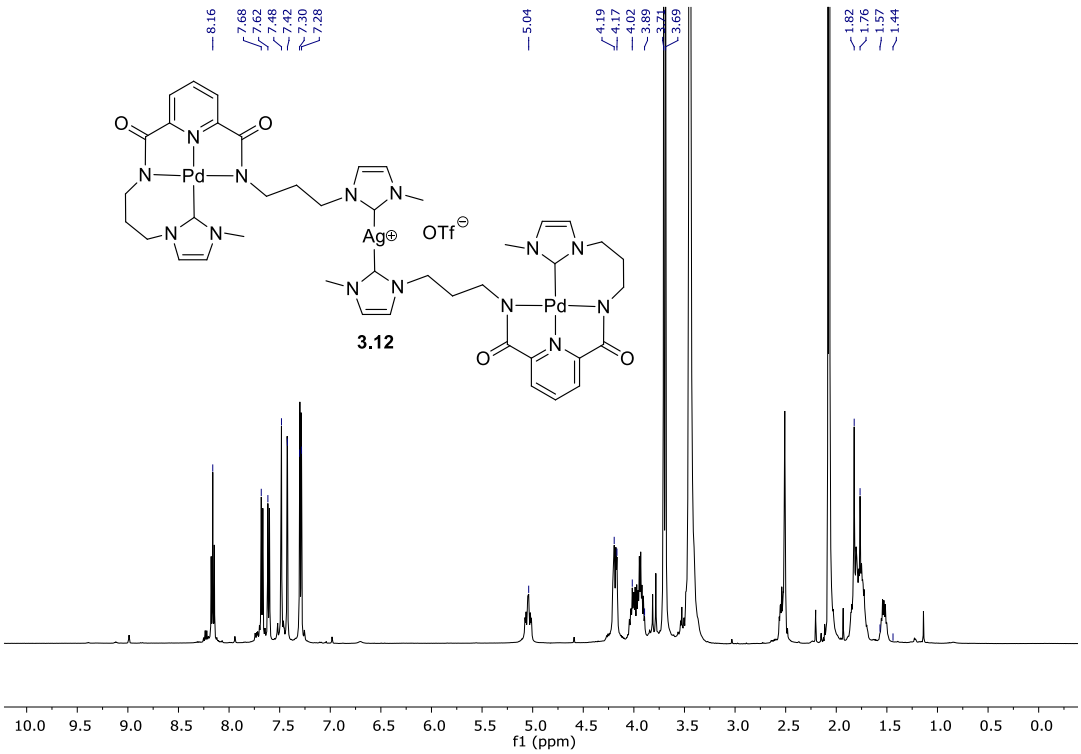

Figure A.3.24. ^{1}H NMR spectrum (500 MHz, DMSO-d_6) of **3.12**.

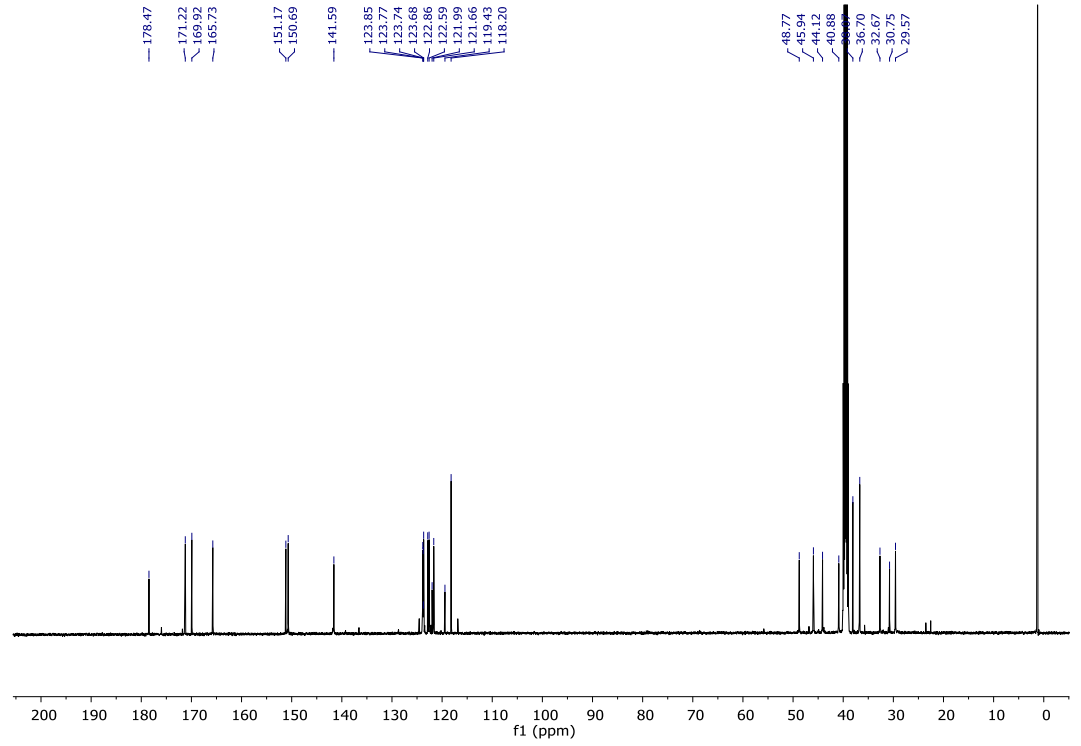

Figure A.3.25. ^{13}C NMR spectrum (126 MHz, DMSO-d_6) of **3.12**.

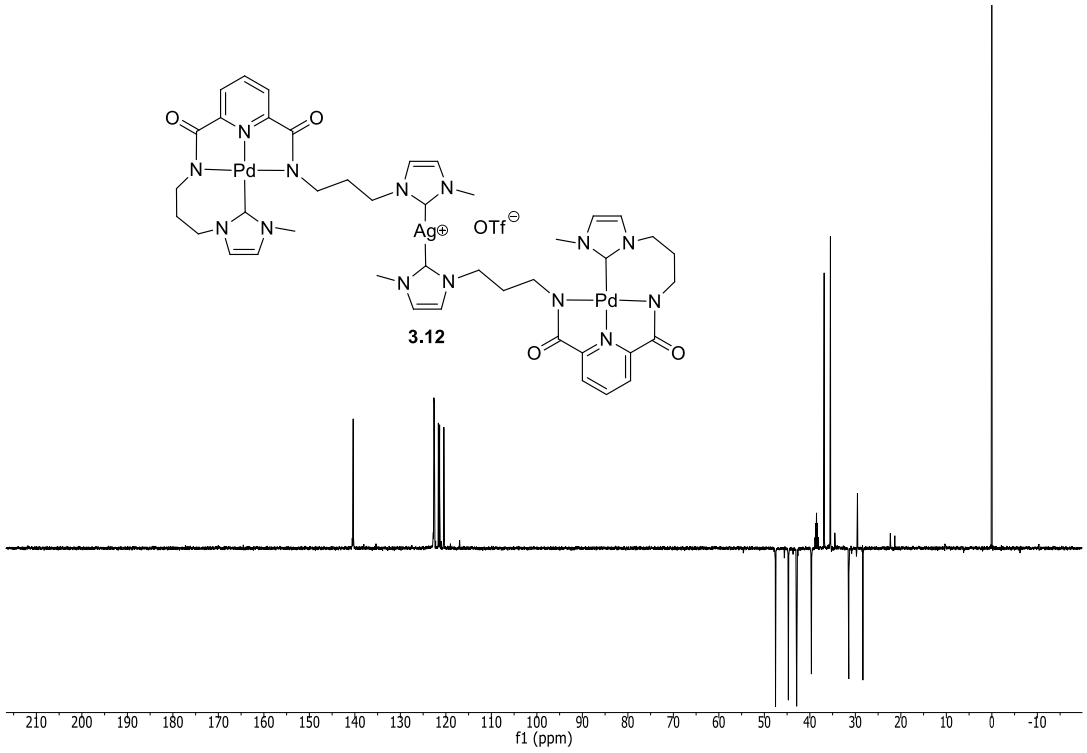

Figure A.3.26. ^{13}C NMR DEPT spectrum (126 MHz, DMSO-d_6) of **3.12**.

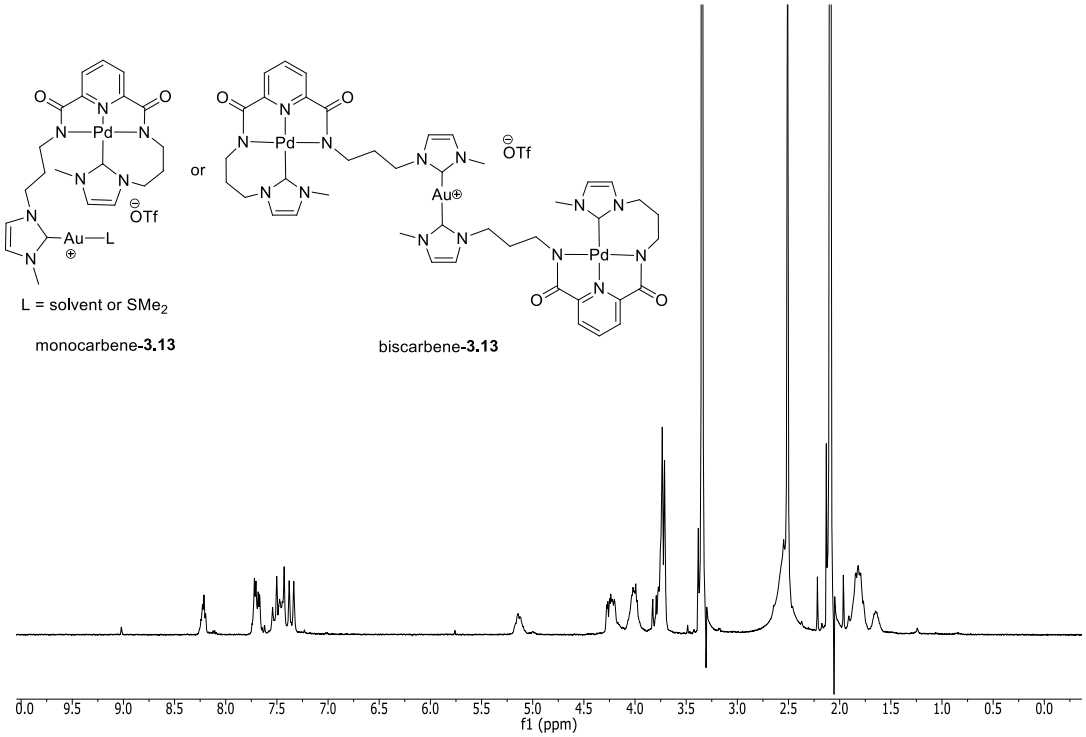

Figure A.3.27. ^{1}H NMR spectrum (500 MHz, DMSO-d_6) of **3.13**.

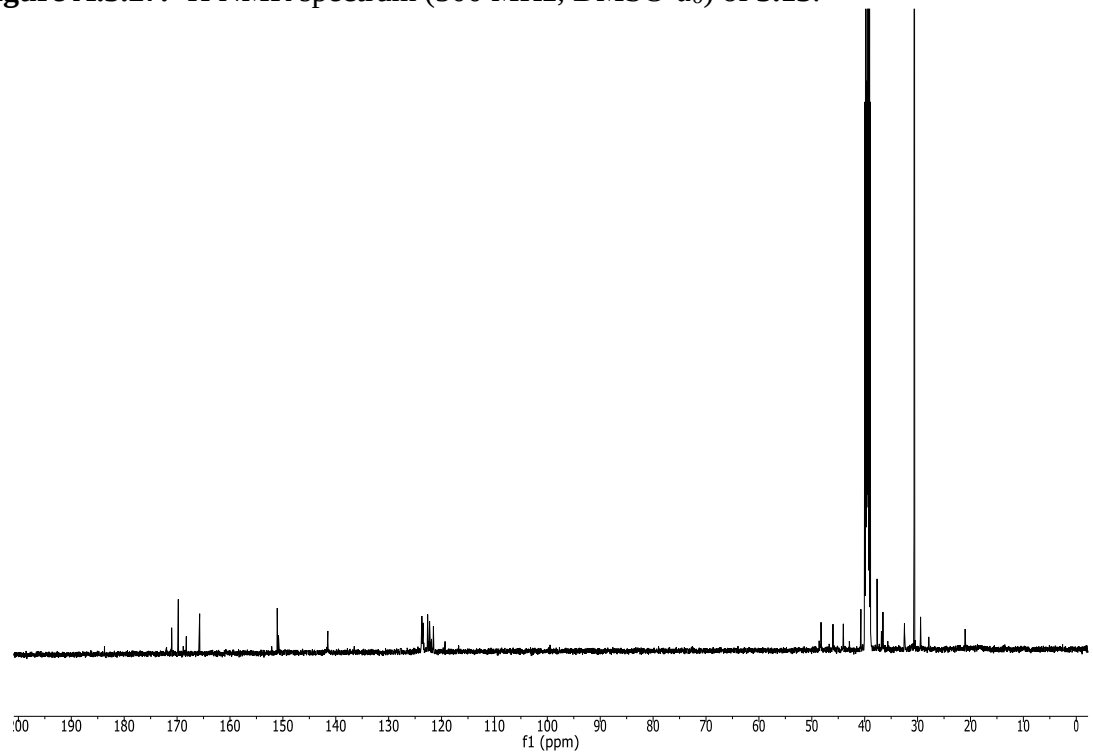

Figure A.3.28. ^{13}C NMR spectrum (126 MHz, DMSO-d_6) of **3.13**.

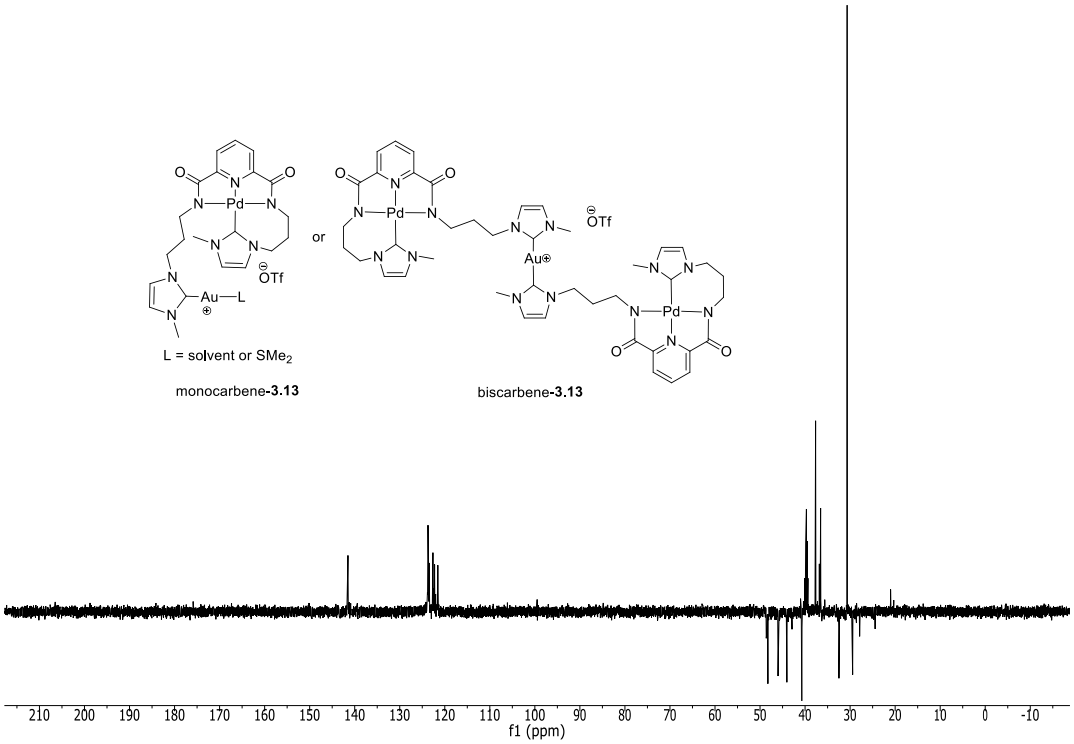

Figure A.3.29. ^{13}C DEPT NMR spectrum (126 MHz, DMSO-d_6) of **3.13**.

A.3.3 *Supplementary Information for XRD Studies*

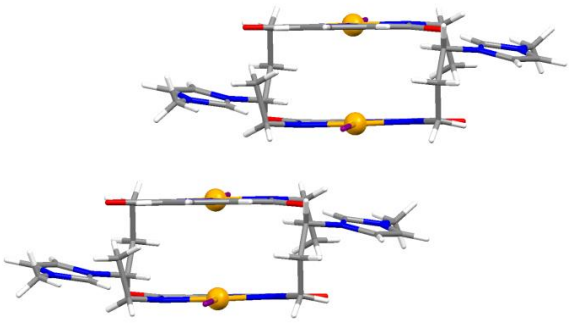

Figure A.3.30. Perspective view of the stacking in complex **3.6** along the Pd–N1 bond (orange ball = Pd).

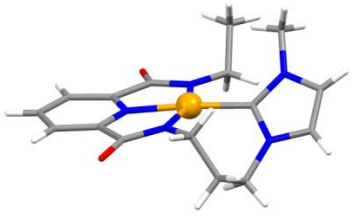

Figure A.3.31. Perspective view of **3.7** showing the diastereotopic protons in the propylene linker.

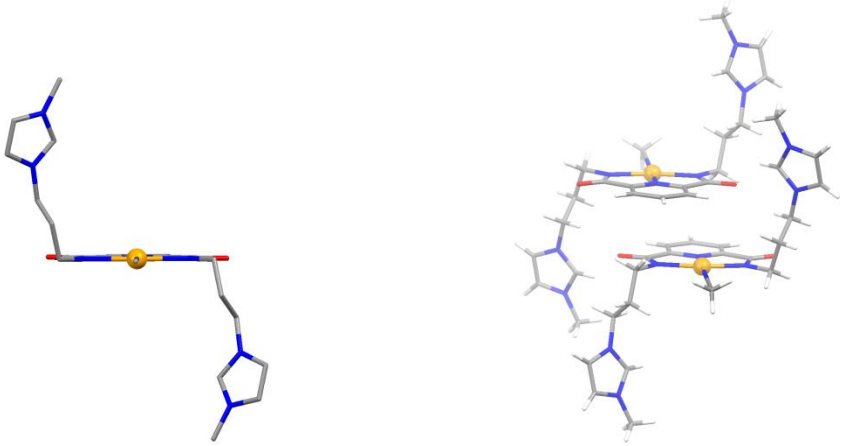

Figure A.3.32. (**A**) Perspective view of complex **3.10** along the Pd–N1 bond and (**B**) perspective view of the stacking in **3.10** (orange ball = Pd).

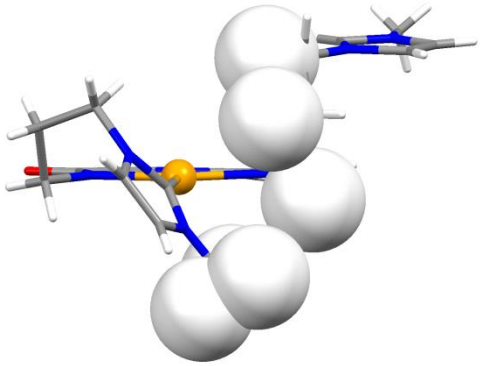

Figure A.3.33. Perspective view of complex **3.11** along the Pd–N1 bond axis (orange ball = Pd; white VDW space fill = selected hydrogen atoms).

Table A.3.1. Selected Bond Distances (Å) in Pd(II) complexes **3.6**, **3.7**, **3.10**, and **3.11**.

	3.6, L = I	**3.7**, L = C15	**3.10**, L = N1S	**3.11,** L = C13
Pd–N1	1.943(8)	1.9607(18)	1.926(5)	1.961(2)
Pd–N2	2.057(7)	2.0299(17)	2.024(4)	2.024(3)
Pd–N3	2.046(8)	2.0522(18)	2.024(4)	2.056(3)
Pd–L	2.030(2)	2.016(2)	2.003(5)	2.010(3)

Table A.3.2. Crystallographic data collection and structure refinement for complexes **3.6** and **3.7**.

	(**3.6**)	(**3.7**)
Formula	$C_{16}H_{20}IN_5O_2Pd$	$C_{16}H_{19}N_5O_2Pd$
Formula weight	547.67	419.76
Crystal size (mm^3)	0.04×0.01×0.01	0.08×0.07×0.06
Crystal system	Monoclinic	Monoclinic
Space group	$P2_1/n$	$P2_1$
a (Å)	14.3180(10)	11.4125(17)
b (Å)	7.8954(6)	9.0341(14)
c (Å)	16.6415(16)	15.501(2)
α (°)	90	90
β (°)	101.627(6)	91.791(2)
γ (°)	90	90
V ($Å^3$)	1842.7(3)	1597.4(4)
Z	4	4
ρ_{calcd} (g cm^{-3})	1.974	1.745
λ (Å)	1.54178	1.54178
T (K)	100(2)	100(2)
F(000)	1064	848
μ (mm^{-1})	21.453	9.546
Abs corr	Multi-scan	Multi-scan
Max, min trans	1.000, 0.764	1.000, 0.761
θ range (°)	3.72-69.82	5.67-68.29
Reflns collected	10540	10797
Indep reflns	3240	2863
R(int)	0.0553	0.0171
Data/restr/param	3240 / 6 / 228	2863 / 0 / 294
[a] R_1; wR_2	0.0494; 0.1294	0.0207;0.0560
GOF (F^2)	1.089	1.107
Largest diff. peak and hole (e $Å^{-3}$)	1.702, -0.797	0.404, -0.575

Table A.3.3. Crystallographic data collection and structure refinement for complexes **3.10** and **3.11**.

	(**3.10**)	(**3.11**)
Formula	$C_{29}H_{36}F_6N_{10}O_8PdS_2$	$C_{23}H_{27.5}F_3N_{7.5}O_5PdS$
Formula weight	937.20	684.49
Crystal size (mm^3)	0.37 x 0.11 x 0.08	0.20×0.09×0.04
Crystal system	Monoclinic	Monoclinic
Space group	C2/c	*P*-1
a (Å)	26.290(9)	8.9399(3)
b (Å)	20.107(7)	10.4834(3)
c (Å)	7.805(3)	14.9913(7)
α (°)	90	95.4870(10)
β (°)	103.851(6)	102.8420(10)
γ (°)	90	94.5980(10)
V ($Å^3$)	4006(2)	1356.11(7)
Z	4	4
ρ_{calcd} (g cm^{-3})	1.554	1.676
λ (Å)	1.54178	1.54178
T (K)	100(2)	100(2)
F(000)	1904	694
μ (mm^{-1})	5.484	6.868
Abs corr	Multi-scan	Multi-scan
Max, min trans	1.000, 0.439	1.000, 0.713
θ range (°)	6.09-68.08	3.04-69.93
Reflns collected	12064	15863
Indep reflns	3548	4750
R(int)	0.0467	0.0166
Data/restr/param	3548 / 0 / 264	4750 / 0 / 381
[a] R_1; wR_2	0.0515;0.1449	0.0330;0.0839
GOF (F^2)	1.086	1.086
Largest diff. peak and hole (e $Å^{-3}$)	0.877, -1.395	2.438, -0.545

A.3.4 *Mass Spectra*

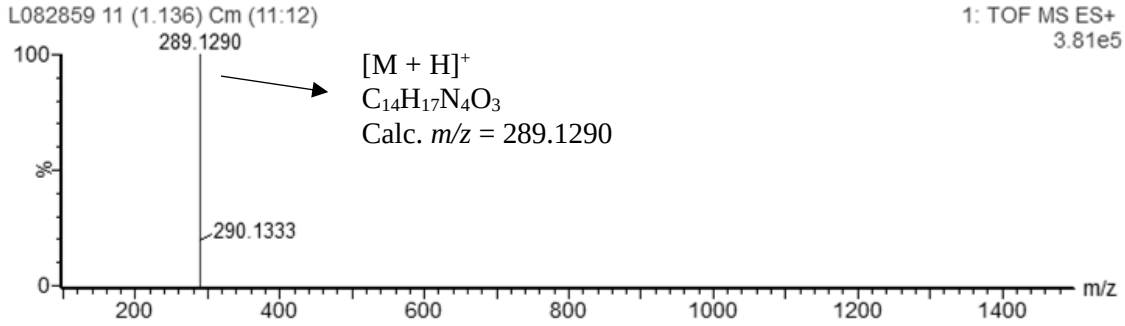

Figure A.3.34. HRMS (ESI$^+$) of ligand **3.1**.

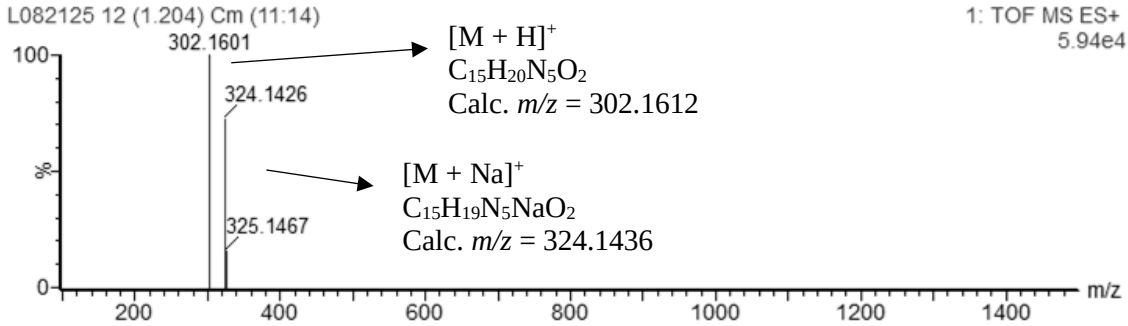

Figure A.3.35. HRMS (ESI$^+$) of ligand **3.2**.

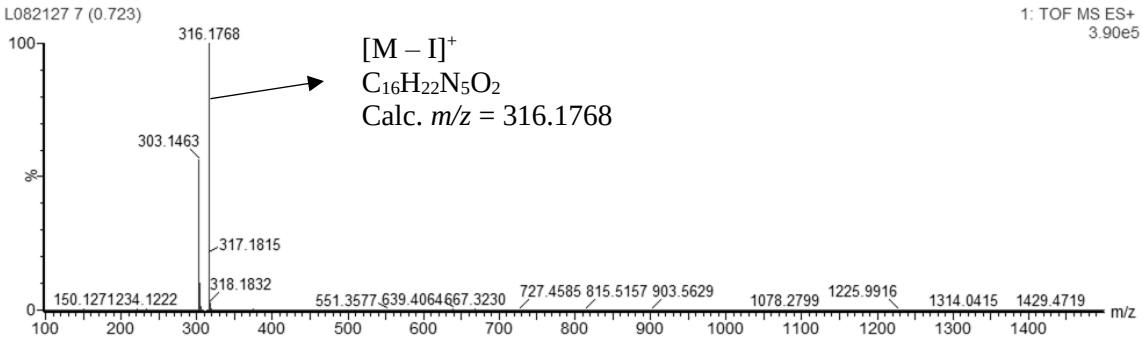

Figure A.3.36. HRMS (ESI$^+$) of ligand **3.3**.

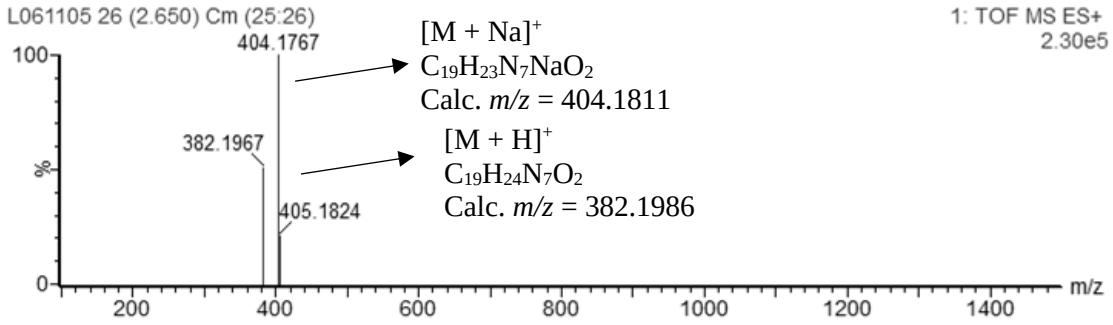

Figure A.3.37. HRMS (ESI$^+$) of ligand **3.4**.

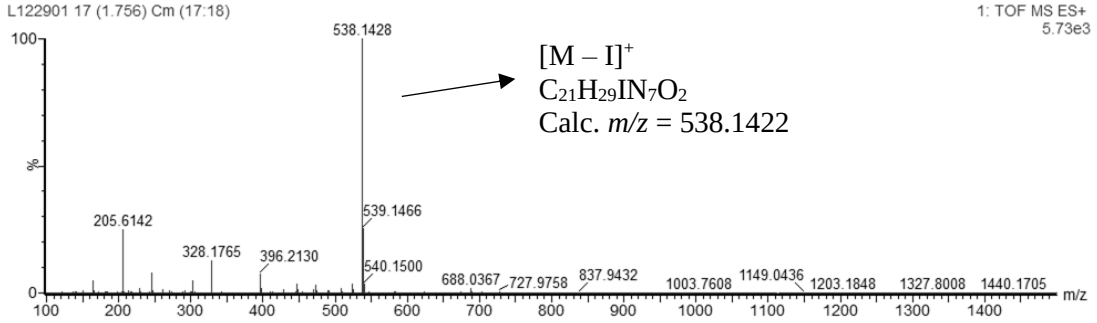

Figure A.3.38. HRMS (ESI$^+$) of ligand **3.5**.

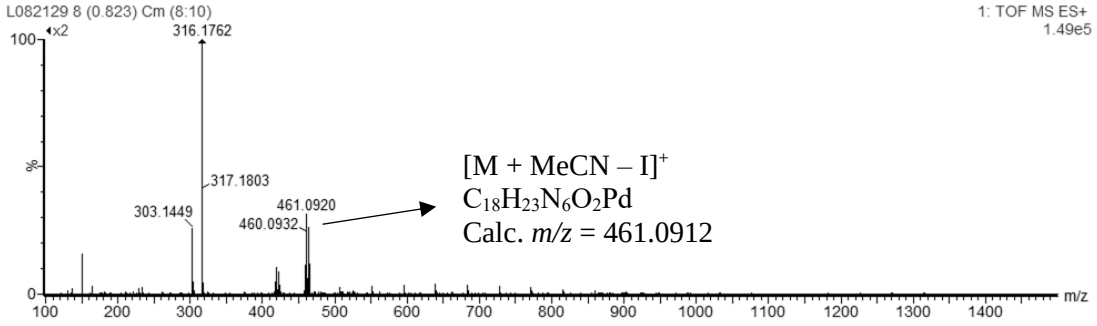

Figure A.3.39. HRMS (ESI$^+$) of complex **3.6**.

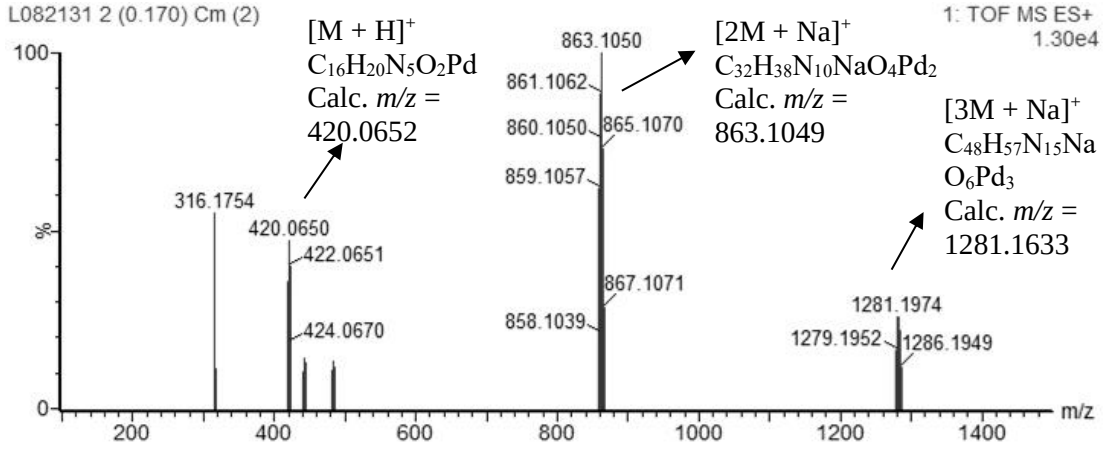

Figure A.3.40. HRMS (ESI$^+$) of complex **3.7**.

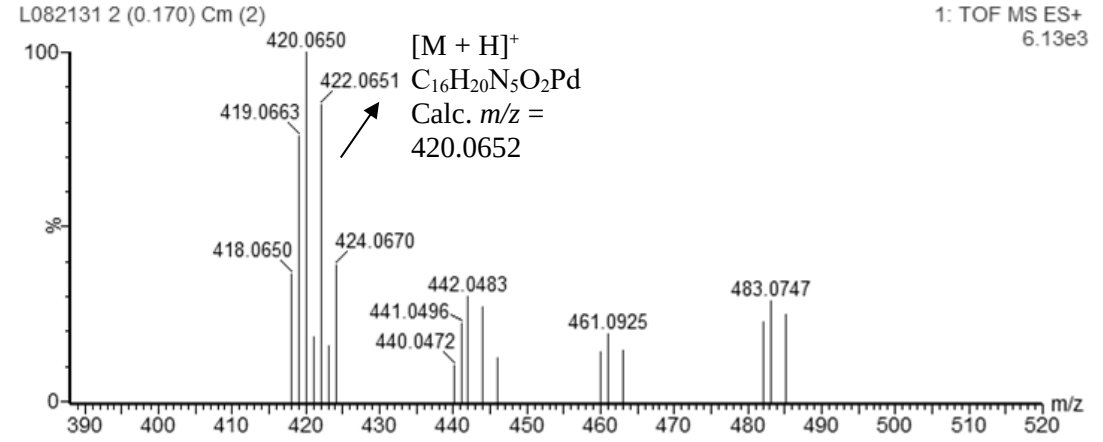

Figure A.3.41. Expanded region of the HRMS (ESI$^+$) of complex **3.7**.

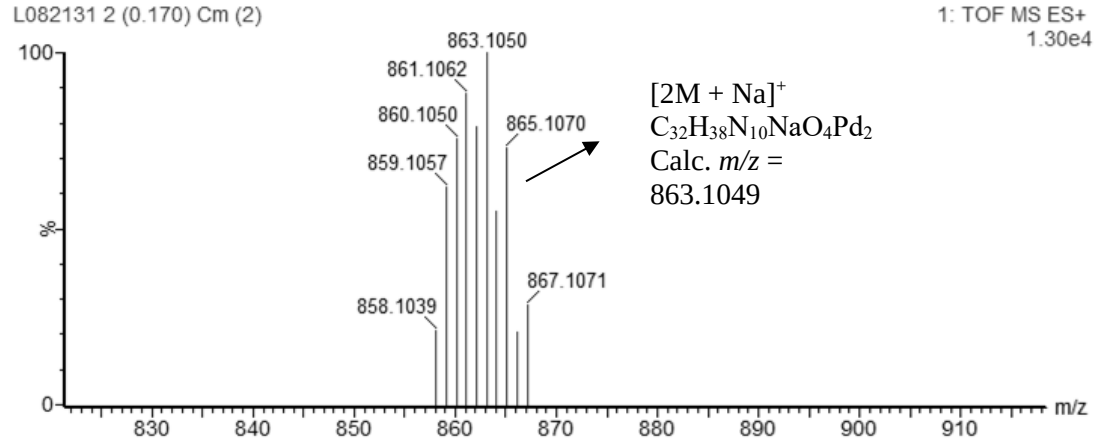

Figure A.3.42. Expanded region of the HRMS (ESI$^+$) of complex **3.7**.

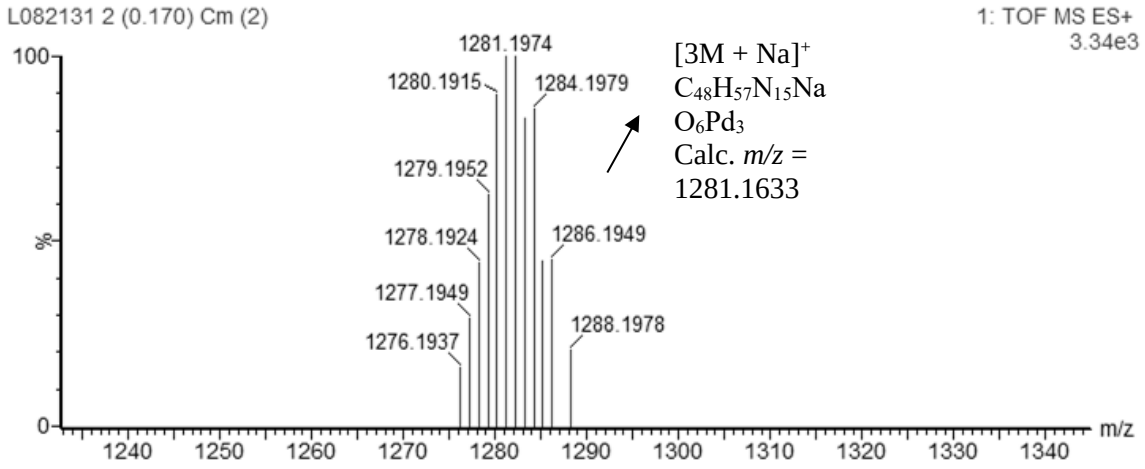

Figure A.3.43. Expanded region of the HRMS (ESI$^+$) of complex **3.7**.

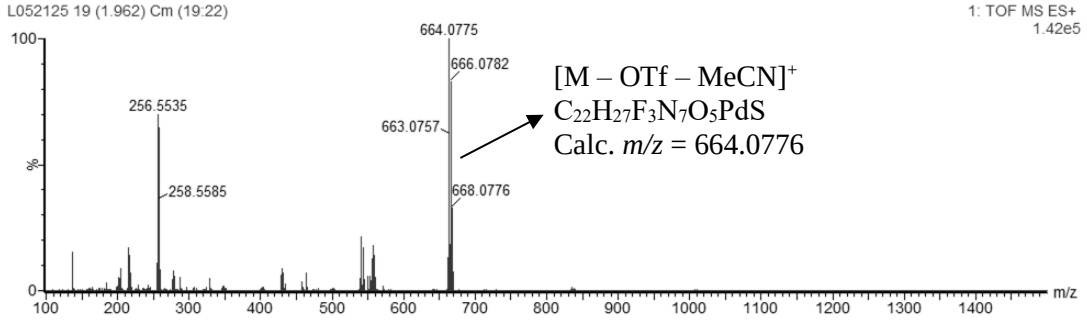

Figure A.3.44. HRMS (ESI$^+$) of complex **3.10**.

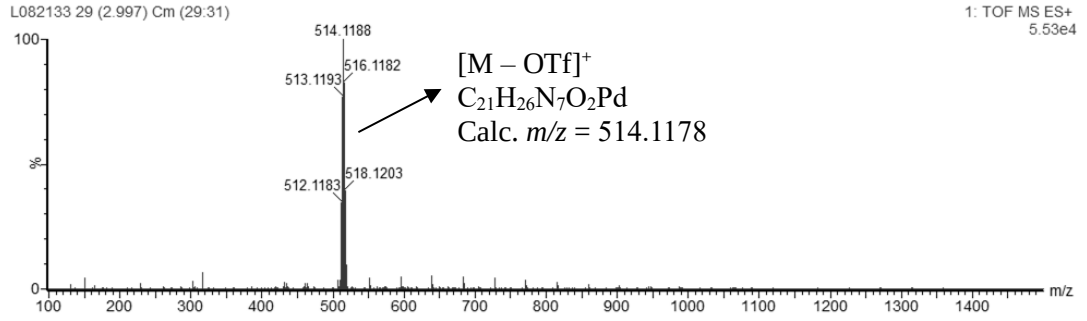

Figure A.3.45. HRMS (ESI$^+$) of complex **3.11**.

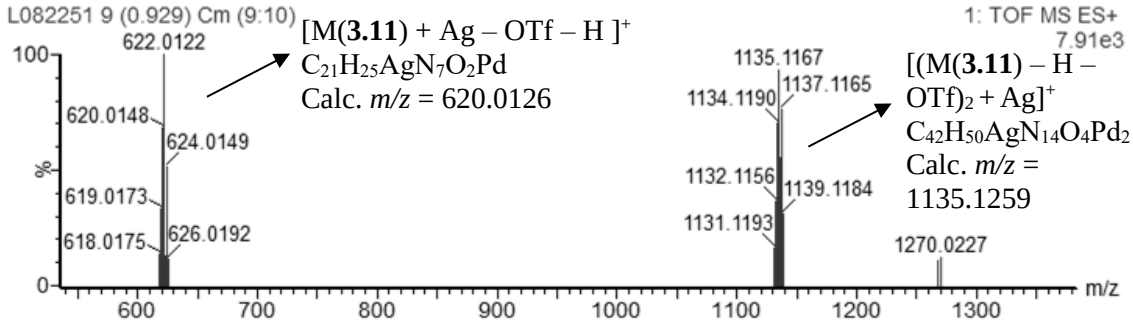

Figure A.3.46. HRMS (ESI$^+$) of complex **3.12**.

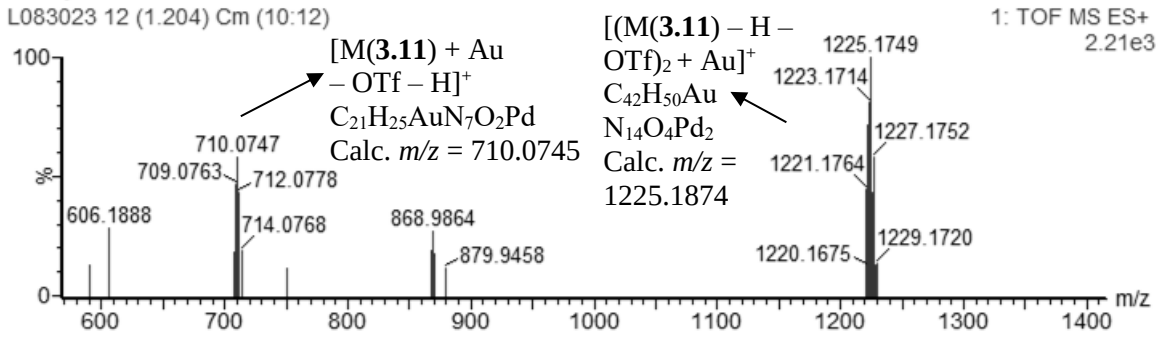

Figure A.3.47. HRMS (ESI$^+$) of complex **3.13**.

A.4 *Supporting Information for Chapter 4*

A.4.1 *Self-Assembly of Coordination Polymers using Pd(OAc)$_2$.*

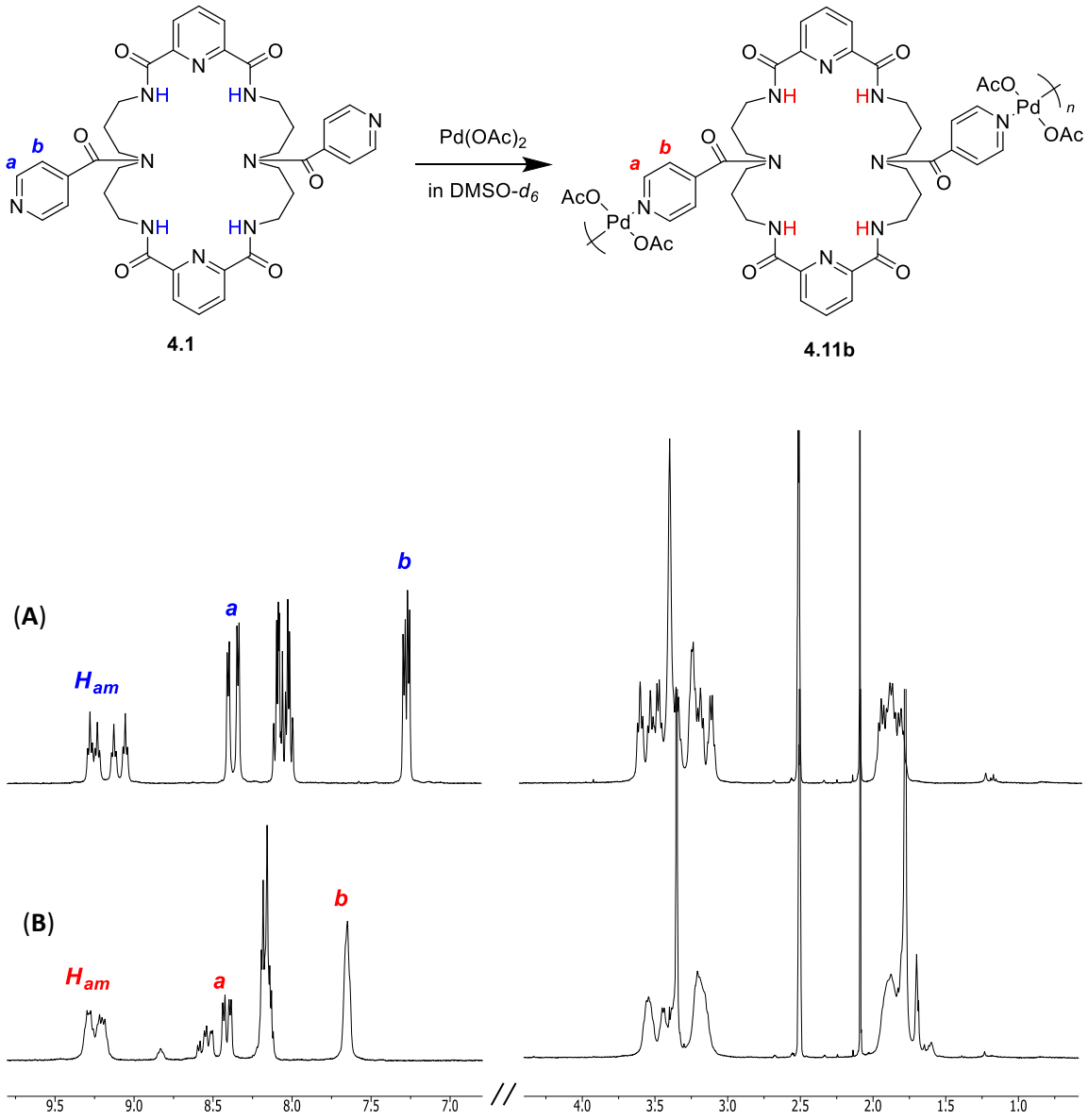

Figure A.4.1. Top: Reaction of $Pd(OAc)_2$ with **4.1** with assignments for the pendant pyridine protons. Bottom: ^{1}H NMR (500 MHz, 298 K, DMSO-d_6) of **4.1** (**A**) before and (**B**) after adding $Pd(OAc)_2$ (2 equiv).

A.4.2 *NMR Spectra of **4.8** and **4.9***

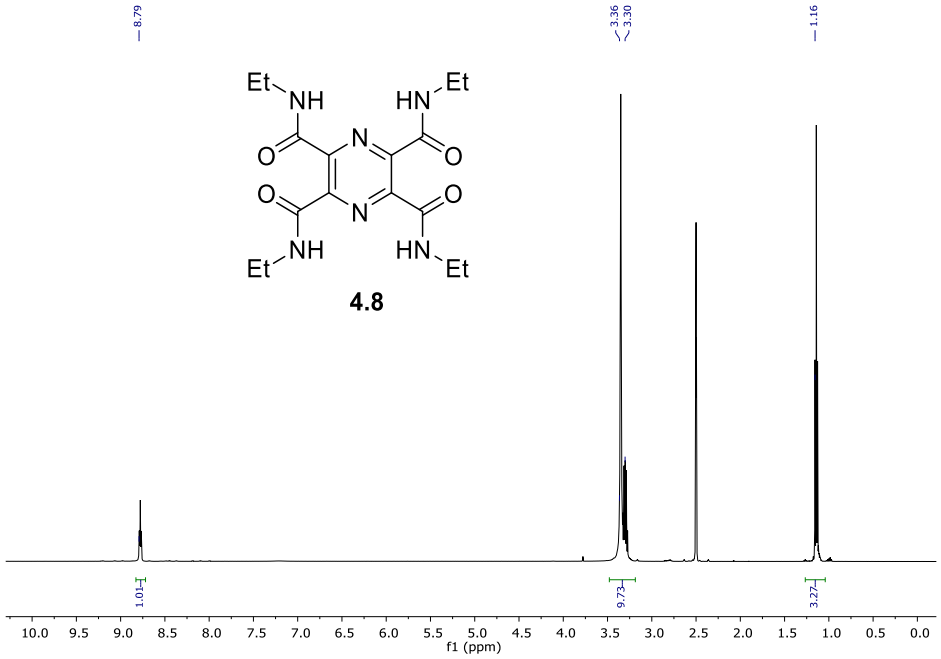

Figure A.4.2. ^{1}H NMR spectrum (500 MHz, DMSO-d_6) of **4.8**.

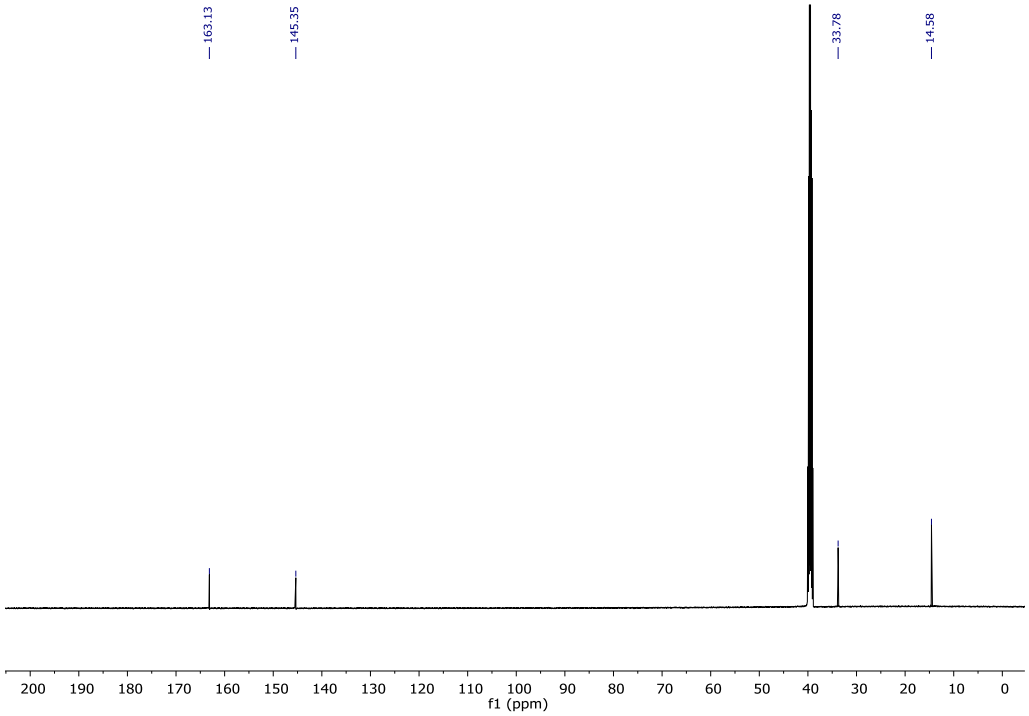

Figure A.4.3. ^{13}C NMR spectrum (126 MHz, DMSO-d_6) of **4.8**.

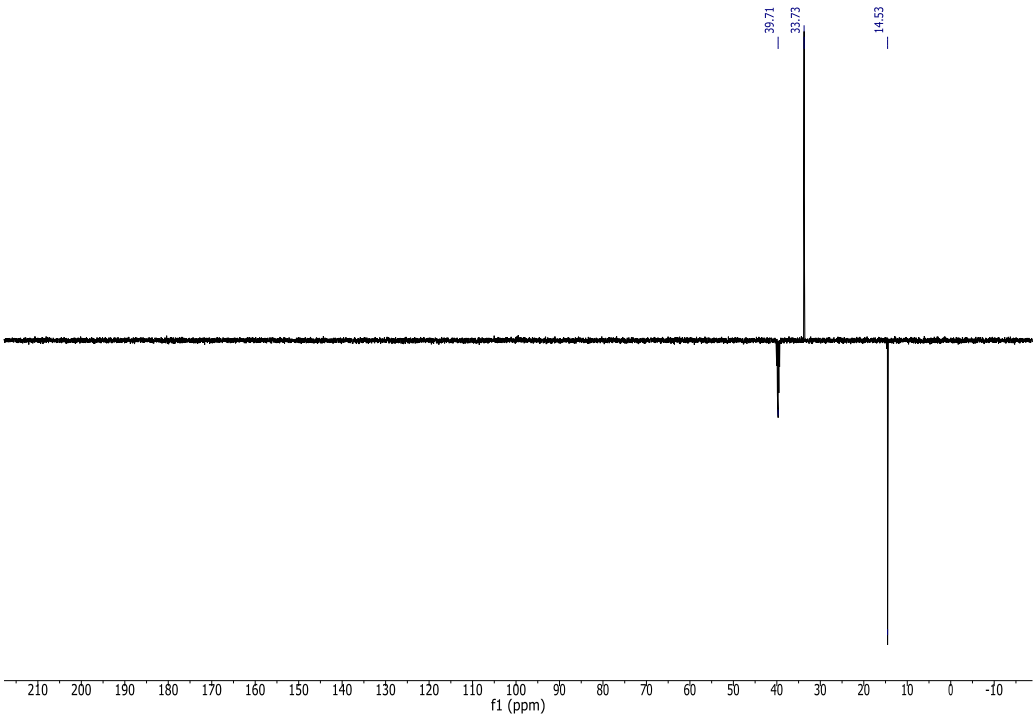

Figure A.4.4. ^{13}C DEPT NMR spectrum (126 MHz, DMSO-d_6) of **4.8**.

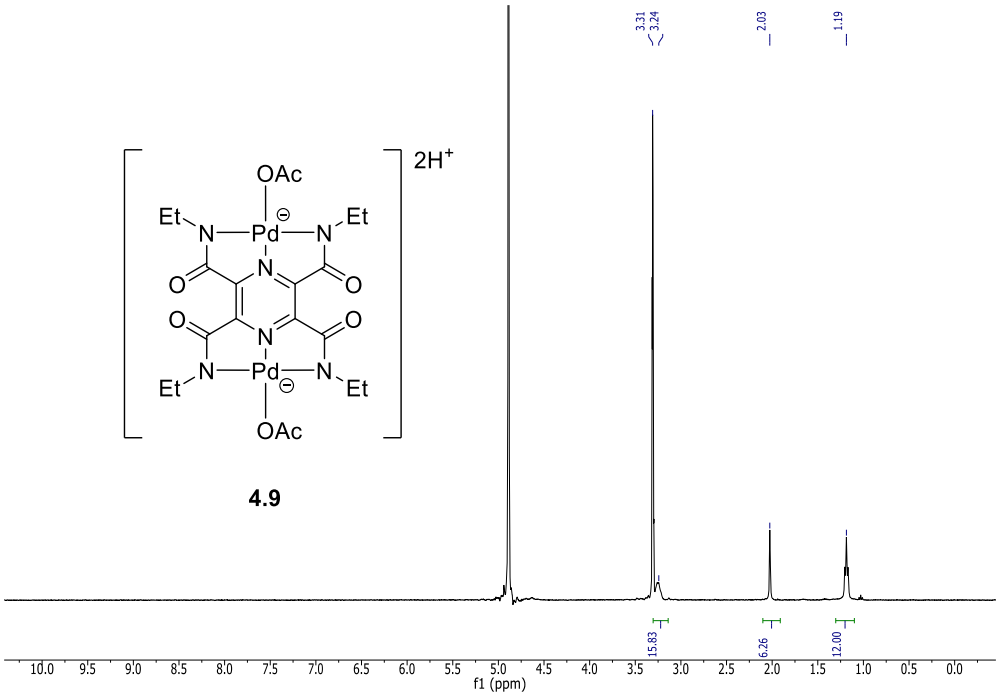

Figure A.4.5. ^{1}H NMR spectrum (500 MHz, CD_3OD) of **4.9**.

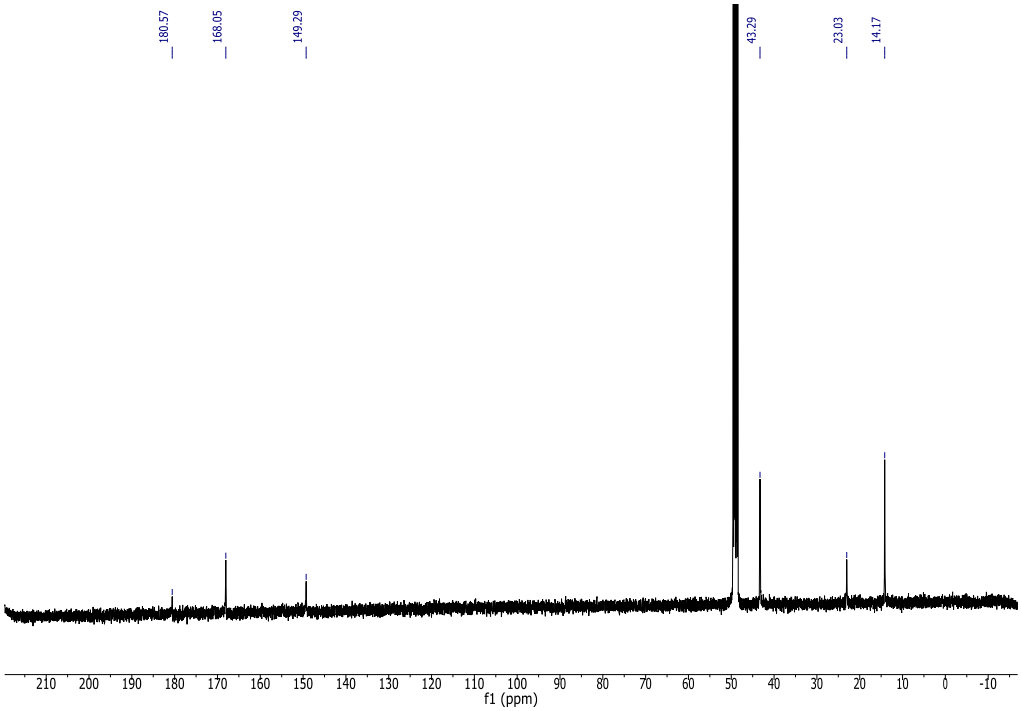

Figure A.4.6. ^{13}C NMR spectrum (126 MHz, CD_3OD) of **4.9**.

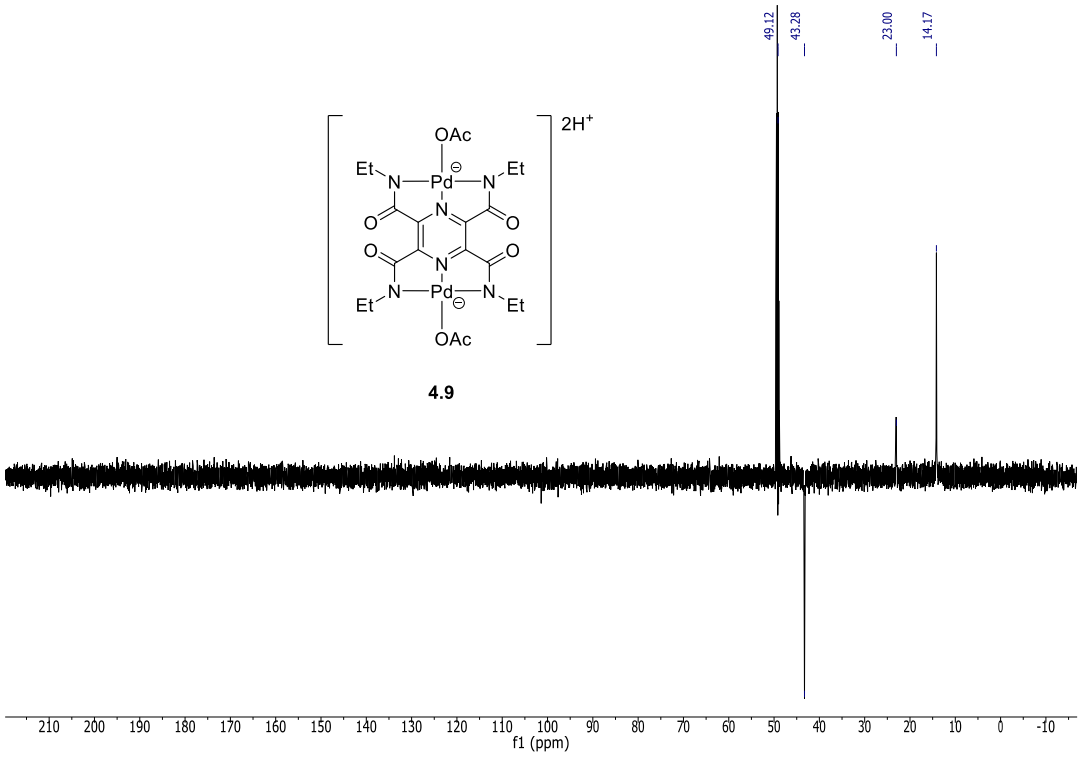

Figure A.4.7. ^{13}C DEPT NMR spectrum (126 MHz, CD_3OD) of **4.9**.

A.4.3 *Mass Spectra*

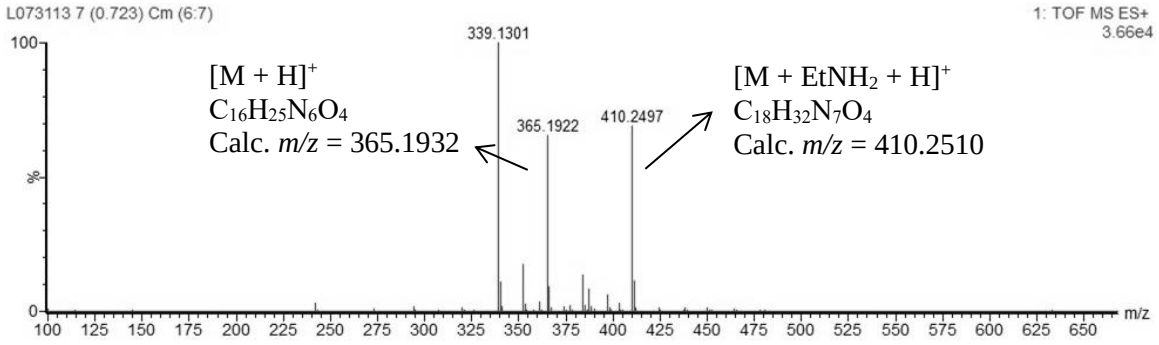

Figure A.4.8. HRMS (ESI^+) of NNN-dipincer ligand **4.8**.

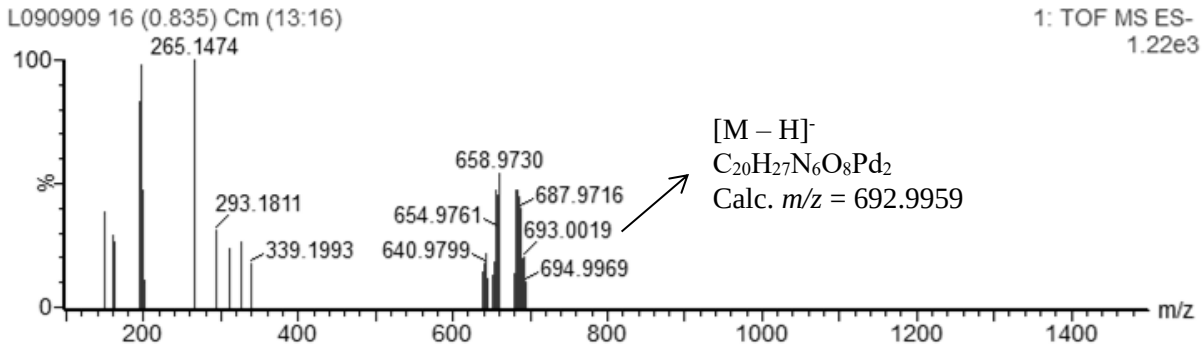

Figure A.4.9. HRMS (ESI^-) of Pd(II) NNN-dipincer complex **4.9**.

A.4.4 *Supporting Information for XRD Studies*

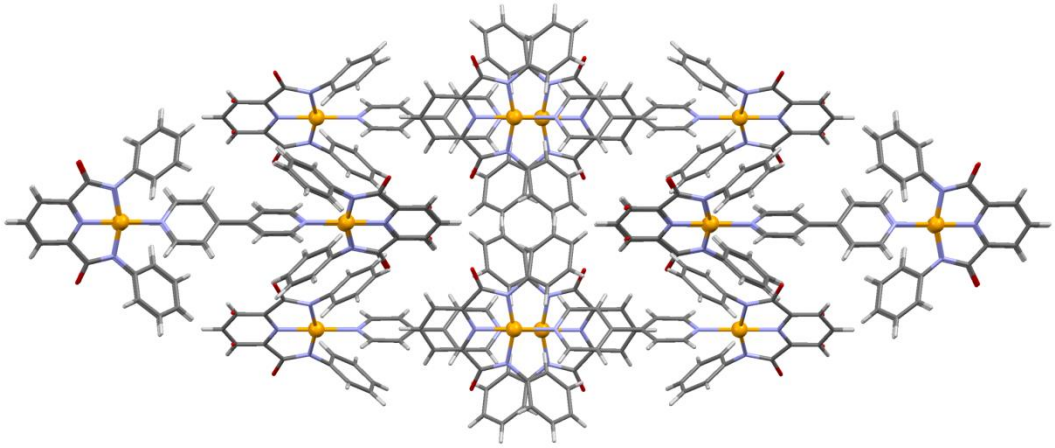

Figure A.4.10. Perspective view of the packing of 4,4-bipyridine dimer complex **4.5**.

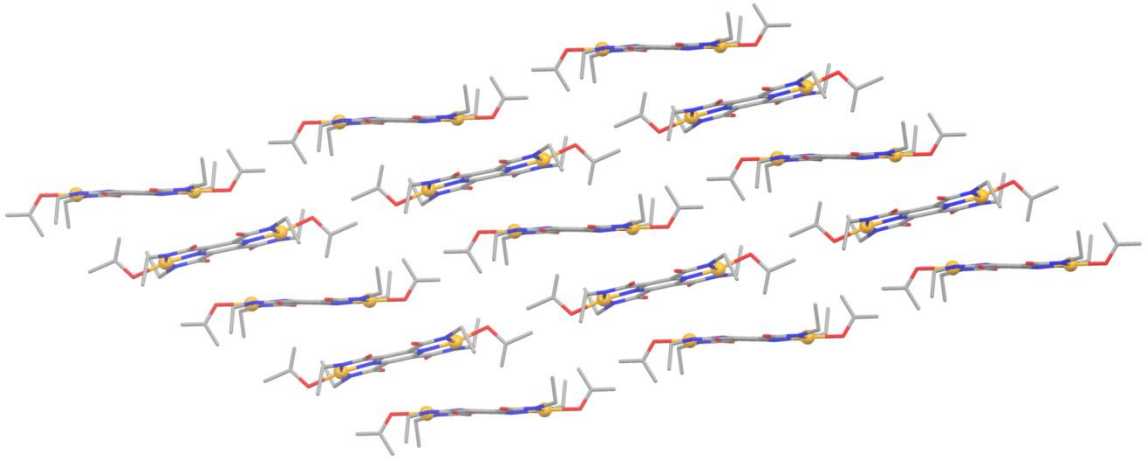

Figure A.4.11. Perspective view of the packing of complex **4.9**.